MEETING OF THE PORTUGUESE SOCIETY FOR NEUROSCIENCES SPN2019

EDITED BY: Sara Xapelli, Cláudia Guimas Almeida and Maria José Diógenes
PUBLISHED IN: Frontiers in Molecular Neuroscience, Frontiers in Neuroscience and Frontiers in Cellular Neuroscience

frontiers Research Topics

frontiers

ISSN 1664-8714
ISBN 978-2-88971-790-3
DOI 10.3389/978-2-88971-790-3

About Frontiers

Frontiers is more than just an open-access publisher of scholarly articles: it is a pioneering approach to the world of academia, radically improving the way scholarly research is managed. The grand vision of Frontiers is a world where all people have an equal opportunity to seek, share and generate knowledge. Frontiers provides immediate and permanent online open access to all its publications, but this alone is not enough to realize our grand goals.

Frontiers Journal Series

The Frontiers Journal Series is a multi-tier and interdisciplinary set of open-access, online journals, promising a paradigm shift from the current review, selection and dissemination processes in academic publishing. All Frontiers journals are driven by researchers for researchers; therefore, they constitute a service to the scholarly community. At the same time, the Frontiers Journal Series operates on a revolutionary invention, the tiered publishing system, initially addressing specific communities of scholars, and gradually climbing up to broader public understanding, thus serving the interests of the lay society, too.

Dedication to Quality

Each Frontiers article is a landmark of the highest quality, thanks to genuinely collaborative interactions between authors and review editors, who include some of the world's best academicians. Research must be certified by peers before entering a stream of knowledge that may eventually reach the public - and shape society; therefore, Frontiers only applies the most rigorous and unbiased reviews.
Frontiers revolutionizes research publishing by freely delivering the most outstanding research, evaluated with no bias from both the academic and social point of view. By applying the most advanced information technologies, Frontiers is catapulting scholarly publishing into a new generation.

What are Frontiers Research Topics?

Frontiers Research Topics are very popular trademarks of the Frontiers Journals Series: they are collections of at least ten articles, all centered on a particular subject. With their unique mix of varied contributions from Original Research to Review Articles, Frontiers Research Topics unify the most influential researchers, the latest key findings and historical advances in a hot research area! Find out more on how to host your own Frontiers Research Topic or contribute to one as an author by contacting the Frontiers Editorial Office: frontiersin.org/about/contact

MEETING OF THE PORTUGUESE SOCIETY FOR NEUROSCIENCES SPN2019

Topic Editors:
Sara Xapelli, University of Lisbon, Portugal
Cláudia Guimas Almeida, New University of Lisbon, Portugal
Maria José Diógenes, University of Lisbon, Portugal

Citation: Xapelli, S., Almeida, C. G., Diógenes, M. J., eds. (2021). Meeting of the Portuguese Society for Neurosciences SPN2019. Lausanne: Frontiers Media SA. doi: 10.3389/978-2-88971-790-3

Table of Contents

frontiers in Molecular Neuroscience

EDITORIAL
published: 07 October 2021
doi: 10.3389/fnmol.2021.753500

Editorial: Meeting of the Portuguese Society for Neurosciences SPN2019

Maria José Diógenes[1,2], *Cláudia Guimas Almeida*[3] *and Sara Xapelli*[1,2]*

[1] *Faculdade de Medicina, Instituto de Medicina Molecular João Lobo Antunes, Universidade de Lisboa, Lisbon, Portugal,*
[2] *Faculdade de Medicina, Instituto de Farmacologia e Neurociências, Universidade de Lisboa, Lisbon, Portugal,*
[3] *iNOVA4Health, Chronic Diseases Research Center (CEDOC), NOVA Medical School (NMS), Universidade Nova de Lisboa, Lisbon, Portugal*

Keywords: neurodevelopment, neurodegeneration, glia and neuroinflammation, drug and addiction, sensory processing, rare disorders, cellular and molecular neurosciences

Editorial on the Research Topic

Meeting of the Portuguese Society for Neurosciences SPN2019

OPEN ACCESS

Edited by:
Jean-Marc Taymans, Institut National de la Santé et de la Recherche Médicale (INSERM), France

Reviewed by:
Gary Leo Dunbar, Central Michigan University, United States

***Correspondence:**
Sara Xapelli
sxapelli@medicina.ulisboa.pt

Specialty section:
This article was submitted to Molecular Signalling and Pathways, a section of the journal Frontiers in Molecular Neuroscience

Received: *04 August 2021*
Accepted: *20 September 2021*
Published: *07 October 2021*

Citation:
Diógenes MJ, Guimas Almeida C and Xapelli S (2021) Editorial: Meeting of the Portuguese Society for Neurosciences SPN2019. Front. Mol. Neurosci. 14:753500. doi: 10.3389/fnmol.2021.753500

The Portuguese Society for Neuroscience meeting (SPN2019) was held in Lisbon from 30th May to 1st June, 2019. The main purpose of this meeting was to promote and develop research in Neurosciences. This interaction took place in a privileged way at this meeting and brought together the vibrant Portuguese Neuroscience community that significantly advances this defying area.

This Research Topic comprises nine manuscripts covering some of the work presented at SPN2019 and hot topics in neurosciences: neurodevelopment; cellular and molecular neurosciences; neurodegeneration; glia and neuroinflammation; drug and addiction; sensory processing; and rare disorders.

In a brief Research Report, Miranda et al. show that cannabidiol, Δ9-tetrahydrocannabinol, and two synthetic cannabinoids (THJ-018 and EG-018) profoundly impact, from toxicity to precocity, developing neurons, highlighting the negative effect of prenatal exposure to natural and synthetic cannabinoids.

A brief Research Report by Neiva et al. shows that methylprednisolone differentially affects GABA and glutamate release from rat hippocampal nerve terminals *via* fast non-genomic mechanisms putatively involving the activation of membrane-bound corticosteroid receptors.

Original Research by Sa de Almeida et al. reveals that microglial Sirtuin 2 (Sirt2) prevents NMDA-mediated excitotoxicity in hippocampal slices in response to an inflammatory signal. Overall, the data suggest a key-protective role for microglial Sirt2 in amnesic deficits associated with neuroinflammation.

Original Research by Fonteles et al. supports that antagonists of ATP receptors P2X7 are protective of dyskinesia induced by dopamine replacement therapy in a Parkinson's disease rat model. These findings suggest P2X7 antagonists as novel candidate anti-dyskinesia drugs.

Original Research by Costa-Pereira et al. describes an enhancement of the descending noradrenergic pain control system due to neuropathy induced by cancer chemotherapy. The authors suggest that potentiation of the antinociception mediated by alpha2-adrenoreceptors may be a therapeutic opportunity.

Original Research by Fabricio de Sousa et al. shows that the cerebellum is vulnerable to metabolic changes due to ultra-endurance racer. High-volume training in rodents induced cerebellar oxidative and inflammatory status and impaired astrocyte reactivity.

Mouro et al. reviewed the recent evidence concerning metabolic, synaptic, functional, and molecular dysfunctions occurring in Rett syndrome. From modulators of GABAergic signaling to cannabinoids and the ketogenic diet, cleverly exploiting the metabolic features of this disease, an ample bulk of evidence has been gathered, creating a plethora of research lines to be followed in the future.

Perdigão et al. reviewed the intracellular trafficking mechanisms of synaptic dysfunction in Alzheimer's disease. They described that in early and late-onset familial Alzheimer's disease the earliest synaptic dysfunctions are characterized by disruptions of the presynaptic vesicle exo- and endocytosis and postsynaptic glutamate receptor endocytosis. While in early-onset familial Alzheimer's disease, synapse dysfunction seems to be triggered by Aβ, in late-onset Alzheimer's disease, there might be a direct synaptic disruption by late-onset Alzheimer's disease trafficking genes, requiring further research.

The mini-review by Gonçalves-Ribeiro et al. discussed the role of the increase in glutamate uptake on hippocampal long-term potentiation and depression beyond excitotoxicity.

Overall, this Research Topic compiling both original and review papers shows the diversity in the neuroscience field ranging from *in vitro* to *in vivo* approaches, including rare to common disorders, neurodevelopment to aging, and molecular to behavioral tests. We hope this collection of articles will be highly attractive to the international neuroscience community.

AUTHOR CONTRIBUTIONS

All authors listed have made a substantial, direct and intellectual contribution to the work, and approved it for publication.

ACKNOWLEDGMENTS

The authors would like to thank the following organizations for their funding: MD has been supported by Fundação para a Ciência e Tecnologia (FCT) Portugal (PTDC/MED-NEU/31929/2017) and Santa Casa da Misericórdia de Lisboa (MB37-2017). The Almeida Lab has been supported by FCT (JPCOFUND/0004/2015); Alzheimer's Association Research Grant (AARG-19-618007); Maratona da Saúde; iNOVA4Health (UID/Multi/04462/2019), a program financially supported by FCT/Ministério da Educação e Ciência, through national funds and co-funded by FEDER under the PT2020 Partnership Agreement. CG salary has been supported by FCT (CEECIND/00410/2017). SX has been supported by FCT (IF/01227/2015).

Conflict of Interest: The authors declare that the research was conducted in the absence of any commercial or financial relationships that could be construed as a potential conflict of interest.

Publisher's Note: All claims expressed in this article are solely those of the authors and do not necessarily represent those of their affiliated organizations, or those of the publisher, the editors and the reviewers. Any product that may be evaluated in this article, or claim that may be made by its manufacturer, is not guaranteed or endorsed by the publisher.

frontiers in Neuroscience

REVIEW
published: 02 July 2019
doi: 10.3389/fnins.2019.00680

From Cannabinoids and Neurosteroids to Statins and the Ketogenic Diet: New Therapeutic Avenues in Rett Syndrome?

Francisco Melo Mouro[1,2], Catarina Miranda-Lourenço[1,2], Ana Maria Sebastião[1,2] and Maria José Diógenes[1,2]**

[1] *Instituto de Farmacologia e Neurociências, Faculdade de Medicina, Universidade de Lisboa, Lisbon, Portugal,* [2] *Instituto de Medicina Molecular João Lobo Antunes, Faculdade de Medicina, Universidade de Lisboa, Lisbon, Portugal*

Rett syndrome (RTT) is an X-linked neurodevelopmental disorder caused mainly by mutations in the *MECP2* gene, being one of the leading causes of mental disability in females. Mutations in the *MECP2* gene are responsible for 95% of the diagnosed RTT cases and the mechanisms through which these mutations relate with symptomatology are still elusive. Children with RTT present a period of apparent normal development followed by a rapid regression in speech and behavior and a progressive deterioration of motor abilities. Epilepsy is one of the most common symptoms in RTT, occurring in 60 to 80% of RTT cases, being associated with worsening of other symptoms. At this point, no cure for RTT is available and there is a pressing need for the discovery of new drug candidates to treat its severe symptoms. However, despite being a rare disease, in the last decade research in RTT has grown exponentially. New and exciting evidence has been gathered and the etiopathogenesis of this complex, severe and untreatable disease is slowly being unfolded. Advances in gene editing techniques have prompted cure-oriented research in RTT. Nonetheless, at this point, finding a cure is a distant reality, highlighting the importance of further investigating the basic pathological mechanisms of this disease. In this review, we focus our attention in some of the newest evidence on RTT clinical and preclinical research, evaluating their impact in RTT symptomatology control, and pinpointing possible directions for future research.

Keywords: Rett syndrome, $GABA_AR$, epilepsy, cholesterol, ketogenic diet, cannabinoids, neurosteroids

OPEN ACCESS

Edited by:
Francisco Ciruela,
University of Barcelona, Spain

Reviewed by:
Maurizio Giustetto,
University of Turin, Italy
Erik B. Oleson,
University of Colorado Denver, United States

****Correspondence:***
Francisco Melo Mouro
fmouro@medicina.ulisboa.pt
Maria José Diógenes
diogenes@medicina.ulisboa.pt

Specialty section:
This article was submitted to Neuropharmacology, a section of the journal Frontiers in Neuroscience

Received: *12 April 2019*
Accepted: *13 June 2019*
Published: *02 July 2019*

Citation:
Mouro FM, Miranda-Lourenço C, Sebastião AM and Diógenes MJ (2019) From Cannabinoids and Neurosteroids to Statins and the Ketogenic Diet: New Therapeutic Avenues in Rett Syndrome? Front. Neurosci. 13:680. doi: 10.3389/fnins.2019.00680

INTRODUCTION

In 1966, the neuro pediatrician Andreas Rett described and published a report concerning a neurodevelopmental disorder affecting females (Rett, 1966; Percy, 2016). In this report, Dr. Rett described a disease characterized as having an early onset of developmental delay followed by a rapid regression, loss of communication ability and fine motor capabilities, as well as, the occurrence of stereotypic hand movements and periodic breathing during wakefulness (Percy, 2016). Today, this disease is known as Rett syndrome (RTT). RTT is a severe neurodevelopmental X-linked disorder affecting almost exclusively female patients, with prevalence of approximately 1:10000 live births (Segatto et al., 2014) and with a high rate of sporadic mutations (Patankar, 2014). Despite its rareness, RTT is still the second most common cause of severe mental retardation in females (De Felice et al., 2012). The majority of RTT cases are characterized by an archetypal clinical scenario, comprised by loss of acquired cognitive, social, and motor skills, in an usual four-stage

neurologic regression, occurring simultaneously with the development of autistic behavior (Hagberg, 2002; Neul et al., 2010; De Felice et al., 2012; Braat and Kooy, 2015). According to Hagberg, stage I is named "early onset stagnation," occurs 6 months to 1.5 years after birth and is characterized by delays on the developmental progress. Subsequently, stage II, or "developmental regression," occurs from year 1 to 4, being characterized by rapid loss of acquired skills and communication and manifestation of mental deficiency. Stage III is termed "pseudostationary period," being characterized by apparent preserved ambulatory ability and restitution of some communicative abilities, while a slow neuromotor regression occurs. Lastly, stage IV or "later motor deterioration," onsets when the ambulation of stage III ceases and its characterized by complete wheelchair dependence, severe disability, wasting and distal distortion. RTT patients can also experience gastrointestinal problems, hypoplasia, early-onset osteoporosis, bruxism and screaming spells (Hagberg, 2002). Reductions in brain weight and cortical atrophy/microencephaly, resulting in a smaller head circumference, were early reported as a common feature occurring in children diagnosed with RTT (Jellinger et al., 1988). As thoroughly reviewed in Kyle et al. (2018), metabolic complications are also known as a common feature in RTT (Justice et al., 2013; Segatto et al., 2014). Also, as revised in Shulyakova et al. (2017), important anomalies in mitochondrial structure and function (altered electron transport chain complex function, increased oxidative stress and elevated levels of lactate and pyruvate in blood and cerebrospinal fluid) have been demonstrated in RTT. The clinical diagnosis of RTT is performed following a battery of co-existing and well-defined set of inclusion and exclusion criteria, which were recently revised (Neul et al., 2010; Kyle et al., 2018).

In Amir et al. (1999), using a systematic gene screening approach, identified mutations in the gene *MECP2* as cause of some cases of RTT. Today, several mutations in the X-linked *MECP2* gene are identified, being acknowledged as the cause of 95% of the classical RTT cases and of 40–50% of the atypical RTT cases (Neul et al., 2010; Zhang et al., 2017), resulting in a wide genetic and phenotypic heterogeneity of this disease (De Felice et al., 2012). *MECP2* is a globally expressed pleiotropic factor, assuming a key role in maintaining homeostasis in different cells and systems (Shulyakova et al., 2017). As expected for a neurological condition (Neul and Zoghbi, 2004), in RTT the higher levels of *MECP2* in the body are expressed in the brain (Shahbazian, 2002). Confirming the importance of *MECP2* presence in the brain, the selective elimination of this gene from neurons (Guy et al., 2007) and oligodendrocytes (Nguyen et al., 2012) triggers RTT-like phenotype in mice (Shulyakova et al., 2017). In atypical RTT variants, mutations in other loci rather than the *MECP2* have been identified (Neul et al., 2010).

A diversity of distinctive variant forms of RTT has been proposed, each of which presents different clinical features. Some of these variants have been identified and described in relatively small populations, which leads to difficulties in the definition of clear clinical characteristics (Neul et al., 2010). Nevertheless, according to Neul et al. (2010), there are three distinctive variants of RTT that have been amply identified and that are well characterized: (1) the preserved speech variant (Zappella, 1992), (2) the congenital variant (Rolando, 1985), and (3) the early seizure variant (Hanefeld, 1985). From these three atypical forms of RTT, the preserved speech variant, or Zappella variant, is the most common one. This variant has clearly defined clinical features and mutations on the *MECP2* gene are identified in most of the diagnosed cases (Zappella, 1992; Renieri et al., 2009; Neul et al., 2010). On the contrary, in diagnosed cases belonging to the congenital and early seizure variants, mutations in the *MECP2* gene are rarely found, while mutations in different genes are reported (Huppke et al., 2000; Archer et al., 2006; Neul et al., 2010; De Felice et al., 2012). Namely, mutations in the *CDKL5* gene have been described in both males and females diagnosed with early-seizure-onset RTT variant (Mari et al., 2005; Scala et al., 2005; Zhao et al., 2014; Zhang et al., 2017). On the other hand, mutations in the FOXG1 gene have been identified in the congenital RTT variant (Zhang et al., 2017), first described by Rolando (1985). The congenital variant of RTT is clinically characterized by hypotonia and developmental delay occurring earlier than in classical RTT variant (Rolando, 1985; Jacob et al., 2009). Importantly, the majority of children diagnosed with the congenital variant of RTT do not present mutations in the *MECP2* or *CDKL5* mutations (Jacob et al., 2009).

The available treatment for RTT is mainly symptomatic. With appropriate social and familiar care, attention to orthopedic complications, physiotherapy to treat and ease muscle rigidity, control of epileptic episodes, and a balanced and healthy nutrition, women with RTT can survive until middle age and older age (Kyle et al., 2018). There is a sudden death rate of 26% in RTT and patients mainly perish due to cardiac complications, respiratory infection and respiratory failure (Kyle et al., 2018). Most of the preclinical and clinical studies in RTT aims at finding ways to prevent or control epileptic episodes, due to the importance that it has for the outcome of RTT prognosis

Abbreviations: 24S-OHC, oxysterol 24(S)-hydroxycholesterol; 3xTg-AD, triple-transgenic mouse model of AD; 3α-HSD, 3α-hydroxysteroid dehydrogenase; 3β-HSD, 3β-hydroxysteroid dehydrogenase; A_1R, adenosine A_1 receptor; $A_{2A}R$, adenosine A_{2A} receptor; AED, anti-epileptic drugs; ALLO, allopregnanolone; ATP, adenosine triphosphate; BBB, blood brain barrier; BDNF, brain-derived neurotrophic factor; BHB, β-hydroxybutyrate; BZD, benzodiazepines; CA1, cornu ammonis 1; cAMP, cyclic adenosine monophosphate; CB_1R, cannabinoid receptor 1; CB_2R, cannabinoid receptor 2; CBC, cannabichromene; CBD, cannabidiol; CBDV, cannabidivarin; CBG, cannabigerol; CBN, cannabinol; CBV, cannabivarin; CDKL5, cyclin-dependent kinase-like 5; CGIC, seven-category caregiver global impression of change questionnaire; CNS, central nervous system; CYP11A1, cytochrome P450 cholesterol side-chain cleavage (P450scc) enzyme; Cyp46a1, cholesterol 24-hydroxylase; ECBS, endocannabinoid system; FDA, United States Food and Drug Administration; FOXG1, forkhead box protein G1; GABA, gamma-aminobutyric acid; $GABA_AR$, $GABA_A$ receptor; $GABA_BR$, $GABA_B$ receptor; GABR, $GABA_A$ receptor subunit; GLU, glutamate; GPR55, G-protein coupled receptor 55; HDL, high density lipoprotein; HMG-CoA, 3-hydroxy-3-methylglutaryl-coA; HMG-CoA-R, 3-hydroxy-3-methylglutaryl-coA reductase; IPSCs, post-synaptic inhibitory potentials; KD, ketogenic diet; LDL, low density lipoprotein; LPI, l-α-lysophosphatidylinositol; MCT, medium chain triglycerides; *MECP2*, methyl-CpG-binding protein 2; PKA, protein kinase A; RISE-SRS, reduced intensity status epilepticus–spontaneous recurrent seizures; RTT, Rett syndrome; SLOS, Smith–Lemli–Opitz syndrome; Sqle, squalene monooxygenase; SRB1, scavenger protein B1; STA, statins; StAR, steroidogenic acute regulatory protein; Tg, transgenic; THCV, Δ^9-tetrahydrocannabivarin; THIP, $GABA_AR$ agonist gaboxadol; TLE, model of temporal lobe epilepsy; $TRPV_1$, transient receptor potential cation channel subfamily V member 1; Δ^8-THC, Δ^8-tetrahydrocannabinol; Δ^9-THC, Δ^9-tetrahydrocannabino.

(Krajnc, 2015; Clarke and Abdala Sheikh, 2018). Therefore, preclinical research in RTT is majorly focused on finding ways of correcting detrimental modifications in neurotransmission occurring in this disease, using *Mecp2*-null mouse models (Clarke and Abdala Sheikh, 2018). Recently, however, a paradigm shift has been proposed. Through gene therapy it was proven that it is possible to reverse RTT symptoms in diseased adult mice by re-activating *Mecp2* expression (Guy et al., 2007). Also, a few years later, it was shown that switching-off the production of Mecp2 protein in adult mice leads to the development of symptoms equivalent to those of mice born with the mutation (McGraw et al., 2011; Clarke and Abdala Sheikh, 2018). Considering that, by rule, neurodevelopmental disorders tend to be non-reversible, such results were received with considerable enthusiasm (Clarke and Abdala Sheikh, 2018). Thus, these studies showed that gene therapy would have to necessarily deliver a working *MECP2* gene throughout the patient life (it would not be sufficient to do it just on child development) and that treatment could be administered regardless of disease stage and/or age (Clarke and Abdala Sheikh, 2018). Although exciting, the above-mentioned discoveries have to be taken carefully. Indeed, in order to work, *MECP2* gene therapy would have to deliver the precise amount of MECP2 protein in each cell of the body, as too much or too few MECP2 protein can trigger RTT-like symptoms (Clarke and Abdala Sheikh, 2018). As a particularly harsh example, in *MECP2* duplication syndrome, an overproduction of MECP2 protein leads to mental disability and autistic-like behavior (Moretti and Zoghbi, 2006; Ramocki et al., 2009). Moreover, even small deviations from the necessary MECP2 protein levels are related with modifications in brain function, which can lead to cognitive and mental disability (Chao and Zoghbi, 2012). Therefore, as mentioned in Clarke and Abdala Sheikh (2018), gene therapy in RTT delivers two major challenges: (1) it potentially means that it would be necessary to deliver the exact right amount of *MECP2* to every cell and (2) in females, it would be necessary to avoid delivering additional copies of the gene to the cells that already express a healthy copy; two pitfalls that are extremely difficult to overcome with the available technology.

At this point, although possible, finding a cure for RTT is a distant reality. In the meanwhile, it is more important than ever to find new treatments to alleviate symptoms, reduce pain and discomfort and increase the quality of life of both the patient and the caregiver. Therefore, in this review we will turn our attention to new discoveries which show potential in RTT preclinical investigation.

DYSFUNCTIONAL GABAR SIGNALING IN RTT: IMPLICATIONS FOR SYMPTOMATOLOGY

Rett syndrome is characterized by structural and molecular deficiencies in synaptic transmission. Evidence displays important modifications in basal transmission, in short and long-term plasticity processes and in neurotransmitter release (Boggio et al., 2010). Studies using different *Mecp2* genetic mutated mice have made it possible to understand that individual phenotypic characteristics of RTT can be associated with dysfunctions in very specific neuronal populations. Indeed, the selective deletion of the *Mecp2* gene from different neuronal populations, in different ages and in distinctive brain regions accounts for specific phenotypical traits of the disease. Thus, such data has led authors to claim that the phenotypical consequences of *Mecp2* deletion are time and region-dependent (Chao et al., 2010). In this regard, dysfunctional GABAergic signaling constitutes a vital element in RTT symptomatology.

The GABAergic signaling system comprises a key pathway commonly disturbed in neurodevelopmental diseases, such as RTT, fragile X syndrome, Dravet Syndrome, neurofibromatosis type I, Tourette syndrome, Down Syndrome and in Autism Spectrum Disorders (Lee and Tierney, 2011; El-Ansary and Al-Ayadhi, 2014; Braat and Kooy, 2015; Kim and Yoon, 2017). GABA is the main inhibitory neurotransmitter in the brain, exerting its actions via the activation of two subtypes of GABA receptors, the ionotropic $GABA_AR$ and the metabotropic $GABA_BR$ (Chebib and Johnston, 1999; Rombo et al., 2016). $GABA_AR$ are ligand-gated receptors responsible for mediating the majority of inhibitory synaptic transmission in the CNS (Reddy, 2010). Structurally, $GABA_AR$ are heteropentamers with five protein subunits that form the chloride ion channel (Reddy, 2010). $GABA_AR$ can be assembled by seven different classes of subunits, some of which comprised by different homologous variants (α_{1-6}, β_{1-3}, γ_{1-3}, σ_{1-3}, δ, θ, ε). Usually, most $GABA_AR$ are composed by α, β, and γ or δ-subunits (Sieghart, 2006). The binding site for the endogenous modulator GABA is located in the cleft between the α and β subunits. Apart from the GABA binding site, there are several other binding sites in the $GABA_AR$ which constitute targets for benzodiazepines and barbiturates (Smith, 2002). Furthermore, each pharmacological effect appears to be directly related with a specific binding site on the receptor surface, which depends on the subunit composition of the receptor (Cai et al., 2018). Post-synaptic $GABA_AR$ are ubiquitously distributed, being responsible for generating the phasic currents in response to presynaptic GABA release. On the other hand, extrasynaptic $GABA_AR$ are preferentially activated when GABA levels are low, being highly sensitive to extracellular GABA concentrations and responsible for generating non-desensitizing tonic inhibition (Wang, 2011; Cai et al., 2018). Despite being exclusively present in a minority of neurons, several clusters of GABAergic interneurons are responsible for regulating and controlling the majority of excitatory neurons. Thus, if an imbalance in the inhibitory system occurs, the following excessive excitatory output leads to disturbances on the excitation/inhibition balance, ultimately resulting in dysfunction of cognitive processes (Braat and Kooy, 2015). Importantly, genetic alterations in GABAergic signaling system has been shown to be involved in several neurodevelopmental diseases (for a detailed review see Braat and Kooy, 2015).

Evidence regarding dysfunctional GABAergic signaling in RTT has been mainly obtained in studies using RTT-mouse models. Such studies have been gathering substantial evidence confirming the critical involvement of GABAergic transmission in RTT symptomatology, highlighting the clinical relevance of

this signaling system. Indeed, an incorrect balance between excitation and inhibition reflecting a dysfunction in GABAergic and glutamatergic signaling systems have been described in *Mecp2*-knockout mice (Dani et al., 2005; Chao et al., 2007; Dani and Nelson, 2009; Calfa et al., 2011). Also, as mentioned before regarding other neuromodulatory systems, the relationship between RTT phenotypical expression and GABAergic signaling is region, time and neuronal population dependent (El-Khoury et al., 2014). Confirming the critical involvement of the GABAergic system in RTT symptomatology, it has been shown that mice with *Mecp2*-deficiency exclusively in GABAergic neurons rapidly develop forepaw stereotyped movements, compulsive grooming, learning and memory deficits, abnormal social behavior, electroencephalography hyperexcitability, lack of motor coordination, severe respiratory dysrhythmias and premature lethality. Additionally, the results of this work also showed that the selective deletion of the *Mecp2* gene in a specific subset of forebrain GABAergic neurons was sufficient to trigger many of the aforementioned symptoms. Thus, these data strongly suggests that the loss of *Mecp2* in GABAergic neurons acts as a pivotal mediator for some characteristic RTT phenotypes (Chao et al., 2010).

The critical relevance of *MECP2* in GABAergic signaling was also shown in other brain regions, such as the hippocampus. Indeed, patch-clamp recordings performed in hippocampal slices obtained from *Mecp2* mutant mice, revealed that hippocampal circuits in CA3 neurons display diminished basal inhibitory rhythmic activity, which, consequently, leaves the circuitry susceptible to hyperexcitability (Zhang et al., 2008). Likewise, in the brain stem, an imbalance between inhibitory and excitatory transmission was reported to occur early at postnatal day 7 in *Mecp2* mutant mice. Additionally, GABAergic transmission was found to be significantly depressed in the same animals, which may be related with deficient presynaptic GABA release and diminished expression levels of subunits α2 and α4 on the post-synaptic $GABA_AR$ (Medrihan et al., 2008). In the thalamus, *Mecp2* differentially regulates the development of GABAergic synapses in excitatory or inhibitory neurons (Zhang Z.W. et al., 2010). Also, in *Mecp2* mutant mice, electrophysiological deficiencies have been reported in norepinephrinergic neurons of the locus coeruleus which receive $GABA_A$ergic inhibitory inputs (Jin et al., 2013a; Zhang X. et al., 2010). In the locus coeruleus, *Mecp2* deficiency leads to simultaneous abnormalities in the pre- and post-synaptic GABAergic component, impairing $GABA_A$ergic and $GABA_B$ergic post-synaptic inhibitory currents and reducing the presynaptic release of GABA (Jin et al., 2013a). Indeed, it has been described that *Mecp2* deficiency abnormally increases extrasynaptic $GABA_AR$ activity, an effect suggested to occur as a compensatory response to the deficient GABA-mediate synaptic inhibition (Zhong et al., 2015).

The above-mentioned evidence highlights the critical role of *MECP2* gene for correct GABAergic signaling in different brain regions. Besides brain region and synaptic location of the receptor, in a recent study it was also shown that selective deletion of *Mecp2* from either parvalbumin-positive neurons or somatostatin-positive neurons leads to different phenotypical outcomes, that together comprise almost the full range of RTT-like phenotypes. Specifically, *Mecp2* deletion from parvalbumin-positive neurons leads to motor, sensory, cognitive and social deficits, while ablation of *Mecp2* from somatostatin-positive neurons originated stereotyped behavior and seizures (Ito-Ishida et al., 2015). Recently, reductions in GABAergic transmission in the nucleus tractus solitarius, a key brain region involved in the integration of respiratory sensory information, were reported (Chen et al., 2018).

Although scarce, there is available data collected from human samples supporting findings in rodent models of RTT (Braat and Kooy, 2015). $GABA_AR$ binding was found to be significantly altered in the basal ganglia (Blue et al., 1999) and in the frontotemporal cortex (Yamashita et al., 1998) in RTT patients. Additionally, a disturbed process of GABAergic neuronal maturation was described in the cerebrospinal fluid of RTT patients (Duarte et al., 2013) (for a more details see Braat and Kooy, 2015). Also, an analysis performed in *post-mortem* human brains, has shown defects in the expression of the GABR gene GABRB3, contained in the human chromosome 15q11-13, in RTT patients (Samaco et al., 2005). Congruently, subsequent evidence obtained with mice models, suggested that *Mecp2* gene is vital for the correct expression of both alleles of GABRB3 in neurons (Hogart et al., 2007).

Considering the anomalies observed in GABAergic signaling in RTT and their crucial role in symptomatology and disease progression, correction of these modifications has been proposed as a therapeutic strategy. Indeed, adjustment of the GABAergic system activity in *Mecp2* mutant mice leads to improvements in several phenotypical features (Braat and Kooy, 2015). In accordance, in a recent study, it was found that an *in vivo* treatment with the inhibitor of GABA reuptake, Tiagabine, significantly increased the life-spam of *Mecp2* knockout mice, although it did not ameliorate motor deficits (El-Khoury et al., 2014). In another study, the benzodiazepine Midazolam transiently abolished breathing abnormalities in *Mecp2* mutant mice (Voituron and Hilaire, 2011). Also, the enhancement of $GABA_AR$-mediated signaling, either through blockade of GABA reuptake or through positive allosteric modulation of the $GABA_AR$, resulted in a significant reduction on respiratory problems (Abdala et al., 2010). Recently, respiratory dysrhythmia has been related with deficient GABAergic signaling in the Kölliker-Fuse area, or subparabrachial nucleus, a brain area responsible for the regulation of breathing rate. Congruently, boosting GABA transmission reduced respiratory arrhythmia in a RTT-mouse model (Abdala et al., 2016). Also, early exposure to the extrasynaptic $GABA_AR$ agonist THIP was shown to regulate neuron hyperexcitability on the locus coeruleus, known to be involved in the regulation of breathing (Zhong et al., 2017). Finally, genetic re-expression of *Mecp2* only in GABAergic neurons of male and female *Mecp2* null mice enhanced inhibitory signaling. Also, it extended animal lifespan, mitigated ataxia, apraxia, and social withdrawal, displaying that the restoration of *Mecp2* expression in GABAergic neurons significantly improves the symptomatology of RTT (Ure et al., 2016; **Figure 1**).

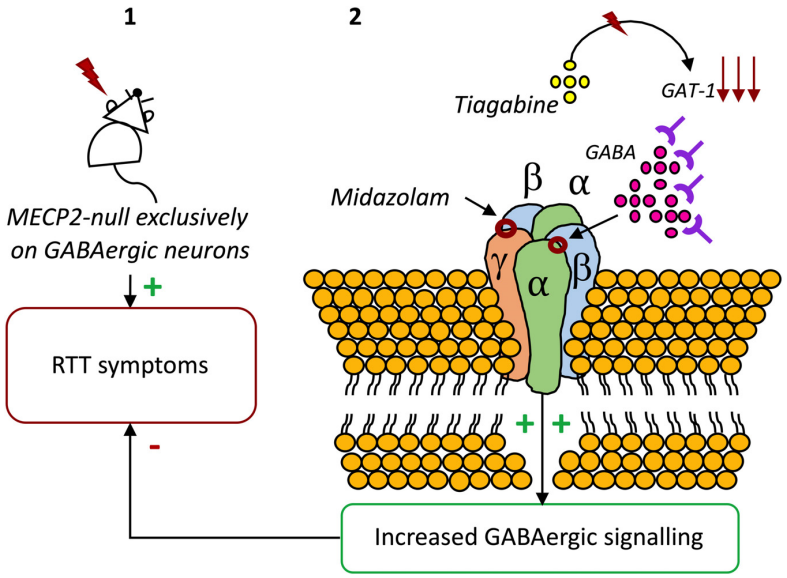

FIGURE 1 | The potential of $GABA_AR$ modulators on RTT. **(1)** Exclusive deletion of *Mecp2* from GABAergic neurons results in almost the full range of neuropsychiatric symptoms of RTT (Chao et al., 2010). **(2)** Blocking GABA reuptake using tiagabine (El-Khoury et al., 2014) or enhancing $GABA_AR$ activity with the benzodiazepine Midazolam increases the life-spam and reduces symptoms in *Mecp2* mutant mice (Voituron and Hilaire, 2011).

Taken together, these results emphasize the crucial role of *MECP2* in GABAergic neurons. Also, they demonstrate a clear relationship between modifications in GABAergic signaling and symptomatology in RTT, highlining the potential of drug agents which correct these modifications to improve RTT symptoms. Therefore, on the following sections we will focus our attention on new findings that, directly or indirectly, involve the modulation of GABAergic signaling in RTT (**Figure 2**).

RTT, A BRAIN DISEASE WITH A METABOLIC BLUEPRINT

Cholesterol and Neurosteroids in Rett Syndrome

Rett syndrome was initially considered to be a metabolic disease (Justice et al., 2013). Indeed, originally, Dr. Rett, convinced of being in the presence of a disease with a clear metabolic component, named it "cerebroatrophic hyperammonaemia" (Kyle et al., 2018). Hyperammonemia is a clinical condition characterized by increased ammonia levels, which manifests itself in a variety of symptoms and signs, including significant CNS abnormalities (Auron and Brophy, 2012). The fact that hyperammonaemia has been detected only in a minority of RTT patients led to the abandonment of the hypothesis of cerebroatrophic hyperammonaemia as the central cause for RTT (Campos-Castelló et al., 1988; Justice et al., 2013). Recently, however, the metabolic components of RTT and its importance for disease progression have been brought again into light.

Cholesterol is a vital component of the cellular membrane structure and a precursor for numerous signaling molecules (Nagy and Ackerman, 2013). Cholesterol does not cross the BBB and therefore brain cholesterol has to be generated locally, which directly contrasts with other organs that are able of acquiring it from circulating lipoproteins (Pfrieger and Ungerer, 2011). In the brain, the production of cholesterol is a highly compartmentalized process presenting a very delicate balance. Its production takes place in the endoplasmic reticulum and requires, as an energy source, the correct functioning of the mitochondria (Justice et al., 2013). Importantly, mitochondrial function and structure is compromised in both RTT patients and *Mecp2* mutant mouse models (Shulyakova et al., 2017). After synthesis, brain cholesterol must be quickly renewed and turned-over, as it can be rapidly oxidized by reactive oxygen species (ROS), known to accumulate whenever mitochondria dysfunction occurs (Justice et al., 2013). To maintain homeostasis, cholesterol must be converted into the 24S-OHC by the neuron-specific enzyme Cyp46a1 (Lund et al., 2003; Kyle et al., 2018). Thus, a tight regulation of cholesterol homeostasis in the brain assumes particular importance: too much or too little cholesterol is detrimental, negatively impacting on cognitive processes, memory and motor skills (Kyle et al., 2018). Concordantly, a vast number of neurological diseases present abnormal lipid synthesis, storage and recycling (Waterham, 2006), namely, SLOS and Niemann–Pick type C disease, Alzheimer's, Parkinson's, and Huntington's diseases, Amyotrophic lateral sclerosis, Fragile X syndrome, and, as recently discovered, RTT (Justice et al., 2013).

Using *Mecp2* mutant mice, a mutagenesis screening to identify genes that influence RTT-linked phenotypes was performed (Buchovecky et al., 2013; Nagy and Ackerman, 2013). To do so, descendent of *MECP2* mice were screened for limp gasping, tremors and activity, and mice that displayed reduced

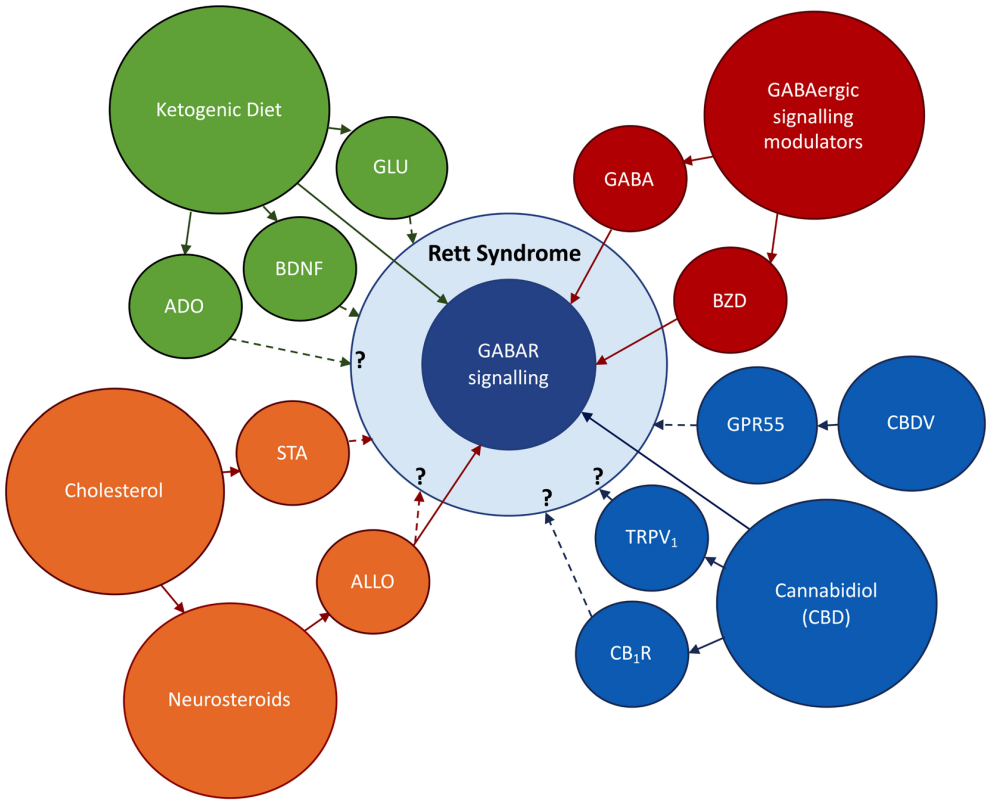

FIGURE 2 | Research topics to be addressed in this review. **In red:** the use of direct and indirect modulators of GABAergic signaling, respectively, benzodiazepines (BZD) and GABA enhancers. **In orange:** Abnormal cholesterol metabolism occurring in RTT, the use of statins (STA) to improve RTT symptoms; the impact of deficits on cholesterol uptake on neurosteroidogenesis; the possible therapeutic actions of the neurosteroid allopregnanolone (ALLO). **In blue:** the use of derivatives of the cannabis plant to ameliorate RTT symptoms; cannabidiol (CBD) has shown promising anti-epileptic effects via GABA-dependent mechanisms; the effects of CBD on CB_1R and $TRPV_1$ and its impact on RTT symptoms are still undisclosed; Cannabidivarin (CBDV) has been identified as a promising therapeutic drug in an RTT-mice model. **In green:** Ketogenic Diet (KD) has potent anticonvulsive actions via GABAergic and glutamatergic (GLU) signaling systems; the KD can also improve RTT symptoms via BDNF-mediated effects or through increases in adenosine production. BNDF signaling is known to be impaired in RTT (Li and Pozzo-Miller, 2014), while unpublished data obtained in our lab points to deregulations in adenosinergic signaling. Direct arrows denote direct interaction with GABAergic signaling system, while doted arrows denote known or undisclosed involvement on RTT pathophysiology.

phenotypic features were bred to establish the hereditability of putative suppressor genes (Buchovecky et al., 2013). This screening highlighted that a mutation in the *Sqle* gene, encoding squalene epoxidase, which is a rate-limiting enzyme in cholesterol biosynthesis, was sufficient to restore function and longevity in *Mecp2* mutant mice. The authors also showed that cholesterol metabolism is perturbed in brains and livers of *Mecp2* mutant male mice, revealing profound and complex dysregulations in cholesterol metabolism. Furthermore, HMG-CoA reductase inhibitors, or statins, were able to ameliorate the systemic imbalance of lipid profile, alleviate motor symptoms and increase longevity in *Mecp2* mutant mice (Buchovecky et al., 2013). Studies with samples collected from human RTT patients have also shown modifications in lipid profile. Directly comparing with age-matched healthy donors, imbalances in both high (HDL) and low (LDL) density lipoprotein levels were found in RTT patients. Accompanying these abnormalities in plasma lipid profile, a marked reduction in SRB1 was detected. SRB1 is ubiquitously expressed, playing vital roles in cellular lipid uptake, mediating, for instance, the uptake of HDL-derived cholesterol in the liver (Sticozzi et al., 2013). Congruently, using freshly isolated human fibroblasts, it has been shown that total cholesterol and LDL levels are significantly increased in RTT patients, while SRB1 expression was quantified has being 70% lower in RTT patients compared with healthy controls (Segatto et al., 2014). On the other hand, and in accordance with data from Buchovecky et al. (2013), cholesterol synthesis was found to be reduced in RTT fibroblasts (Segatto et al., 2014). Therefore, these data provided strong evidence toward the importance of cholesterol homeostasis in RTT. Also, imbalances in cholesterol metabolism can affect the synthesis of steroid hormones, among which neurosteroids can have an important role in several brain diseases, as it will be approached in the following section.

Neurosteroids: The Way Is Through the $GABA_AR$

Neurosteroids were described, for the first time, has having anesthetic and anticonvulsive actions in the late 1940s (Selye, 1941; Selye and Masson, 1942; Clarke, 1973; Reddy and

Estes, 2016). Almost half a century later, alphaxolone, a synthetic neurosteroid, was found to increase synaptic inhibition through $GABA_AR$ activation (Harrison and Simmonds, 1984), which constituted a major advanced in neurosteroid research (Majewska et al., 1986).

Neuroactive steroids are steroid molecules synthesized in the brain that modulate neuronal excitability by rapid non-genomic actions (Reddy, 2010). Cholesterol constitutes the raw material for the biosynthesis of all steroid hormones (Hu et al., 2010). *De novo* synthesis of neurosteroids is a sequential and highly compartmentalized process involving, as first step, the translocation of cholesterol from the cytoplasm to the inner mitochondrial membrane. Once inside the mitochondria, cholesterol is converted into pregnenolone, the precursor of all steroid hormones (Reddy, 2010; Melcangi et al., 2014). Pregnenolone is then transformed into progesterone by the action of the enzyme 3β-HSD (Melcangi et al., 2008). The conversion of cholesterol to pregnenolone in the mitochondria is, consequently, the first rate-limiting step in the biosynthesis of all steroid hormones (Stoffel-Wagner, 2003). ALLO is derived from progesterone by 5α-reductase and 3α-HSD (Liu and Wong-Riley, 2010), and is viewed as the most potent endogenous modulator of the GABAergic system via interaction with the $GABA_AR$ (Hosie et al., 2006; Reddy, 2010; **Figure 3**).

Recent studies indicate that neurosteroids have anxiolytic, antidepressant and antipsychotic properties. Furthermore, neurosteroids stimulate neurogenesis, facilitate regeneration of neurons after injury, promote myelinization, and improve cognition (Reddy and Estes, 2016; Cai et al., 2018). The development of new analogous neurosteroid agents with promising therapeutic properties has resulted in four compounds tested in clinical trials for epilepsy, traumatic brain injury, status epilepticus and Fragile X syndrome. Also, several synthetic neurosteroids have been prepared for therapeutic use in the past decades, among which, the best-known are, the aforementioned alphaxolone, and also alphadolone, minaxolone, and ganaxolone (Reddy and Estes, 2016).

Neurosteroids have been implicated in the behavioral profile of some neurologic diseases. In SLOS, an autosomal recessive disorder which develops due to an inborn error in cholesterol metabolism (Tint et al., 1994; Aneja and Tierney, 2008; Lee and Tierney, 2011), impaired neurosteroid synthesis or the synthesis of an inhibitory analog form of neurosteroids on the brain have been proposed to occur (Porter, 2002). Congruently, urinary analysis has allowed the identification of neurosteroid-like compounds in SLOS patients, being foreseeable that this abnormal synthesis also occurs in the brain (Marcos et al., 2004; Lee and Tierney, 2011). In Fragile X syndrome, patients show autism-like phenotypes characterized by cognitive impairment, anxiety, mood swings and behavioral and learning difficulties (Reddy and Estes, 2016). A clinical trial using ganaxolone was found to be safe but produced no significant effects on the outcome measures in the overall population of the study. However, specific subsets of the children with Fragile X syndrome enrolled on the clinical trial, particularly the ones with higher anxiety, lower cognitive abilities and who have frequent seizure episodes, might benefit from treatment with this neurosteroid (Ligsay et al., 2017).

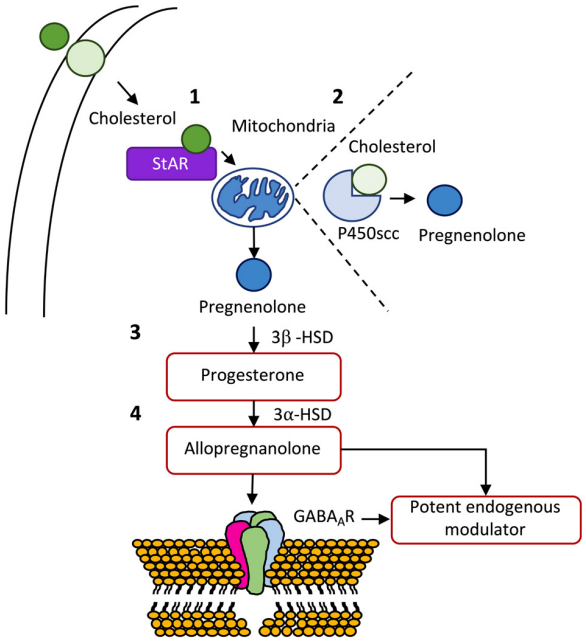

FIGURE 3 | *De novo* synthesis of some important neurosteroids. **(1)** After being transported from the outer to the inner membrane, cholesterol is transported from the outer to the inner membrane of the mitochondria by steroidogenic acute regulatory protein (StAR). **(2)** Once inside the mitochondria, cholesterol is transformed in pregnenolone, the mother of all steroid hormones, by cytochrome P450 cholesterol side-chain cleavage (P450scc) enzyme (CYP11A1). **(3)** Pregnenolone can be, subsequently, transformed into progesterone by 3β-hydroxysteroid dehydrogenase (3β-HSD), which in turn, can originate allopregnanolone through the action of 3α-hydroxysteroid dehydrogenase (3α-HSD). **(4)** Allopregnanolone is viewed as the most potent endogenous modulator of the GABAergic system via interaction with the $GABA_A$ receptor (for a detailed review see Melcangi et al., 2014).

Recently, it has been described that ALLO (Meletti et al., 2017) and progesterone (Meletti et al., 2018) are decreased in cerebrospinal fluid (CSF) of patients affected by status epilepticus. Progesterone levels were found to be 64% lower than in healthy controls (Meletti et al., 2018). Interestingly, neurosteroids are also being proposed for the treatment of schizophrenia, as neurosteroids show promising anti-psychotic potential (Cai et al., 2018).

The therapeutic potential of neurosteroids is mainly related with their ability to rapidly modulate the activity of the GABAergic neurons, known to be involved in the pathophysiology of several psychiatric disorders (Mellédo and Baker, 2002; Dubrovsky, 2005; Marx et al., 2006) and neurodegenerative diseases (Carunchio et al., 2008; Li et al., 2016; Kim and Yoon, 2017; Lozovaya et al., 2018), and commonly disturbed in neurodevelopmental diseases (see section "Dysfunctional GABAR Signalling in RTT: Implications for Symptomatology"). The modulatory effects of neurosteroids on $GABA_AR$ are unique and extremely complex, depending on

several factors, such as, the subunit composition of the receptor, the receptor localization, concentration and the structure of the neurosteroid (Sieghart, 2006; Reddy, 2010; Reddy and Jian, 2010; Wang, 2011; Reddy and Estes, 2016; Cai et al., 2018). Previous studies have shown that specific combinations of subunits in the $GABA_AR$ confer more or less affinity for neurosteroids, but that ALLO enhances $GABA_A$ergic transmission whenever the $GABA_AR$ are composed by any α subunit (Puia et al., 1993, 2003; Maitra and Reynolds, 1999; Belelli et al., 2002). Importantly, both post-synaptic $GABA_AR$ and extrasynaptic $GABA_AR$ are highly sensible to neurosteroid modulation. In particular, extrasynaptic $GABA_AR$ containing the δ subunit located in specific brain regions as the hypothalamus, hippocampal dentate gyrus and cerebellum, are highly sensitive to neurosteroids, which may open a therapeutic window for the use of neurosteroids in several brain diseases, including RTT (Smith, 2002; Reddy and Estes, 2016). Indeed, neurosteroids have been proposed as a viable alternative to overcome benzodiazepine tolerance, as they can bind and enhance the activity of all $GABA_AR$ isoforms, including extrasynaptic $GABA_AR$ containing the highly neurosteroid sensitive δ subunit (Brown et al., 2002; Uusi-Oukari and Korpi, 2010; Meera et al., 2011; Rogawski et al., 2013; Carver and Reddy, 2016).

Also, unlike benzodiazepines, neurosteroids are able of modulating the activity of $GABA_AR$ that lack the mandatory γ subunit, which confers benzodiazepine sensitivity to the $GABA_AR$ (Bianchi and Macdonald, 2003). In this regard, neurosteroids have been tested in super refractory status epilepticus with mixed-results (Broomall et al., 2014; Rosenthal et al., 2017; Vaitkevicius et al., 2017). Analogs of ALLO were found to be protective against partial seizures induced by electrical stimulation in animals (Kaminski et al., 2004; **Figure 4**).

The role of ALLO as a neuroprotective agent starts before birth. Indeed, ALLO levels fluctuate during perinatal periods (Bernardi et al., 1998; Concas et al., 1998; Genazzani et al., 1998; Grobin and Morrow, 2001; Jin et al., 2013b) and its actions are known to contribute to neuroprotection of the fetal brain (Liu and Wong-Riley, 2010). In rats, ALLO levels drop immediately after birth, keeping a steady decline until a temporary elevation at 10 to 14 days postnatal, then decrease to a steady low level 3 weeks after birth (Grobin and Morrow, 2001). The drop in ALLO levels seems to coincide with drastic reductions in progesterone levels immediately after birth (Paoletti et al., 2006). Relevantly, in *MECP2* mutant mice, the reductions in ALLO levels coincide with the onset of RTT symptoms in such animals (Jin et al., 2013b).

There are very few examples of the use of neurosteroids in RTT available on literature. Jin et al. (2013b), using an optogenetic approach to directly stimulate $GABA_AR$ in the locus coeruleus, found that ALLO increases the amplitude, frequency and decay time of $GABA_A$ergic inhibitory post-synaptic currents (IPSCs). In this study, the authors described a time-dependent modulation of $GABA_A$ergic transmission by ALLO in *Mecp2* mutant mice. Like in wild-type mice, during the first 2 weeks of the postnatal period, ALLO increases $GABA_A$ergic inhibitory post-synaptic potentials and suppresses neuronal excitability in locus coeruleus neurons of *Mecp2* mutant mice. However, such effect abruptly deteriorates at 3 weeks of age in *Mecp2* deficient mice, which coincides with the onset of RTT symptoms. Therefore, the authors hypothesize that, in *MECP2* mutant mice, declines in progesterone levels after birth may lead to decreases in ALLO biosynthesis which in turn, becomes insufficient to potentiate $GABA_A$ergic transmission through the $GABA_AR$ (Jin et al., 2013b). There is, also, the possibility that the subunit composition of the $GABA_AR$ shifts during development (Rissman and Mobley, 2011; Datta et al., 2015) or in pathophysiological conditions (Drexel et al., 2013; Govindpani et al., 2017; Kwakowsky et al., 2018) and also that it varies accordingly to temporal and local constrains (Walton et al., 2017). Thus, these modifications in $GABA_AR$ composition may change the receptor sensibility to neurosteroids in *Mecp2* mutant mice (Jin et al., 2013b) (see **Figure 5**). Also, $GABA_AR$ sensitivity toward ALLO can shift due to neurosteroid withdrawal (Gulinello et al., 2001; Mascia et al., 2002; Boggio et al., 2010), long-term steroid administration

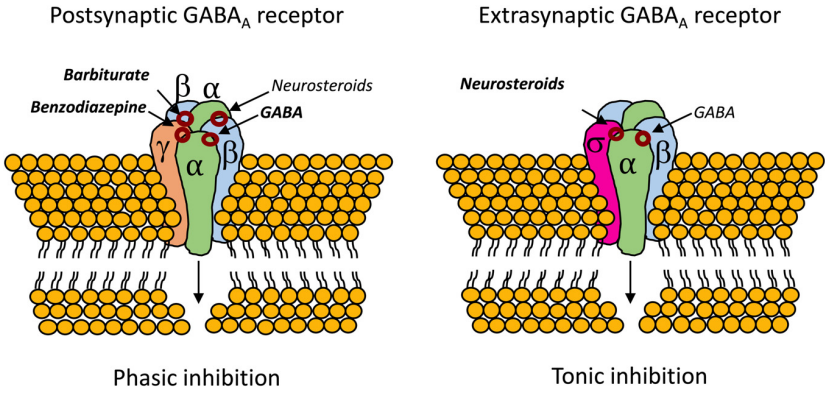

FIGURE 4 | Binding sites for neurosteroids on the postsynaptic and extrasynaptic $GABA_AR$ (Reddy, 2011; Cai et al., 2018). Contrary to benzodiazepines, which require the mandatory γ subunit, neurosteroids can act on $GABA_AR$ whenever they are composed by α subunits (Bianchi and Macdonald, 2003). The extrasynaptic $GABA_AR$ usually contains the highly neurosteroid sensitive δ subunit, which opens an exploitable therapeutic window, especially in cases of benzodiazepine tolerance (Brown et al., 2002; Uusi-Oukari and Korpi, 2010; Meera et al., 2011; Rogawski et al., 2013; Carver and Reddy, 2016).

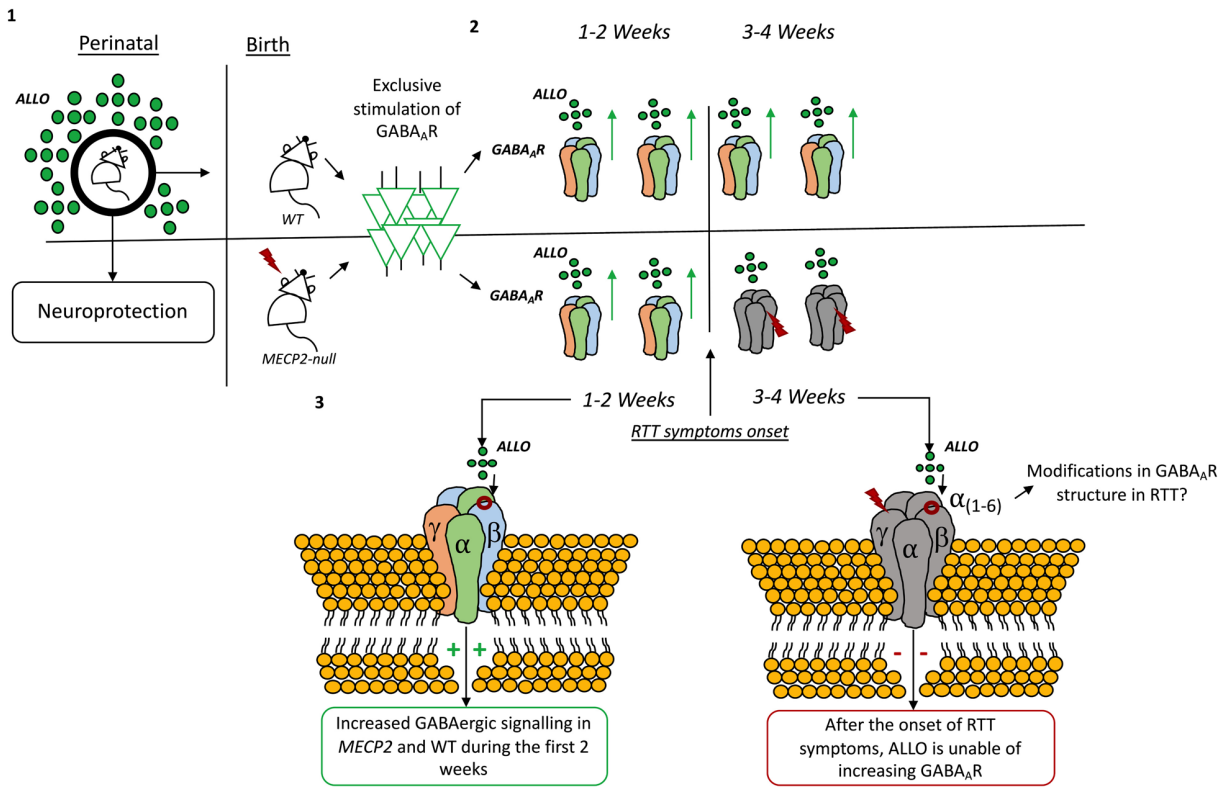

FIGURE 5 | Time-dependent modulation by allopregnanolone on GABA$_A$R signaling. **(1)** Allopregnanolone actions are known to contribute to neuroprotection of the fetal brain (Liu and Wong-Riley, 2010). In rats, allopregnanolone levels change immediately after birth and during the first weeks of life (Grobin and Morrow, 2001). **(2)** By exclusively stimulating the GABA$_A$-ergic neurons in the locus coeruleus it was found that allopregnanolone increases the amplitude, frequency and decay time of GABA$_A$R inhibitory post-synaptic currents (IPSCs) both in wild-type and *Mecp2* mutant animals. **(3)** However, after the first 2 weeks, allopregnanolone effects are lost in *Mecp2*-null animals, coinciding with the onset of RTT symptoms in such animals (Jin et al., 2013b). The drop in allopregnanolone levels seems to coincide with drastic reductions in progesterone levels immediately after birth (Paoletti et al., 2006). Modifications in the composition of the GABA$_A$R can also be responsible for the effect (Jin et al., 2013b).

(Follesa et al., 2002) and age (Shen et al., 2007), amongst other factors [reviewed in Mellon (2007)]. Other studies have shown that ALLO stimulates GABA$_A$ergic currents in the hippocampus (Park et al., 2011), cerebellum (Cooper et al., 1999), and neocortex (Puia et al., 2003).

Evidence displaying the existing of a time-dependent modulation of GABA$_A$ergic transmission by ALLO in *Mecp2* mutant mice is certainly important, as it shows how the GABAergic system is vulnerable and mutable in RTT. However, there is an ample bulk of evidence displaying that, even in wild-type animals, changes in GABA$_A$R sensitivity toward neurosteroids occur during embryonic development and even later in puberty. These changes can potentially lead to different effects of ALLO and other neurosteroids during development (Follesa et al., 2002). Thus, the GABA$_A$R subunit composition may shift accordingly to the developmental stage. Therefore, the existing time-dependent GABA$_A$R sensitivity to neurosteroids can reflect a changeable requirement of neurosteroid actions by the GABAergic system, which, in turn, may be related with the hormonal milieu of the specific period of life (Colciago and Magnaghi, 2016). Also, either physiological or pathophysiological conditions can change the way neurosteroids act on the GABAergic system. Understanding how the subunit composition of the GABA$_A$R shifts in wild-type animals comparing to RTT mouse models, may offer important insight to elucidate the role and therapeutic potential of neurosteroids in RTT. Also, it would be relevant to study how the existent imbalances in cholesterol metabolism can impact the biosynthesis of neurosteroids in RTT.

The effects of ALLO on hippocampal-dependent memory are a great example of how the actions of neurosteroids can shift according to physiological/pathological conditions. GABA$_A$R in the dentate gyrus, where ALLO is actively metabolized, display low sensitivity to this neurosteroid. In turn, lower ALLO metabolism in the CA1 region of the hippocampus suggests that local steroid metabolism plays a crucial role in the regulation of GABA$_A$R-mediated inhibition in a regionally dependent manner (Belelli and Herd, 2003), specifically in brain regions devoted to memory formation and consolidation (Colciago and Magnaghi, 2016). This is strengthened by observations that ALLO increases neurogenesis, neuronal survival and reduces apoptosis in the hippocampus (Charalampopoulos et al., 2008; Rossetti et al., 2015). ALLO also increases the density of dendritic spines, the number of mature excitatory synapses and induces the formation of clusters of the actin binding protein debrin

(Shimizu et al., 2015), which is known to be decreased in the brain of Alzheimer's disease patients and individuals with mild cognitive impairment (Harigaya et al., 1996; Counts et al., 2012). Congruently, using an Alzheimer's disease mice model, ALLO restored hippocampal-dependent learning and memory deficits and induced survival of newly generated cells in 3xTgAD mice and non-Tg aged mice (Singh et al., 2012). Thus, in 3xTgAD mice it has been proposed that an early deficit in neurosteroid synthesis may contribute to the cognitive phenotype of AD and that ALLO shows the potential to function as a regenerative therapeutic tool to delay or even prevent characteristic neurogenic and cognitive deficits of Alzheimer's disease (Wang et al., 2010; Singh et al., 2012). In addition, ALLO was found to significantly reduce amyloid-β accumulation in the hippocampus, cortex and amygdala, to reduce microglia activation and increase expression of liver-X-receptor, pregnane-X-receptor and HMG-CoA-R, three vital proteins involved in cholesterol homeostasis and clearance from the brain (Chen et al., 2011). Despite the clear effects of ALLO on the molecular mechanisms of hippocampal memory, on the other hand, it has been described that ALLO impairs recognition memory consolidation and contextual fear memory in wild-type mice (Misane et al., 2013; Rabinowitz et al., 2014), and spatial learning in rats (Johansson et al., 2002; Matthews et al., 2002; Turkmen et al., 2004). Importantly, *Mecp2* mutant mice display learning and memory impairments, besides the classic breathing abnormalities, hypoactivity, motor deficits, anxiety alterations and stereotypies. Likewise, *Mecp2* mutant mice have reduced hippocampus, amygdala and striatum volumes and an overall reduction in brain volume (Stearns et al., 2007). Therefore, direct research on the possible restorative effects of neurosteroids in RTT could constitute an interesting and potentially successful approach.

Epilepsy in RTT: CBD to the Rescue?

Epilepsy is fairly a common comorbidity in RTT, with reports showing its presence in 60–80% of patients. In RTT, there is no unambiguous pattern of seizure episodes, and almost all seizure types are reported (Krajnc, 2015). The manifestations of seizures seems to constitute an age-related event (Chapleau et al., 2013), with onset usually in stage II or III (see section "Introduction"), around 4 years of age, but with possibility of maximal onset age between 7 and 12 years (Krajnc, 2015). In RTT, due to limited experience of epilepsy treatment, there are no definitive recommendations regarding treatment approach with the anticonvulsants currently available. Therefore, the choice of treatment for epilepsy in RTT can be challenging (Krajnc, 2015), being considered a major problem in RTT treatment (Chapleau et al., 2013). Additionally, evidence suggests that the prevalence of drug resistance epilepsy in patients with RTT is about the same as in other newly diagnosed epilepsies, in which 20 to 40% of the patients become refractory to treatment (French, 2007). However, prevention and efficient management of epileptic episodes is of major importance in RTT, as the severity and frequency of epileptic episodes are strong determinants to the clinical severity of RTT phenotype (Krajnc, 2015; Clarke and Abdala Sheikh, 2018).

A number of different AED are used in treatment of epilepsy in RTT, either in monotherapy or combined therapy, and its selection varies from case to case (Krajnc, 2015). Regardless of their many mechanisms of action, one of the main targets of several AEDs is the GABAergic signaling system (Greenfield, 2013). For instance, the effects of valproate acid, one of the most commonly prescribed AEDs, on the GABA signaling system (such as, increased GABA turnover and consequent enhancement of synaptic and extrasynaptic inhibition) are important for its antiseizure actions (Löscher, 1989; Greenfield, 2013; Rogawski et al., 2016). On the other hand, the effects of AEDs on GABAergic signaling can be more direct, like the ones of benzodiazepines, which act as direct agonists of $GABA_AR$, known to have a specific binding site for this type of drugs. Benzodiazepines are known for augmenting the amplitude (Macdonald and Barker, 1978) or decay time (Tietz et al., 1999) of $GABA_AR$-evoked IPSCs (Greenfield, 2013). However, in order to mediate increases in $GABA_AR$ currents, the receptor must have in its composition a γ subunit and the selectivity of each benzodiazepine depends on the specific α subunit (for detailed review see Riss et al., 2008). The clinical advantages of benzodiazepines relate with its efficacy against many seizure types (Riss et al., 2008), rapidity of onset, minimal toxicity, possibility of administration via several routes and high efficacy track-record (Macdonald and Barker, 1978). However, its use is limited by adverse side effects, such as cognitive impairment and sedation, tolerance, withdrawal and drug interactions (Riss et al., 2008). Tolerance to benzodiazepine treatment has been associated with time-dependent modifications in $GABA_AR$ subunit composition (Betjemann and Lowenstein, 2015). Namely, the internalization of subunits β_{1-3} and γ_2 on the $GABA_AR$, may lead do decreased inhibition of synaptic transmission (Goodkin et al., 2008). Although benzodiazepines are not commonly prescribed as AED in RTT cases, different studies using RTT-mice models have shown the promising effects of benzodiazepines midazolam (Voituron and Hilaire, 2011) and diazepam (Abdala et al., 2010), particularly attenuating respiratory defects.

Recently, natural constituents of the cannabis plant have been emerging as promising AEDs. Importantly, the ECBS stands as a promising pharmacological target in RTT (Vigli et al., 2018; Zamberletti et al., 2019). The ECBS is a complex neuromodulatory system that regulates important physiological processes (Kano et al., 2009), such as, anxiety and stress (Jenniches et al., 2016), social behavior (Wei et al., 2017), motor coordination (El Manira and Kyriakatos, 2010) and memory/learning (Marsicano and Lafenêtre, 2009). Importantly, these are behaviors usually compromised in RTT (Vigli et al., 2018). Cannabinoids modulate neuronal activity mainly via the CB_1R and CB_2R. CB_1R activation is linked with neuroprotection by controlling excitotoxicity via inhibition of excessive excitatory transmission and consequent calcium release (Vendel and de Lange, 2014). Indeed, the control of excitotoxicity constitutes a major physiological role of the ECBS (Kano et al., 2009). Although the CB_1R is classically denoted as a $G_{i/o}$ protein coupled receptor, mainly linked with inhibitory effects, CB_1R coupling to G proteins is mutable. CB_1R is now believed to have very few "intrinsic" properties, being the cellular consequences

of its activation likely a reflex of cell type and/or location in which the receptor is situated, their activity in different brain regions and due to temporal constrains (Busquets-Garcia et al., 2018). Contrary to initial belief, which placed CB_2R exclusively in the immune system (Kano et al., 2009), CB_2R are now known to be present in neurons, microglia and astrocytes (for a review see Solymosi and Kofalvi, 2017). CB_2R are involved in the control of glial activation and inflammation and on the regulation of neuronal excitability (Solymosi and Kofalvi, 2017). Moreover, CB_2R levels can increase in neurons and astrocytes under very specific circumstances, such as, in situations of neuroinflammation and in certain diseases (Onaivi et al., 2012; Di Marzo et al., 2015; Fernández-Ruiz et al., 2015). Related with its physiological roles, the lack of psychoactivity associated with CB_2R activation, has made this receptor a particular promising therapeutic target for cannabis-based therapies (Cassano et al., 2017). For thorough reviews on the ECBS and its actions, natural cannabinoids and their molecular targets, and the clinical applications of cannabinoids (see Kano et al., 2009; Morales et al., 2017; Solymosi and Kofalvi, 2017).

Today, more than 120 phytocannabinoids (natural occurring cannabinoids) have been identified as constituents of the cannabis plant. The most abundant cannabinoids in the cannabis plant are delta-9-tetrahydrocannabinoid, or Δ^9-THC, followed by Δ^8-THC, CBN, CBD, CBG, CBC, THCV, CBV, and CBDV (Morales et al., 2017). From all the natural constituents of the cannabis plant, CBD, a non-psychoactive cannabinoid (Loewe, 1946; Pertwee, 2009), is being widely studied given its high therapeutic value. CBD has been shown, both in humans and rodents, to have antiseizure (Jones et al., 2010; Pamplona and Coan, 2017; Perucca, 2017; Zaheer et al., 2018), anti-inflammatory (Malfait et al., 2000; Nagarkatti et al., 2009; Petrosino et al., 2018), antioxidant (Hampson et al., 2000), and anti-psychotic properties (Zuardi et al., 1991, 2012; Iseger and Bossong, 2015), to have neuroprotective effects (Iuvone et al., 2009; Fernández-Ruiz et al., 2013), to reduce nausea (Parker et al., 2011; Mersiades et al., 2018) and to work as an anxiolytic and anti-depressive drug (de Mello Schier et al., 2014; Blessing et al., 2015; Zuardi et al., 2017). Furthermore, CBD is known to potentiate the clinical efficacy of Δ^9-THC, increasing the durability of its beneficial effects, while preventing its psychoactive effects (Russo and Guy, 2006; Solymosi and Kofalvi, 2017). CBD acts as a surprisingly high potent antagonist at both the CB_1R and the CB_2R (Thomas et al., 2009). Recently, it has also been proposed that CBD acts as a negative allosteric modulator (NAM) at the CB_1R (Laprairie et al., 2015). Many of CBD therapeutic properties have been suggested to occur due to its effect at the $TRPV_1$ (Morales et al., 2017).

The medical use of cannabis has been increasing and the full potential of the cannabis plant is yet to be unfold. Cannabis-based drugs are been used, or proposed for use, in neuropathic pain and muscle spasticity associated with Multiple Sclerosis (Fitzpatrick and Downer, 2017; Solymosi and Kofalvi, 2017; Rice and Cameron, 2018), neurodegenerative diseases (Fagan and Campbell, 2014; Basavarajappa et al., 2017; Navarro et al., 2018), chronic pain (Carter et al., 2015; Pascual et al., 2018), to alleviate AIDS-related weight loss (Badowski and Perez, 2016; Rock and Parker, 2016) and to reduce vomiting and nausea associated with chemotherapy (Badowski and Yanful, 2018). Most relevantly for this work, cannabinoid use is being increasingly proposed as a very promising anti-epileptic drug, even in cases of treatment-resistant epilepsy (Maa and Figi, 2014; O'Connell et al., 2017; Pamplona and Coan, 2017). In a recent clinical trial, CBD significantly reduced convulsive-seizure frequency in Dravet syndrome patients (Devinsky et al., 2017). In a double-blind placebo-controlled trial, 120 children suffering with Dravet syndrome and drug-resistance epilepsy received either CBD (oral solution 20 mg/kg per day) or placebo over 14 weeks. In the CBD group, 43% of the patients had a reduction of 50% in seizure frequency, as opposed to a 27% decrease in the placebo group. Furthermore, 5% of the patients treated with CBD became seizure-free compared with a 0% incident in the placebo group. On the CGIC, a Likert-like scale questionnaire which allows assessing improvement after a treatment comparing with a baseline period (ranging from 1, very much improved to 7 very much worse), in the CBD group, 62% of the patients increased at least one category on the CGIC compared with 27% on the placebo group. Treatment with CBD provoked more adverse side effects reflected on diarrhea, vomiting, fatigue, pyrexia, somnolence, and some abnormalities on liver-function tests (Devinsky et al., 2017). About 1 year after this clinical trial, the FDA approved Epidiolex® (CBD) oral solution for treatment in Dravet and Lennox–Gastaut syndromes, two diseases that, in resemblance with RTT, present refractory epilepsy and high mortality rates. Also, Nabiximols (Sativex®), a combination of CBD and Δ^9-THC, is approved to treat muscle spasticity in Multiple Sclerosis (Novotna et al., 2011), an abnormality in muscle tone present in RTT (Kyle et al., 2018).

The mechanism by which CBD exerts anticonvulsive effects is still not completely clarified. Recently, however, using human recombinant $GABA_AR$, CBD was shown to act as a positive allosteric modulator of the $GABA_AR$, with the effects being selective for the β-subunit (higher in receptors with β2/β3 over β1 subunits) and the maximum effect being detected in receptors which included the α2-subunit (Bakas et al., 2017). The authors hypothesized that these results may explain the anticonvulsant and anxiolytic properties of this compound (Bakas et al., 2017). Indeed, previously, it was reported that CBD attenuated seizures in two well characterized seizure models, the acute pilocarpine TLE and the penicillin model of partial seizure (Jones et al., 2012). Curiously, in the acute epilepsy model using pilocarpine, a muscarinic acetylcholine receptor agonist, the antiseizure effects of CBD were modest and the drug was not able of reducing mortality and severity of episodes. On the other hand, using the penicillin model, a selective antagonist of the $GABA_AR$, CBD had a powerful antiseizure effect, significantly reducing the number of animals experiencing tonic-clonic episodes and their mortality. Importantly, CBD exerted only minor negligible motor effects (Jones et al., 2012). At the time, the authors speculated that the antiseizure effect of CBD could be occurring via a GABAergic-mediated mechanism (Jones et al., 2012). In support of this hypothesis, a previous study had shown an anticonvulsive action of CBD on several seizure models mediated *via* disinhibition of GABA release (Consroe et al.,

1982; Jones et al., 2012). In a very recent study, CBD was shown to have antiseizure effects in several models of acute epilepsy (Patra et al., 2019). Additionally, this study showed, for the first time, that chronic CBD administration improves seizure burden ratio, attenuates cognitive impairment and reduces motor comorbidities, well after the onset of symptoms in the RISE-SRS TLE (Patra et al., 2019). Thus, the results of this study are particularly relevant for research in RTT, considering the positive effects of a chronic administration of CBD on both seizures and motor impairment, which constitute two common comorbidities in RTT. Additionally, cognitive impairment is also characteristic of RTT and, therefore, finding that CBD improves cognition in models of acute and chronic epilepsy in also relevant for cannabinoid-related research in RTT.

Direct evidence of cannabinoid use in RTT mice models is objectively scarce in literature. To the best of our knowledge, there are only two reports evaluating the impact of a chronic treatment with a phytocannabinoid in an RTT-mice model. In both these reports (Vigli et al., 2018; Zamberletti et al., 2019), the authors used CBDV, a propyl analog of CBD devoid of psychoactive actions (Morales et al., 2017). CBDV has very weak activity at the CB_1R and CB_2R (Hill et al., 2013; Rosenthaler et al., 2014; Morales et al., 2017) and it has been proposed to activate the TRPV1 (Iannotti et al., 2014). Additionally, an effect of CBDV on the deorphanized cannabinoid receptor GPR55 has been described. Besides some cannabinoids, GPR55 is also activated by LPI. Notably, it has been found that CBDV is a potent inhibitor of LPI-induced GPR55 signaling (Lauckner et al., 2008; Anavi-Goffer et al., 2012). As stated in Vigli et al. (2018), GPR55 has been implied in important cognitive processes, such as, spatial memory regulation (Marichal-Cancino et al., 2018), social behavior (Kramar et al., 2017) and motor function (Bjursell et al., 2016). Moreover, in a recent work, CBDV was shown to attenuate seizures and social withdrawal in a mice model of Dravet syndrome (Kaplan et al., 2017). Concerning cannabinoids and RTT, the administration of CBDV by intraperitoneal injection (escalating dose ranging from 2 to 100 mg/kg of body weight) to *Mecp2*-308 male mice during 14 days, rescued sociability impairments, improved the general health status and increased the brain weight of these animals. Furthermore, a molecular analysis of GPR55 levels, revealed an up-regulation of this receptor in the hippocampus (Vigli et al., 2018). These results showed, for the first time, the clinical potential of non-psychoactive constituents of the cannabis plant and also the important role of the GPR55 as a promising drug-target on RTT. Very recently, a new study using CBDV has confirmed the potential of this particular phytocannabinoid in RTT. In this study, chronic administration of CBDV (0.2 to 2 mg/kg) was shown to completely rescue cognitive deficits, delaying neurological (although transiently) and motor impairments in male *MECP2* mutant mice (Zamberletti et al., 2019). Importantly, CBDV administration normalized BDNF and insulin growth factor 1 (IGF1) levels and restored normal signaling in the PI3K/AKT/mTOR pathway at an advanced stage of the disease. Interestingly, *Mecp2* deletion in this RTT mouse model provoked upregulation of CB_1R and CB_2R and CBDV treatment led to a normalization of these changes (Zamberletti et al., 2019). Although these two independent studies suggest a promising role of CBDV as a therapeutic drug in RTT, the fact that different molecular modifications in the ECBS were detected in each model, highlight the necessity of further studies.

The promising antiseizure effects of CBD, even in cases of refractory-epilepsy, observed in both clinical trials with humans and in laboratory animals, the effects of combinations of CBD and Δ^9-THC in controlling muscle spasticity and motor symptoms, and the positive results of CBDV administration in two different mouse models of RTT, place cannabinoids as a viable therapeutic strategy in RTT. Moreover, CBD positively modifies impairments in motor, cognitive and social processes in animal models, further highlighting the potential of cannabinoid molecules to tackle RTT-symptomology.

The Use of the Ketogenic Diet

Around 100 years ago, it was noted that a high fat diet could have long-lasting effects in preventing seizures without inducing significant caloric deprivation (Rogawski et al., 2016). These findings resulted on the creation of the KD, trademarked by an increase in the production in the liver of ketones bodies, such as BHB, acetoacetate and acetone (Peterman, 1924; Freeman and Kossoff, 2010; Rogawski et al., 2016). The fact that the KD was created in a time where the available AEDs were very limited, contributed for a rapid gain in popularity of this diet (Rogawski et al., 2016). However, the development of the antiepileptic drug phenytoin substantially decreased the use of the KD. In the last 30 years, interest in using the KD resurged, especially in children presenting refractory epilepsy (Rogawski et al., 2016).

An abnormal increase of ketone bodies in the blood was early suggested as the underlaying mechanism of the anticonvulsive properties of low carbohydrate KD (Talbot et al., 1927; Huttenlocher, 1976). Subsequently, many other possible mechanisms were enounced, such as, pH changes, anticonvulsive effects of hyperlipidemia, effects of the KD directly on sodium and potassium balance, and also an effect on cerebral metabolism, reflected on the change of glucose, as the main source of energy, to BHB, as a consequence of carbohydrate restriction (for details see Huttenlocher, 1976). To clarify these questions, Peter Huttenlocher designed a new KD in which ketonemia was induced by feeding of MCT. In his report of 1976, the MCT diet was administered to 18 children and he observed no differences in hyperlipidemia, no significant changes in pH, considerable reductions in blood glucose levels in one-third of the children and a gradual increase in plasma BHB and acetoacetate levels during a diet that was kept from 3 months to 4 years. Furthermore, plasma levels of BHB showed a significant correlation with the anticonvulsive effects of the MCT diet and, along with ketonemia, were rapidly abolished by intravenous infusion of glucose (Huttenlocher, 1976). Today, the mechanisms behind the anticonvulsive actions of the KD are fairly well characterized (for a detailed review see Rogawski et al., 2016).

One of the proposed mechanisms of action of the KD are increases in the synthesis of GABA and decreases in the

synthesis of excitatory neurotransmitters, such as glutamate (Rogawski et al., 2016). Indeed, it has been suggested that one of the anticonvulsive mechanisms of the KD relates with modifications in the way glutamate is processed in the brain. Particularly, due to a more active astrocytic metabolism, the conversion of glutamate to glutamine is increased, resulting in a more efficient removal of glutamate and increased GABA synthesis (Yudkoff et al., 2008). A study with 26 children suffering from refractory epilepsy, revealed that the KD increases levels of GABA in the cerebrospinal fluid, without affecting glutamate concentration. In this study, the results showed higher GABA levels in the responders to the diet compared with non-responders. Furthermore, the anticonvulsive action of the diet was more evident (90% reduction in seizures) in children who had higher levels of GABA at the beginning of the treatment and in whom a gradual increase in GABA levels during treatment was registered. Also, the anticonvulsive effects of the diet seem to be age-dependent, with younger children being the best responders (Dahlin et al., 2005). However, studies with animal models performed to confirm a GABAergic-mediated mechanism of anticonvulsive actions of the KD have produced mixed-results (Hartman et al., 2007). If, on one hand, the KD administered to mice fails to confer protection against the clonic seizures induced by $GABA_AR$ antagonist pentylenetetrazol, on the other hand, it is much more effective protecting against seizures induced by the maximal electroshock test, a test in which the classical anticonvulsive drugs targeting the GABAergic system only confer weak protection (Uhlemann and Neims, 1972; Hartman et al., 2007). On the contrary, the KD was found to protect against seizures induced by $GABA_AR$ antagonists pentylenetetrazol, bicuculline, and picrotoxin in rats (for a detailed review see Hartman et al., 2007). It has also been suggested that ketone bodies, such as acetoacetate, compete with chloride for the allosteric binding site at the vesicular glutamate transporter, thus inhibiting exocytotic glutamate release (Juge et al., 2010). Additionally, the authors of this work showed that acetoacetate protected against seizure-like activity induced by 4-aminopyridine (Juge et al., 2010). Recently, using the spontaneously epileptic Kcna1-null mice, the ketone body BHB was shown to exert anti-seizure effects, restore impairments in synaptic plasticity processes and raise the threshold of mitochondrial permeability transition (Kim et al., 2015; Rogawski et al., 2016).

Concerning the clinical use of the KD in RTT, Haas et al. (1986), reported a clinical study were the MCT KD was used in 7 girls diagnosed with RTT who presented anticonvulsive resistant seizures. Among the 5 girls capable of tolerating the diet, the KD improved seizure control, slightly ameliorated behavior and motor skills and increased bodyweight. The results from this work led the authors to suggest that, considering the defects in the carbohydrate metabolism occurring in RTT, the KD stands as a logical choice in this disease (Haas et al., 1986). Surprisingly, until very recently, this was the only clinical report of the use of KD in RTT. Indeed, evidence of the application of the KD in RTT is extremely hard to find in the literature. In Liebhaber et al. (2003) reported a case of an RTT patient who was treated with the KD for 4 years. The treatment started when the patient was 8 years old and presented a refractory epilepsy. The diet led to a 70% reduction in seizure frequency and improved contact and behavior. In Giampietro et al. (2006) reported a case with a female patient suffering from an atypical RTT variant in which the KD significantly reduced seizure occurrence. In 2011, a long-term follow-up of the use of the KD in 226 patients with refractory epilepsy was reported. This report included one patient with RTT, which presented a 75–99% seizure reduction after KD (Caraballo et al., 2011). Evidence on the use of the KD in RTT-mouse models is also scarce. In the only direct approach available in the literature, it has been described that a restricted KD positively impacts anxiety and motor measures in a male mutant *Mecp2* mice. However, the authors also showed that the results of the KD were very similar to the ones from a calorie restriction diet, concluding that, most likely, it was the caloric restriction that produced the positive outcomes, rather than the composition of the KD by itself (Mantis et al., 2009).

Reports on the use of the KD in autism spectrum disorders and other brain diseases are also available in literature. With relevance for the phenotypic expression of RTT, it has been described that 4 weeks of a KD regime increases the social behavior of wild-type rats, registered in three different social interaction protocols. On the other hand, the exogenous administration of ketone bodies had no effects on social interaction in the same paradigms (Kasprowska-Liśkiewicz et al., 2017). Also, in an EL mice model (Meidenbauer et al., 2011), which presents autism spectrum disorders phenotype and comorbid epilepsy, the KD was shown to improve sociability and reduce repetitive behavior (Ruskin et al., 2017). Using the same animal model, the KD was shown to induce a 1 month delay in epileptogenesis (Todorova et al., 2000) and to have anticonvulsive actions (Mantis et al., 2004). In an Huntington's disease mice model, the KD was shown to produce positive outcomes on weight lose without affecting cognitive processes (Ruskin et al., 2011). More recently, in an animal model of autism induced by prenatal exposure to valproic acid, the KD was, once again, associated with improvement in social behavior (Castro et al., 2017).

Another potential mechanism of action underlying the anticonvulsive effects of the KD involves the modulation of adenosine receptor activity (Masino et al., 2013; Rogawski et al., 2016). Adenosine is an ubiquitous neuromodulator affecting the action and activity of several neurotransmitter receptors (Sebastião and Ribeiro, 2015). A_1R activity mediates the inhibitory effects of adenosine, including inhibition of neurotransmitter release and changes in post-synaptic membrane conductance (Dunwiddie and Masino, 2001). On the other hand, the $A_{2A}R$ mediates the excitatory effects of adenosine by coupling to G_s proteins, consequently leading to stimulation of adenylate cyclase, increases in intracellular cAMP levels and PKA activation (Sebastião and Ribeiro, 2015). Relevantly, caffeine, the most widely consumed legal drug in the world, is a non-selective antagonist at the A_1R and $A_{2A}R$ (Fredholm et al., 1999). Recently, the KD was demonstrated to suppress seizures in a transgenic mice model with spontaneous seizures by activation of the A_1R (Masino et al., 2011) and similar results were shown in an *in vitro* mimic of the KD (Kawamura et al., 2010). Adenosine is directly synthetized from ATP and given that ATP levels are increased in

the KD it is feasible that it results in an increase in adenosine synthesis (Rogawski et al., 2016). Adenosine receptor activity, particularly $A_{2A}R$ activity, is also known to directly facilitate the actions of the important BDNF (Diógenes et al., 2004, 2007; Fernandes et al., 2008; Fontinha et al., 2008; Vaz et al., 2015). Importantly, BDNF expression is impaired in RTT and it has been suggested that it can have important therapeutic actions in RTT (reviewed in Katz, 2014; Li and Pozzo-Miller, 2014).

In conclusion, if, on one hand, it is particularly well accepted and proven that the KD has powerful antiseizure actions (although the mechanisms of action are still not completely described) (Vining et al., 1998; Hassan et al., 1999; Neal et al., 2008), on the other hand, reports on the application of this diet to RTT cases and in RTT-mice models are scarce. The lack of research is even more surprising considering the positive results shown in both clinical studies with humans and in

TABLE 1 | Summary of the main topics of this review and future directions.

From cannabinoids and neurosteroids to statins and the ketogenic diet: new therapeutic avenues in Rett syndrome?				
GABAergic signaling	***Cholesterol metabolism***	***Neurosteroids***	***Cannabinoids***	***Ketogenic diet***
The GABAergic signaling system comprises a key pathway commonly disturbed in neurodevelopmental diseases (Braat and Kooy, 2015). In RTT, $GABA_A$ergic transmission is intimately related with symptoms and disease progression (Chao et al., 2010; El-Khoury et al., 2014). An incorrect balance between excitation and inhibition reflecting a dysfunction in GABAergic and glutamatergic signaling systems have been described in *Mecp2*-KO mice (Chao et al., 2007; Calfa et al., 2011). The relationship between RTT phenotypical expression and GABAergic signaling is region, time and neuronal population dependent (Chao et al., 2010; El-Khoury et al., 2014). *MECP2* absence exclusively in GABAergic neurons has been found to trigger almost the full range of RTT symptomatology in mice (Chao et al., 2010). The use of benzodiazepines, acting as agonists of the $GABA_AR$, improve RTT symptoms in mice (Voituron and Hilaire, 2011). Íncreasing GABA availability by blocking its reuptake with Tiagabine, has been shown to reduce RTT symptoms.	Cholesterol metabolism is abnormal in brain and livers of *Mecp2* mutant mice (Buchovecky et al., 2013). A mutation in the Sqle gene was sufficient to restore function and longevity in *Mecp2* mutant mice (Buchovecky et al., 2013). Statins ameliorate the systemic imbalance of lipid profile, alleviated motor symptoms and conferred increased longevity in Mecp2 mutant mice (Buchovecky et al., 2013). In samples collected from RTT patients the total cholesterol level is altered (Sticozzi et al., 2013; Segatto et al., 2014). Modifications in mitochondrial structure and function have been described (Shulyakova et al., 2017). Cholesterol influences the production of neurosteroids (Reddy, 2010).	Allopregnanolone (ALLO) is the most powerful endogenous allosteric modulator of the $GABA_AR$ (Hosie et al., 2006; Reddy, 2010). Neurosteroids are being proposed as an alternative to benzodiazepines (Reddy and Estes, 2016) and also as antipsychotics (Cai et al., 2018). In *MECP2* mutant mice, allopregnanolone increases the amplitude, frequency and decay time of $GABA_AR$ IPSCs (Jin et al., 2013b). Changes in subunit composition on the $GABA_AR$ might be responsible for different responses to allopregnanolone (Paoletti et al., 2006; Jin et al., 2013b). Reductions in neurosteroids were found on status epilepticus (Meletti et al., 2017, 2018). In SLOS, an abnormal synthesis of neurosteroids occurs (Marcos et al., 2004; Lee and Tierney, 2011). Ganaxolone showed promising results in a clinical trial in Fragile X syndrome (Ligsay et al., 2017).	The endocannabinoid system (ECBS) is involved in the regulation of several behavioral processes found to be compromised in RTT (Vigli et al., 2018). Cannabis-based therapies are being proposed as anti-epileptic drugs (AED) even in cases of drug resistant epilepsy (Maa and Figi, 2014; O'Connell et al., 2017; Pamplona and Coan, 2017). Nabiximols (Sativex), a combination of CBD and Δ^9-THC, is approved to treat muscle spasticity in Multiple Sclerosis (Novotna et al., 2011), a comorbidity frequently reported in RTT (Kyle et al., 2018). Epidiolex (CBD) has been approved to treat epilepsy in Dravet syndrome (Devinsky et al., 2017), a disease that present refractory epilepsy and high mortality rates. The antiepileptic actions of CBD can be mediated via GABAergic signaling (Bakas et al., 2017). Administration of CBDV to *Mecp2*-null mice rescued sociability impairments, improved the general health status and increased the brain weight of these animals (Vigli et al., 2018).	The ketogenic diet (KD) has strong antiepileptic actions (Rogawski et al., 2016). The anticonvulsive actions of the KD can be mediated via GABAergic signaling mechanism (Rogawski et al., 2016), or be related with increases in adenosine and BDNF signaling (Masino et al., 2011). The use of the KD in RTT has shown promising results in controlling epilepsy (Haas et al., 1986; Liebhaber et al., 2003; Giampietro et al., 2006; Caraballo et al., 2011). The KD has also shown positive results in refractory epilepsy and in intractable epilepsy (Neal et al., 2008; Rogawski et al., 2016). In *Mecp2* null mice models, the KD ameliorated anxiety and motor measurements, although clarification is required (Mantis et al., 2009). In Autism and Huntington's disease mice models, the KD has been shown to improve sociability, to reduce repetitive behavior and increase body weight (Todorova et al., 2000; Mantis et al., 2004; Meidenbauer et al., 2011; Ruskin et al., 2011, 2017; Castro et al., 2017; Kasprowska-Liśkiewicz et al., 2017).
Future directions				
To better characterize the modifications occurring in $GABA_AR$ composition during RTT progression (Jin et al., 2013b). To further evaluate the impact of strategies which, directly or indirectly, increase GABAergic signaling in RTT mice models.	To comprehend the cellular mechanisms behind the dysregulations in cholesterol metabolism (Buchovecky et al., 2013).	To directly evaluate the impact of neurosteroid treatment in *Mecp2* mutant mice phenotype. To understand how modifications occurring in $GABA_AR$ composition during RTT progression affect neurosteroid actions (Jin et al., 2013b).	Study the ECBS in RTT mice models. Understand the impact of CBD and THC in RTT symptoms in trials with humans and in preclinical studies using RTT mice models.	Reinstate the interest in the use of the KD in RTT, particularly considering its antiseizure actions, advancing with new studies, both in humans and in RTT-mice models.

RTT mouse-models. Relevantly, a prospective study with 145 children aged between 2 and 16 years, suffering from intractable epilepsy and who had never experienced the KD, showed that 3 months of diet resulted in a 75% seizure reduction rate, with 38% of the children in the experimental group experiencing a reduction of 50% in seizures. Also, five children experienced reductions of 90% in seizures and one child became seizure free (Neal et al., 2008). Importantly, in children allocated to the control group who continued their usual treatment with AED, some of them experienced worsening of symptoms and none became seizure-free (Neal et al., 2008; Masino et al., 2013).

CONCLUSION AND FINAL REMARKS

The present review summarizes important recent evidence concerning metabolic, synaptic, functional and molecular dysfunctions occurring in RTT (see **Table 1**). Due to the ubiquitous role of *MECP2* gene, it has been a tremendous challenge to comprehend and characterize the mechanisms through which *MECP2* mutations lead to symptomatology in RTT. With the development and improvement of gene-editing technologies, research in RTT has drifted from "therapy-directed" to "cure-oriented" investigation. However, the path for a definitive cure is paved with many challenges and, most likely, this achievement in not around the corner. Meanwhile, it is paramount to better understand this disease and to improve the available treatment by exploring new therapeutic avenues. In this work, we reviewed promising evidence on different research lines that may have an important impact in the field. From modulators of GABAergic signaling, to cannabinoids and the KD, and cleverly exploiting the metabolic features of this disease, an ample bulk of evidence has been gathered, creating a plethora of research lines to be followed in the future. RTT is a devastating disease, both for the patient and for the caregivers, and clinical and preclinical research directed at finding new therapeutic approaches are more important than ever, now that we are beginning to understand some of the mechanisms of this disease.

Summarizing, in the future it would be interesting to: (1) better characterize the modifications occurring in $GABA_AR$ composition during RTT disease progression; (2) study how cholesterol imbalances impact on neurosteroid production in RTT and their potential therapeutic use in this disease; (3) disclose the cellular mechanisms behind the dysregulations in cholesterol metabolism; (4) directly study the immense potentiality of CBD and other cannabinoids on RTT mouse-models and in controlled clinical trials with humans; (5) reinstate the interest in the use of the KD in RTT, particularly considering its antiseizure actions, advancing with new studies, both in humans and in RTT-mouse models; (6) to design further studies on the therapeutic properties of statins in RTT, and (7) continue to research mitochondria dynamics in RTT and its role on the disease progression and symptomatology.

AUTHOR CONTRIBUTIONS

FM and MD wrote the manuscript. CM-L revised and assisted on manuscript writing. AS revised the manuscript. All authors contributed to the final version of the manuscript.

FUNDING

FM was in receipt of a fellowship (IMM/CT/8-2018). The authors would like to thank the following organizations for their funding: AdoRett – LISBOA-01-0145-FEDER-031929; the Association Française du Syndrome de Rett Program "Educação pela Ciência" | Bolsas CHLN/FMUL; GAPIC. Project No. 20190017; Twinning action (SynaNet) from the EU H2020 Programme; and the UID/BIM/50005/2019, project financed by the FCT/Ministério da Ciência, Tecnologia e Ensino Superior (MCTES), through the Fundos do Orçamento de Estado.

REFERENCES

Abdala, A. P., Toward, M. A., Dutschmann, M., Bissonnette, J. M., and Paton, J. F. R. (2016). Deficiency of GABAergic synaptic inhibition in the kölliker-fuse area underlies respiratory dysrhythmia in a mouse model of Rett syndrome. *J. Physiol.* 594, 223–237. doi: 10.1113/JP270966

Abdala, A. P. L., Dutschmann, M., Bissonnette, J. M., and Paton, J. F. R. (2010). Correction of respiratory disorders in a mouse model of Rett syndrome. *Proc. Natl. Acad. Sci. U.S.A.* 107, 18208–18213. doi: 10.1073/pnas.1012104107

Amir, R. E., Van den Veyver, I. B., Wan, M., Tran, C. Q., Francke, U., and Zoghbi, H. Y. (1999). Rett syndrome is caused by mutations in X-linked MECP2, encoding methyl-CpG-binding protein 2. *Nat. Genet.* 23, 185–188. doi: 10.1038/13810

Anavi-Goffer, S., Baillie, G., Irving, A. J., Gertsch, J., Greig, I. R., Pertwee, R. G., et al. (2012). Modulation of l-α-lysophosphatidylinositol/GPR55 mitogen-activated protein kinase (MAPK) signaling by Cannabinoids. *J. Biol. Chem.* 287, 91–104. doi: 10.1074/jbc.M111.296020

Aneja, A., and Tierney, E. (2008). Autism: the role of cholesterol in treatment. *Int. Rev. Psychiatry* 20, 165–170. doi: 10.1080/09540260801889062

Archer, H. L., Evans, J., Edwards, S., Colley, J., Newbury-Ecob, R., O'Callaghan, F., et al. (2006). CDKL5 mutations cause infantile spasms, early onset seizures, and severe mental retardation in female patients. *J. Med. Genet.* 43, 729–734. doi: 10.1136/jmg.2006.041467

Auron, A., and Brophy, P. D. (2012). Hyperammonemia in review: pathophysiology, diagnosis, and treatment. *Pediatr. Nephrol.* 27, 207–222. doi: 10.1007/s00467-011-1838-5

Badowski, M. E., and Perez, S. E. (2016). Clinical utility of dronabinol in the treatment of weight loss associated with HIV and AIDS. *HIV AIDS* 8, 37–45. doi: 10.2147/HIV.S81420

Badowski, M. E., and Yanful, P. K. (2018). Dronabinol oral solution in the management of anorexia and weight loss in AIDS and cancer. *Ther. Clin. Risk Manag.* 14, 643–651. doi: 10.2147/TCRM.S126849

Bakas, T., van Nieuwenhuijzen, P. S., Devenish, S. O., McGregor, I. S., Arnold, J. C., and Chebib, M. (2017). The direct actions of cannabidiol and 2-arachidonoyl glycerol at GABA A receptors. *Pharmacol. Res.* 119, 358–370. doi: 10.1016/j.phrs.2017.02.022

Basavarajappa, B. S., Shivakumar, M., Joshi, V., and Subbanna, S. (2017). Endocannabinoid system in neurodegenerative disorders. *J. Neurochem.* 142, 624–648. doi: 10.1111/jnc.14098

Belelli, D., Casula, A., Ling, A., and Lambert, J. J. (2002). The influence of subunit composition on the interaction of neurosteroids with GABA(A) receptors. *Neuropharmacology* 43, 651–661.

Belelli, D., and Herd, M. B. (2003). The contraceptive agent Provera enhances GABA(A) receptor-mediated inhibitory neurotransmission in the rat hippocampus: evidence for endogenous neurosteroids? *J. Neurosci.* 23, 10013–10020.

Bernardi, F., Salvestroni, C., Casarosa, E., Nappi, R. E., Lanzone, A., Luisi, S., et al. (1998). Aging is associated with changes in allopregnanolone concentrations in brain, endocrine glands and serum in male rats. *Eur. J. Endocrinol.* 138, 316–321.

Betjemann, J. P., and Lowenstein, D. H. (2015). Status epilepticus in adults. *Lancet Neurol.* 14, 615–624. doi: 10.1016/S1474-4422(15)00042-3

Bianchi, M. T., and Macdonald, R. L. (2003). Neurosteroids shift partial agonist activation of GABA(A) receptor channels from low- to high-efficacy gating patterns. *J. Neurosci.* 23, 10934–10943.

Bjursell, M., Ryberg, E., Wu, T., Greasley, P. J., Bohlooly-Y, M., and Hjorth, S. (2016). Deletion of Gpr55 results in subtle effects on energy metabolism, motor activity and thermal pain sensation. *PLoS One* 11:e0167965. doi: 10.1371/journal.pone.0167965

Blessing, E. M., Steenkamp, M. M., Manzanares, J., and Marmar, C. R. (2015). Cannabidiol as a potential treatment for anxiety disorders. *Neurotherapeutics* 12, 825–836. doi: 10.1007/s13311-015-0387-1

Blue, M. E., Naidu, S., and Johnston, M. V. (1999). Altered development of glutamate and GABA receptors in the basal ganglia of girls with Rett syndrome. *Exp. Neurol.* 156, 345–352. doi: 10.1006/exnr.1999.7030

Boggio, E. M., Lonetti, G., Pizzorusso, T., and Giustetto, M. (2010). Synaptic determinants of Rett syndrome. *Front. Synapt. Neurosci.* 2:28. doi: 10.3389/fnsyn.2010.00028

Braat, S., and Kooy, R. F. (2015). The GABAA receptor as a therapeutic target for neurodevelopmental disorders. *Neuron* 86, 1119–1130. doi: 10.1016/j.neuron.2015.03.042

Broomall, E., Natale, J. E., Grimason, M., Goldstein, J., Smith, C. M., Chang, C., et al. (2014). Pediatric super-refractory status epilepticus treated with allopregnanolone. *Ann. Neurol.* 76, 911–915. doi: 10.1002/ana.24295

Brown, N., Kerby, J., Bonnert, T. P., Whiting, P. J., and Wafford, K. A. (2002). Pharmacological characterization of a novel cell line expressing human alpha(4)beta(3)delta GABA(A) receptors. *Br. J. Pharmacol.* 136, 965–974. doi: 10.1038/sj.bjp.0704795

Buchovecky, C. M., Turley, S. D., Brown, H. M., Kyle, S. M., McDonald, J. G., Liu, B., et al. (2013). A suppressor screen in Mecp2 mutant mice implicates cholesterol metabolism in Rett syndrome. *Nat. Genet.* 45, 1013–1020. doi: 10.1038/ng.2714

Busquets-Garcia, A., Bains, J., and Marsicano, G. (2018). CB1 receptor signaling in the brain: extracting specificity from ubiquity. *Neuropsychopharmacology* 43, 4–20. doi: 10.1038/npp.2017.206

Cai, H., Cao, T., Zhou, X., and Yao, J. K. (2018). Neurosteroids in schizophrenia: pathogenic and therapeutic implications. *Front. Psychiatry* 9:73. doi: 10.3389/fpsyt.2018.00073

Calfa, G., Hablitz, J. J., and Pozzo-Miller, L. (2011). Network hyperexcitability in hippocampal slices from Mecp2 mutant mice revealed by voltage-sensitive dye imaging. *J. Neurophysiol.* 105, 1768–1784. doi: 10.1152/jn.00800.2010

Campos-Castelló, J., Peral Guerra, M., Riviere Gómez, A., Oliete García, F., Herranz Tanarro, J., Toledano Barrero, M., et al. (1988). [Rett's syndrome: study of 15 cases]. *An. Esp. Pediatr.* 28, 286–292.

Caraballo, R., Vaccarezza, M., Cersósimo, R., Rios, V., Soraru, A., Arroyo, H., et al. (2011). Long-term follow-up of the ketogenic diet for refractory epilepsy: multicenter Argentinean experience in 216 pediatric patients. *Seizure* 20, 640–645. doi: 10.1016/j.seizure.2011.06.009

Carter, G. T., Javaher, S. P., Nguyen, M. H., Garret, S., and Carlini, B. H. (2015). Re-branding cannabis: the next generation of chronic pain medicine? *Pain Manag.* 5, 13–21. doi: 10.2217/pmt.14.49

Carunchio, I., Mollinari, C., Pieri, M., Merlo, D., and Zona, C. (2008). GABA A receptors present higher affinity and modified subunit composition in spinal motor neurons from a genetic model of amyotrophic lateral sclerosis. *Eur. J. Neurosci.* 28, 1275–1285. doi: 10.1111/j.1460-9568.2008.06436.x

Carver, C. M., and Reddy, D. S. (2016). Neurosteroid structure-activity relationships for functional activation of extrasynaptic δGABA(A) receptors. *J. Pharmacol. Exp. Ther.* 357, 188–204. doi: 10.1124/jpet.115.229302

Cassano, T., Calcagnini, S., Pace, L., De Marco, F., Romano, A., and Gaetani, S. (2017). Cannabinoid receptor 2 signaling in neurodegenerative disorders: from pathogenesis to a promising therapeutic target. *Front. Neurosci.* 11:30. doi: 10.3389/fnins.2017.00030

Castro, K., Baronio, D., Perry, I. S., Riesgo, R. D. S., and Gottfried, C. (2017). The effect of ketogenic diet in an animal model of autism induced by prenatal exposure to valproic acid. *Nutr. Neurosci.* 20, 343–350. doi: 10.1080/1028415X.2015.1133029

Chao, H.-T., Chen, H., Samaco, R. C., Xue, M., Chahrour, M., Yoo, J., et al. (2010). Dysfunction in GABA signalling mediates autism-like stereotypies and Rett syndrome phenotypes. *Nature* 468, 263–269. doi: 10.1038/nature09582

Chao, H.-T., and Zoghbi, H. Y. (2012). MeCP2: only 100% will do. *Nat. Neurosci.* 15, 176–177. doi: 10.1038/nn.3027

Chao, H.-T., Zoghbi, H. Y., and Rosenmund, C. (2007). MeCP2 controls excitatory synaptic strength by regulating glutamatergic synapse number. *Neuron* 56, 58–65. doi: 10.1016/j.neuron.2007.08.018

Chapleau, C. A., Lane, J., Pozzo-Miller, L., and Percy, A. K. (2013). Evaluation of current pharmacological treatment options in the management of Rett syndrome: from the present to future therapeutic alternatives. *Curr. Clin. Pharmacol.* 8, 358–369.

Charalampopoulos, I., Remboutsika, E., Margioris, A. N., and Gravanis, A. (2008). Neurosteroids as modulators of neurogenesis and neuronal survival. *Trends Endocrinol. Metab.* 19, 300–307. doi: 10.1016/j.tem.2008.07.004

Chebib, M., and Johnston, G. A. R. (1999). The "ABC" of gaba receptors: a brief review. *Clin. Exp. Pharmacol. Physiol.* 26, 937–940. doi: 10.1046/j.1440-1681.1999.03151.x

Chen, C.-Y., Di Lucente, J., Lin, Y.-C., Lien, C.-C., Rogawski, M. A., Maezawa, I., et al. (2018). Defective GABAergic neurotransmission in the nucleus tractus solitarius in Mecp2-null mice, a model of Rett syndrome. *Neurobiol. Dis.* 109, 25–32. doi: 10.1016/j.nbd.2017.09.006

Chen, S., Wang, J. M., Irwin, R. W., Yao, J., Liu, L., and Brinton, R. D. (2011). Allopregnanolone promotes regeneration and reduces β-amyloid burden in a preclinical model of Alzheimer's disease. *PLoS One* 6:e24293. doi: 10.1371/journal.pone.0024293

Clarke, A. J., and Abdala Sheikh, A. P. (2018). A perspective on "cure" for Rett syndrome. *Orphanet J. Rare Dis.* 13:44. doi: 10.1186/s13023-018-0786-6

Clarke, R. S. (1973). Anaesthesia and carbohydrate metabolism. *Br. J. Anaesth.* 45, 237–243.

Colciago, A., and Magnaghi, V. (2016). Neurosteroids involvement in the epigenetic control of memory formation and storage. *Neural Plast.* 2016:5985021. doi: 10.1155/2016/5985021

Concas, A., Mostallino, M. C., Porcu, P., Follesa, P., Barbaccia, M. L., Trabucchi, M., et al. (1998). Role of brain allopregnanolone in the plasticity of gamma-aminobutyric acid type A receptor in rat brain during pregnancy and after delivery. *Proc. Natl. Acad. Sci. U.S.A.* 95, 13284–13289.

Consroe, P., Benedito, M. A., Leite, J. R., Carlini, E. A., and Mechoulam, R. (1982). Effects of cannabidiol on behavioral seizures caused by convulsant drugs or current in mice. *Eur. J. Pharmacol.* 83, 293–298.

Cooper, E. J., Johnston, G. A., and Edwards, F. A. (1999). Effects of a naturally occurring neurosteroid on GABAA IPSCs during development in rat hippocampal or cerebellar slices. *J. Physiol.* 521(Pt 2), 437–449.

Counts, S. E., He, B., Nadeem, M., Wuu, J., Scheff, S. W., and Mufson, E. J. (2012). Hippocampal drebrin loss in mild cognitive impairment. *Neurodegener. Dis.* 10, 216–219. doi: 10.1159/000333122

Dahlin, M., Elfving, A., Ungerstedt, U., and Amark, P. (2005). The ketogenic diet influences the levels of excitatory and inhibitory amino acids in the CSF in children with refractory epilepsy. *Epilepsy Res.* 64, 115–125. doi: 10.1016/j.eplepsyres.2005.03.008

Dani, V. S., Chang, Q., Maffei, A., Turrigiano, G. G., Jaenisch, R., and Nelson, S. B. (2005). Reduced cortical activity due to a shift in the balance between excitation and inhibition in a mouse model of Rett syndrome. *Proc. Natl. Acad. Sci. U.S.A.* 102, 12560–12565. doi: 10.1073/pnas.0506071102

Dani, V. S., and Nelson, S. B. (2009). Intact long-term potentiation but reduced connectivity between neocortical layer 5 pyramidal neurons in a mouse model of Rett syndrome. *J. Neurosci.* 29, 11263–11270. doi: 10.1523/JNEUROSCI.1019-09.2009

Datta, D., Arion, D., and Lewis, D. A. (2015). Developmental expression patterns of GABAA receptor subunits in layer 3 and 5 pyramidal cells of monkey prefrontal cortex. *Cereb. Cortex* 25, 2295–2305. doi: 10.1093/cercor/bhu040

De Felice, C., Signorini, C., Leoncini, S., Pecorelli, A., Durand, T., Valacchi, G., et al. (2012). The role of oxidative stress in Rett syndrome: an overview: oxidative stress and Rett syndrome. *Ann. N.Y. Acad. Sci.* 1259, 121–135. doi: 10.1111/j.1749-6632.2012.06611.x

de Mello Schier, A. R., de Oliveira Ribeiro, N. P., Coutinho, D. S., Machado, S., Arias-Carrión, O., Crippa, J. A., et al. (2014). Antidepressant-like and anxiolytic-like effects of cannabidiol: a chemical compound of *Cannabis sativa*. *CNS Neurol Disord. Drug Targets* 13, 953–960.

Devinsky, O., Cross, J. H., Laux, L., Marsh, E., Miller, I., Nabbout, R., et al. (2017). Trial of cannabidiol for drug-resistant seizures in the dravet syndrome. *N. Engl. J. Med.* 376, 2011–2020. doi: 10.1056/NEJMoa1611618

Di Marzo, V., Stella, N., and Zimmer, A. (2015). Endocannabinoid signalling and the deteriorating brain. *Nat. Rev. Neurosci.* 16, 30–42. doi: 10.1038/nrn3876

Diógenes, M. J., Assaife-Lopes, N., Pinto-Duarte, A., Ribeiro, J. A., and Sebastião, A. M. (2007). Influence of age on BDNF modulation of hippocampal synaptic transmission: interplay with adenosine A2A receptors. *Hippocampus* 17, 577–585. doi: 10.1002/hipo.20294

Diógenes, M. J., Fernandes, C. C., Sebastião, A. M., and Ribeiro, J. A. (2004). Activation of adenosine A2A receptor facilitates brain-derived neurotrophic factor modulation of synaptic transmission in hippocampal slices. *J. Neurosci.* 24, 2905–2913. doi: 10.1523/JNEUROSCI.4454-03.2004

Drexel, M., Kirchmair, E., and Sperk, G. (2013). Changes in the expression of GABAA receptor subunit mRNAs in parahippocampal areas after kainic acid induced seizures. *Front. Neural Circ.* 7:142. doi: 10.3389/fncir.2013.00142

Duarte, S. T., Armstrong, J., Roche, A., Ortez, C., Pérez, A., O'Callaghan, M., et al. (2013). Abnormal expression of cerebrospinal fluid cation chloride cotransporters in patients with Rett syndrome. *PLoS One* 8:e068851. doi: 10.1371/journal.pone.0068851

Dubrovsky, B. O. (2005). Steroids, neuroactive steroids and neurosteroids in psychopathology. *Progr. Neuro Psychopharmacol. Biol. Psychiatry* 29, 169–192. doi: 10.1016/j.pnpbp.2004.11.001

Dunwiddie, T. V., and Masino, S. A. (2001). The role and regulation of adenosine in the central nervous system. *Annu. Rev. Neurosci.* 24, 31–55. doi: 10.1146/annurev.neuro.24.1.31

El Manira, A., and Kyriakatos, A. (2010). The role of endocannabinoid signaling in motor control. *Physiology* 25, 230–238. doi: 10.1152/physiol.00007.2010

El-Ansary, A., and Al-Ayadhi, L. (2014). GABAergic/glutamatergic imbalance relative to excessive neuroinflammation in autism spectrum disorders. *J. Neuroinflam.* 11:189. doi: 10.1186/s12974-014-0189-0

El-Khoury, R., Panayotis, N., Matagne, V., Ghata, A., Villard, L., and Roux, J.-C. (2014). GABA and glutamate pathways are spatially and developmentally affected in the brain of Mecp2-deficient mice. *PLoS One* 9:e92169. doi: 10.1371/journal.pone.0092169

Fagan, S. G., and Campbell, V. A. (2014). The influence of cannabinoids on generic traits of neurodegeneration: cannabinoids and neurodegeneration. *Br. J. Pharmacol.* 171, 1347–1360. doi: 10.1111/bph.12492

Fernandes, C. C., Pinto-Duarte, A., Ribeiro, J. A., and Sebastião, A. M. (2008). Postsynaptic action of brain-derived neurotrophic factor attenuates alpha7 nicotinic acetylcholine receptor-mediated responses in hippocampal interneurons. *J. Neurosci.* 28, 5611–5618. doi: 10.1523/JNEUROSCI.5378-07.2008

Fernández-Ruiz, J., Moro, M. A., and Martínez-Orgado, J. (2015). Cannabinoids in neurodegenerative disorders and stroke/brain trauma: from preclinical models to clinical applications. *Neurotherapeutics* 12, 793–806. doi: 10.1007/s13311-015-0381-7

Fernández-Ruiz, J., Sagredo, O., Pazos, M. R., García, C., Pertwee, R., Mechoulam, R., et al. (2013). Cannabidiol for neurodegenerative disorders: important new clinical applications for this phytocannabinoid? *Br. J. Clin. Pharmacol.* 75, 323–333. doi: 10.1111/j.1365-2125.2012.04341.x

Fitzpatrick, J.-M. K., and Downer, E. J. (2017). Toll-like receptor signalling as a cannabinoid target in multiple sclerosis. *Neuropharmacology* 113, 618–626. doi: 10.1016/j.neuropharm.2016.04.009

Follesa, P., Porcu, P., Sogliano, C., Cinus, M., Biggio, F., Mancuso, L., et al. (2002). Changes in GABAA receptor gamma 2 subunit gene expression induced by long-term administration of oral contraceptives in rats. *Neuropharmacology* 42, 325–336.

Fontinha, B. M., Diógenes, M. J., Ribeiro, J. A., and Sebastião, A. M. (2008). Enhancement of long-term potentiation by brain-derived neurotrophic factor requires adenosine A2A receptor activation by endogenous adenosine. *Neuropharmacology* 54, 924–933. doi: 10.1016/j.neuropharm.2008.01.011

Fredholm, B. B., Bättig, K., Holmén, J., Nehlig, A., and Zvartau, E. E. (1999). Actions of caffeine in the brain with special reference to factors that contribute to its widespread use. *Pharmacol. Rev.* 51, 83–133.

Freeman, J. M., and Kossoff, E. H. (2010). Ketosis and the ketogenic diet, 2010: advances in treating epilepsy and other disorders. *Adv. Pediatr.* 57, 315–329. doi: 10.1016/j.yapd.2010.08.003

French, J. A. (2007). Refractory epilepsy: clinical overview. *Epilepsia* 48, 3–7. doi: 10.1111/j.1528-1167.2007.00992.x

Genazzani, A. R., Petraglia, F., Bernardi, F., Casarosa, E., Salvestroni, C., Tonetti, A., et al. (1998). Circulating levels of allopregnanolone in humans: gender, age, and endocrine influences. *J. Clin. Endocrinol. Metab.* 83, 2099–2103. doi: 10.1210/jcem.83.6.4905

Giampietro, P. F., Schowalter, D. B., Merchant, S., Campbell, L. R., Swink, T., and Roa, B. B. (2006). Widened clinical spectrum of the Q128P MECP2 mutation in Rett syndrome. *Childs Nerv. Syst.* 22, 320–324. doi: 10.1007/s00381-005-1155-z

Goodkin, H. P., Joshi, S., Mtchedlishvili, Z., Brar, J., and Kapur, J. (2008). Subunit-specific trafficking of GABA(A) receptors during status epilepticus. *J. Neurosci.* 28, 2527–2538. doi: 10.1523/JNEUROSCI.3426-07.2008

Govindpani, K., Calvo-Flores Guzmán, B., Vinnakota, C., Waldvogel, H. J., Faull, R. L., and Kwakowsky, A. (2017). Towards a better understanding of GABAergic remodeling in alzheimer's disease. *Int. J. Mol. Sci.* 18:1813. doi: 10.3390/ijms18081813

Greenfield, L. J. (2013). Molecular mechanisms of antiseizure drug activity at GABAA receptors. *Seizure* 22, 589–600. doi: 10.1016/j.seizure.2013.04.015

Grobin, A. C., and Morrow, A. L. (2001). 3Alpha-hydroxy-5alpha-pregnan-20-one levels and GABA(A) receptor-mediated 36Cl(-) flux across development in rat cerebral cortex. *Brain Res. Dev. Brain Res.* 131, 31–39.

Gulinello, M., Gong, Q. H., Li, X., and Smith, S. S. (2001). Short-term exposure to a neuroactive steroid increases alpha4 GABA(A) receptor subunit levels in association with increased anxiety in the female rat. *Brain Res.* 910, 55–66.

Guy, J., Gan, J., Selfridge, J., Cobb, S., and Bird, A. (2007). Reversal of neurological defects in a mouse model of Rett syndrome. *Science* 315, 1143–1147. doi: 10.1126/science.1138389

Haas, R. H., Rice, M. A., Trauner, D. A., Merritt, T. A., Opitz, J. M., and Reynolds, J. F. (1986). Therapeutic effects of a ketogenic diet in Rett syndrome. *Am. J. Med. Genet.* 25, 225–246. doi: 10.1002/ajmg.1320250525

Hagberg, B. (2002). Clinical manifestations and stages of Rett syndrome. *Ment. Retardat. Dev. Disabil. Res. Rev.* 8, 61–65. doi: 10.1002/mrdd.10020

Hampson, A. J., Grimaldi, M., Lolic, M., Wink, D., Rosenthal, R., and Axelrod, J. (2000). Neuroprotective antioxidants from marijuana. *Ann. N.Y. Acad. Sci.* 899, 274–282.

Hanefeld, F. (1985). The clinical pattern of the Rett syndrome. *Brain Dev.* 7, 320–325.

Harigaya, Y., Shoji, M., Shirao, T., and Hirai, S. (1996). Disappearance of actin-binding protein, drebrin, from hippocampal synapses in Alzheimer's disease. *J. Neurosci. Res.* 43, 87–92. doi: 10.1002/jnr.490430111

Harrison, N. L., and Simmonds, M. A. (1984). Modulation of the GABA receptor complex by a steroid anaesthetic. *Brain Res.* 323, 287–292.

Hartman, A. L., Gasior, M., Vining, E. P. G., and Rogawski, M. A. (2007). The neuropharmacology of the ketogenic diet. *Pediatr. Neurol.* 36, 281–292. doi: 10.1016/j.pediatrneurol.2007.02.008

Hassan, A. M., Keene, D. L., Whiting, S. E., Jacob, P. J., Champagne, J. R., and Humphreys, P. (1999). Ketogenic diet in the treatment of refractory epilepsy in childhood. *Pediatr. Neurol.* 21, 548–552.

Hill, T. D. M., Cascio, M.-G., Romano, B., Duncan, M., Pertwee, R. G., Williams, C. M., et al. (2013). Cannabidivarin-rich cannabis extracts are anticonvulsant in mouse and rat via a CB1 receptor-independent mechanism. *Br. J. Pharmacol.* 170, 679–692. doi: 10.1111/bph.12321

Hogart, A., Nagarajan, R. P., Patzel, K. A., Yasui, D. H., and LaSalle, J. M. (2007). 15q11-13 GABAA receptor genes are normally biallelically expressed in brain yet are subject to epigenetic dysregulation in autism-spectrum disorders. *Hum. Mol. Genet.* 16, 691–703. doi: 10.1093/hmg/ddm014

Hosie, A. M., Wilkins, M. E., da Silva, H. M. A., and Smart, T. G. (2006). Endogenous neurosteroids regulate GABAA receptors through two discrete transmembrane sites. *Nature* 444, 486–489. doi: 10.1038/nature05324

Hu, J., Zhang, Z., Shen, W.-J., and Azhar, S. (2010). Cellular cholesterol delivery, intracellular processing and utilization for biosynthesis of steroid hormones. *Nutr. Metab.* 7:47. doi: 10.1186/1743-7075-7-47

Huppke, P., Laccone, F., Krämer, N., Engel, W., and Hanefeld, F. (2000). Rett syndrome: analysis of MECP2 and clinical characterization of 31 patients. *Hum. Mol. Genet.* 9, 1369–1375.

Huttenlocher, P. R. (1976). Ketonemia and seizures: metabolic and anticonvulsant effects of two ketogenic diets in childhood epilepsy. *Pediatr. Res.* 10, 536–540. doi: 10.1203/00006450-197605000-00006

Iannotti, F. A., Hill, C. L., Leo, A., Alhusaini, A., Soubrane, C., Mazzarella, E., et al. (2014). Nonpsychotropic plant cannabinoids, cannabidivarin (CBDV) and cannabidiol (CBD), activate and desensitize transient receptor potential vanilloid 1 (TRPV1) channels in vitro: potential for the treatment of neuronal hyperexcitability. *ACS Chem. Neurosci.* 5, 1131–1141. doi: 10.1021/cn5000524

Iseger, T. A., and Bossong, M. G. (2015). A systematic review of the antipsychotic properties of cannabidiol in humans. *Schizophr Res.* 162, 153–161. doi: 10.1016/j.schres.2015.01.033

Ito-Ishida, A., Ure, K., Chen, H., Swann, J. W., and Zoghbi, H. Y. (2015). Loss of MeCP2 in parvalbumin-and somatostatin-expressing neurons in mice leads to distinct Rett syndrome-like phenotypes. *Neuron* 88, 651–658. doi: 10.1016/j.neuron.2015.10.029

Iuvone, T., Esposito, G., De Filippis, D., Scuderi, C., and Steardo, L. (2009). Cannabidiol: a promising drug for neurodegenerative disorders? *CNS Neurosci. Ther.* 15, 65–75. doi: 10.1111/j.1755-5949.2008.00065.x

Jacob, F. D., Ramaswamy, V., Andersen, J., and Bolduc, F. V. (2009). Atypical Rett syndrome with selective FOXG1 deletion detected by comparative genomic hybridization: case report and review of literature. *Eur. J. Hum. Genet.* 17, 1577–1581. doi: 10.1038/ejhg.2009.95

Jellinger, K., Armstrong, D., Zoghbi, H. Y., and Percy, A. K. (1988). Neuropathology of Rett syndrome. *Acta Neuropathol.* 76, 142–158. doi: 10.1007/BF00688098

Jenniches, I., Ternes, S., Albayram, O., Otte, D. M., Bach, K., Bindila, L., et al. (2016). Anxiety, stress, and fear response in mice with reduced endocannabinoid levels. *Biol. Psychiatry* 79, 858–868. doi: 10.1016/j.biopsych.2015.03.033

Jin, X., Cui, N., Zhong, W., Jin, X.-T., and Jiang, C. (2013a). GABAergic synaptic inputs of locus coeruleus neurons in wild-type and Mecp2-null mice. *Am. J. Physiol. Cell Physiol.* 304, C844–C857. doi: 10.1152/ajpcell.00399.2012

Jin, X., Zhong, W., and Jiang, C. (2013b). Time-dependent modulation of GABAA-ergic synaptic transmission by allopregnanolone in locus coeruleus neurons of Mecp2-null mice. *Am. J. Physiol. Cell Physiol.* 305, C1151–C1160. doi: 10.1152/ajpcell.00195.2013

Johansson, I.-M., Birzniece, V., Lindblad, C., Olsson, T., and Bäckström, T. (2002). Allopregnanolone inhibits learning in the morris water maze. *Brain Res.* 934, 125–131. doi: 10.1016/S0006-8993(02)02414-9

Jones, N. A., Glyn, S. E., Akiyama, S., Hill, T. D. M., Hill, A. J., Weston, S. E., et al. (2012). Cannabidiol exerts anti-convulsant effects in animal models of temporal lobe and partial seizures. *Seizure* 21, 344–352. doi: 10.1016/j.seizure.2012.03.001

Jones, N. A., Hill, A. J., Smith, I., Bevan, S. A., Williams, C. M., Whalley, B. J., et al. (2010). Cannabidiol displays antiepileptiform and antiseizure properties in vitro and in vivo. *J. Pharmacol. Exp. Ther.* 332, 569–577. doi: 10.1124/jpet.109.159145

Juge, N., Gray, J. A., Omote, H., Miyaji, T., Inoue, T., Hara, C., et al. (2010). Metabolic control of vesicular glutamate transport and release. *Neuron* 68, 99–112. doi: 10.1016/j.neuron.2010.09.002

Justice, M. J., Buchovecky, C. M., Kyle, S. M., and Djukic, A. (2013). A role for metabolism in Rett syndrome pathogenesis: new clinical findings and potential treatment targets. *Rare Dis.* 1:e27265. doi: 10.4161/rdis.27265

Kaminski, R. M., Livingood, M. R., and Rogawski, M. A. (2004). Allopregnanolone analogs that positively modulate GABA receptors protect against partial seizures induced by 6-Hz electrical stimulation in mice. *Epilepsia* 45, 864–867. doi: 10.1111/j.0013-9580.2004.04504.x

Kano, M., Ohno-Shosaku, T., Hashimotodani, Y., Uchigashima, M., and Watanabe, M. (2009). Endocannabinoid-mediated control of synaptic transmission. *Physiol. Rev.* 89, 309–380. doi: 10.1152/physrev.00019.2008

Kaplan, J. S., Stella, N., Catterall, W. A., and Westenbroek, R. E. (2017). Cannabidiol attenuates seizures and social deficits in a mouse model of dravet syndrome. *PNAS* 114, 11229–11234. doi: 10.1073/pnas.1711351114

Kasprowska-Liśkiewicz, D., Liśkiewicz, A. D., Nowacka-Chmielewska, M. M., Nowicka, J., Małecki, A., and Barski, J. J. (2017). The ketogenic diet affects the social behavior of young male rats. *Physiol. Behav.* 179, 168–177. doi: 10.1016/j.physbeh.2017.06.007

Katz, D. M. (2014). "Brain-Derived Neurotrophic Factor and Rett Syndrome," in *Neurotrophic Factors Handbook of Experimental Pharmacology*, eds G. R. Lewin and B. D. Carter (Heidelberg: Springer), 481–495.

Kawamura, M., Ruskin, D. N., and Masino, S. A. (2010). Metabolic autocrine regulation of neurons involves cooperation among pannexin hemichannels, adenosine receptors, and KATP channels. *J. Neurosci.* 30, 3886–3895. doi: 10.1523/JNEUROSCI.0055-10.2010

Kim, D. Y., Simeone, K. A., Simeone, T. A., Pandya, J. D., Wilke, J. C., Ahn, Y., et al. (2015). Ketone bodies mediate anti-seizure effects through mitochondrial permeability transition. *Ann. Neurol.* 78, 77–87. doi: 10.1002/ana.24424

Kim, Y. S., and Yoon, B.-E. (2017). Altered GABAergic signaling in brain disease at various stages of life. *Exp. Neurobiol.* 26:122. doi: 10.5607/en.2017.26.3.122

Krajnc, N. (2015). Management of epilepsy in patients with Rett syndrome: perspectives and considerations. *Therapeu. Clin. Risk Manag.* 11, 925–932. doi: 10.2147/TCRM.S55896

Kramar, C., Loureiro, M., Renard, J., and Laviolette, S. R. (2017). Palmitoylethanolamide modulates GPR55 receptor signaling in the ventral hippocampus to regulate mesolimbic dopamine activity, social interaction, and memory processing. *Cannabis Cannabinoid Res.* 2, 8–20. doi: 10.1089/can.2016.0030

Kwakowsky, A., Calvo-Flores Guzmán, B., Pandya, M., Turner, C., Waldvogel, H. J., and Faull, R. L. (2018). GABAA receptor subunit expression changes in the human Alzheimer's disease hippocampus, subiculum, entorhinal cortex and superior temporal gyrus. *J. Neurochem.* 145, 374–392. doi: 10.1111/jnc.14325

Kyle, S. M., Vashi, N., and Justice, M. J. (2018). Rett syndrome: a neurological disorder with metabolic components. *Open Biol.* 8:170216. doi: 10.1098/rsob.170216

Laprairie, R. B., Bagher, A. M., Kelly, M. E. M., and Denovan-Wright, E. M. (2015). Cannabidiol is a negative allosteric modulator of the cannabinoid CB 1 receptor: negative allosteric modulation of CB 1 by cannabidiol. *Br. J. Pharmacol.* 172, 4790–4805. doi: 10.1111/bph.13250

Lauckner, J. E., Jensen, J. B., Chen, H.-Y., Lu, H.-C., Hille, B., and Mackie, K. (2008). GPR55 is a cannabinoid receptor that increases intracellular calcium and inhibits M current. *Proc. Natl. Acad. Sci. U.S.A.* 105, 2699–2704. doi: 10.1073/pnas.0711278105

Lee, R. W. Y., and Tierney, E. (2011). Hypothesis: the role of sterols in autism spectrum disorder. *Autism Res. Treat.* 2011, 1–7. doi: 10.1155/2011/653570

Li, W., and Pozzo-Miller, L. (2014). BDNF deregulation in Rett syndrome. *Neuropharmacology* 76(Pt C), 737–746. doi: 10.1016/j.neuropharm.2013.03.024

Li, Y., Sun, H., Chen, Z., Xu, H., Bu, G., and Zheng, H. (2016). Implications of GABAergic Neurotransmission in Alzheimer's Disease. *Front Aging Neurosci.* 8:31. doi: 10.3389/fnagi.2016.00031

Liebhaber, G. M., Riemann, E., and Matthias Baumeister, F. A. (2003). Ketogenic diet in Rett syndrome. *J. Child Neurol.* 18, 74–75. doi: 10.1177/08830738030180011801

Ligsay, A., Van Dijck, A., Nguyen, D. V., Lozano, R., Chen, Y., Bickel, E. S., et al. (2017). A randomized double-blind, placebo-controlled trial of ganaxolone in children and adolescents with fragile X syndrome. *J. Neurodev. Disord.* 9:26. doi: 10.1186/s11689-017-9207-8

Liu, Q., and Wong-Riley, M. T. T. (2010). Postnatal development of N-methyl-D-aspartate receptor subunits 2A, 2B, 2C, 2D, and 3B immunoreactivity in brain stem respiratory nuclei of the rat. *Neuroscience* 171, 637–654. doi: 10.1016/j.neuroscience.2010.09.055

Loewe, S. (1946). Studies on the pharmacology and acute toxicity of compounds with marihuana activity. *J. Pharmacol. Exp. Ther.* 88, 154–161.

Löscher, W. (1989). Valproate enhances GABA turnover in the substantia nigra. *Brain Res.* 501, 198–203.

Lozovaya, N., Eftekhari, S., Cloarec, R., Gouty-Colomer, L. A., Dufour, A., Riffault, B., et al. (2018). GABAergic inhibition in dual-transmission cholinergic and GABAergic striatal interneurons is abolished in

Parkinson disease. *Nat. Commun.* 9:1422. doi: 10.1038/s41467-018-03802-y

Lund, E. G., Xie, C., Kotti, T., Turley, S. D., Dietschy, J. M., and Russell, D. W. (2003). Knockout of the cholesterol 24-hydroxylase gene in mice reveals a brain-specific mechanism of cholesterol turnover. *J. Biol. Chem.* 278, 22980–22988. doi: 10.1074/jbc.M303415200

Maa, E., and Figi, P. (2014). The case for medical marijuana in epilepsy. *Epilepsia* 55, 783–786. doi: 10.1111/epi.12610

Macdonald, R., and Barker, J. L. (1978). Benzodiazepines specifically modulate GABA-mediated postsynaptic inhibition in cultured mammalian neurones. *Nature* 271, 563–564.

Maitra, R., and Reynolds, J. N. (1999). Subunit dependent modulation of GABAA receptor function by neuroactive steroids. *Brain Res.* 819, 75–82.

Majewska, M. D., Harrison, N. L., Schwartz, R. D., Barker, J. L., and Paul, S. M. (1986). Steroid hormone metabolites are barbiturate-like modulators of the GABA receptor. *Science* 232, 1004–1007.

Malfait, A. M., Gallily, R., Sumariwalla, P. F., Malik, A. S., Andreakos, E., Mechoulam, R., et al. (2000). The nonpsychoactive cannabis constituent cannabidiol is an oral anti-arthritic therapeutic in murine collagen-induced arthritis. *PNAS* 97, 9561–9566. doi: 10.1073/pnas.160105897

Mantis, J. G., Centeno, N. A., Todorova, M. T., McGowan, R., and Seyfried, T. N. (2004). Management of multifactorial idiopathic epilepsy in EL mice with caloric restriction and the ketogenic diet: role of glucose and ketone bodies. *Nutr. Metab.* 1:11. doi: 10.1186/1743-7075-1-11

Mantis, J. G., Fritz, C. L., Marsh, J., Heinrichs, S. C., and Seyfried, T. N. (2009). Improvement in motor and exploratory behavior in Rett syndrome mice with restricted ketogenic and standard diets. *Epilepsy Behav.* 15, 133–141. doi: 10.1016/j.yebeh.2009.02.038

Marcos, J., Guo, L.-W., Wilson, W. K., Porter, F. D., and Shackleton, C. (2004). The implications of 7-dehydrosterol-7-reductase deficiency (smith-lemli-opitz syndrome) to neurosteroid production. *Steroids* 69, 51–60.

Mari, F., Azimonti, S., Bertani, I., Bolognese, F., Colombo, E., Caselli, R., et al. (2005). CDKL5 belongs to the same molecular pathway of MeCP2 and it is responsible for the early-onset seizure variant of Rett syndrome. *Hum. Mol. Genet.* 14, 1935–1946. doi: 10.1093/hmg/ddi198

Marichal-Cancino, B. A., Fajardo-Valdez, A., Ruiz-Contreras, A. E., Méndez-Díaz, M., and Prospéro-García, O. (2018). Possible role of hippocampal GPR55 in spatial learning and memory in rats. *Acta Neurobiol. Exp.* 78, 41–50. doi: 10.21307/ane-2018-001

Marsicano, G., and Lafenêtre, P. (2009). "Roles of the Endocannabinoid System in Learning and Memory," in *Behavioral Neurobiology of the Endocannabinoid System*, eds D. Kendall and S. Alexander (Berlin: Springer), 201–230.

Marx, C. E., Stevens, R. D., Shampine, L. J., Uzunova, V., Trost, W. T., Butterfield, M. I., et al. (2006). Neuroactive steroids are altered in schizophrenia and bipolar disorder: relevance to pathophysiology and therapeutics. *Neuropsychopharmacology* 31, 1249–1263. doi: 10.1038/sj.npp.1300952

Mascia, M. P., Biggio, F., Mancuso, L., Cabras, S., Cocco, P. L., Gorini, G., et al. (2002). Changes in GABA(A) receptor gene expression induced by withdrawal of, but not by long-term exposure to, ganaxolone in cultured rat cerebellar granule cells. *J. Pharmacol. Exp. Ther.* 303, 1014–1020. doi: 10.1124/jpet.102.040063

Masino, S. A., Kawamura, M., Cote, J. L., Williams, R. B., and Ruskin, D. N. (2013). Adenosine and autism: a spectrum of opportunities. *Neuropharmacology* 68, 116–121. doi: 10.1016/j.neuropharm.2012.08.013

Masino, S. A., Li, T., Theofilas, P., Sandau, U. S., Ruskin, D. N., Fredholm, B. B., et al. (2011). A ketogenic diet suppresses seizures in mice through adenosine A_1 receptors. *J. Clin. Invest.* 121, 2679–2683. doi: 10.1172/JCI57813

Matthews, D. B., Morrow, A. L., Tokunaga, S., and McDaniel, J. R. (2002). Acute ethanol administration and acute allopregnanolone administration impair spatial memory in the Morris water task. *Alcohol. Clin. Exp. Res.* 26, 1747–1751. doi: 10.1097/01.ALC.0000037219.79257.17

McGraw, C. M., Samaco, R. C., and Zoghbi, H. Y. (2011). Adult neural function requires MeCP2. *Science* 333, 186–186. doi: 10.1126/science.1206593

Medrihan, L., Tantalaki, E., Aramuni, G., Sargsyan, V., Dudanova, I., Missler, M., et al. (2008). Early defects of GABAergic synapses in the brain stem of a MeCP2 mouse model of Rett syndrome. *J. Neurophysiol.* 99, 112–121. doi: 10.1152/jn.00826.2007

Meera, P., Wallner, M., and Otis, T. S. (2011). Molecular basis for the high THIP/gaboxadol sensitivity of extrasynaptic GABA(A) receptors. *J. Neurophysiol.* 106, 2057–2064. doi: 10.1152/jn.00450.2011

Meidenbauer, J. J., Mantis, J. G., and Seyfried, T. N. (2011). The EL mouse: a natural model of autism and epilepsy. *Epilepsia* 52, 347–357. doi: 10.1111/j.1528-1167.2010.02898.x

Melcangi, R. C., Garcia-Segura, L. M., and Mensah-Nyagan, A. G. (2008). Neuroactive steroids: state of the art and new perspectives. *Cell. Mol. Life Sci.* 65, 777–797. doi: 10.1007/s00018-007-7403-5

Melcangi, R. C., Giatti, S., Calabrese, D., Pesaresi, M., Cermenati, G., Mitro, N., et al. (2014). Levels and actions of progesterone and its metabolites in the nervous system during physiological and pathological conditions. *Prog. Neurobiol.* 113, 56–69. doi: 10.1016/j.pneurobio.2013.07.006

Meletti, S., Lucchi, C., Monti, G., Giovannini, G., Bedin, R., Trenti, T., et al. (2017). Decreased allopregnanolone levels in cerebrospinal fluid obtained during status epilepticus. *Epilepsia* 58, e16–e20. doi: 10.1111/epi.13625

Meletti, S., Lucchi, C., Monti, G., Giovannini, G., Bedin, R., Trenti, T., et al. (2018). Low levels of progesterone and derivatives in cerebrospinal fluid of patients affected by status epilepticus. *J. Neurochem.* 147, 275–284. doi: 10.1111/jnc.14550

Mellédo, J.-M. L., and Baker, G. B. (2002). Neuroactive steroids and anxiety disorders. *J. Psychiatry Neurosci.* 27, 161–165.

Mellon, S. H. (2007). Neurosteroid regulation of central nervous system development. *Pharmacol. Ther.* 116, 107–124. doi: 10.1016/j.pharmthera.2007.04.011

Mersiades, A. J., Tognela, A., Haber, P. S., Stockler, M., Lintzeris, N., Simes, J., et al. (2018). Oral cannabinoid-rich THC/CBD cannabis extract for secondary prevention of chemotherapy-induced nausea and vomiting: a study protocol for a pilot and definitive randomised double-blind placebo-controlled trial (CannabisCINV). *BMJ Open* 8:e020745. doi: 10.1136/bmjopen-2017-020745

Misane, I., Kruis, A., Pieneman, A. W., Ögren, S. O., and Stiedl, O. (2013). GABA(A) receptor activation in the CA1 area of the dorsal hippocampus impairs consolidation of conditioned contextual fear in C57BL/6J mice. *Behav. Brain Res.* 238, 160–169. doi: 10.1016/j.bbr.2012.10.027

Morales, P., Hurst, D. P., and Reggio, P. H. (2017). "Molecular Targets of the Phytocannabinoids: A Complex Picture," in *Phytocannabinoids*, eds A. D. Kinghorn, H. Falk, S. Gibbons, and J. Kobayashi (Cham: Springer International Publishing), 103–131.

Moretti, P., and Zoghbi, H. Y. (2006). MeCP2 dysfunction in Rett syndrome and related disorders. *Curr. Opin. Genet. Dev.* 16, 276–281. doi: 10.1016/j.gde.2006.04.009

Nagarkatti, P., Pandey, R., Rieder, S. A., Hegde, V. L., and Nagarkatti, M. (2009). Cannabinoids as novel anti-inflammatory drugs. *Future Med. Chem.* 1, 1333–1349. doi: 10.4155/fmc.09.93

Nagy, G., and Ackerman, S. L. (2013). Cholesterol metabolism and Rett syndrome pathogenesis. *Nat. Genet.* 45, 965–967. doi: 10.1038/ng.2738

Navarro, G., Borroto-Escuela, D., Angelats, E., Etayo, Í, Reyes-Resina, I., Pulido-Salgado, M., et al. (2018). Receptor-heteromer mediated regulation of endocannabinoid signaling in activated microglia. role of CB1 and CB2 receptors and relevance for Alzheimer's disease and levodopa-induced dyskinesia. *Brain Behav. Immun.* 67, 139–151. doi: 10.1016/j.bbi.2017.08.015

Neal, E. G., Chaffe, H., Schwartz, R. H., Lawson, M. S., Edwards, N., Fitzsimmons, G., et al. (2008). The ketogenic diet for the treatment of childhood epilepsy: a randomised controlled trial. *Lancet Neurol.* 7, 500–506. doi: 10.1016/S1474-4422(08)70092-9

Neul, J. L., Kaufmann, W. E., Glaze, D. G., Christodoulou, J., Clarke, A. J., Bahi-Buisson, N., et al. (2010). Rett syndrome: revised diagnostic criteria and nomenclature. *Ann. Neurol.* 68, 944–950. doi: 10.1002/ana.22124

Neul, J. L., and Zoghbi, H. Y. (2004). Rett syndrome: a prototypical neurodevelopmental disorder. *Neuroscientist* 10, 118–128. doi: 10.1177/1073858403260995

Nguyen, M. V. C., Du, F., Felice, C. A., Shan, X., Nigam, A., Mandel, G., et al. (2012). MeCP2 is critical for maintaining mature neuronal networks and global brain anatomy during late stages of postnatal brain development and in the mature adult brain. *J. Neurosci.* 32, 10021–10034. doi: 10.1523/JNEUROSCI.1316-12.2012

Novotna, A., Mares, J., Ratcliffe, S., Novakova, I., Vachova, M., Zapletalova, O., et al. (2011). A randomized, double-blind, placebo-controlled, parallel-group,

enriched-design study of nabiximols* (sativex), as add-on therapy, in subjects with refractory spasticity caused by multiple sclerosis: Sativex for refractory spasticity in MS. *Eur. J. Neurol.* 18, 1122–1131. doi: 10.1111/j.1468-1331.2010.03328.x

O'Connell, B. K., Gloss, D., and Devinsky, O. (2017). Cannabinoids in treatment-resistant epilepsy: a review. *Epilepsy Behav.* 70, 341–348. doi: 10.1016/j.yebeh.2016.11.012

Onaivi, E. S., Ishiguro, H., Gu, S., and Liu, Q.-R. (2012). CNS effects of CB2 cannabinoid receptors: beyond neuro-immuno-cannabinoid activity. *J. Psychopharmacol.* 26, 92–103. doi: 10.1177/0269881111400652

Pamplona, F. A., and Coan, A. C. (2017). Potential clinical benefits of CBD-rich cannabis extracts over purified CBD in treatment-resistant epilepsy: observational data meta-analysis. *bioRxiv* doi: 10.1101/212662

Paoletti, A. M., Romagnino, S., Contu, R., Orrù, M. M., Marotto, M. F., Zedda, P., et al. (2006). Observational study on the stability of the psychological status during normal pregnancy and increased blood levels of neuroactive steroids with GABA-A receptor agonist activity. *Psychoneuroendocrinology* 31, 485–492. doi: 10.1016/j.psyneuen.2005.11.006

Park, H.-M., Choi, I.-S., Nakamura, M., Cho, J.-H., Lee, M.-G., and Jang, I.-S. (2011). Multiple effects of allopregnanolone on GABAergic responses in single hippocampal CA3 pyramidal neurons. *Eur. J. Pharmacol.* 652, 46–54. doi: 10.1016/j.ejphar.2010.10.097

Parker, L. A., Rock, E. M., and Limebeer, C. L. (2011). Regulation of nausea and vomiting by cannabinoids. *Br. J. Pharmacol.* 163, 1411–1422. doi: 10.1111/j.1476-5381.2010.01176.x

Pascual, D., Sánchez-Robles, E. M., García, M. M., and Goicoechea, C. (2018). Chronic pain and cannabinoids. great expectations or a christmas carol. *Biochem. Pharmacol.* 157, 33–42. doi: 10.1016/j.bcp.2018.07.033

Patankar, J. V. (2014). Cholesterol metabolism is a potential therapeutic target for Rett syndrome. *Clin. Genet.* 85, 229–230. doi: 10.1111/cge.12284

Patra, P. H., Barker-Haliski, M., White, H. S., Whalley, B. J., Glyn, S., Sandhu, H., et al. (2019). Cannabidiol reduces seizures and associated behavioral comorbidities in a range of animal seizure and epilepsy models. *Epilepsia* 60, 303–314. doi: 10.1111/epi.14629

Percy, A. K. (2016). Progress in Rett Syndrome: from discovery to clinical trials. *Wien. Med. Wochensch.* 166, 325–332. doi: 10.1007/s10354-016-0491-9

Pertwee, R. G. (2009). Cannabinoid pharmacology: the first 66 years: cannabinoid pharmacology. *Br. J. Pharmacol.* 147, S163–S171. doi: 10.1038/sj.bjp.0706406

Perucca, E. (2017). Cannabinoids in the treatment of epilepsy: hard evidence at last? *J Epilepsy Res.* 7, 61–76. doi: 10.14581/jer.17012

Peterman, M. G. (1924). The ketogenic diet in the treatment of epilepsy: a preliminary report. *Am. J. Dis. Child* 28, 28–33. doi: 10.1001/archpedi.1924.04120190031004

Petrosino, S., Verde, R., Vaia, M., Allarà, M., Iuvone, T., and Di Marzo, V. (2018). Anti-inflammatory properties of cannabidiol, a nonpsychotropic cannabinoid, in experimental allergic contact dermatitis. *J. Pharmacol. Exp. Ther.* 365, 652–663. doi: 10.1124/jpet.117.244368

Pfrieger, F. W., and Ungerer, N. (2011). Cholesterol metabolism in neurons and astrocytes. *Prog. Lipid Res.* 50, 357–371. doi: 10.1016/j.plipres.2011.06.002

Porter, F. D. (2002). Malformation syndromes due to inborn errors of cholesterol synthesis. *J. Clin. Invest.* 110, 715–724. doi: 10.1172/JCI16386

Puia, G., Duciæ, I., Vicini, S., and Costa, E. (1993). Does neurosteroid modulatory efficacy depend on GABAA receptor subunit composition? *Recept. Channels* 1, 135–142.

Puia, G., Mienville, J.-M., Matsumoto, K., Takahata, H., Watanabe, H., Costa, E., et al. (2003). On the putative physiological role of allopregnanolone on GABA(A) receptor function. *Neuropharmacology* 44, 49–55.

Rabinowitz, A., Cohen, S. J., Finn, D. A., and Stackman, R. W. (2014). The neurosteroid allopregnanolone impairs object memory and contextual fear memory in male C57BL/6J mice. *Horm Behav.* 66, 238–246. doi: 10.1016/j.yhbeh.2014.05.005

Ramocki, M. B., Peters, S. U., Tavyev, Y. J., Zhang, F., Carvalho, C. M. B., Schaaf, C. P., et al. (2009). Autism and other neuropsychiatric symptoms are prevalent in individuals with MeCP2 duplication syndrome. *Ann. Neurol.* 66, 771–782. doi: 10.1002/ana.21715

Reddy, D. S. (2010). *"Neurosteroids," in Progress in Brain Research*. Amsterdam: Elsevier.

Reddy, D. S. (2011). Role of anticonvulsant and antiepileptogenic neurosteroids in the pathophysiology and treatment of epilepsy. *Front. Endocrinol.* 2:38. doi: 10.3389/fendo.2011.00038

Reddy, D. S., and Estes, W. A. (2016). Clinical potential of neurosteroids for CNS disorders. *Trends Pharmacol. Sci.* 37, 543–561. doi: 10.1016/j.tips.2016.04.003

Reddy, D. S., and Jian, K. (2010). The testosterone-derived neurosteroid androstanediol is a positive allosteric modulator of GABAA receptors. *J. Pharmacol. Exp. Ther.* 334, 1031–1041. doi: 10.1124/jpet.110.169854

Renieri, A., Mari, F., Mencarelli, M. A., Scala, E., Ariani, F., Longo, I., et al. (2009). Diagnostic criteria for the Zappella variant of Rett syndrome (the preserved speech variant). *Brain Dev.* 31, 208–216. doi: 10.1016/j.braindev.2008.04.007

Rett, A. (1966). [On a unusual brain atrophy syndrome in hyperammonemia in childhood]. *Wien. Med. Wochenschr.* 116, 723–726.

Rice, J., and Cameron, M. (2018). Cannabinoids for treatment of MS symptoms: state of the evidence. *Curr. Neurol. Neurosci. Rep.* 18:50. doi: 10.1007/s11910-018-0859-x

Riss, J., Cloyd, J., Gates, J., and Collins, S. (2008). Benzodiazepines in epilepsy: pharmacology and pharmacokinetics. *Acta Neurol. Scand.* 118, 69–86. doi: 10.1111/j.1600-0404.2008.01004.x

Rissman, R. A., and Mobley, W. C. (2011). Implications for treatment: GABAA receptors in aging, down syndrome and Alzheimer's disease. *J. Neurochem.* 117, 613–622. doi: 10.1111/j.1471-4159.2011.07237.x

Rock, E. M., and Parker, L. A. (2016). Cannabinoids as potential treatment for chemotherapy-induced nausea and vomiting. *Front. Pharmacol.* 7:221. doi: 10.3389/fphar.2016.00221

Rogawski, M. A., Löscher, W., and Rho, J. M. (2016). Mechanisms of action of antiseizure drugs and the ketogenic diet. *Cold Spring Harb. Perspect. Med.* 6:a022780. doi: 10.1101/cshperspect.a022780

Rogawski, M. A., Loya, C. M., Reddy, K., Zolkowska, D., and Lossin, C. (2013). Neuroactive steroids for the treatment of status epilepticus. *Epilepsia* 54(Suppl. 6), 93–98. doi: 10.1111/epi.12289

Rolando, S. (1985). Rett syndrome: report of eight cases. *Brain Dev.* 7, 290–296.

Rombo, D. M., Ribeiro, J. A., and Sebastião, A. M. (2016). Hippocampal GABAergic transmission: a new target for adenosine control of excitability. *J. Neurochem.* 139, 1056–1070. doi: 10.1111/jnc.13872

Rosenthal, E. S., Claassen, J., Wainwright, M. S., Husain, A. M., Vaitkevicius, H., Raines, S., et al. (2017). Brexanolone as adjunctive therapy in super-refractory status epilepticus. *Ann. Neurol.* 82, 342–352. doi: 10.1002/ana.25008

Rosenthaler, S., Pöhn, B., Kolmanz, C., Huu, C. N., Krewenka, C., Huber, A., et al. (2014). Differences in receptor binding affinity of several phytocannabinoids do not explain their effects on neural cell cultures. *Neurotoxicol. Teratol.* 46, 49–56. doi: 10.1016/j.ntt.2014.09.003

Rossetti, M. F., Varayoud, J., Moreno-Piovano, G. S., Luque, E. H., and Ramos, J. G. (2015). Environmental enrichment attenuates the age-related decline in the mRNA expression of steroidogenic enzymes and reduces the methylation state of the steroid 5α-reductase type 1 gene in the rat hippocampus. *Mol. Cell. Endocrinol.* 412, 330–338. doi: 10.1016/j.mce.2015.05.024

Ruskin, D. N., Fortin, J. A., Bisnauth, S. N., and Masino, S. A. (2017). Ketogenic diets improve behaviors associated with autism spectrum disorder in a sex-specific manner in the EL mouse. *Physiol. Behav.* 168, 138–145. doi: 10.1016/j.physbeh.2016.10.023

Ruskin, D. N., Ross, J. L., Kawamura, M., Ruiz, T. L., Geiger, J. D., and Masino, S. A. (2011). A ketogenic diet delays weight loss and does not impair working memory or motor function in the R6/2 1J mouse model of huntington's disease. *Physiol. Behav.* 103, 501–507. doi: 10.1016/j.physbeh.2011.04.001

Russo, E., and Guy, G. W. (2006). A tale of two cannabinoids: The therapeutic rationale for combining tetrahydrocannabinol and cannabidiol. *Med. Hypoth.* 66, 234–246. doi: 10.1016/j.mehy.2005.08.026

Samaco, R. C., Hogart, A., and LaSalle, J. M. (2005). Epigenetic overlap in autism-spectrum neurodevelopmental disorders: MECP2 deficiency causes reduced expression of UBE3A and GABRB3. *Hum. Mol. Genet.* 14, 483–492. doi: 10.1093/hmg/ddi045

Scala, E., Ariani, F., Mari, F., Caselli, R., Pescucci, C., Longo, I., et al. (2005). CDKL5/STK9 is mutated in Rett syndrome variant with infantile spasms. *J. Med. Genet.* 42, 103–107. doi: 10.1136/jmg.2004.026237

Sebastião, A. M., and Ribeiro, J. A. (2015). Neuromodulation and metamodulation by adenosine: impact and subtleties upon synaptic plasticity regulation. *Brain Res.* 1621, 102–113. doi: 10.1016/j.brainres.2014.11.008

Segatto, M., Trapani, L., Di Tunno, I., Sticozzi, C., Valacchi, G., Hayek, J., et al. (2014). Cholesterol metabolism is altered in Rett syndrome: a study on plasma and primary cultured fibroblasts derived from patients. *PLoS One* 9:e104834. doi: 10.1371/journal.pone.0104834

Selye, H. (1941). On the hormonal activity of a steroid compound. *Science* 94:94. doi: 10.1126/science.94.2430.94

Selye, H., and Masson, G. (1942). Additional steroids with luteoid activity. *Science* 96:358. doi: 10.1126/science.96.2494.358

Shahbazian, M. D. (2002). Insight into Rett syndrome: MeCP2 levels display tissue- and cell-specific differences and correlate with neuronal maturation. *Hum. Mol. Genet.* 11, 115–124. doi: 10.1093/hmg/11.2.115

Shen, H., Gong, Q. H., Aoki, C., Yuan, M., Ruderman, Y., Dattilo, M., et al. (2007). Reversal of neurosteroid effects at alpha4beta2delta GABAA receptors triggers anxiety at puberty. *Nat. Neurosci.* 10, 469–477. doi: 10.1038/nn1868

Shimizu, H., Ishizuka, Y., Yamazaki, H., and Shirao, T. (2015). Allopregnanolone increases mature excitatory synapses along dendrites via protein kinase A signaling. *Neuroscience* 305, 139–145. doi: 10.1016/j.neuroscience.2015.07.079

Shulyakova, N., Andreazza, A. C., Mills, L. R., and Eubanks, J. H. (2017). Mitochondrial dysfunction in the pathogenesis of Rett syndrome: implications for mitochondria-targeted therapies. *Front. Cell. Neurosci.* 11:58. doi: 10.3389/fncel.2017.00058

Sieghart, W. (2006). Structure, pharmacology, and function of GABAA receptor subtypes. *Adv. Pharmacol.* 54, 231–263.

Singh, C., Liu, L., Wang, J. M., Irwin, R. W., Yao, J., Chen, S., et al. (2012). Allopregnanolone restores hippocampal-dependent learning and memory and neural progenitor survival in aging 3xTgAD and nonTg mice. *Neurobiol. Aging* 33, 1493–1506. doi: 10.1016/j.neurobiolaging.2011.06.008

Smith, S. S. (2002). Withdrawal properties of a neuroactive steroid: implications for GABAA receptor gene regulation in the brain and anxiety behavior. *Steroids* 67, 519–528. doi: 10.1016/S0039-128X(01)00170-2

Solymosi, K., and Kofalvi, A. (2017). Cannabis: a treasure trove or pandora's box? *Mini Rev. Med. Chem.* 17, 1223–1291. doi: 10.2174/1389557516666161004162133

Stearns, N. A., Schaevitz, L. R., Bowling, H., Nag, N., Berger, U. V., and Berger-Sweeney, J. (2007). Behavioral and anatomical abnormalities in Mecp2 mutant mice: a model for Rett syndrome. *Neuroscience* 146, 907–921. doi: 10.1016/j.neuroscience.2007.02.009

Sticozzi, C., Belmonte, G., Pecorelli, A., Cervellati, F., Leoncini, S., Signorini, C., et al. (2013). Scavenger receptor B1 post-translational modifications in Rett syndrome. *FEBS Lett.* 587, 2199–2204. doi: 10.1016/j.febslet.2013.05.042

Stoffel-Wagner, B. (2003). Neurosteroid biosynthesis in the human brain and its clinical implications. *Ann. N. Y. Acad. Sci.* 1007, 64–78.

Talbot, F. B., Metcalf, K. M., and Moriarty, M. E. (1927). Epilepsy: chemical investigations of rational treatment by production of ketosis. *Am. J. Dis. Child.* 33, 218–225. doi: 10.1001/archpedi.1927.04130140038005

Thomas, A., Baillie, G. L., Phillips, A. M., Razdan, R. K., Ross, R. A., and Pertwee, R. G. (2009). Cannabidiol displays unexpectedly high potency as an antagonist of CB1 and CB2 receptor agonists in vitro: Cannabinoid antagonism by cannabidiol. *Br. J. Pharmacol.* 150, 613–623. doi: 10.1038/sj.bjp.0707133

Tietz, E. I., Zeng, X. J., Chen, S., Lilly, S. M., Rosenberg, H. C., and Kometiani, P. (1999). Antagonist-induced reversal of functional and structural measures of hippocampal benzodiazepine tolerance. *J. Pharmacol. Exp. Ther.* 291, 932–942.

Tint, G. S., Irons, M., Elias, E. R., Batta, A. K., Frieden, R., Chen, T. S., et al. (1994). Defective cholesterol biosynthesis associated with the Smith-Lemli-Opitz syndrome. *N. Engl. J. Med.* 330, 107–113. doi: 10.1056/NEJM199401133300205

Todorova, M. T., Tandon, P., Madore, R. A., Stafstrom, C. E., and Seyfried, T. N. (2000). The ketogenic diet inhibits epileptogenesis in EL mice: a genetic model for idiopathic epilepsy. *Epilepsia* 41, 933–940.

Turkmen, S., Lundgren, P., Birzniece, V., Zingmark, E., Backstrom, T., and Johansson, I.-M. (2004). 3β-20β-dihydroxy-5α-pregnane (UC1011) antagonism of the GABA potentiation and the learning impairment induced in rats by allopregnanolone. *Eur. J. Neurosci.* 20, 1604–1612. doi: 10.1111/j.1460-9568.2004.03610.x

Uhlemann, E. R., and Neims, A. H. (1972). Anticonvulsant properties of the ketogenic diet in mice. *J. Pharmacol. Exp. Ther.* 180, 231–238.

Ure, K., Lu, H., Wang, W., Ito-Ishida, A., Wu, Z., He, L., et al. (2016). Restoration of Mecp2 expression in GABAergic neurons is sufficient to rescue multiple disease features in a mouse model of Rett syndrome. *eLife* 5:e14198. doi: 10.7554/eLife.14198

Uusi-Oukari, M., and Korpi, E. R. (2010). Regulation of GABAA receptor subunit expression by pharmacological agents. *Pharmacol. Rev.* 62, 97–135. doi: 10.1124/pr.109.002063

Vaitkevicius, H., Husain, A. M., Rosenthal, E. S., Rosand, J., Bobb, W., Reddy, K., et al. (2017). First-in-man allopregnanolone use in super-refractory status epilepticus. *Ann. Clin. Transl. Neurol.* 4, 411–414. doi: 10.1002/acn3.408

Vaz, S. H., Lérias, S. R., Parreira, S., Diógenes, M. J., and Sebastião, A. M. (2015). Adenosine A2A receptor activation is determinant for BDNF actions upon GABA and glutamate release from rat hippocampal synaptosomes. *Purinerg. Signal* 11, 607–612. doi: 10.1007/s11302-015-9476-1

Vendel, E., and de Lange, E. C. M. (2014). Functions of the CB1 and CB2 receptors in neuroprotection at the level of the blood–brain barrier. *NeuroMol. Med.* 16, 620–642. doi: 10.1007/s12017-014-8314-x

Vigli, D., Cosentino, L., Raggi, C., Laviola, G., Woolley-Roberts, M., and De Filippis, B. (2018). Chronic treatment with the phytocannabinoid cannabidivarin (CBDV) rescues behavioural alterations and brain atrophy in a mouse model of Rett syndrome. *Neuropharmacology* 140, 121–129. doi: 10.1016/j.neuropharm.2018.07.029

Vining, E. P., Freeman, J. M., Ballaban-Gil, K., Camfield, C. S., Camfield, P. R., Holmes, G. L., et al. (1998). A multicenter study of the efficacy of the ketogenic diet. *Arch. Neurol.* 55, 1433–1437.

Voituron, N., and Hilaire, G. (2011). The benzodiazepine Midazolam mitigates the breathing defects of Mecp2-deficient mice. *Respir. Physiol. Neurobiol.* 177, 56–60. doi: 10.1016/j.resp.2011.02.002

Walton, J. C., McNeill, J. K., Oliver, K. A., and Albers, H. E. (2017). Temporal regulation of GABAA receptor subunit expression: role in synaptic and extrasynaptic communication in the suprachiasmatic nucleus. *eNeuro* 4:ENEURO.0352-16.2017. doi: 10.1523/ENEURO.0352-16.2017

Wang, J. M., Singh, C., Liu, L., Irwin, R. W., Chen, S., Chung, E. J., et al. (2010). Allopregnanolone reverses neurogenic and cognitive deficits in mouse model of Alzheimer's disease. *Proc. Natl. Acad. Sci. U.S.A.* 107, 6498–6503. doi: 10.1073/pnas.1001422107

Wang, M. (2011). Neurosteroids and GABA-A receptor function. *Front. Endocrinol.* 2:44. doi: 10.3389/fendo.2011.00044

Waterham, H. R. (2006). Defects of cholesterol biosynthesis. *FEBS Lett.* 580, 5442–5449. doi: 10.1016/j.febslet.2006.07.027

Wei, D., Allsop, S., Tye, K., and Piomelli, D. (2017). Endocannabinoid signaling in the control of social behavior. *Trends Neurosci.* 40, 385–396. doi: 10.1016/j.tins.2017.04.005

Yamashita, Y., Matsuishi, T., Ishibashi, M., Kimura, A., Onishi, Y., Yonekura, Y., et al. (1998). Decrease in benzodiazepine receptor binding in the brains of adult patients with Rett syndrome. *J. Neurol. Sci.* 154, 146–150.

Yudkoff, M., Daikhin, Y., Horyn, O., Nissim, I., and Nissim, I. (2008). Ketosis and brain handling of glutamate, glutamine, and GABA. *Epilepsia* 49(Suppl. 8), 73–75. doi: 10.1111/j.1528-1167.2008.01841.x

Zaheer, S., Kumar, D., Khan, M. T., Giyanwani, P. R., and Kiran, F. N. U. (2018). Epilepsy and cannabis: a literature review. *Cureus* 10:e3278. doi: 10.7759/cureus.3278

Zamberletti, E., Gabaglio, M., Piscitelli, F., Brodie, J. S., Woolley-Roberts, M., Barbiero, I., et al. (2019). Cannabidivarin completely rescues cognitive deficits and delays neurological and motor defects in male Mecp2 mutant mice. *J. Psychopharmacol.* doi: 10.1177/0269881119844184 [Epub ahead of print].

Zappella, M. (1992). The Rett girls with preserved speech. *Brain Dev.* 14, 98–101.

Zhang, L., He, J., Jugloff, D. G. M., and Eubanks, J. H. (2008). The MeCP2-null mouse hippocampus displays altered basal inhibitory rhythms and is prone to hyperexcitability. *Hippocampus* 18, 294–309. doi: 10.1002/hipo.20389

Zhang, Q., Wang, J., Li, J., Bao, X., Zhao, Y., Zhang, X., et al. (2017). Novel FOXG1 mutations in Chinese patients with Rett syndrome or Rett-like mental retardation. *BMC Med. Genet.* 18:96. doi: 10.1186/s12881-017-0455-y

Zhang, X., Cui, N., Wu, Z., Su, J., Tadepalli, J. S., Sekizar, S., et al. (2010). Intrinsic membrane properties of locus coeruleus neurons in Mecp2-null mice. *Am. J. Physiol. Cell Physiol.* 298, C635–C646. doi: 10.1152/ajpcell.00442.2009

Zhang, Z.-W., Zak, J. D., and Liu, H. (2010). MeCP2 is required for normal development of GABAergic circuits in the

thalamus. *J. Neurophysiol.* 103, 2470–2481. doi: 10.1152/jn.00601.2009

Zhao, Y., Zhang, X., Bao, X., Zhang, Q., Zhang, J., Cao, G., et al. (2014). Clinical features and gene mutational spectrum of CDKL5-related diseases in a cohort of Chinese patients. *BMC Med. Genet.* 15:24. doi: 10.1186/1471-2350-15-24

Zhong, W., Cui, N., Jin, X., Oginsky, M. F., Wu, Y., Zhang, S., et al. (2015). Methyl CpG binding protein 2 gene disruption augments tonic currents of γ-aminobutyric acid receptors in locus coeruleus neurons: impact on neuronal excitability and breathing. *J. Biol. Chem.* 290, 18400–18411. doi: 10.1074/jbc.M115.650465

Zhong, W., Johnson, C. M., Cui, N., Oginsky, M. F., Wu, Y., and Jiang, C. (2017). Effects of early-life exposure to THIP on brainstem neuronal excitability in the Mecp2-null mouse model of Rett syndrome before and after drug withdrawal. *Physiol. Rep.* 5:e13110. doi: 10.14814/phy2.13110

Zuardi, A. W., Antunes Rodrigues, J., and Cunha, J. M. (1991). Effects of cannabidiol in animal models predictive of antipsychotic activity. *Psychopharmacology* 104, 260–264. doi: 10.1007/BF02244189

Zuardi, A. W., Crippa, J. A. S., Hallak, J. E. C., Bhattacharyya, S., Atakan, Z., Martin-Santos, R., et al. (2012). A critical review of the antipsychotic effects of cannabidiol: 30 years of a translational investigation. *Curr. Pharm. Des.* 18, 5131–5140.

Zuardi, A. W., de Souza Crippa, J. A., Hallak, J. E. C., Campos, A. C., and Guimarães, F. S. (2017). "Chapter e13 - The Anxiolytic Effects of Cannabidiol (CBD)," in *Handbook of Cannabis and Related Pathologies*, ed. V. R. Preedy (San Diego: Academic Press), e131–e139.

Conflict of Interest Statement: The authors declare that the research was conducted in the absence of any commercial or financial relationships that could be construed as a potential conflict of interest.

frontiers in Cellular Neuroscience

MINI REVIEW
published: 06 August 2019
doi: 10.3389/fncel.2019.00357

Glutamate Transporters in Hippocampal LTD/LTP: Not Just Prevention of Excitotoxicity

*Joana Gonçalves-Ribeiro[1,2], Carolina Campos Pina[1,2], Ana Maria Sebastião[1,2] and Sandra Henriques Vaz[1,2]**

[1] *Instituto de Medicina Molecular João Lobo Antunes, Faculdade de Medicina, Universidade de Lisboa, Lisbon, Portugal,*
[2] *Instituto de Farmacologia e Neurociências, Faculdade de Medicina, Universidade de Lisboa, Lisbon, Portugal*

Glutamate uptake is a process mediated by sodium-dependent glutamate transporters, preventing glutamate spillover from the synapse. Typically, astrocytes express higher amounts of glutamate transporters, thus being responsible for most of the glutamate uptake; nevertheless, neurons can also express these transporters, albeit in smaller concentrations. When not regulated, glutamate uptake can lead to neuronal death. Indeed, the majority of the studies regarding glutamate transporters have focused on excitotoxicity and the subsequent neuronal loss. However, later studies have found that glutamate uptake is not a static process, evincing a possible correlation between this phenomenon and the efficiency of synaptic transmission and plasticity. In this review, we will focus on the role of the increase in glutamate uptake that occurs during long-term potentiation (LTP) in the hippocampus, as well as on the impairment of long-term depression (LTD) under the same conditions. The mechanism underpinning the modulatory effect of glutamate transporters over synaptic plasticity still remains unascertained; yet, it appears to have a more prominent effect over the *N*-methyl-D-aspartate receptor (NMDAR), despite changes in other glutamate receptors may also occur.

Keywords: glutamate transporters, synaptic plasticity, tripartite synapse, astrocytes, NMDAR

OPEN ACCESS

Edited by:
Cláudia Guimas Almeida,
New University of Lisbon, Portugal

Reviewed by:
Daniela Marazziti,
Italian National Research Council (CNR), Italy
Paula Agostinho,
University of Coimbra, Portugal

***Correspondence:**
Sandra Henriques Vaz
svaz@medicina.ulisboa.pt

Specialty section:
This article was submitted to Non-Neuronal Cells, a section of the journal Frontiers in Cellular Neuroscience

Received: *25 March 2019*
Accepted: *18 July 2019*
Published: *06 August 2019*

Citation:
Gonçalves-Ribeiro J, Pina CC, Sebastião AM and Vaz SH (2019) Glutamate Transporters in Hippocampal LTD/LTP: Not Just Prevention of Excitotoxicity. Front. Cell. Neurosci. 13:357. doi: 10.3389/fncel.2019.00357

INTRODUCTION

Glutamate was first classified as a neurotransmitter in the 1950s (Hayashi, 1952), and is presently acknowledged as the major excitatory neurotransmitter in the mammalian brain. Having a pivotal role in neuronal signaling, it has been vastly implied in several brain functions, such as cognition, memory, and learning (for review see Zhou and Danbolt, 2014). Within the Central Nervous System (CNS), glutamate acts by binding to receptors coupled to ionotropic channels, as *N*-methyl-D-aspartate (NMDAR), α-amino-3-hydroxy-5-methyl-4-isoxazole propionic acid (AMPAR) and kainite receptors, and metabotropic glutamate receptors (mGluRs). mGluRs can be subclassified into three distinct categories in accordance to sequence homology, G-protein coupling and ligand selectivity: Group I includes mGluR1 and mGluR5, Group II includes mGluR2 and mGluR3, and Group III includes mGluRs 4, 6, 7, and 8 (for review see Niswender and Conn, 2010). Paradoxically, in spite of its critical role in overall CNS functionality, glutamate can also act as a neurotoxin (Choi et al., 1987). When in abnormally high concentrations, glutamate can severely damage neurons, or

even lead to neural death, by overactivation of NMDA or AMPA receptors in a process referred to as excitotoxicity, suggesting a thorough regulation of its concentration is required for proper neuronal signaling. This regulation is primarily performed by high-affinity glutamate transporters, but also by passive diffusion, albeit to a lesser extent (Barbour and Häusser, 1997).

Neurotransmitter uptake is crucial for normal synaptic transmission, being performed by astrocytes and neurons. For this purpose, both cell types express distinct transporters, each corresponding to specific neurotransmitter, which are responsible for the recycling and the regulation of the synaptic concentration of the neurotransmitter, directly influencing several aspects of synaptic communication, such as the duration of postsynaptic responses. Accordingly, glutamate transporters are responsible for clearing glutamate from the extracellular space into the cell, in order for it to be either metabolized or recycled, in compliance with the cell's needs. So far, five high-affinity glutamate transporters have been identified and characterized in the CNS: Glutamate Aspartate Transporter (GLAST) (Storck et al., 1992), Glutamate Transporter type 1 (GLT-1) (Pines et al., 1992), Excitatory amino-acid transporter 4 (EAAT4) (Fairman et al., 1995) and Excitatory amino-acid transporter 5 (EAAT5) (Arriza et al., 1997).

Several studies support the notion that glutamate transporter expression is not uniform among distinct cell types and brain regions. GLT-1 and GLAST are the most copious transporters in the forebrain (Danbolt, 2001; Takahashi et al., 2015), being responsible for approximately 90% of total glutamate transport and subsequently, for maintaining extracellular glutamate at optimal levels, thus preventing excitotoxic events. This is further supported by studies of GLT-1-KO (Tanaka et al., 1997) and GLAST-KO (Watase et al., 1998) phenotypes, as mice suffered from lethal seizures and impaired motor coordination, respectively, strongly indicating glutamate transporters are key regulators of neuronal excitability. Immunostaining for GLT-1 in tissue reports a more prominent expression in the cortex and hippocampus (Danbolt, 2001), being found almost exclusively in glial cells. This transporter has three known isoforms (GLT-1a, GLT-1b and GLT-1c) with different relative expressions. EAAC1 (EAAT3) is exclusively expressed in neurons. GLAST expression is more pronounced in the cerebellum, EAAT4 in the cerebellar Purkinje cells and EAAT5 in the retina (Danbolt, 2001).

Glutamate transport mediated by high-affinity transporters in an electrogenic process characterized by the translocation of net positive charge during each transport cycle. The inward transport of a glutamate anion is coupled with three Na^+ ions, accompanied by the simultaneous outflux one K^+ ion, indicating glutamate transport is a sodium-dependent process driven by electrochemical gradients across the cell membrane (Kanner, 2006).

As aforementioned, glutamate transporters prevent excitotoxicity, a phenomenon vastly implied in multiple neurological disorders, such as epilepsy, Parkinson's disease (Van Laar et al., 2015), Alzheimer's disease (Hynd et al., 2004; Esposito et al., 2013), and Amyotrophic Lateral Sclerosis (ALS) (Van Den Bosch et al., 2006), thus emphasizing the importance of a thorough regulation of glutamate uptake. Indeed, the majority of studies regarding glutamate uptake have focused on its impact on neuropathologies, however, in more recent years, there has been a gradually increasing interest in the putative role of these transporter in synaptic transmission. Although glutamate transporters do not exactly bind to glutamate, they do compete with glutamate receptors for this neurotransmitter, implying receptor activation can be modulated by transporter activity. Since the activation of postsynaptic glutamate receptors affects synaptic transmission, glutamate transporters are able to influence synaptic transmission via a regulation of glutamate levels. Modulation of glutamate transport can be associated with a variety of factors ranging from neural stimulation to protein synthesis and ion channel, as will be further discussed. In fact, there is growing evidences supporting glutamate transporters are not static but extremely dynamic proteins, which can be found internalized in the intracellular space, and when in the membrane, display the ability to diffuse through glia surface (Pita-Almenar et al., 2012; Murphy-Royal et al., 2015), likely shaping the distribution of extracellular glutamate.

GLUTAMATE TRANSPORTERS IMPACT WITHIN THE SYNAPSE

Glutamate transporters and receptors have similar affinities for glutamate (Arriza et al., 1994), and taking into consideration that glutamate transport is not solely a mechanisms for shutting down neurotransmitter action, it should be noted that these can also be regarded as a diffusion sink capable of modifying synaptic responses on a millisecond time scale by sequestering glutamate at the binding sites within the transporter (Wadiche et al., 1995). Thus, glutamate transporters do play an important role in synaptic transmission, being crucial for maintaining optimal extracellular glutamate levels. AMPAR and NMDAR have a higher expression in the synapse, where glutamate transporters are unlikely to have any sort of competition, due to space constraints. Nevertheless, on account of its privileged localization, glutamate transporters may easily counteract the action of a fraction of extrasynaptic NMDAR in hippocampal synapse and mGlurRs, which are highly concentrated at the perisynaptic membrane of neurons (Baude et al., 1993). Accordingly, the activity of glutamate transporters can be modulated in order to regulate synaptic transmission. This is possible since glutamate transporters can act as diffusion sinks for glutamate and also as a consequence of their high dynamism in the membrane, allowing the adjustment of its activity in different stages of long-term potentiation (LTP). This modulation can be achieved by either exocytosis or endocytosis of transporters, membrane surface diffusion (Murphy-Royal et al., 2015; Al Awabdh et al., 2016) in co-cultures of neurons and astrocytes, brain slices and living mice. In the hippocampal neuropil, an area with a high-density of synapses, pharmacological blockade of glutamate transporters prolonged NMDAR-mediated Excitatory postsynaptic currents (EPSCs) in CA1 pyramidal neurons that had suffered high stimulation, but not in those subjected to low stimulation, suggesting glutamate transporters restrict glutamate spillover from neighboring synapses, and revealing that, in this

region, independent synapses can collaborate with each other via glutamate transporter (Arnth-Jensen et al., 2002). Both LTP and long-term depression (LTD) induction depend on the activation of NMDAR and mGluR (Anwyl, 2009; Gladding et al., 2009; Lüscher and Malenka, 2012) and these receptors can be modulated by extracellular glutamate concentration, which is mediated by glutamate release in the synaptic cleft, glutamate diffusion plus glutamate uptake. In the CA1 region, neuronal glutamate transporters are able to control the level of NMDAR activation (Diamond, 2001) modulating neuronal excitability by regulating Kv2.1 channels (Mulholland et al., 2008). mGluR EPSCs are also potentiated by glutamate transporters inhibition in both cortex and hippocampus (Huang et al., 2004; Otis et al., 2004), constituting a possible candidate to suffer modulation by glutamate transporters. It appears that by competing with postsynaptic glutamate receptors, glutamate transporters mediate the level of activity of these receptors, making them relevant in synaptic plasticity.

Glutamate Uptake in LTP

Long term potentiation is a form of synaptic plasticity where a persistent strengthening of synapses based on recent patterns of activity occurs (Bliss and Lomo, 1973), resulting in a long-lasting increase in signal transmission between neurons (for a deeper review see: Nicoll, 2017). Maintenance and modulation of LTP is usually associated with G-protein coupled receptor (GPCR) and/or protein phosphorylation, typically by a heightening of EPSCs (Betke et al., 2012). In the CA1 region, glutamate uptake is not homogenous throughout LTP and it is well established that LTP induction elicits glutamate uptake enhancement (Pita-Almenar et al., 2006, 2012) by increasing expression of glutamate transporters at the membrane. However, this modulation of uptake is regulated by distinct pathways in early-LTP and late-LTP. During early-LTP, glutamate uptake increase is insensitive to dihydrokainate (DHK), a selective GLT-1 inhibitor, being mostly secured by an enhanced expression of EAAC1 at the membrane level. There are no studies confirming an increase of glutamate transporters synthesis, just increase of uptake during LTP and transporter expression at the membrane level (Pita-Almenar et al., 2006). Conversely, late-LTP was DHK sensitive and required macromolecular synthesis mediated by phosphatase kinase C (PKC) (Pita-Almenar et al., 2006). Since PKC is a protein-related to Ca^{2+} signaling (Huang, 1989), this suggests that glutamate uptake modulation can be influenced by changes in intracellular Ca^{2+} concentration. This is noteworthy considering the majority of glutamate uptake is mediated by glial glutamate transporters, along with the fact that astrocytes show excitability by Ca^{2+} signaling (Araque et al., 1999; Perea and Araque, 2005; Sherwood et al., 2017). Actually, in astrocytic cultures, chelation of Ca^{2+} can prevent the modulation of glutamate and GABA transporters (Leonova et al., 2001; Matsuura et al., 2002; Cristovao-Ferreira et al., 2011; Jacob et al., 2014). LTP is impaired in hippocampal slices of GLT-1KO mice but this was overcome in the presence of low concentrations of NMDAR antagonists (Katagiri et al., 2001). This suggests that GLT-1 mediates NMDAR activity by controlling the levels of extracellular glutamate, and this is plausible explanation of how glutamate transporters modulate synaptic transmission, by regulating the activation of postsynaptic glutamate receptors via a control of the concentrations of glutamate present at the synaptic cleft.

As mentioned before, glutamate uptake mediated by glutamate transporters is an electrogenic process and, therefore, the concentrations of K^+, Na^+ and H^+ directly influence glutamate uptake and, subsequently, synaptic plasticity. In glutamate transporters, the inward flow of a glutamate anion and three Na^+ ions is simultaneously accompanied by the outflow of one K^+ ion (Kanner, 2006). Therefore, glutamate uptake can be modulated by the extracellular concentration of both Na^+ and K^+ ions. Changes in synaptic plasticity by modulating concentrations of K^+ has been correlated with glutamate transporters (Kucheryavykh et al., 2007; Mulholland et al., 2008). Knockout of astrocytic K^+ channel impaired glutamate uptake and enhanced short term potentiation (Djukic et al., 2007). This can be due to the fact that increased extracellular K^+ impairs the electrogenic process of the glutamate transporters, compromising normal uptake activity. EphA4, a receptor tyrosine kinase, reduces both GLT-1 and GLAST expression, leading to LTP impairment, which was rescued by pharmacological inhibition of glutamate transporters (Carmona et al., 2009). Surprisingly, we did not find any interactions of glutamate transporters with the sodium potassium pump (Na^+/K^+-ATPase), a ubiquitous membrane protein (Lees, 1991) at the electrophysiological level. However, there are some studies suggesting a possible correlation between these two proteins such as co-localization in the hippocampus (Rose et al., 2009). Ouabain, a specific antagonist of Na^+/K^+-ATPase, inhibits glutamate uptake in synaptosomes and also exhibits a bimodal effect by only inhibiting at high concentrations in cultures of astrocytes (Rose et al., 2009; Illarionava et al., 2014). In fetal human astrocytes, glutamate transporters activity can enhance Na^+/K^+-ATPase activity as well as cell surface expression (Gegelashvili et al., 2007), hinting on a possible interaction between these proteins. This can be interesting since Na^+/K^+-ATPase modulation has been correlated with changes in synaptic transmission (Scuri et al., 2007; Diaz et al., 2013).

LTP induction and maintenance require optimal glutamate extracellular concentration (Katagiri et al., 2001), which is secured by glutamate transporters, mostly expressed in astrocytes, being glutamate transport a key factor for the induction and maintenance of hippocampal LTP. Hence, during LTP, there is an increase of glutamate uptake activity mainly in astrocytes (**Figure 1A**).

Glutamate Uptake in LTD

LTD comprehends a form of synaptic plasticity where a weakening of synapses occurs by a reduction of the efficiency. This can be interpreted as an internalization of AMPA receptors in the postsynaptic membrane, triggered by synaptic activation of either NMDARs or mGluRs (Collingridge et al., 2010). The impact of glutamate uptake in LTD is not as well understood as in LTP, but some studies suggest a possible correlation between these two mechanisms. As glutamate transporters are not enzymes, there are no available agonists capable of enhancing

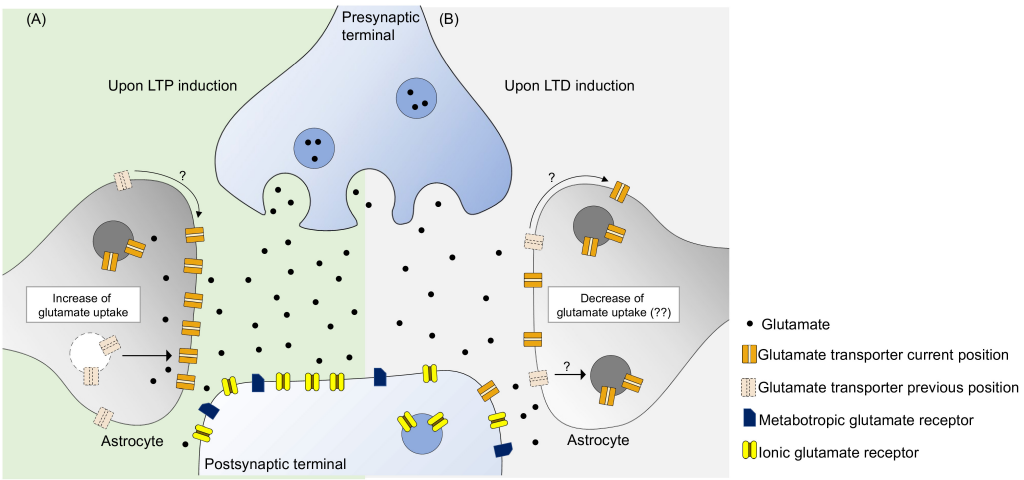

FIGURE 1 | Glutamate transporters have the ability to monitor the concentration of synaptic glutamate, potentially controlling the activity of glutamate metabotropic and ionic receptors. **(A)** During LTP induction there is an increase of glutamate transport activity probably due to an increase of glutamate transporters near synaptic cleft. This can be due to a intracellular trafficking from the intracellular space to the membrane and surface diffusion to the synaptic region, leading to an optimal activation of postsynaptic receptors. **(B)** As for LTD induction, the specific role of glutamate uptake is yet to be revealed. It is know that increase of glutamate transporters decreases LTD, perhaps by not activating postsynaptic receptors to an optimal level. Furthermore, blockade of glutamate uptake enhances LTD suggesting that glutamate uptake may not be static during this phenomenon. We propose that there occurs some sort of glutamate uptake decrease either by removing glutamate transporters by internalization or by surface diffusion.

its activity, making it difficult to "synthetically" elicit an increase in glutamate uptake. One way to do it is to treat living mice, brain slices or cultures with ceftriaxone, a beta-lactam antibiotic that enhances GLT-1 expression (Rothstein et al., 2005; Omrani et al., 2009; Bajrektarevic and Nistri, 2017). Chronic ceftriaxone treatment in Wistar rats increased GLT-1 expression, which produced an impairment in LTD in hippocampus mossy fibers CA3 (MF-CA3) synapses (Omrani et al., 2009), an effect reversed by the blockade of GLT-1 with DHK. This can be explained by a restraining of the level of activation of peri-synaptic mGluRs as a result of increased glutamate clearance by glutamate transporters, since, in these synapses, LTD is mGluR dependent (Yokoi et al., 1996), which, as above mentioned, is a receptor that can be modulated by glutamate uptake. Behavior can also affect the activity of glutamate transporters. It is known that stress enhances LTD and decreases LTP (Pan Wong et al., 2007). One study suggests that this stress-mediated LTD enhancement in the CA1 region of the hippocampus is done through the blockade of glutamate transporters, since both LTD enhancement and decreased uptake were reversed when animals had been previously treated with glucocorticoid receptor antagonist, RU38486, before stress induction (Yang et al., 2005). It is not exclusively in the hippocampus that glutamate transporters are relevant in LTD, existing connections in other brain regions, such as the amygdala (Tsvetkov et al., 2004) and the cerebellum (Brasnjo and Otis, 2001), where similar mechanisms can also occur.

To our knowledge, the role of glutamate transporters in hippocampal LTD, under physiological conditions, still remains elusive. Enhancement of glutamate uptake activity impairs LTD, however, this does not necessarily mean that uptake decreases in order to achieve LTD, although some alterations are expected. The fact that blockade of glutamate uptake enhanced LTD (Yang et al., 2005; Omrani et al., 2009), allied to increase produced the opposite effect, suggests that during LTD there can be a decrease of functional transporters in the membrane, leading to an optimal activation of glutamate receptors. Perhaps, in a similar way to what occurs with AMPA receptors, glutamate transporters are also internalized by cells and translocated to the plasma membrane upon an appropriate stimulus (**Figure 1B**). Further studies need to be made in order to grasp the role of glutamate transporters in LTD, in which transporters have not been subjected to any form of treatment.

CONCLUSION

Glutamate clearance by high affinity transporters is essential for the maintenance of glutamate homeostasis, which requires a functional level of expression of glutamate transporters at the membrane level of both astrocytes and neurons. Glutamate uptake is not a static process and can be finely adjusted in accordance to synaptic needs. Glutamate transporters are able to control the level of activation of glutamate receptors by controlling the level of glutamate present at the synaptic level. These changes can be achieved either by an over or under expression of glutamate transporters, altered cellular trafficking or changes in the transporter conformation, all processes that affect the affinity of these transporters for glutamate. For LTP, glutamate uptake needs to be enhanced when compared to basal levels (Pita-Almenar et al., 2006, 2012). Noting that late LTP requires protein expression, an increase in glutamate transporters is not surprising at this point. Conversely, despite some reports suggest causality between

glutamate uptake and LTD, this interaction remains poorly comprehended. An increase of glutamate uptake activity is not favorable for LTD maintenance (Omrani et al., 2009), while a stress-mediated inhibition of glutamate transporters enhances it (Yang et al., 2005). Nonetheless, we did not find what occurs to glutamate transporters throughout a "standard" LTD. In both LTP and LTD phenomena, the impact of glutamate transporters is seemingly achieved by a fine regulation of the activation of peri- and extrasynaptic NMDARs and mGluRs. Further studies are essential for a better comprehension of the importance of glutamate uptake for synaptic transmission and plasticity, namely by clarifying how these transporters modulate such physiological processes.

The study of transporter activity has proven to be particularly challenging, mostly on account of a lack of suitable methodologies. Techniques used for assessing receptor function are not applicable to transporters, and genetic approaches, as up- or down-regulating glutamate transport, although feasible, are not sensitive to variations in transporter activity, and thus, are unable to shed some light on the functional role of transporters during LTP or LTD. Blockade of glutamate transporters through the application of antagonists allows the inference of some of its putative functions in synaptic plasticity, however, it does not help in the clarification of the impact of enhanced glutamate transport. To our knowledge, the only current method is the application of ceftriaxone (Omrani et al., 2009), which acts by increasing GLT-1 expression levels and, concomitantly, by increasing glutamate uptake. In Murphy-Royal et al., 2015, GLT-1 surface diffusion was blocked by a cross-linking technique (Heine et al., 2008), which itself had an impact on synaptic transmission. Perhaps, the manipulation or the monitoring of this diffusion of transporters at an *in situ* or *in vivo* model could constitute a suitable approach for better comprehending how exactly do glutamate transporter influence synaptic signaling and plasticity. Additionally, glutamate imaging could also allow a more direct observation of the behavior of glutamate transporters in seconds, or even millisecond, timescale (Dulla et al., 2008; Okubo et al., 2010), and it can constitute a means for understanding how glutamate transporters impact glutamate dynamics (Hefendehl et al., 2016; Pinky et al., 2018). Whole cell patch clamp constitutes a powerful tool for measuring glutamate uptake in astrocytes (Bergles and Jahr, 1997), and dual-patch recordings could emerge as a plausible method for simultaneously recording glutamate uptake and neuronal excitability, and ultimately, correlate these two events.

In sum, sufficient evidence indicates the critical participation of glutamate transporters in synaptic transmission and synaptic plasticity in the hippocampus and other areas, and additional studies are required in order to better comprehend the mechanisms by which glutamate transporters and, subsequently, glutamate uptake impacts synaptic transmission and plasticity.

AUTHOR CONTRIBUTIONS

All authors listed have made a substantial, direct and intellectual contribution to the work, and approved it for publication.

FUNDING

This work was supported by UID/BIM/50005/2019 [project finnanced by Fundação para a Ciência e a Tecnologia (FCT)/Ministério da Ciência, Tecnologia e Ensino Superior (MCTES) through Fundos do Orçamento de Estado] and PTDC/BTM-SAL/32147/2017 (FCT). JG-R was in receipt of an FCT fellowship (iMM/BI/96-2018).

REFERENCES

Al Awabdh, S., Gupta-Agarwal, S., Sheehan, D. F., Muir, J., Norkett, R., Twelvetrees, A. E., et al. (2016). Neuronal activity mediated regulation of glutamate transporter GLT-1 surface diffusion in rat astrocytes in dissociated and slice cultures. *Glia* 64, 1252–1264. doi: 10.1002/glia.22997

Anwyl, R. (2009). Metabotropic glutamate receptor-dependent long-term potentiation. *Neuropharmacology* 56, 735–740. doi: 10.1016/j.neuropharm.2009.01.002

Araque, A., Parpura, V., Sanzgiri, R. P., and Haydon, P. G. (1999). Tripartite synapses: glia, the unacknowledged partner. *Trends Neurosci.* 22, 208–215. doi: 10.1016/s0166-2236(98)01349-6

Arnth-Jensen, N., Jabaudon, D., and Scanziani, M. (2002). Cooperation between independent hippocampal synapses is controlled by glutamate uptake. *Nat. Neurosci.* 5, 325–331. doi: 10.1038/nn825

Arriza, J. L., Eliasof, S., Kavanaugh, M. P., and Amara, S. G. (1997). Excitatory amino acid transporter 5, a retinal glutamate transporter coupled to a chloride conductance. *Proc. Natl. Acad. Sci. U.S.A.* 94, 4155–4160. doi: 10.1073/pnas.94.8.4155

Arriza, J. L., Fairman, W. A., Wadiche, J. I., Murdoch, G. H., Kavanaugh, M. P., and Amara, S. G. (1994). Functional comparisons of three glutamate transporter subtypes cloned from human motor cortex. *J. Neurosci.* 14, 5559–5569. doi: 10.1523/jneurosci.14-09-05559.1994

Bajrektarevic, D., and Nistri, A. (2017). Ceftriaxone-mediated upregulation of the glutamate transporter GLT-1 contrasts neurotoxicity evoked by kainate in rat organotypic spinal cord cultures. *Neurotoxicology* 60, 34–41. doi: 10.1016/J.NEURO.2017.02.013

Barbour, B., and Häusser, M. (1997). Intersynaptic diffusion of neurotransmitter. *Trends Neurosci.* 20, 377–384.

Baude, A., Nusser, Z., Roberts, J. D., Mulvihill, E., McIlhinney, R. A., and Somogyi, P. (1993). The metabotropic glutamate receptor (mGluR1 alpha) is concentrated at perisynaptic membrane of neuronal subpopulations as detected by immunogold reaction. *Neuron* 11, 771–787. doi: 10.1016/0896-6273(93)90086-7

Bergles, D. E., and Jahr, C. E. (1997). Synaptic activation of glutamate transporters in hippocampal astrocytes. *Neuron* 19, 1297–1308. doi: 10.1016/S0896-6273(00)80420-1

Betke, K. M., Wells, C. A., and Hamm, H. E. (2012). GPCR mediated regulation of synaptic transmission. *Prog. Neurobiol.* 96, 304–321. doi: 10.1016/j.pneurobio.2012.01.009

Bliss, T. V., and Lomo, T. (1973). Long-lasting potentiation of synaptic transmission in the dentate area of the anaesthetized rabbit following stimulation of the perforant path. *J. Physiol.* 232, 331–356. doi: 10.1113/jphysiol.1973.sp010273

Brasnjo, G., and Otis, T. S. (2001). Neuronal glutamate transporters control activation of postsynaptic metabotropic glutamate receptors and influence

cerebellar long-term depression. *Neuron* 31, 607–616. doi: 10.1016/S0896-6273(01)00377-374

Carmona, M. A., Murai, K. K., Wang, L., Roberts, A. J., and Pasquale, E. B. (2009). Glial ephrin-A3 regulates hippocampal dendritic spine morphology and glutamate transport. *Proc. Natl. Acad. Sci. U.S.A.* 106, 12524–12529. doi: 10.1073/pnas.0903328106

Choi, D. W., Maulucci-Gedde, M., and Kriegstein, A. R. (1987). Glutamate neurotoxicity in cortical cell culture. *J. Neurosci.* 7, 357–368. doi: 10.1523/JNEUROSCI.07-02-00357.1987

Collingridge, G. L., Peineau, S., Howland, J. G., and Wang, Y. T. (2010). Long-term depression in the CNS. *Nat. Rev. Neurosci.* 11, 459–473. doi: 10.1038/nrn2867

Cristovao-Ferreira, S., Navarro, G., Brugarolas, M., Perez-Capote, K., Vaz, S. H., Fattorini, G., et al. (2011). Modulation of GABA transport by adenosine A1R-A2AR heteromers, which are coupled to both Gs- and Gi/o-Proteins. *J. Neurosci.* 31, 15629–15639. doi: 10.1523/JNEUROSCI.2526-11.2011

Danbolt, N. C. (2001). Glutamate uptake. *Prog. Neurobiol.* 65, 1–105. doi: 10.1016/S0301-0082(00)00067-68

Diamond, J. S. (2001). Neuronal glutamate transporters limit activation of NMDA receptors by neurotransmitter spillover on CA1 pyramidal cells. *J. Neurosci.* 21, 8328–8338. doi: 10.1523/JNEUROSCI.21-21-08328.2001

Diaz, M. R., Wadleigh, A., Kumar, S., De Schutter, E., and Valenzuela, C. F. (2013). Na+/K+-ATPase inhibition partially mimics the ethanol-induced increase of the golgi cell-dependent component of the tonic GABAergic current in rat cerebellar granule cells. *PLoS One* 8:e55673. doi: 10.1371/journal.pone.0055673

Djukic, B., Casper, K. B., Philpot, B. D., Chin, L.-S., and Mccarthy, K. D. (2007). Conditional knock-out of Kir4.1 leads to glial membrane depolarization, inhibition of potassium and glutamate uptake and enhanced short-term synaptic potentiation. *J. Neurosci.* 27, 11354–11365. doi: 10.1523/JNEUROSCI.0723-07.2007

Dulla, C., Tani, H., Okumoto, S., Frommer, W. B., Reimer, R. J., and Huguenard, J. R. (2008). Imaging of glutamate in brain slices using FRET sensors. *J. Neurosci. Methods* 168, 306–319. doi: 10.1016/j.jneumeth.2007.10.017

Esposito, Z., Belli, L., Toniolo, S., Sancesario, G., Bianconi, C., and Martorana, A. (2013). Amyloid β, glutamate, excitotoxicity in Alzheimer's disease: are we on the right track? *CNS Neurosci. Ther.* 19, 549–555. doi: 10.1111/cns.12095

Fairman, W. A., Vandenberg, R. J., Arriza, J. L., Kavanaught, M. P., and Amara, S. G. (1995). An excitatory amino-acid transporter with properties of a ligand-gated chloride channel. *Nature* 375, 599–603. doi: 10.1038/375599a0

Gegelashvili, M., Rodriguez-Kern, A., Sung, L., Shimamoto, K., and Gegelashvili, G. (2007). Glutamate transporter GLAST/EAAT1 directs cell surface expression of FXYD2/γ subunit of Na, K-ATPase in human fetal astrocytes. *Neurochem. Int.* 50, 916–920. doi: 10.1016/j.neuint.2006.12.015

Gladding, C. M., Fitzjohn, S. M., and Molnár, E. (2009). Metabotropic glutamate receptor-mediated long-term depression: molecular mechanisms. *Pharmacol. Rev.* 61, 395–412. doi: 10.1124/pr.109.001735

Hayashi, T. (1952). A physiological study of epileptic seizures following cortical stimulation in animals and its application to human clinics. *Jpn. J. Physiol.* 3, 46–64. doi: 10.2170/jjphysiol.3.46

Hefendehl, J. K., LeDue, J., Ko, R. W. Y., Mahler, J., Murphy, T. H., and MacVicar, B. A. (2016). Mapping synaptic glutamate transporter dysfunction *in vivo* to regions surrounding Aβ plaques by iGluSnFR two-photon imaging. *Nat. Commun.* 7:13441. doi: 10.1038/ncomms13441

Heine, M., Groc, L., Frischknecht, R., Béïque, J.-C., Lounis, B., Rumbaugh, G., et al. (2008). Surface mobility of postsynaptic AMPARs tunes synaptic transmission. *Science* 320, 201–205. doi: 10.1126/science.1152089

Huang, K. P. (1989). The mechanism of protein kinase C activation. *Trends Neurosci.* 12, 425–432. doi: 10.1016/0166-2236(89)90091-x

Huang, Y. H., Sinha, S. R., Tanaka, K., Rothstein, J. D., and Bergles, D. E. (2004). Astrocyte glutamate transporters regulate metabotropic glutamate receptor-mediated excitation of hippocampal interneurons. *J. Neurosci.* 24, 4551–4559. doi: 10.1523/JNEUROSCI.5217-03.2004

Hynd, M., Scott, H. L., and Dodd, P. R. (2004). Glutamate-mediated excitotoxicity and neurodegeneration in Alzheimer?s disease. *Neurochem. Int.* 45, 583–595. doi: 10.1016/j.neuint.2004.03.007

Illarionava, N. B., Brismar, H., Aperia, A., and Gunnarson, E. (2014). Role of Na,K-ATPase α1 and α2 isoforms in the support of astrocyte glutamate uptake. *PLoS One* 9:e98469. doi: 10.1371/journal.pone.0098469

Jacob, P. F., Vaz, S. H., Ribeiro, J. A., and Sebastião, A. M. (2014). P2Y1 receptor inhibits GABA transport through a calcium signalling-dependent mechanism in rat cortical astrocytes. *Glia* 62, 1211–1226. doi: 10.1002/glia.22673

Kanner, B. I. (2006). Structure and function of sodium-coupled GABA and glutamate transporters. *J. Membr. Biol.* 213, 89–100. doi: 10.1007/s00232-006-0877-875

Katagiri, H., Tanaka, K., and Manabe, T. (2001). Requirement of appropriate glutamate concentrations in the synaptic cleft for hippocampal LTP induction. *Eur. J. Neurosci.* 14, 547–553. doi: 10.1046/j.0953-816x.2001.01664.x

Kucheryavykh, Y. V., Kucheryavykh, L. Y., Nichols, C. G., Maldonado, H. M., Baksi, K., Reichenbach, A., et al. (2007). Downregulation of Kir4.1 inward rectifying potassium channel subunits by RNAi impairs potassium transfer and glutamate uptake by cultured cortical astrocytes. *Glia* 55, 274–281. doi: 10.1002/glia.20455

Lees, G. J. (1991). Inhibition of sodium-potassium-ATPase: a potentially ubiquitous mechanism contributing to central nervous system neuropathology. *Brain Res. Rev.* 16, 283–300. doi: 10.1016/0165-0173(91)90011-V

Leonova, J., Thorlin, T., Åberg, N. D., Eriksson, P. S., Rönnbäck, L., and Hansson, E. (2001). Endothelin-1 decreases glutamate uptake in primary cultured rat astrocytes. *Am. J. Physiol. Physiol.* 281, C1495–C1503. doi: 10.1152/ajpcell.2001.281.5.C1495

Lüscher, C., and Malenka, R. C. (2012). NMDA receptor-dependent long-term potentiation and long-term depression (LTP/LTD). *Cold Spring Harb. Perspect. Biol.* 4:a005710. doi: 10.1101/cshperspect.a005710

Matsuura, S., Ikegaya, Y., Yamada, M. K., Nishiyama, N., and Matsuki, N. (2002). Endothelin downregulates the glutamate transporter GLAST in cAMP-differentiated astrocytes in vitro. *Glia* 37, 178–182. doi: 10.1002/glia.10020

Mulholland, P. J., Carpenter-Hyland, E. P., Hearing, M. C., Becker, H. C., Woodward, J. J., and Chandler, L. J. (2008). Glutamate transporters regulate extrasynaptic NMDA receptor modulation of Kv2.1 Potassium Channels. *J. Neurosci.* 28, 8801–8809. doi: 10.1523/JNEUROSCI.2405-08.2008

Murphy-Royal, C., Dupuis, J. P., Varela, J. A., Panatier, A., Pinson, B., Baufreton, J., et al. (2015). Surface diffusion of astrocytic glutamate transporters shapes synaptic transmission. *Nat. Neurosci.* 18, 219–226. doi: 10.1038/nn.3901

Nicoll, R. A. (2017). Review a brief history of long-term potentiation. *Neuron* 93, 281–290. doi: 10.1016/j.neuron.2016.12.015

Niswender, C. M., and Conn, P. J. (2010). Metabotropic glutamate receptors: physiology, pharmacology, and disease. *Annu. Rev. Pharmacol. Toxicol.* 50, 295–322. doi: 10.1146/annurev.pharmtox.011008.145533

Okubo, Y., Sekiya, H., Namiki, S., Sakamoto, H., Iinuma, S., Yamasaki, M., et al. (2010). Imaging Extrasynaptic Glutamate Dynamics in the Brain. *Proc. Natl. Acad. Sci. U.S.A.* 107, 6526–6531. doi: 10.1073/pnas.0913154107

Omrani, A., Melone, M., Bellesi, M., Safiulina, V., Aida, T., Tanaka, K., et al. (2009). Up-regulation of GLT-1 severely impairs LTD at mossy fibre-CA3 synapses. *J. Physiol.* 587, 4575–4588. doi: 10.1113/jphysiol.2009.177881

Otis, T. S., Brasnjo, G., Dzubay, J. A., and Pratap, M. (2004). Interactions between glutamate transporters and metabotropic glutamate receptors at excitatory synapses in the cerebellar cortex. *Neurochem. Int.* 45, 537–544. doi: 10.1016/j.neuint.2003.11.007

Pan Wong, T., Howland, J. G., Robillard, J. M., Ge, Y., Yu, W., Titterness, A. K., et al. (2007). Hippocampal long-term depression mediates acute stress-induced spatial memory retrieval impairment. *Proc. Natl. Acad. Sci. U.S.A.* 104, 11471–11476. doi: 10.1073/pnas.0702308104

Perea, G., and Araque, A. (2005). Glial calcium signaling and neuron–glia communication. *Cell Calcium* 38, 375–382. doi: 10.1016/J.CECA.2005.06.015

Pines, G., Danbolt, N. C., Bjørås, M., Zhang, Y., Bendahan, A., Eide, L., et al. (1992). Cloning and expression of a rat brain L-glutamate transporter. *Nature* 360, 464–467. doi: 10.1038/360464a0

Pinky, N. F., Wilkie, C. M., Barnes, J. R., and Parsons, M. P., (2018). Region- and activity-dependent regulation of extracellular glutamate. *J. Neurosci.* 38, 5351–5366. doi: 10.1523/JNEUROSCI.3213-17.2018

Pita-Almenar, J. D., Collado, M. S., Colbert, C. M., and Eskin, A. (2006). Different mechanisms exist for the plasticity of glutamate reuptake during early long-term potentiation (LTP) and late LTP. *J. Neurosci.* 26, 10461–10471. doi: 10.1523/JNEUROSCI.2579-06.2006

Pita-Almenar, J. D., Zou, S., Colbert, C. M., and Eskin, A. (2012). Relationship between increase in astrocytic GLT-1 glutamate transport and late-LTP. *Learn. Mem.* 19, 615–626. doi: 10.1101/lm.023259.111

Rose, E. M., Koo, J. C. P., Antflick, J. E., Ahmed, S. M., Angers, S., and Hampson, D. R. (2009). Glutamate transporter coupling to Na,K-ATPase. *J. Neurosci.* 29, 8143–8155. doi: 10.1523/JNEUROSCI.1081-09.2009

Rothstein, J. D., Patel, S., Regan, M. R., Haenggeli, C., Huang, Y. H., Bergles, D. E., et al. (2005). β-Lactam antibiotics offer neuroprotection by increasing glutamate transporter expression. *Nature* 433, 73–77. doi: 10.1038/nature 03180

Scuri, R., Lombardo, P., Cataldo, E., Ristori, C., and Brunelli, M. (2007). Inhibition of Na+/K+ ATPase potentiates synaptic transmission in tactile sensory neurons of the leech. *Eur. J. Neurosci.* 25, 159–167. doi: 10.1111/j.1460-9568.2006. 05257.x

Sherwood, M. W., Arizono, M., Hisatsune, C., Bannai, H., Ebisui, E., Sherwood, J. L., et al. (2017). Astrocytic IP 3 Rs: contribution to Ca 2+ signalling and hippocampal LTP. *Glia* 65, 502–513. doi: 10.1002/glia.23107

Storck, T., Schulte, S., Hofmann, K., and Stoffel, W. (1992). Structure, expression, and functional analysis of a Na(+)-dependent glutamate/aspartate transporter from rat brain. *Proc. Natl. Acad. Sci. U.S.A.* 89, 10955–10959. doi: 10.1073/pnas. 89.22.10955

Takahashi, K., Foster, J. B., and Lin, C.-L. G. (2015). Glutamate transporter EAAT2: regulation, function, and potential as a therapeutic target for neurological and psychiatric disease. *Cell. Mol. Life Sci.* 72, 3489–3506. doi: 10.1007/s00018-015-1937-1938

Tanaka, K., Watase, K., Manabe, T., Yamada, K., Watanabe, M., Takahashi, K., et al. (1997). Epilepsy and exacerbation of brain injury in mice lacking the glutamate transporter GLT-1. *Science* 276, 1699–1702. doi: 10.1126/science.276.5319.1699

Tsvetkov, E., Shin, R. M., and Bolshakov, V. Y. (2004). Glutamate uptake determines pathway specificity of long-term potentiation in the neural circuitry of fear conditioning. *Neuron* 41, 139–151. doi: 10.1016/s0896-6273(03)00800-6

Van Den Bosch, L., Van Damme, P., Bogaert, E., and Robberecht, W. (2006). The role of excitotoxicity in the pathogenesis of amyotrophic lateral sclerosis. *Biochim. Biophys. Acta* 1762, 1068–1082. doi: 10.1016/j.bbadis.2006. 05.002

Van Laar, V. S., Roy, N., Liu, A., Rajprohat, S., Arnold, B., Dukes, A. A., et al. (2015). Glutamate excitotoxicity in neurons triggers mitochondrial and endoplasmic reticulum accumulation of Parkin, and, in the presence of N-acetyl cysteine, mitophagy. *Neurobiol. Dis.* 74, 180–193. doi: 10.1016/j.nbd.2014.11.015

Wadiche, J. I., Arriza, J. L., Amara, S. G., and Kavanaugh, M. P. (1995). Kinetics of a human glutamate transporter. *Neuron* 14, 1019–1027. doi: 10.1016/0896-6273(95)90340-90342

Watase, K., Hashimoto, K., Kano, M., Yamada, K., Watanabe, M., Inoue, Y., et al. (1998). Motor discoordination and increased susceptibility to cerebellar injury in GLAST mutant mice. *Eur. J. Neurosci.* 10, 976–988. doi: 10.1046/j.1460-9568. 1998.00108.x

Yang, C.-H., Huang, C.-C., and Hsu, K.-S. (2005). Behavioral stress enhances hippocampal CA1 long-term depression through the blockade of the glutamate uptake. *J. Neurosci.* 25, 4288–4293. doi: 10.1523/JNEUROSCI.0406-05.2005

Yokoi, M., Kobayashi, K., Manabe, T., Takahashi, T., Sakaguchi, I., Katsuura, G., et al. (1996). Impairment of hippocampal mossy fiber LTD in mice lacking mGluR2. *Science* 273, 645–647. doi: 10.1126/science.273.5275.645

Zhou, Y., and Danbolt, N. C. (2014). Glutamate as a neurotransmitter in the healthy brain. *J. Neural Transm.* 121, 799–817. doi: 10.1007/s00702-014-1180-1188

Conflict of Interest Statement: The authors declare that the research was conducted in the absence of any commercial or financial relationships that could be construed as a potential conflict of interest.

frontiers in Neuroscience

ORIGINAL RESEARCH
published: 15 January 2020
doi: 10.3389/fnins.2019.01413

Role of Spinal Cord α_2-Adrenoreceptors in Noradrenergic Inhibition of Nociceptive Transmission During Chemotherapy-Induced Peripheral Neuropathy

*José Tiago Costa-Pereira[1,2,3], Joana Ribeiro[1,2,3], Isabel Martins[1,2,3] and Isaura Tavares[1,2,3]**

[1] Unit of Experimental Biology, Department of Biomedicine, Faculty of Medicine, University of Porto, Porto, Portugal, [2] Institute of Molecular and Cell Biology, University of Porto, Porto, Portugal, [3] I3S-Institute for Investigation and Innovation in Health, University of Porto, Porto, Portugal

Chemotherapy-induced peripheral neuropathy (CIPN) is a problem during cancer treatment and for cancer survivors but the central mechanisms underlying CIPN remain understudied. This study aims to determine if CIPN is associated with alterations of noradrenergic modulation of nociceptive transmission at the spinal cord. CIPN was induced in male Wistar rats by paclitaxel injections. One month after CIPN induction, the behavioral effects of the administration of reboxetine (noradrenaline reuptake inhibitor), clonidine (agonist of α_2-adrenoreceptors; α_2_AR) and atipamezole (antagonist of α_2_AR) were evaluated using the von Frey and cold plate tests. Furthermore, we measured the expression of the noradrenaline biosynthetic enzyme dopamine-β-hydroxylase (DBH) and of α_2_AR in the spinal dorsal horn. Reboxetine and clonidine reversed the behavioral signs of CIPN whereas the opposite occurred with atipamezole. In the 3 pharmacological approaches, a higher effect was detected in mechanical allodynia, the pain modality which is under descending noradrenergic control. DBH expression was increased at the spinal dorsal horn of paclitaxel-injected animals. The enhanced noradrenergic inhibition during CIPN may represent an adaptation of the descending noradrenergic pain control system to the increased arrival of peripheral nociceptive input. A potentiation of the α_2_AR mediated antinociception at the spinal cord may represent a therapeutic opportunity to face CIPN.

Keywords: descending pain modulation, antidepressants, paclitaxel, chemotherapy side-effects, cancer treatment, pain

OPEN ACCESS

Edited by:
Sara Xapelli,
University of Lisbon, Portugal

Reviewed by:
Philippe Séguéla,
McGill University, Canada
Temugin Berta,
University of Cincinnati, United States

***Correspondence:**
Isaura Tavares
isatav@med.up.pt

Specialty section:
This article was submitted to Neuropharmacology, a section of the journal Frontiers in Neuroscience

Received: *26 July 2019*
Accepted: *13 December 2019*
Published: *15 January 2020*

Citation:
Costa-Pereira JT, Ribeiro J, Martins I and Tavares I (2020) Role of Spinal Cord α_2-Adrenoreceptors in Noradrenergic Inhibition of Nociceptive Transmission During Chemotherapy-Induced Peripheral Neuropathy. Front. Neurosci. 13:1413. doi: 10.3389/fnins.2019.01413

INTRODUCTION

Chemotherapy is the most common approach for cancer treatment but it frequently induces neuropathy. This chemotherapy-induced peripheral neuropathy (CIPN) is a clinical problem that may impose changes in cancer treatment and can persist after cessation of chemotherapy (Mantyh, 2006; Seretny et al., 2014). CIPN is characterized by multiple sensory features which include changes in pain responses, such as spontaneous pain, allodynia and hyperalgesia.

The neurotoxic mechanisms underlying CIPN depend on the cytostatic drug (Kerckhove et al., 2017). Paclitaxel, one of the most effective cytostatic drug, has been shown to cause CIPN in humans and in animal models (Polomano et al., 2001; Cavaletti and Marmiroli, 2010). Increases in nociceptive behavioral responses in paclitaxel-induced CIPN models were ascribed to peripheral fiber loss, mitochondrial swelling and vacuolization of peripheral axons and hyperexcitability of dorsal root ganglion neurons (Cliffer et al., 1998; Flatters and Bennett, 2006; Boehmerle et al., 2014; Yadav et al., 2015). The central changes during paclitaxel-induced CIPN remain understudied but since paclitaxel has a very low ability to cross the blood-brain barrier (Cavaletti and Marmiroli, 2010), it is likely that the central changes during paclitaxel-induced CIPN are caused by the neurotoxic effects triggered by the cytostatic at the periphery. At the spinal cord, paclitaxel-injected animals show increased spontaneous activity of wide-dynamic range neurons (Cata et al., 2006) and reduced local GABAergic tonic inhibition (Yadav et al., 2015). At the supraspinal level, the periaqueductal gray matter (PAG), a key area of the descending pain modulatory system, shows increases in spontaneous and evoked neuronal firing (Samineni et al., 2017). Furthermore, in a recent exploratory study using diffusion weighted magnetic resonance, alterations in the activity of the PAG were reported (Ferris et al., 2019). Using an animal model of paclitaxel-induced CIPN, we recently reported increases in the activity of serotoninergic neurons of the rostroventromedial medulla (RVM), an area that relays descending modulation from the PAG to the spinal cord (Costa-Pereira et al., 2019).

CIPN is empirically treated with antidepressant drugs which increase noradrenaline (NA) and serotonin (5-HT) levels (Sisignano et al., 2014), but the relative contribution of each neurochemical system is starting to be unraveled. Using the paclitaxel-induced CIPN model, we have recently described an involvement of 5-HT with an enhanced facilitatory effect of 5-HT3 receptors at the spinal cord (Costa-Pereira et al., 2019). Nothing is known about descending noradrenergic modulation in the paclitaxel-induced CIPN model. This is important since descending pain modulation has some distinct features between different preclinical models (Porreca et al., 2002; Ossipov et al., 2014). Furthermore descending modulatory systems are crucial to balance between inhibition (antinociception) and facilitation (pro-nociception) (Tracey and Mantyh, 2007; Heinricher et al., 2009). An imbalance of descending modulation toward facilitation was proposed to account for chronic pain installation. It is well established that NA release at the spinal dorsal horn is mainly originated from the pontine locus coeruleus (LC) (Pertovaara, 2006; Heinricher et al., 2009) and leads to analgesia by activating spinal α_{2A}-adrenoreceptors (α_{2A}-AR) which block the nociceptive transmission at the spinal dorsal horn, both pre and postsynaptically (Kawasaki et al., 2003; Pertovaara, 2013). Intrathecal administration of α_2-AR agonists induces antinociception in humans and animal models whereas the opposite occurs with α_2-AR antagonists (Eisenach et al., 1996; Budai et al., 1998). However, NA may trigger pain facilitation after brain release (Bie et al., 2003; Ortiz et al., 2008; Martins et al., 2015). Further adding complexity to the studies of noradrenergic pain modulation, an effect of the pain model was reported. In traumatic neuropathic pain models, noradrenergic upregulation occurs with increased spinal NA levels and enhanced potency of α_2-AR (Ma and Eisenach, 2003; Bantel et al., 2005) but with the progression of traumatic neuropathy, a gradual loss of descending noradrenergic inhibition occurs (Hughes et al., 2013, 2015). In diabetic neuropathy the descending noradrenergic inhibition is impaired and NA exerts pain facilitation at the spinal level (Kinoshita et al., 2013). These results show that the specificities of each preclinical pain model should be considered in the studies of descending noradrenergic pain control.

To evaluate if descending noradrenergic modulation of spinal nociceptive transmission is altered during paclitaxel-induced CIPN, we used a validated model of paclitaxel-induced CIPN to study the noradrenergic modulation of nociceptive transmission at the spinal cord. We first evaluated the nociceptive behavioral effects of the administration of reboxetine (noradrenaline reuptake inhibitor), clonidine (agonist of α_2-adrenoreceptors; α_2_AR) and atipamezole (antagonist of α_2_AR). Then we evaluated the immunohistochemical expression of the noradrenaline synthetizing enzyme, dopamine-β-hydroxylase (DBH), at the spinal dorsal horn. We analyzed the expression of α_2_AR at the spinal dorsal horn, using immunohistochemistry and western blot approaches.

MATERIALS AND METHODS

Animals

Wistar male rats (weighing 175–190 g; Charles River, France) were housed in a 12/12 h light/dark environment at 22 ± 2°C and received food and water *ad libitum*. All behavioral experiments were conducted in the light phase. The animals were acclimated to the housing facility for a least 1 week before the onset of experiments. The animals were randomly housed in pairs and selected from the cage before each procedure.

The experiments were approved by the Animal Ethical Committee of the Faculty of Medicine of University of Porto and Directorate-General of Food and Veterinary Medicine–Portuguese National Authority for Animal Health (license 0421/000/000/2018) and performed in accordance with the European Community Council Directive (2010/63/EU) and the ethical guidelines of the International Association for the Study of Pain (IASP) in conscious animals (Zimmermann, 1983).

Induction of the CIPN Model

The CIPN model was induced as described previously (Polomano et al., 2001). Briefly, paclitaxel (Taxol®) (2.0 mg Kg^{-1} – cumulative dose of 8.0 mg Kg^{-1}) (Tocris, United Kingdom) was dissolved in a solution of 4% Dimethyl Sulfoxide (DMSO). Rats weighing 190-200 g received an intraperitoneal (i.p.) injection of the paclitaxel solution in 4 alternate days (day 1, 3, 5, and 7). The injections were performed between 9 a.m. and 11 a.m. Control animals were injected with 4% DMSO. The DMSO concentration was elected based on previous studies showing that it is the minimal concentration of DMSO required to resuspend

paclitaxel and it does not induce any toxic effects (Worthley and Schott, 1969; Chen et al., 2011; Braz et al., 2015).

Drug Delivery and Behavioral Evaluation

Three weeks after CIPN induction, all rats weighing 290–300 g underwent surgical implantation of sterile silicone catheter (0.31 × 0.64 × 0.17 mm; Freudenberg, Germany). Briefly, the animals were deeply anesthetized with medetomidine (0.25 mg Kg^{-1}) and ketamine hydrochloride (60 mg Kg^{-1}) and the catheter was inserted in the subarachnoid space in caudal direction until the tip reached the L4/L5 spinal cord segment. After surgery, the rats were single-housed to avoid interfering with cagemate's catheter. The correct placement of the intrathecal catheter was confirmed after dissection. The few animals presenting severe signs of locomotor impairment after surgery were excluded from the study. The animals were then used in pharmacological experiments to test the behavioral nociceptive effects of reboxetine (NA reuptake inhibitor), atipamezole (α_{2A}–AR blockade) and clonidine (α_{2A}–AR agonist). All experiments were performed 30 days after the first paclitaxel injection.

Reboxetine Experiments

To study the effects of NA reuptake inhibition on nociceptive behaviors, we injected the selective reuptake inhibitor, reboxetine mesylate (10 mg Kg^{-1}) (Tocris Bioscience, United Kingdom) (DMSO: $n = 5$; paclitaxel: $n = 5$) using the i.p. route. Reboxetine was dissolved in saline and the control groups were injected with saline (DMSO: $n = 5$; paclitaxel: $n = 5$). Previous study showed reboxetine did not affect motor performance (Lapmanee et al., 2013).

The effects of reboxetine on mechanical allodynia were evaluated before (T0) and at 30, 60, 120, and 240 min after injection. To evaluate mechanical nociceptive responses, we used the von Frey test as described previously in the CIPN model (Costa-Pereira et al., 2019). Briefly, the test was performed after 20 min acclimatization to equipment, according to the "up and down" method (Chaplan et al., 1994), which consists on the application of monofilaments between 0.4 and 26.0 g (Stoelting, United States) starting with the 2.0 g monofilament. Each animal was tested twice at an interval of 3–5 min, each value obtained was logarithmic transformed and averaged.

The effects of reboxetine on cold hyperalgesia were assessed at 30 min, the time that has been previously shown to be of maximum reboxetine (Hughes et al., 2015), which was further confirmed by the present results using the von Frey test. Cold responses were studied as described previously (Costa-Pereira et al., 2019) using the cold plate test. After a training period of 3 days for habituation purposes in the device, the animals were placed on the plate at 0°C and the withdrawal latency was recorded. The cut-off period of 60 s was applied to avoid any tissue damage.

Atipamezole Experiments

To evaluate the effects of the blockade of spinal α_{2A}–AR on nociceptive behaviors, we administered the α_{2A}–*AR* antagonist atipamezole (Tocris Bioscience, United Kingdom) at 5 μg (DMSO: $n = 5$; paclitaxel: $n = 4$). Atipamezole was administered using the intrathecal route and was dissolved in 0.9% saline solution. Based on previous study (Dimitrov et al., 2013), we assessed the effects of atipamezole on mechanical and cold hypersensitivity 30 min after antagonist injection. Atipamezole did not induce any sedative effects (Pertovaara et al., 1994).

Clonidine Experiments

To assess the effects of the activation of spinal α_{2A}–AR on nociceptive behaviors, we intrathecally administered the agonist clonidine (Sigma-Aldrich, United States) at 3 doses: 0.1 μg (DMSO: $n = 6$; paclitaxel $n = 7$), 1 μg (DMSO: $n = 7$; paclitaxel $n = 7$) or 10 μg (DMSO: $n = 8$; paclitaxel $n = 6$). Clonidine was dissolved in 0.9% saline solution and the respective control groups were injected with saline (DMSO: $n = 7$; paclitaxel $n = 6$). Mechanical and thermal hypersensitivity were evaluated before and 30 min after clonidine injection, which has previously been shown to be the time of the maximal drug effect (Yaksh et al., 1995). In order to evaluate possible sedative effects of the higher clonidine dose (10 μg), 2 additional animals were tested in the rotarod as described previously (Vanderah et al., 2001). Briefly, the test was performed using DMSO-injected animals after training once a day for three consecutive days. Training consisted on placing the rats on a rotating rod (Ugo Basile, Varese, Italy) with the rate of rotation set at 10 rpm, until they fell off or until reaching a cutoff time set at 180 s. The evaluated animals remained on the rod for 180 s which indicates that the animals did not have motor impairments after clonidine injection.

Immunohistochemistry

Thirty days after the first paclitaxel injection, the rats were deeply anesthetized with an overdose of an i.p. injection of sodium pentobarbital (65 mg Kg^{-1}) and perfused with 100 ml of calcium free Tyrode's solution, followed by 750 ml of 4% paraformaldehyde in 0.1M phosphate buffer. The lumbar spinal cord segments were removed, immersed in a fixative for 4 h and cryopreserved in a 30% sucrose solution. The segments were then sliced at 30 μm in a freezing microtome and used for the DBH and α_{2A}-AR immunoreactions described below. The L4 and L5 sections were used for immunodetection of DBH (DMSO: $n = 6$; paclitaxel: $n = 5$) and α_{2A}- AR (DMSO: $n = 5$; paclitaxel: $n = 5$).

Dopamine-β-Hydroxylase (DBH) Immunoreaction

For the DBH-immunoreaction, one in every fourth spinal L4 and L5 sections were incubated with a monoclonal anti-DBH primary antibody (Millipore Catalogue No. MAB308) diluted at 1:5000, followed by a horse biotinylated anti-mouse secondary antibody (Dako, Denmark; 1:200). After several washes, the sections were incubated in PBS-T containing the avidin-biotin complex (1:200; ABC, Vector, United States). The bound peroxidase was revealed using 0.0125% 3,3′- diaminobenzidine tetrahydrochloride (DAB) (Sigma-Aldrich, United States). The immunodetection of DBH-immunoreactive fibers was assessed as described above.

The DBH labeled sections were observed using a light microscope (Axioskop 40 model, Zeiss®, Switzerland) coupled to a high-resolution digital camera (Leica EC3 model) and the LAS 4.6.0. software (Leica Microsystems®) and maintaining the same

exposure and light settings. The quantification of DBH labeling of 3 randomly taken L4 and L5 spinal sections was performed on the ImageJ® software (U. S. National Institutes of Health, United States) based on a method previously described (Hughes et al., 2013; Costa-Pereira et al., 2019). Briefly, the mean level of background was determined for each section and lamina using ROI analysis of small areas without DBH immunoreaction. The threshold level for DBH positive pixels was adjusted at a value of 5 standard deviations above the mean background level. The mean percentage of DBH positive pixels in laminae I-II, lamina III, IV, and V was then calculated.

The total DBH fibers length in each lamina of spinal dorsal horn were also calculated using a semi quantitative skeleton analysis adapted from Willing et al. (2017). Briefly, after an adjustment of the threshold level as abovementioned, the images were converted to binary images, skeletonized using the skeleton macro from ImageJ and evaluated in terms of number of pixels occupied by skeletons. The number of pixels were then converted to millimeter scale.

α_{2A}-AR Immunoreaction

For the α_{2A}-AR immunoreaction, one in every fourth spinal sections was incubated with a rabbit-raised anti-α_{2A} primary antibody (Neuromics; Cat. No. RA14110), diluted at 1:500, followed by incubation for 1 h with a donkey anti-rabbit Alexa 488 (Molecular Probes®; 1:1000). Photomicrographs were taken under the same time exposure, capture parameters and laser light wavelength (488 nm) on an ApoTome Slider (Zeiss®) fluorescence microscope coupled to the AxioVision Rel. 4.8. software (Zeiss®). The images were analyzed in order to calculate the percentage of pixels occupied by α_{2A}-AR immunoreactivity, size and number of α_{2A}-AR positive neurons in the spinal dorsal horn of 5 randomly taken sections using the ROI manager. The mean percentage of α_{2A}-AR positive pixels in laminae I-II was automatically calculated by the ImageJ software. The size and number of α_{2A}-AR positive neurons were also automatically quantified using the "Analyze Particles" function of ImageJ software.

Western- Blot Analysis of α_{2A} AR

The dorsal portion of the L4 and L5 segments from DMSO ($n = 5$) and paclitaxel-injected animals ($n = 5$) were homogenized with lysis buffer (TBS-T: 20 mM Tris HCl pH 7.4; 150 mM NaCl; 0.1% Triton X-100) containing phosphatase inhibitors and protease inhibitor. A total of 20 μg of protein was loaded and electrophoresed on 12% SDS-PAGE. The proteins were then electroblotted onto nitrocellulose membranes. After incubation with 5% of Blotting-Grade Blocker (Bio-Rad, United States), the membrane was incubated with rabbit anti-α_{2A}-ARs (Neuromics; Cat. No. RA14110) diluted at 1:1000, followed by an anti-rabbit secondary antibody conjugated to horseradish peroxidase (HRP) (1:10000; Jackson Immunoresearch Europe, United Kingdom). The immunoreactive bands were detected by Chemidoc system (Bio-Rad, United States). Glyceraldehyde 3-phosphate dehydrogenase (GAPDH) was used as loading protein internal control, with the membranes being incubated with mouse anti-GAPDH (1:10000; Abcam, United Kingdom) followed by incubation in anti-mouse secondary antibody conjugated to HRP (1:10000; Jackson Immunoresearch Europe, United Kingdom). Semi-quantification of bands was performed using Image Lab software (Bio-Rad, United States) and expressed in arbitrary units. The results of the quantification of α_{2A}-AR expression were presented as normalized for GAPDH.

Specificity of Primary Antibodies

The specificity of the primary anti-DBH antibody was previously demonstrated (Howorth et al., 2009). We tested the specificity of alpha2AR using Western blot of liver samples since the liver tissue does not express mRNA for the receptor (Handy et al., 1993). No band was detected in the blot.

Statistical Analysis

The behavioral results obtained in the Von Frey and cold plate tests were analyzed by two-way repeated measures of ANOVA followed by Tukey's *post hoc* for multiple comparisons. The analysis of the percentage of change obtained in the von Frey and cold plate tests were conducted by ordinary two-way ANOVA followed by Tukey's *post hoc* for multiple comparisons. DBH and α_{2A}-ARs expression in DMSO- and paclitaxel-injected animals were compared by unpaired *t*-test. Statistical analysis was performed by GraphPad Prism (GraphPad Software, United States). Data are presented as mean ± SD. $P < 0.05$ was considered statistically significant values.

RESULTS

In order to evaluate if increasing NA levels or interfering with the function of $\alpha_{2_}$AR differentially affect nociceptive behavioral responses of control and paclitaxel- injected animals, we administered reboxetine, atipamezole or clonidine.

Antinociceptive Effects of Reboxetine

In order to evaluate the behavioral nociceptive effects of an increase of NA levels, we injected the selective NA reuptake inhibitor reboxetine 30 days after the first paclitaxel administration. The results of paclitaxel administration in mechanical and cold sensitivities are shown in **Figure 1**. The analysis of the effects of reboxetine in the von Frey test (**Figures 1A–C**), showed that in DMSO-injected animals (**Figure 1A**) there was a significant interaction between treatments (saline vs. reboxetine) and time [$F(4,32) = 17.60$, $p < 0.0001$]. Reboxetine significantly increased paw withdrawal thresholds at 30 min after injection compared to saline ($p = 0.0091$) and before the injection (T0; $p = 0.0064$). The paw withdrawal thresholds returned to the baseline values 60 min after injection of reboxetine. The analysis of the effects of reboxetine in paclitaxel-injected animals (**Figure 1B**) revealed a significant interaction between treatment and time [$F(4,32) = 62.73$, $p < 0.0001$]. Reboxetine significantly increased paw withdrawal thresholds at 30 and 60 min after injection compared with saline and with T0 ($p < 0.001$). Paw withdrawal thresholds returned to the baseline values 120 min after injection of reboxetine. The injection of saline

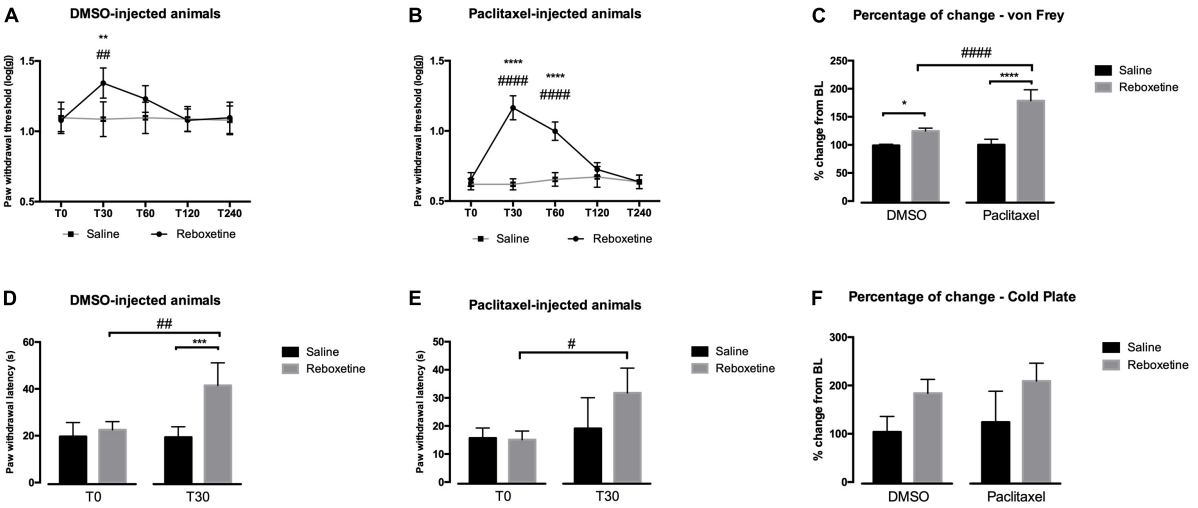

FIGURE 1 | Nociceptive behavioral effects of the administration of reboxetine (30 days after the first paclitaxel injection). **(A,B)** Show a time-course analysis of paw withdrawal thresholds in the von Frey test of DMSO- and paclitaxel-injected rats, respectively, after saline or reboxetine administration. **(D,E)** Show the paw withdrawal latency in the cold plate test at baseline (T0) and 30 min (T30) after saline or reboxetine administration. Data are presented as mean ± SD. $^{*}p < 0.05$; $^{**}p < 0.01$; $^{***}p < 0.001$; $^{****}p < 0.0001$ vs. saline; $^{\#}p < 0.05$; $^{\#\#}p < 0.01$; $^{\#\#\#\#}p < 0.001$ vs. baseline (T0). Graphs **(C,F)** show the percentage of change from baseline of paw withdrawal thresholds and latencies after saline or reboxetine injection in the von Frey **(C)** and cold plate **(F)** tests. Data are presented as mean ± SD (saline: DMSO and paclitaxel $n = 5$; reboxetine at 10 mg/kg: DMSO and paclitaxel $n = 5$). $^{*}p < 0.05$; $^{****}p < 0.0001$ vs. saline; $^{\#\#\#\#}p < 0.001$ vs. DMSO.

did not affect the behavioral responses of DMSO- and paclitaxel-injected animals (**Figures 1A,B**). Overall, the analysis of the variation from baseline, 30 min after injection of reboxetine or saline, revealed a significant interaction between treatments and experimental groups (DMSO *vs.* paclitaxel) [$F(1,16) = 27.53$; $p < 0.0001$; **Figure 1C**]. The increase of withdrawal thresholds was higher after reboxetine than after saline injection both in the DMSO- ($p = 0.0116$) and paclitaxel-group ($p < 0.0001$). The injection of reboxetine induced significantly higher percentages of change in the paclitaxel-group (178.75 ± 19.50%) than in DMSO-group (124.62 ± 5.23%; $p < 0.0001$).

The analysis of the effects of reboxetine in the cold plate test is shown in **Figures 1D–F**. In DMSO-injected animals (**Figure 1D**), reboxetine induced a significant interaction between treatments and time [$F(1,8) = 23.12$, $p = 0.0013$]. Reboxetine significantly increased paw withdrawal latency compared to saline injection ($p = 0.0002$) and T0 ($p = 0.0012$). The analysis of the effects of reboxetine in paclitaxel-injected animals (**Figure 1E**) revealed a significant interaction between treatments and time [$F(1,8) = 5.466$, $p = 0.0476$]. Reboxetine significantly increased the paw withdrawal latency compared to T0 ($p = 0.0127$). No statistically significant alterations in paw withdraw latency were induced after saline injection in DMSO- and paclitaxel-injected animals (**Figures 1D,E**). The overall analysis of the variation (**Figure 1F**) only revealed an effect of treatment [$F(1,16) = 18.60$, $p = 0.0005$] but no effects of the group [$F(1,16) = 1.404$, $p = 0.2533$] or interaction [$F(1,16) = 0.017$, $p = 0.8969$] which indicates that reboxetine increased significantly withdrawal latencies in both experimental groups compared with saline but without significant differences between the group (DMSO: 183.92 ± 28.77%; paclitaxel: 209.09 ± 37.09%).

Pronociceptive Effects of Atipamezole

Since reboxetine administration had an effect at behavioral responses, we then evaluated if blocking α_{2A}-AR at the spinal cord by intrathecal administration of atipamezole, an α_{2A}-AR antagonist, also affected nociceptive behavioral responses. The behavioral effects of intrathecal are shown in **Figure 2**. Overall, the analysis of the effects of atipamezole in the von Frey test (**Figure 2A**) showed a significant interaction between groups (DMSO *vs.* paclitaxel) and time [$F(1,7) = 57.37$, $p = 0.0001$]. In comparison with the respective values at T0, the administration of atipamezole decreased paw withdrawal thresholds in the DMSO ($p = 0.0087$) and paclitaxel group ($p < 0.0001$). After atipamezole injection, the paw withdrawal thresholds of paclitaxel-injected animals were significantly lower than DMSO-treated animals ($p < 0.0001$). At baseline, the experimental groups were statistically different ($p < 0.0001$).

The analysis of the effects of atipamezole in the cold plate test (**Figure 2B**) showed a significant interaction between groups and time [$F(1,7) = 8.048$, $p = 0.0252$]. Compared to baseline, atipamezole significantly decreased paw withdrawal latencies in the DMSO ($p < 0.0001$) and paclitaxel groups ($p = 0.0051$). In the DMSO group, atipamezole decreased withdrawal latencies to values similar to those of the paclitaxel group at T0 ($p = 0.1105$; **Figure 2B**). Paw withdrawal latencies in the paclitaxel group were significantly lower than in the DMSO group after atipamezole injection ($p < 0.0001$). At T0, the DMSO- and paclitaxel groups were statistically different ($p < 0.0001$).

Antinociceptive Effects of Clonidine

Based on the results obtained with reboxetine and atipamezole, we then evaluated if activating α_{2A}-AR at the spinal cord by

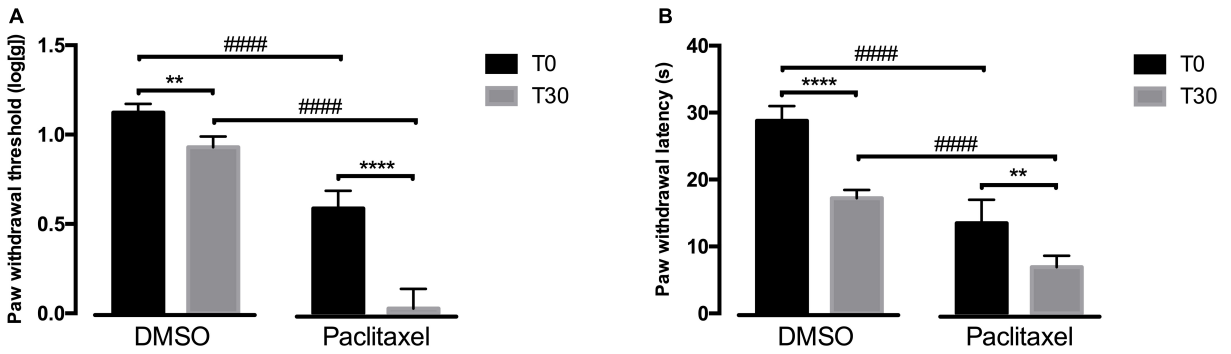

FIGURE 2 | Nociceptive behavioral effects after the administration of atipamezole (30 days after the first paclitaxel injection). **(A)** Shows paw withdrawal threshold in the von Frey test at baseline (T0) and 30 min (T30) after atipamezole administration. **(B)** Shows paw withdrawal latency in the cold plate test at T0 and T30 after atipamezole administration. Data are presented as mean ± SD (DMSO $n = 5$; paclitaxel $n = 4$). $^{**}p < 0.01$; $^{****}p < 0.0001$ vs. baseline (T0); $^{\#\#\#\#}p < 0.0001$ vs. DMSO.

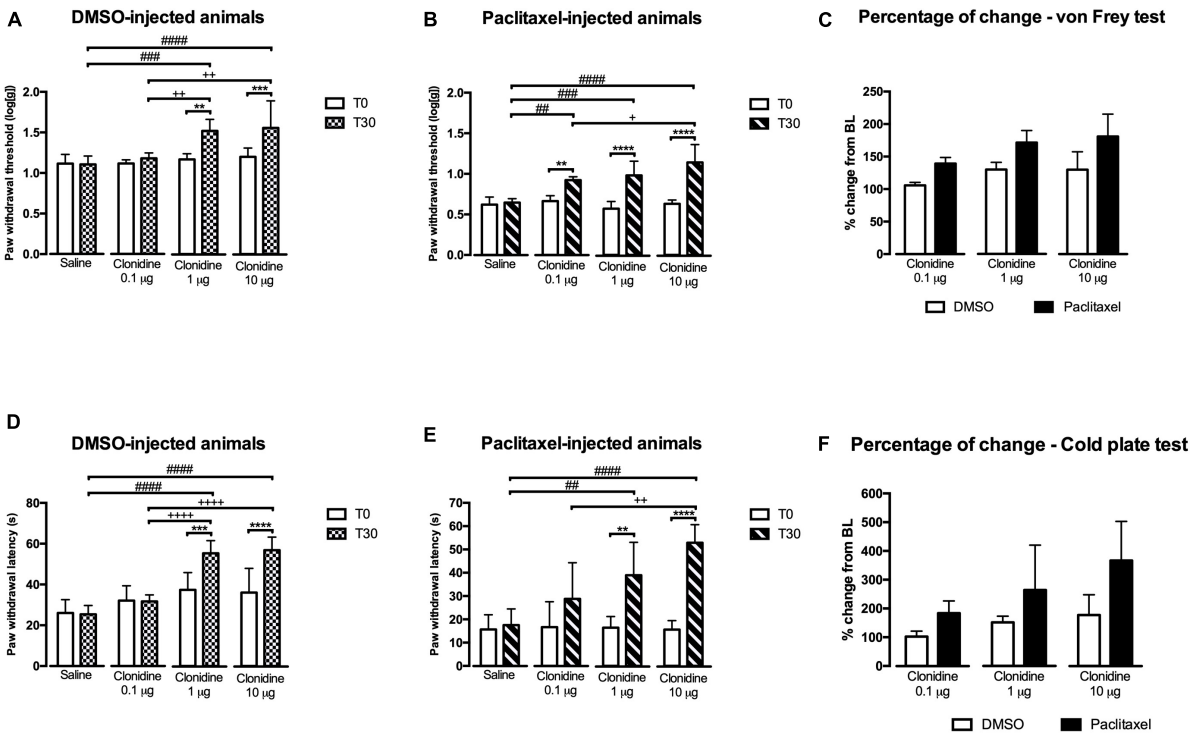

FIGURE 3 | Nociceptive behavioral effects of the administration of clonidine (30 days after the first paclitaxel injection). **(A,B)** Show paw withdrawal thresholds in the von Frey test at baseline (T0) and 30 min (T30) after saline or clonidine administration. **(D,E)** Show paw withdrawal latencies in the cold plate test at T0 and T30 after saline or clonidine administration. **(C,F)** Show the percentage of change from baseline of paw withdrawal thresholds and latencies, in the von Frey **(C)** and cold plate **(D)** tests. Data are presented as mean ± SD (saline: DMSO $n = 7$; paclitaxel $n = 6$; clonidine at 0.1 µg: DMSO $n = 6$; paclitaxel $n = 7$; clonidine at 1 µg: DMSO $n = 7$; paclitaxel $n = 7$; clonidine at 10 µg: DMSO $n = 8$; paclitaxel $n = 6$). $^{**}p < 0.01$; $^{***}p < 0.001$; $^{****}p < 0.0001$ vs. baseline (T0); $^{\#\#}p < 0.01$; $^{\#\#\#}p < 0.001$; $^{\#\#\#\#}p < 0.0001$ vs. saline. $^{+}p < 0.05$; $^{++}p < 0.01$; $^{++++}p < 0.0001$ vs. clonidine 0.1 µg.

intrathecal administration of 3 doses of clonidine, an α_{2A}-AR agonist, also affected nociceptive behavior. The results of the study of the effects of 3 clonidine doses (0.1, 1, and 10 µg) are shown in **Figure 3**. In the von Frey test, the analysis of the effects of clonidine in DMSO-injected animals (**Figure 3A**) revealed a significant interaction between treatments and time [$F(3,24) = 7.589$, $p = 0.0010$]. The lower dose of clonidine (0.1 µg) produced no effects compared to T0 and saline. The higher doses of clonidine significantly increased paw withdrawal thresholds compared to T0 (1 µg: $p = 0.003$; 10 µg: $p = 0.001$), saline (1 µg: $p = 0.0003$; 10 µg: $p < 0.0001$), and clonidine at 0.1 µg (1 µg: $p = 0.0077$; 10 µg: $p = 0.0015$). No differences were detected between clonidine at 1 and 10 µg. Saline injection produced no significant effects and

no differences were detected between the animals at baseline. The effects of clonidine in paclitaxel-injected animals in the von Frey test (**Figure 3B**) revealed a significant interaction between treatment and time [$F(3,22) = 16.63$, $p < 0.0001$]. The 3 doses of clonidine significantly increased paw withdrawal thresholds compared to baseline (0.1 μg: $p = 0.0030$; 1 μg: $p < 0.0001$; 10 μg: $p < 0.0001$) and saline (0.1 μg: $p = 0.0020$; 1 μg: $p = 0.0001$; 10 μg: $p < 0.0001$). Clonidine at 10 μg, showed higher withdrawal thresholds compared to clonidine at 0.1 μg ($p = 0.0257$; **Figure 3B**). No differences were detected between clonidine 0.1 and 1 μg neither between clonidine 1 and 10 μg. At T0, the paw withdrawal thresholds were not significantly different between the different conditions (saline and 3 doses of clonidine). The analysis of the variation from baseline (**Figure 3C**) showed an effect of experimental group [$F(1,35) = 43.29$; $p < 0.0001$] and treatment [$F(2,35) = 10.13$; $p = 0.0003$] but no interaction [$F(2,35) = 0.613$; $p = 0.5473$]. The 3 doses of clonidine significantly increased withdrawal thresholds in the paclitaxel group compared with DMSO group. Overall, the effects of the lower dose (0.1 μg) were significantly lower than the intermediate (1 μg; $p = 0.0042$) and the higher dose (10 μg; $p = 0.0030$). No statistically significant differences were detected between the doses of 1 and 10 μg.

In the cold plate test, the effects of clonidine in DMSO-injected animals (**Figure 3D**) showed a significant interaction between treatment and time [$F(3,24) = 24.19$, $p < 0.0001$]. The lower dose of clonidine (0.1 μg) produced no effects compared to T0 and saline. The higher doses of clonidine significantly increased paw withdrawal latency compared to T0 (1 μg: $p = 0.0009$; 10 μg: $p < 0.0001$), to saline (1 μg: $p < 0.0001$; 10 μg: $p < 0.0001$) and to clonidine at 0.1 μg (1 μg: $p < 0.0001$; 10 μg: $p < 0.0001$). No differences were detected between clonidine at 1 and 10 μg. Saline injection produced no significant effects and no differences were detected between the animals at baseline. The analysis of the effects of clonidine in paclitaxel-injected animals in the cold test (**Figure 3E**) revealed a significant interaction between treatments and time [$F(3,44) = 7.087$, $p = 0.0005$]. The lower dose of clonidine (0.1 μg) produced no effects compared to T0 and saline. The higher doses of clonidine significantly increased paw withdrawal latency compared to baseline (1 μg: $p = 0.0025$; 10 μg: $p < 0.0001$) and saline (1 μg: $p = 0.0076$; 10 μg: $p < 0.0001$). Clonidine at 10 μg showed higher withdrawal latencies compared to clonidine at 0.1 μg ($p = 0.001$; **Figure 3E**). No differences were detected between clonidine 1 and 10 μg (**Figure 3E**). Overall, the analysis of the variation from baseline (**Figure 3F**) revealed an effect of the experimental group [$F(1,35) = 20.07$; $p < 0.0001$] and treatment [$F(2,35) = 6.689$; $p = 0.0035$] but no interaction [$F(2,35) = 1.257$; $p = 0.2971$]. Therefore, the variation is higher in paclitaxel- than DMSO-injected animals. Overall the effects of the lower dose (0.1 μg) are significantly lower than the higher dose (10 μg; $p = 0.0079$).

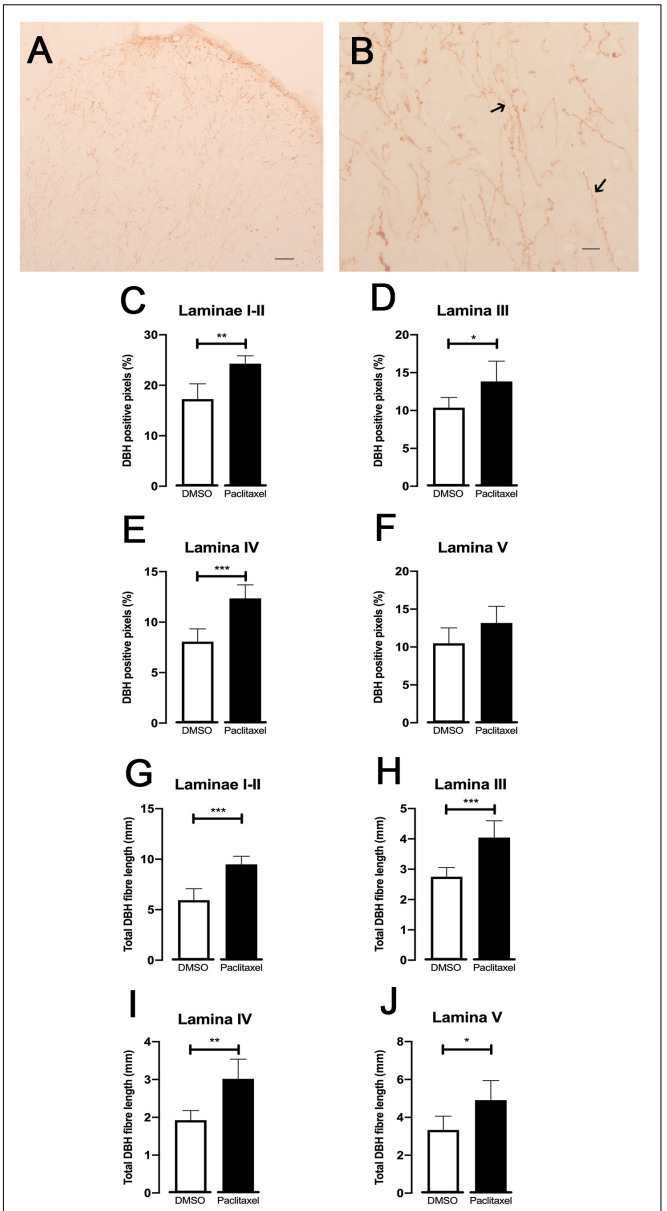

FIGURE 4 | Spinal noradrenergic system evaluated by DBH immunoreaction (30 days after the first paclitaxel injection). Representative photomicrographs of DBH expression at the spinal dorsal horn **(A,B).** The details of fibers namely varicosities are better depicted in **(B)** (arrows). Scale bar in **(A,B)** 200 and 25 μm, respectively. The mean percentages of DBH positive pixels evaluated using the ROI manager are shown in laminae I-II **(C)**, III **(D)**, IV **(E),** and V **(F).** The total length of DBH-immunoreactive fibers quantified using skeleton macro is shown in laminae I-II **(G)**, III **(H)**, IV **(I),** and V **(J).** Data are presented as mean ± SD (DMSO $n = 6$; paclitaxel $n = 6$). $^{*}p < 0.05$; $^{**}p < 0.01$; $^{***}p < 0.001$ paclitaxel vs. DMSO.

DBH-Immunoreaction at the Spinal Cord

To evaluate if the noradrenergic innervation of the spinal dorsal horn is affected during CIPN, the DBH expression was analyzed (**Figure 4**). DBH-immunoreactive fibers were clearly recognized by the brown axons and varicosities scattered throughout the spinal dorsal horn (**Figures 4A,B**). The sections from paclitaxel-injected animals presented significantly higher percentages of DBH-positive pixels compared to the DMSO-injected animals in laminae I–II

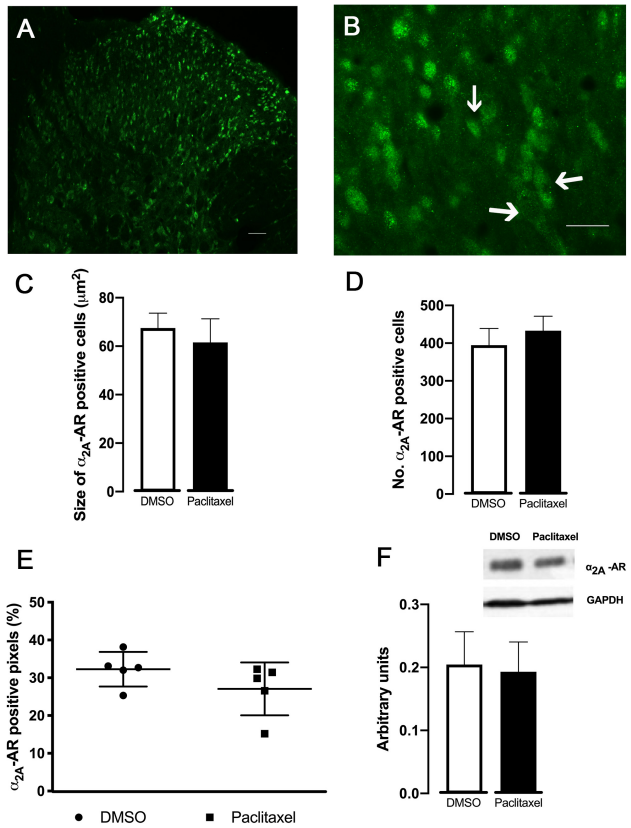

FIGURE 5 | Expression of α_{2A}-AR in the spinal dorsal horn (30 days after the first paclitaxel injection). Representative photomicrographs of a α_{2A}-AR positive pixels at laminae I–II are shown in **(A,B)**. The immunolabelling occurs in structures with neuronal morphology, which are better represented by arrows in **(B)**. Scale bar in **(A,B)**: 100 and 50 μm, respectively. **(C,D)** Show the size and the number of α_{2A}-AR positive neurons, respectively, determined in laminae I-II in DMSO- and paclitaxel-injected animals. **(E)** Represents the percentage of α_{2A}-AR positive pixels in laminae I-II of DMSO- and paclitaxel-injected animals. Data are presented as mean ± SD (DMSO n = 5; paclitaxel n = 5). **(F)** Depicts the quantification of α_{2A}–AR assessed by western-blotting from DMSO- and paclitaxel-injected animals. GAPDH was used as a control of the western-blotting procedure. Data are presented as mean ± SD (DMSO n = 5; paclitaxel n = 5).

(p = 0.0011; **Figure 4C**), lamina III (p = 0.0216; **Figure 4D**), and IV (p = 0.0004; **Figure 4E**). No statistically significantly differences were detected in lamina V (p = 0.0652; **Figure 4F**). The total length of DBH-positive fibers was also analyzed (**Figures 4G–J**). Paclitaxel-injected animals showed longer DBH-positive fibers compared to DMSO-injected animals in laminae I–II (p = 0.0002; **Figure 4G**), lamina III (p = 0.0008; **Figure 4H**), IV (p = 0.0013; **Figure 4I**), and V (p = 0.0158; **Figure 4J**).

Spinal Expression of α_{2A}-AR

In order to evaluate if the higher effects of α_{2A}-AR ligands observed in paclitaxel-injected animals were related to changes in receptor expression, the analysis of the α_{2A}-AR expression at the spinal dorsal horn was performed (**Figure 5**). The immunofluorescence quantification of the superficial dorsal horn (laminae I-II) (**Figure 5E**) revealed that the percentage of α_{2A}-AR positive pixels were not statistically significant different between DMSO- and paclitaxel-injected animals (p = 0.2017). Likewise, the analysis of size and number of α_{2A}-AR positive objects did not show significantly differences between experimental groups (p = 0.2804 and p = 0.1820, respectively; **Figures 5C,D**).

The western-blotting analysis (**Figure 5F**) did not show statistically significant differences between DMSO- and paclitaxel-injected animals (p = 0.7174).

DISCUSSION

The present study shows, for the first time, that the noradrenergic modulation of spinal nociceptive transmission is altered in an animal model of paclitaxel-induced CIPN. This is relevant since the study of descending pain modulation should take into account the specific features of the preclinical model (Porreca et al., 2002; Ossipov et al., 2014) and descending noradrenergic modulation was never studied in the paclitaxel-induced CIPN model. To study noradrenergic modulation of nociceptive transmission at the spinal cord in paclitaxel-induced CIPN, we performed behavioral and structural studies. Regarding the behavioral studies, paclitaxel-injected animals treated with the selective NA reuptake inhibitor reboxetine showed a decrease of nociceptive behaviors. The antinociceptive effects of reboxetine were much more robust in paclitaxel-injected animals than in controls, both in magnitude and duration. Considering the increased NA levels in the spinal cord after reboxetine injection (Nakajima et al., 2012), the present findings showing antinociceptive effects after reboxetine administration indicate an increased recruitment of descending noradrenergic pain inhibition during paclitaxel-induced CIPN. The reboxetine data are further supported by the results of the intrathecal administration of the α_{2A}-AR antagonist atipamezole and of the α_{2A}-AR agonist clonidine since both drugs induced higher behavioral effects in paclitaxel-injected animals. The results suggest a relation between the dose and the magnitude of behavioral antinociceptive responses. Furthermore, the lowest clonidine dose (0.1 μg) failed to show an effect in DMSO-injected animals whereas in paclitaxel-injected animals it induced an antinociceptive effect. The clonidine data reinforce the hypothesis that in paclitaxel-induced CIPN there is an increased recruitment of noradrenergic modulation at the spinal cord. Incidentally, it should be noted that the current pharmacological studies support the existence of tonic noradrenergic inhibition since the intrathecal administration of atipamezole and clonidine to DMSO-injected animals altered their behavioral nociceptive responses. The existence of a tonic noradrenergic inhibition is a question under dispute since some studies show that atipamezole induces mechanical and cold allodynia in control animals (Xu et al., 1999), whereas others failed to show effects (Wei and Pertovaara, 2006; Patel et al., 2018). The role of the descending noradrenergic system during chronic pain installation is interesting. In traumatic pain models, some studies reported plastic changes

and functional upregulation of spinal α_2-AR (Stone et al., 1999; Ma and Eisenach, 2003; Bantel et al., 2005; Hayashida et al., 2008). This was proposed to compensate the enhanced nociceptive peripheral input, through increased noradrenaline levels and enhancement of the potency of α_2-AR at the spinal cord. With the progression of traumatic neuropathy, a gradual loss of descending noradrenergic inhibition occurs along with an increase of descending facilitation (Viisanen and Pertovaara, 2007; Rahman et al., 2008; Hughes et al., 2013, 2015; Patel et al., 2018). By studying paclitaxel-induced CIPN using a short duration, the present result indicates that CIPN is similar to short-term models of traumatic neuropathy. Since the duration of neuropathy also affects the features of descending modulation, we will increase the duration of our studies in the paclitaxel-induced CIPN model to evaluate if a switch of descending noradrenergic modulation from inhibitory to facilitatory could account for the intensification of CIPN after long term chemotherapy treatments, a current problem for cancer survivors (Mantyh, 2006; Seretny et al., 2014).

As to the structural data, the levels of DBH in the spinal dorsal horn cord were higher in paclitaxel-injected animals. The analysis of the laminar distribution in what concerns the length of fibers and positive-pixels showed that the increase was due to contribution of all the spinal laminae. The increase in the DBH levels at the spinal cord matches the results obtained in traumatic neuropathic pain models (Ma and Eisenach, 2003) and indicates increased noradrenergic innervation of the spinal dorsal horn in chronic pain situations. The higher potency of atipamezole and clonidine in paclitaxel-injected animals cannot be explained by an increase in the expression of α_{2A}-AR at the superficial dorsal horn (laminae I–II), as no differences were found in the expression of α_{2A}-AR between paclitaxel- and DMSO-injected animals. An increase of potency of α_2-AR without changes in receptor expression may be due to increased efficiency of G-protein coupled α_2-AR (Bantel et al., 2005; Chen et al., 2007). The antinociceptive effects of clonidine are well reported in clinical studies (Rauck et al., 2015) and in models of traumatic peripheral nerve injury (Hayashida et al., 2008). Clonidine acts at presynaptic α_2-AR located on the central terminals of primary afferents and on postsynaptic dorsal horn α_2-AR (Pan et al., 2002; Mitrovic et al., 2003). In the present study, we cannot discriminate between the pre- and postsynaptic components of α_2-AR. Paclitaxel induces abnormal outgrowth of primary afferent sensory neurons (Letourneau and Ressler, 1984; Cliffer et al., 1998) but since no changes in α_2-AR expression were detected in the present study, it is likely that the primary afferents which express α_2-AR are not structurally affected during CINP. The neurochemical nature of primary affect fibers damaged by paclitaxel is starting to be studied with indications that NMDA receptors are affected (Xie et al., 2016; Chen et al., 2019). Another emergent issue is the cell type which expresses α_2-AR since at the spinal cord the receptors are present in neurons and glial cells (Xu et al., 2010). No differences were detected in the number and size of cell profiles immunostained for α_2-AR between the experimental groups and most of the immunostained profiles were large and similar to neurons. Detailed comparisons of the expression of α_2-AR in neurons and glial cells (astrocytes and microglia) between control and paclitaxel-injected animals can provide evidence about a possible role of spinal glia during CIPN. The behavioral studies with reboxetine, atipamezole and clonidine clearly showed more pronounced drug effects in mechanical allodynia than in cold hyperalgesia. This is an interesting finding since mechanical allodynia is a sensory modality predominantly modulated supraspinally, namely by brainstem centers engaged in noradrenergic inhibitory control (Xu et al., 1999; Saade et al., 2006; Hughes et al., 2015). The LC is likely to be the main source of the increased descending input since it is, by large, the main source of noradrenergic fibers at the spinal cord in the rat strain used in the present study (Tavares et al., 1997). Noradrenergic modulation from the LC is an important coordinator of the balance between inhibition and facilitation of descending pain control (Rahman et al., 2008; Martins et al., 2015). We showed antinociceptive effects of NA in paclitaxel-injected animals which indicates that during CIPN noradrenergic modulation from the LC preserves its inhibitory tone. We have recently shown that in paclitaxel-induced CIPN there is an increased activation of serotoninergic RVM neurons (Costa-Pereira et al., 2019). Since the RVM targets the LC and this connection is relevant for descending noradrenergic pain modulation (Sim and Joseph, 1992; Bahari and Meftahi, 2019) it is possible that the activation of RVM neurons recently reported in the paclitaxel-induced CIPN model (Costa-Pereira et al., 2019) is a trigger of increased recruitment of noradrenergic descending modulation during CIPN.

Patients affected by CIPN are empirically treated with antidepressant drugs which potentiate the effects of NA and serotonin but the relative contribution of each neurochemical system is unknown (Sisignano et al., 2014). By showing that in the paclitaxel CIPN model, the inhibitory function of the noradrenergic system is potentiated and based on our recent demonstration that the serotoninergic system exerts pronociceptive effects mediated by spinal 5HT3 receptors (Costa-Pereira et al., 2019), we propose that treating CIPN with drugs that mainly target the noradrenergic system may be a valuable approach in the future of cancer treatment. However, further preclinical studies are necessary namely in what concerns the evaluation of the mechanisms of noradrenergic modulation of nociceptive transmission during CIPN in female animals. Although no differences in the sex differences in mechanical allodynia were detected between male and female rodents (Hwang et al., 2012; Naji-Esfahani et al., 2016), one study showed sex differences in cold allodynia (Ward et al., 2011). To better envisage the translational perspectives of the present study, it is important to include female animals inasmuch that paclitaxel is used in the treatment of tumors that affect women, such as breast, cervical and ovarian cancers (Cavaletti and Marmiroli, 2010).

DATA AVAILABILITY STATEMENT

The datasets generated for this study are available on request to the corresponding author.

ETHICS STATEMENT

The animal study was reviewed and approved by the Institutional Animal Care and Use Committee of the Faculty of Medicine of the University of Porto.

AUTHOR CONTRIBUTIONS

JC-P, IM, and IT participated in study design and planning of experiments, wrote the first versions of the manuscript. JC-P and JR performed the experiments. JC-P, JR, and IM analyzed the data. All authors revised the manuscript.

FUNDING

This study was supported by a grant of Norte 2020/NORTE-01-0145-FEDER-000008. JC-P is recipient of a Ph.D. grant of NORTE-08-5369-FSE-000026. The sponsors had no role in study design, collection, analysis, interpretation of data, and writing of the manuscript for publication.

REFERENCES

Bahari, Z., and Meftahi, G. H. (2019). Spinal alpha2 -adrenoceptors and neuropathic pain modulation; therapeutic target. *Br. J. Pharmacol.* 176, 2366–2381. doi: 10.1111/bph.14580

Bantel, C., Eisenach, J. C., Duflo, F., Tobin, J. R., and Childers, S. R. (2005). Spinal nerve ligation increases alpha2-adrenergic receptor G-protein coupling in the spinal cord. *Brain Res.* 1038, 76–82. doi: 10.1016/j.brainres.2005.01.016

Bie, B., Fields, H. L., Williams, J. T., and Pan, Z. Z. (2003). Roles of alpha1- and alpha2-adrenoceptors in the nucleus raphe magnus in opioid analgesia and opioid abstinence-induced hyperalgesia. *J. Neurosci.* 23, 7950–7957. doi: 10.1523/jneurosci.23-21-07950.2003

Boehmerle, W., Huehnchen, P., Peruzzaro, S., Balkaya, M., and Endres, M. (2014). Electrophysiological, behavioral and histological characterization of paclitaxel, cisplatin, vincristine and bortezomib-induced neuropathy in C57Bl/6 mice. *Sci. Rep.* 4:6370. doi: 10.1038/srep06370

Braz, J. M., Wang, X., Guan, Z., Rubenstein, J. L., and Basbaum, A. I. (2015). Transplant-mediated enhancement of spinal cord GABAergic inhibition reverses paclitaxel-induced mechanical and heat hypersensitivity. *Pain* 156, 1084–1091. doi: 10.1097/j.pain.0000000000000152

Budai, D., Harasawa, I., and Fields, H. L. (1998). Midbrain periaqueductal gray (PAG) inhibits nociceptive inputs to sacral dorsal horn nociceptive neurons through alpha2-adrenergic receptors. *J. Neurophysiol.* 80, 2244–2254. doi: 10.1152/jn.1998.80.5.2244

Cata, J. P., Weng, H. R., Chen, J. H., and Dougherty, P. M. (2006). Altered discharges of spinal wide dynamic range neurons and down-regulation of glutamate transporter expression in rats with paclitaxel-induced hyperalgesia. *Neuroscience* 138, 329–338. doi: 10.1016/j.neuroscience.2005.11.009

Cavaletti, G., and Marmiroli, P. (2010). Chemotherapy-induced peripheral neurotoxicity. *Nat. Rev. Neurol.* 6, 657–666. doi: 10.1038/nrneurol.2010.160

Chaplan, S. R., Bach, F. W., Pogrel, J. W., Chung, J. M., and Yaksh, T. L. (1994). Quantitative assessment of tactile allodynia in the rat paw. *J. Neurosci. Methods* 53, 55–63. doi: 10.1016/0165-0270(94)90144-9

Chen, S. R., Pan, H. M., Richardson, T. E., and Pan, H. L. (2007). Potentiation of spinal alpha(2)-adrenoceptor analgesia in rats deficient in TRPV1-expressing afferent neurons. *Neuropharmacology* 52, 1624–1630. doi: 10.1016/j.neuropharm.2007.03.009

Chen, Y., Chen, S. R., Chen, H., Zhang, J., and Pan, H. L. (2019). Increased alpha2delta-1-NMDA receptor coupling potentiates glutamatergic input to spinal dorsal horn neurons in chemotherapy-induced neuropathic pain. *J. Neurochem.* 148, 252–274. doi: 10.1111/jnc.14627

Chen, Y., Yang, C., and Wang, Z. J. (2011). Proteinase-activated receptor 2 sensitizes transient receptor potential vanilloid 1, transient receptor potential vanilloid 4, and transient receptor potential ankyrin 1 in paclitaxel-induced neuropathic pain. *Neuroscience* 193, 440–451. doi: 10.1016/j.neuroscience.2011.06.085

Cliffer, K. D., Siuciak, J. A., Carson, S. R., Radley, H. E., Park, J. S., Lewis, D. R., et al. (1998). Physiological characterization of Taxol-induced large-fiber sensory neuropathy in the rat. *Ann. Neurol.* 43, 46–55. doi: 10.1002/ana.410430111

Costa-Pereira, J. T., Serrao, P., Martins, I., and Tavares, I. (2019). Serotoninergic pain modulation from the rostral ventromedial medulla (RVM) in chemotherapy-induced neuropathy: the role of spinal 5-HT3 receptors. *Eur. J. Neurosci.* doi: 10.1111/ejn.14614 [Epub ahead of print].

Dimitrov, E. L., Kuo, J., Kohno, K., and Usdin, T. B. (2013). Neuropathic and inflammatory pain are modulated by tuberoinfundibular peptide of 39 residues. *Proc. Natl. Acad. Sci. U.S.A.* 110, 13156–13161. doi: 10.1073/pnas.1306342110

Eisenach, J. C., De Kock, M., and Klimscha, W. (1996). alpha(2)-adrenergic agonists for regional anesthesia. A clinical review of clonidine (1984-1995). *Anesthesiology* 85, 655–674. doi: 10.1097/00000542-199609000-00026

Ferris, C. F., Nodine, S., Pottala, T., Cai, X., Knox, T. M., Fofana, F. H., et al. (2019). Alterations in brain neurocircuitry following treatment with the chemotherapeutic agent paclitaxel in rats. *Neurobiol. Pain* 6:100034. doi: 10.1016/j.ynpai.2019.100034

Flatters, S. J., and Bennett, G. J. (2006). Studies of peripheral sensory nerves in paclitaxel-induced painful peripheral neuropathy: evidence for mitochondrial dysfunction. *Pain* 122, 245–257. doi: 10.1016/j.pain.2006.01.037

Handy, D. E., Flordellis, C. S., Bogdanova, N. N., Bresnahan, M. R., and Gavras, H. (1993). Diverse tissue expression of rat alpha 2-adrenergic receptor genes. *Hypertension* 21, 861–865. doi: 10.1161/01.hyp.21.6.861

Hayashida, K., Clayton, B. A., Johnson, J. E., and Eisenach, J. C. (2008). Brain derived nerve growth factor induces spinal noradrenergic fiber sprouting and enhances clonidine analgesia following nerve injury in rats. *Pain* 136, 348–355. doi: 10.1016/j.pain.2007.07.014

Heinricher, M. M., Tavares, I., Leith, J. L., and Lumb, B. M. (2009). Descending control of nociception: specificity, recruitment and plasticity. *Brain Res. Rev.* 60, 214–225. doi: 10.1016/j.brainresrev.2008.12.009

Howorth, P. W., Teschemacher, A. G., and Pickering, A. E. (2009). Retrograde adenoviral vector targeting of nociresponsive pontospinal noradrenergic neurons in the rat in vivo. *J. Comp. Neurol.* 512, 141–157. doi: 10.1002/cne.21879

Hughes, S., Hickey, L., Donaldson, L. F., Lumb, B. M., and Pickering, A. E. (2015). Intrathecal reboxetine suppresses evoked and ongoing neuropathic pain behaviours by restoring spinal noradrenergic inhibitory tone. *Pain* 156, 328–334. doi: 10.1097/01.j.pain.0000460313.73358.31

Hughes, S. W., Hickey, L., Hulse, R. P., Lumb, B. M., and Pickering, A. E. (2013). Endogenous analgesic action of the pontospinal noradrenergic system spatially restricts and temporally delays the progression of neuropathic pain following tibial nerve injury. *Pain* 154, 1680–1690. doi: 10.1016/j.pain.2013.05.010

Hwang, B. Y., Kim, E. S., Kim, C. H., Kwon, J. Y., and Kim, H. K. (2012). Gender differences in paclitaxel-induced neuropathic pain behavior and analgesic response in rats. *Korean J. Anesthesiol.* 62, 66–72. doi: 10.4097/kjae.2012.62.1.66

Kawasaki, Y., Kumamoto, E., Furue, H., and Yoshimura, M. (2003). Alpha 2 adrenoceptor-mediated presynaptic inhibition of primary

afferent glutamatergic transmission in rat substantia gelatinosa neurons. *Anesthesiology* 98, 682–689. doi: 10.1097/00000542-200303000-00016

Kerckhove, N., Collin, A., Conde, S., Chaleteix, C., Pezet, D., and Balayssac, D. (2017). Long-term effects, pathophysiological mechanisms, and risk factors of chemotherapy-induced peripheral neuropathies: a comprehensive literature review. *Front. Pharmacol.* 8:86. doi: 10.3389/fphar.2017.00086

Kinoshita, J., Takahashi, Y., Watabe, A. M., Utsunomiya, K., and Kato, F. (2013). Impaired noradrenaline homeostasis in rats with painful diabetic neuropathy as a target of duloxetine analgesia. *Mol. Pain* 9:59. doi: 10.1186/1744-8069-9-59

Lapmanee, S., Charoenphandhu, J., and Charoenphandhu, N. (2013). Beneficial effects of fluoxetine, reboxetine, venlafaxine, and voluntary running exercise in stressed male rats with anxiety- and depression-like behaviors. *Behav. Brain Res.* 250, 316–325. doi: 10.1016/j.bbr.2013.05.018

Letourneau, P. C., and Ressler, A. H. (1984). Inhibition of neurite initiation and growth by taxol. *J. Cell Biol.* 98, 1355–1362. doi: 10.1083/jcb.98.4.1355

Ma, W., and Eisenach, J. C. (2003). Chronic constriction injury of sciatic nerve induces the up-regulation of descending inhibitory noradrenergic innervation to the lumbar dorsal horn of mice. *Brain Res.* 970, 110–118. doi: 10.1016/s0006-8993(03)02293-5

Mantyh, P. W. (2006). Cancer pain and its impact on diagnosis, survival and quality of life. *Nat. Rev. Neurosci.* 7, 797–809. doi: 10.1038/nrn1914

Martins, I., Carvalho, P., De Vries, M. G., Teixeira-Pinto, A., Wilson, S. P., Westerink, B. H., et al. (2015). Increased noradrenergic neurotransmission to a pain facilitatory area of the brain is implicated in facilitation of chronic pain. *Anesthesiology* 123, 642–653. doi: 10.1097/ALN.0000000000000749

Mitrovic, I., Margeta-Mitrovic, M., Bader, S., Stoffel, M., Jan, L. Y., and Basbaum, A. I. (2003). Contribution of GIRK2-mediated postsynaptic signaling to opiate and alpha 2-adrenergic analgesia and analgesic sex differences. *Proc. Natl. Acad. Sci. U.S.A.* 100, 271–276. doi: 10.1073/pnas.0136822100

Naji-Esfahani, H., Vaseghi, G., Safaeian, L., Pilehvarian, A. A., Abed, A., and Rafieian-Kopaei, M. (2016). Gender differences in a mouse model of chemotherapy-induced neuropathic pain. *Lab. Anim.* 50, 15–20. doi: 10.1177/0023677215575863

Nakajima, K., Obata, H., Iriuchijima, N., and Saito, S. (2012). An increase in spinal cord noradrenaline is a major contributor to the antihyperalgesic effect of antidepressants after peripheral nerve injury in the rat. *Pain* 153, 990–997. doi: 10.1016/j.pain.2012.01.029

Ortiz, J. P., Close, L. N., Heinricher, M. M., and Selden, N. R. (2008). Alpha(2)-noradrenergic antagonist administration into the central nucleus of the amygdala blocks stress-induced hypoalgesia in awake behaving rats. *Neuroscience* 157, 223–228. doi: 10.1016/j.neuroscience.2008.08.051

Ossipov, M. H., Morimura, K., and Porreca, F. (2014). Descending pain modulation and chronification of pain. *Curr. Opin. Support Palliat. Care* 8, 143–151. doi: 10.1097/SPC.0000000000000055

Pan, Y. Z., Li, D. P., and Pan, H. L. (2002). Inhibition of glutamatergic synaptic input to spinal lamina II(o) neurons by presynaptic alpha(2)-adrenergic receptors. *J. Neurophysiol.* 87, 1938–1947. doi: 10.1152/jn.00575.2001

Patel, R., Qu, C., Xie, J. Y., Porreca, F., and Dickenson, A. H. (2018). Selective deficiencies in descending inhibitory modulation in neuropathic rats: implications for enhancing noradrenergic tone. *Pain* 159, 1887–1899. doi: 10.1097/j.pain.0000000000001300

Pertovaara, A. (2006). Noradrenergic pain modulation. *Prog. Neurobiol.* 80, 53–83. doi: 10.1016/j.pneurobio.2006.08.001

Pertovaara, A. (2013). The noradrenergic pain regulation system: a potential target for pain therapy. *Eur. J. Pharmacol.* 716, 2–7. doi: 10.1016/j.ejphar.2013.01.067

Pertovaara, A., Hamalainen, M. M., Kauppila, T., Mecke, E., and Carlson, S. (1994). Dissociation of the alpha 2-adrenergic antinociception from sedation following microinjection of medetomidine into the locus coeruleus in rats. *Pain* 57, 207–215. doi: 10.1016/0304-3959(94)90225-9

Polomano, R. C., Mannes, A. J., Clark, U. S., and Bennett, G. J. (2001). A painful peripheral neuropathy in the rat produced by the chemotherapeutic drug, paclitaxel. *Pain* 94, 293–304. doi: 10.1016/s0304-3959(01)00363-3

Porreca, F., Ossipov, M. H., and Gebhart, G. F. (2002). Chronic pain and medullary descending facilitation. *Trends Neurosci.* 25, 319–325. doi: 10.1016/s0166-2236(02)02157-4

Rahman, W., D'mello, R., and Dickenson, A. H. (2008). Peripheral nerve injury-induced changes in spinal alpha(2)-adrenoceptor-mediated modulation of mechanically evoked dorsal horn neuronal responses. *J. Pain* 9, 350–359. doi: 10.1016/j.jpain.2007.11.010

Rauck, R. L., North, J., and Eisenach, J. C. (2015). Intrathecal clonidine and adenosine: effects on pain and sensory processing in patients with chronic regional pain syndrome. *Pain* 156, 88–95. doi: 10.1016/j.pain.0000000000000007

Saade, N. E., Al Amin, H., Chalouhi, S., Baki, S. A., Jabbur, S. J., and Atweh, S. F. (2006). Spinal pathways involved in supraspinal modulation of neuropathic manifestations in rats. *Pain* 126, 280–293. doi: 10.1016/j.pain.2006.07.010

Samineni, V. K., Premkumar, L. S., and Faingold, C. L. (2017). Neuropathic pain-induced enhancement of spontaneous and pain-evoked neuronal activity in the periaqueductal gray that is attenuated by gabapentin. *Pain* 158, 1241–1253. doi: 10.1097/j.pain.0000000000000905

Seretny, M., Currie, G. L., Sena, E. S., Ramnarine, S., Grant, R., Macleod, M. R., et al. (2014). Incidence, prevalence, and predictors of chemotherapy-induced peripheral neuropathy: a systematic review and meta-analysis. *Pain* 155, 2461–2470. doi: 10.1016/j.pain.2014.09.020

Sim, L. J., and Joseph, S. A. (1992). Efferent projections of the nucleus raphe magnus. *Brain Res. Bull.* 28, 679–682. doi: 10.1016/0361-9230(92)90246-t

Sisignano, M., Baron, R., Scholich, K., and Geisslinger, G. (2014). Mechanism-based treatment for chemotherapy-induced peripheral neuropathic pain. *Nat. Rev. Neurol.* 10, 694–707. doi: 10.1038/nrneurol.2014.211

Stone, L. S., Vulchanova, L., Riedl, M. S., Wang, J., Williams, F. G., Wilcox, G. L., et al. (1999). Effects of peripheral nerve injury on alpha-2A and alpha-2C adrenergic receptor immunoreactivity in the rat spinal cord. *Neuroscience* 93, 1399–1407. doi: 10.1016/s0306-4522(99)00209-2

Tavares, I., Lima, D., and Coimbra, A. (1997). The pontine A5 noradrenergic cells which project to the spinal cord dorsal horn are reciprocally connected with the caudal ventrolateral medulla in the rat. *Eur. J. Neurosci.* 9, 2452–2461. doi: 10.1111/j.1460-9568.1997.tb01662.x

Tracey, I., and Mantyh, P. W. (2007). The cerebral signature for pain perception and its modulation. *Neuron* 55, 377–391. doi: 10.1016/j.neuron.2007.07.012

Vanderah, T. W., Suenaga, N. M., Ossipov, M. H., Malan, T. P. Jr, Lai, J., and Porreca, F. (2001). Tonic descending facilitation from the rostral ventromedial medulla mediates opioid-induced abnormal pain and antinociceptive tolerance. *J. Neurosci.* 21, 279–286. doi: 10.1523/jneurosci.21-01-00279.2001

Viisanen, H., and Pertovaara, A. (2007). Influence of peripheral nerve injury on response properties of locus coeruleus neurons and coeruleospinal antinociception in the rat. *Neuroscience* 146, 1785–1794. doi: 10.1016/j.neuroscience.2007.03.016

Ward, S. J., Ramirez, M. D., Neelakantan, H., and Walker, E. A. (2011). Cannabidiol prevents the development of cold and mechanical allodynia in paclitaxel-treated female C57Bl6 mice. *Anesth. Analg.* 113, 947–950. doi: 10.1213/ANE.0b013e3182283486

Wei, H., and Pertovaara, A. (2006). Spinal and pontine alpha2-adrenoceptors have opposite effects on pain-related behavior in the neuropathic rat. *Eur. J. Pharmacol.* 551, 41–49. doi: 10.1016/j.ejphar.2006.08.064

Willing, J., Cortes, L. R., Brodsky, J. M., Kim, T., and Juraska, J. M. (2017). Innervation of the medial prefrontal cortex by tyrosine hydroxylase immunoreactive fibers during adolescence in male and female rats. *Dev. Psychobiol.* 59, 583–589. doi: 10.1002/dev.21525

Worthley, E. G., and Schott, C. D. (1969). The toxicity of four concentrations of DMSO. *Toxicol. Appl. Pharmacol.* 15, 275–281. doi: 10.1016/0041-008x(69)90027-1

Xie, J. D., Chen, S. R., Chen, H., Zeng, W. A., and Pan, H. L. (2016). Presynaptic N-Methyl-d-aspartate (n.d.) receptor activity is increased through protein Kinase C in paclitaxel-induced neuropathic pain. *J. Biol. Chem.* 291, 19364–19373. doi: 10.1074/jbc.M116.732347

Xu, B., Zhang, W. S., Yang, J. L., Lu, N., Deng, X. M., Xu, H., et al. (2010). Evidence for suppression of spinal glial activation by dexmedetomidine in

a rat model of monoarthritis. *Clin. Exp. Pharmacol. Physiol.* 37, e158–e166. doi: 10.1111/j.1440-1681.2010.05426.x

Xu, M., Kontinen, V. K., and Kalso, E. (1999). Endogenous noradrenergic tone controls symptoms of allodynia in the spinal nerve ligation model of neuropathic pain. *Eur. J. Pharmacol.* 366, 41–45. doi: 10.1016/s0014-2999(98)00910-8

Yadav, R., Yan, X., Maixner, D. W., Gao, M., and Weng, H. R. (2015). Blocking the GABA transporter GAT-1 ameliorates spinal GABAergic disinhibition and neuropathic pain induced by paclitaxel. *J. Neurochem.* 133, 857–869. doi: 10.1111/jnc.13103

Yaksh, T. L., Pogrel, J. W., Lee, Y. W., and Chaplan, S. R. (1995). Reversal of nerve ligation-induced allodynia by spinal alpha-2 adrenoceptor agonists. *J. Pharmacol. Exp. Ther.* 272, 207–214.

Zimmermann, M. (1983). Ethical guidelines for investigations of experimental pain in conscious animals. *Pain* 16, 109–110. doi: 10.1016/0304-3959(83)90201-4

Conflict of Interest: The authors declare that the research was conducted in the absence of any commercial or financial relationships that could be construed as a potential conflict of interest.

frontiers in Cellular Neuroscience

REVIEW
published: 17 April 2020
doi: 10.3389/fncel.2020.00072

Intracellular Trafficking Mechanisms of Synaptic Dysfunction in Alzheimer's Disease

*Catarina Perdigão, Mariana A. Barata, Margarida N. Araújo, Farzaneh S. Mirfakhar, Jorge Castanheira and Cláudia Guimas Almeida**

Laboratory Neuronal Trafficking in Aging, CEDOC Chronic Diseases Research Center, NOVA Medical School, Universidade NOVA de Lisboa, Lisbon, Portugal

Alzheimer's disease (AD) is the most common neurodegenerative disease characterized by progressive memory loss. Although AD neuropathological hallmarks are extracellular amyloid plaques and intracellular tau tangles, the best correlate of disease progression is synapse loss. What causes synapse loss has been the focus of several researchers in the AD field. Synapses become dysfunctional before plaques and tangles form. Studies based on early-onset familial AD (eFAD) models have supported that synaptic transmission is depressed by β-amyloid (Aβ) triggered mechanisms. Since eFAD is rare, affecting only 1% of patients, research has shifted to the study of the most common late-onset AD (LOAD). Intracellular trafficking has emerged as one of the pathways of LOAD genes. Few studies have assessed the impact of trafficking LOAD genes on synapse dysfunction. Since endocytic traffic is essential for synaptic function, we reviewed Aβ-dependent and independent mechanisms of the earliest synaptic dysfunction in AD. We have focused on the role of intraneuronal and secreted Aβ oligomers, highlighting the dysfunction of endocytic trafficking as an Aβ-dependent mechanism of synapse dysfunction in AD. Here, we reviewed the LOAD trafficking genes APOE4, ABCA7, BIN1, CD2AP, PICALM, EPH1A, and SORL1, for which there is a synaptic link. We conclude that in eFAD and LOAD, the earliest synaptic dysfunctions are characterized by disruptions of the presynaptic vesicle exo- and endocytosis and of postsynaptic glutamate receptor endocytosis. While in eFAD synapse dysfunction seems to be triggered by Aβ, in LOAD, there might be a direct synaptic disruption by LOAD trafficking genes. To identify promising therapeutic targets and biomarkers of the earliest synaptic dysfunction in AD, it will be necessary to join efforts in further dissecting the mechanisms used by Aβ and by LOAD genes to disrupt synapses.

Keywords: late-onset Alzheimer's disease, synapses, endocytosis, β-amyloid, APOE4, PICALM, BIN1, CD2AP

OPEN ACCESS

Edited by:
Alessandro Tozzi, University of Perugia, Italy

Reviewed by:
Gunnar Keppler Gouras, Lund University, Sweden
Davide Tampellini, Institut National de la Santé et de la Recherche Médicale (INSERM), France

***Correspondence:**
Cláudia Guimas Almeida
claudia.almeida@nms.unl.pt

Specialty section:
This article was submitted to Cellular Neuropathology, a section of the journal Frontiers in Cellular Neuroscience

Received: *02 February 2020*
Accepted: *12 March 2020*
Published: *17 April 2020*

Citation:
Perdigão C, Barata MA, Araújo MN, Mirfakhar FS, Castanheira J and Guimas Almeida C (2020) Intracellular Trafficking Mechanisms of Synaptic Dysfunction in Alzheimer's Disease. Front. Cell. Neurosci. 14:72. doi: 10.3389/fncel.2020.00072

INTRODUCTION

Alzheimer's disease (AD), the most common neurodegenerative disease, affecting 1 in 10 people over 65 years old, remains without adequate treatment. By the age of 85, one in three people develops the disease (Alzheimer's Association, 2019). Functionally, a progressive loss of memory and cognitive impairment leads to a loss of autonomy and independance. Neuropathologically,

AD is characterized by two hallmark proteinaceous aggregates, extracellular amyloid plaques and intracellular neurofibrillary tangles. The AD brain volume is dramatically reduced, mainly due to extensive cortical neuronal death. These are hallmark phenotypes of a disease in which pathological mechanisms can start 30 years before diagnosis. Importantly, the synapse loss is the best pathological correlate of cognitive impairment in AD, which can exceed and precede the existing neuronal cell death (Tampellini and Gouras, 2010). Among the earliest disease phenotypes are intracellular β-amyloid (Aβ) accumulation and synapse dysfunction. Synapse dysfunction can remain silent, at least initially, due to the reserve brain capacity to compensate for the affected neurons. Cognitive impairment likely manifests when the pathology spreads throughout the brain. Thus, it has become apparent that the next step for AD research is to focus on identifying novel therapeutic strategies targeted at the earliest mechanisms of synaptic dysfunction.

AD has two forms (Katzman, 1976), the familial early-onset (eFAD) and sporadic late-onset (LOAD), depending on if it occurs before or after the age of 65. eFAD is the result of dominantly inherited mutations in the amyloid precursor protein (APP) and presenilin (PSEN1 and PSEN2; Selkoe and Hardy, 2016). These mutations lead to increased production of Aβ, the main component of amyloid plaques, or a higher ratio of longer Aβ peptides (Aβ42/43) to Aβ40. Aβ42, while accounting for only 10% of the total Aβ produced, is more hydrophobic and has a higher capacity of aggregating into oligomers. Currently, evidence strongly supports that soluble Aβ oligomers are more toxic than insoluble fibrils (plaques). The production of Aβ42 occurs intracellularly, where it accumulates before being secreted and deposited into amyloid plaques extracellularly (Gouras et al., 2005). Aβ oligomerization, particularly of Aβ42 peptides, begins intracellularly (Tampellini and Gouras, 2010). Intraneuronal Aβ correlates with cognitive dysfunction better than amyloid plaques (Billings et al., 2005; Takahashi et al., 2017). Aβ42 oligomerization precedes tau aggregation (Billings et al., 2005; Bilousova et al., 2016). Thus, we did not include tau-dependent synaptic dysfunction in this review; nevertheless, since tau aggregation is a determinant for the propagation and progression of the pathology, we recommend a recent review on the topic (Tracy and Gan, 2018).

In contrast with eFAD, LOAD is likely multifactorial, caused by a combination of aging, lifestyle, and genetic factors. Given the prediction for heritability of AD to be between 58 and 79%, geneticists have been looking for gene variants in LOAD patients (Gatz et al., 2006). Apolipoprotein E-ε4 was the first genetic risk factor identified and is the most significant one (Strittmatter et al., 1993). However, it does not account for all genetic susceptibility (Stocker et al., 2018). Thus, genome-wide association studies (GWAS) conducted since 2007 have identified several additional genetic risk factors associated with LOAD (Grupe et al., 2007; Harold et al., 2009; Hollingworth et al., 2011; Naj et al., 2014). A recent meta-analysis of GWAS expanded the initial "Top 10" genes (Lambert et al., 2013[1]) to 37 LOAD putative risk factors (Jansen et al., 2019; Kunkle et al., 2019). Now it is crucial to determine how these genes contribute to AD functionally. We, along with other resesarchers, have performed gene ontology (GO) analysis and LOAD risk factors group in three main pathways: endocytic trafficking, immune response, and lipid metabolism (**Figure 1**). Interestingly, some genes, such as ABCA7 and TREM2, are grouped in more than one pathway. Indeed, it is essential to keep in mind that these biological pathways intersect; for example, lipid metabolism influences trafficking at many levels (Huijbregts et al., 2000) and trafficking in microglia influences the immune response (McQuade and Blurton-Jones, 2019). Most attention has been given to how the loss of function of these genes impacts Aβ, generation (reviewed in Guimas Almeida et al., 2018), aggregation (Zhang et al., 2018), and clearance (Van Acker et al., 2019). Recently reviewed data indicates that LOAD microglia risk genes may impact synapses (Rajendran and Paolicelli, 2018).

Here, we will review the importance of neuronal endocytic trafficking for synapses (Barry and Ziff, 2002), how Aβ can have a physiological synaptic role, and how intraneuronal and secreted Aβ oligomers affect synapses, highlighting Aβ-dependent consequences to synaptic endocytic trafficking. Importantly, we will highlight recent data on how LOAD risk genes related to trafficking may impact synapse dysfunction, in particular, the ones related to endocytic protein trafficking (BIN1, SORL1, PICALM, CD2AP), to lipid trafficking (APOE and ABCA7), and synapses (EPH1A).

SYNAPTIC ENDOCYTIC TRAFFICKING

Presynaptic Trafficking

Cycles of synaptic vesicles (SV) exocytosis and endocytosis at the presynaptic active zone membrane mediate neurotransmitter release. This presynaptic trafficking begins with the arrival of an action potential that opens Ca^{2+} channels, which triggers exocytosis of readily releasable SV pool (RRP), which comprises the SVs that are docked and primed for exocytosis. There is also the SV reserve pool, which is mobilized only during periods of intense neuronal activity. After exocytosis, there are different routes of endocytosis to recycle SVs. SV components and newly added membrane need to be recycled to ensure repeated rounds of release.

The SV fusion machinery is composed of the SNARE (soluble N-ethylmaleimide-sensitive factor attachment protein receptor) complex proteins synaptobrevin/VAMP2, syntaxin-1, and SNAP-25 and SM proteins ("Sec1/Munc-18-like proteins"), which promote the assembly of the fusogenic SNARE complex. To trigger exocytosis, Ca^{2+} binds to synaptotagmin-1, the SV calcium sensor protein that, by interacting with the SNARE complex, modulates its assembly or its coupling to the plasma membrane, enabling fusion (Tucker et al., 2004; Wang et al., 2011; Dittman and Ryan, 2019). Upon fusion, NSF promotes the disassembly and recycling of the SNARE complex

[1]https://www.alzforum.org/alzgene

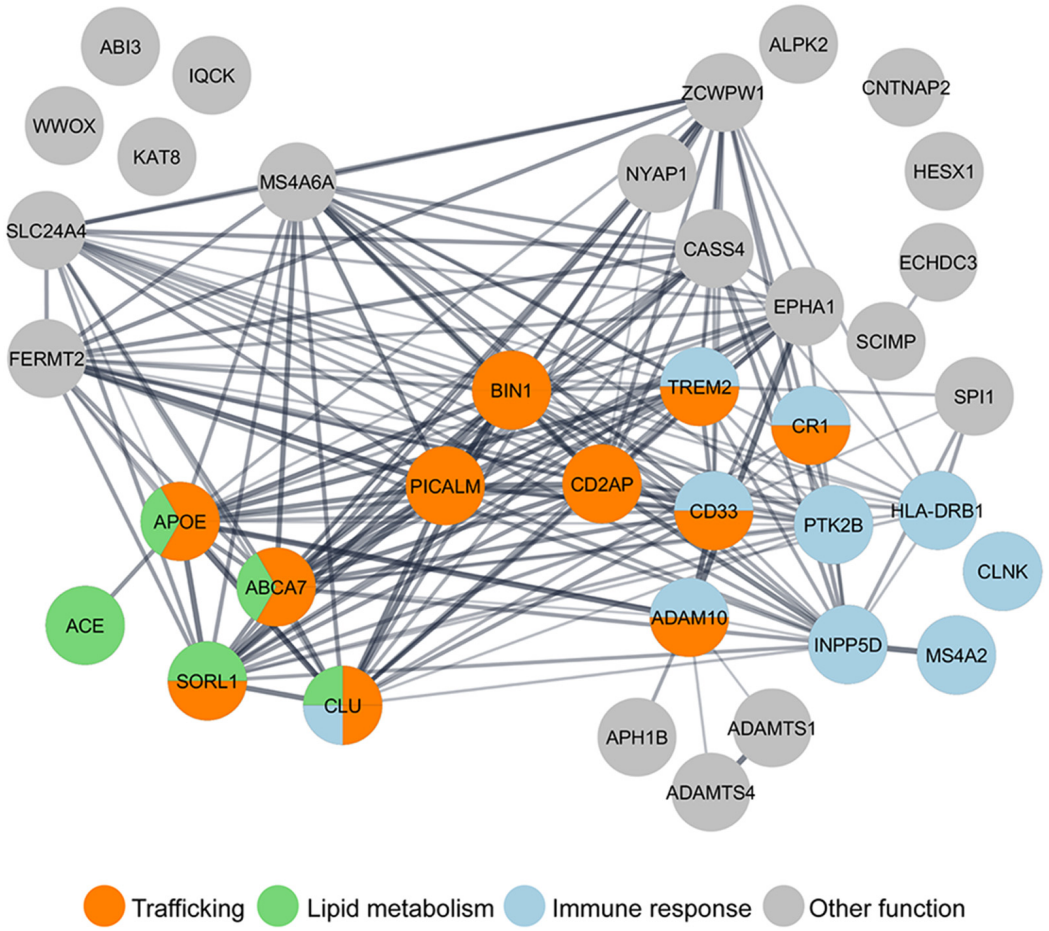

FIGURE 1 | Gene ontology (GO) analysis of LOAD risk factors reveals the enrichment of genes in the trafficking pathway. Nearly half of the 37 LOAD putative risk factors identified by genome-wide association studies (GWAS) meta-analysis (Lambert et al., 2013; Jansen et al., 2019; Kunkle et al., 2019), have been functionally grouped by GO analysis in three main pathways: trafficking (orange), immune response (blue), and lipid metabolism (green). GO analysis was performed using the Cytoscape StringApp (Doncheva et al., 2019).

(Südhof, 2013). SV recycling follows exocytosis to regulate the presynaptic plasma membrane area and locally regenerate SVs (Kononenko and Haucke, 2015; Azarnia Tehran et al., 2018; Chanaday et al., 2019). There are probably several routes of SV recycling. Here, we focus on endocytic recycling that starts with endocytosis of SV proteins. When SVs fuse, they intermix with the plasma membrane (Fernández-Alfonso et al., 2006); therefore, SV recycling requires sorting and reformation. Considering the high number of SVs, their identity and uniformity, protein sorting, and SV reformation are significant tasks for the presynaptic endocytic machinery. Presynaptic endocytosis can be mediated by clathrin, by bulk endocytosis, or by ultrafast endocytosis. Upon the formation of the presynaptic early endosome, SVs need to be accurately reformed, which requires endocytic adaptors such as the assembly protein complex 2 (AP-2) to sort cargo into clathrin-coated pits. AP-3 is an alternative adaptor that can sort SV cargo at endosomes into reforming SVs but independently of clathrin (Milosevic, 2018). Other clathrin adaptors are neuronal-specific such as AP180 and LOAD risk factor CALM (for LOAD risk factors, see below). These proteins are essential for VAMP2 sorting by still unclear mechanisms. Other endocytic adaptors are required to ensure sorting fidelity, such as stonin 2 and synaptic vesicle 2 (SV2A; Kononenko and Haucke, 2015; Gordon and Cousin, 2016). After the assembly of endocytic vesicles, the BAR domain proteins, endophilin, amphiphysin, and SNX9/18 form the vesicle neck and recruit dynamin, which is responsible for membrane scission. Then, endophilin recruits synaptojanin-1 to shed the coat off of the released endocytic vesicles (Kononenko and Haucke, 2015).

Postsynaptic Trafficking

In the postsynaptic site, activation of neurotransmitter-gated ion channels occurs by the presynaptic release of neurotransmitters. In an excitatory synapse, the principal neurotransmitter released is glutamate, which binds NMDA (N-methyl-D-aspartic acid) receptors, kainate receptors, and AMPA (α-amino-3-hydroxy-5-methyl-4-isoxazole propionic

acid) receptors (Waites et al., 2005). Brief periods of high neuronal excitability activate NMDARs and induce Ca^{2+} influx, leading to a long-lasting increase in synaptic efficacy. Repetitive low-frequency stimulation produces long-term depression (LTD), with a decrease in synaptic strength (Kessels and Malinow, 2009). Plasticity at synapses, i.e., changes in the onset or magnitude of long-term potentiation (LTP) and LTD, can be regulated postsynaptically by changing the number, types, or properties of neurotransmitter receptors (reviewed in Henley and Wilkinson, 2016). Regulated trafficking of AMPARs underlies activity-induced changes in synaptic transmission, and therefore their abundance at synapses can significantly strengthen or weaken synaptic transmission (Malinow and Malenka, 2002; Bredt and Nicoll, 2003; Newpher and Ehlers, 2008). AMPAR subunits can have long- (GluA1, GluA2L, and GluA4) or short-tailed carboxyl-terminals (GluA2, GluA3, and GluA4S), which impact their trafficking (Shepherd and Huganir, 2007; Hanley, 2008). The recycling or functional insertion of AMPARs into the postsynaptic membrane is dependent on AMPAR-binding proteins, phosphorylation, and ubiquitination events (Derkach et al., 1999, 2007; Malinow and Malenka, 2002; Schwarz et al., 2010). The addition of long-tailed AMPARs to the postsynaptic membrane is correlated with synaptic strengthening and, therefore, with LTP (Hayashi et al., 2000; Kakegawa et al., 2004), while LTD is associated with the removal of synaptic long- or short-tailed AMPARs (Malinow and Malenka, 2002; Sheng and Hyoung Lee, 2003).

Aβ Physiological Role at Synapses

Although in AD, high Aβ concentration has a toxic effect, endogenous Aβ concentration has a physiological synaptic role. Aβ physiological function was first proposed in 2003 by the Malinow lab and described that blocking Aβ endogenous production by gamma-secretase inhibition potentiated synaptic transmission (Kamenetz et al., 2003). In contrast, in 2008, the Arancio lab showed that exogenous picomolar concentrations of Aβ, monomers and oligomers, increase LTP, while high nanomolar amounts of Aβ reduce LTP (Puzzo et al., 2008). In agreement, the Slutsky lab showed that increasing endogenous Aβ, by inhibition of neprilysin-mediated degradation, potentiates synaptic transmission (Abramov et al., 2009). Importantly, SV recycling was first identified to be endogenously regulated by Aβ. The Slutsky lab elegantly demonstrated that increasing Aβ by neprilysin inhibition increases SV recycling, while decreasing physiological Aβ levels by anti-Aβ antibody-promoted degradation, in contrast, decreases SV recycling (Abramov et al., 2009). More recent data indicate that exogenous picomolar preparations of oligomeric Aβ42 can augment neurotransmitter release and the length of the postsynaptic density, resulting in a late-LTP (Gulisano et al., 2019). The mechanisms of how endogenous Aβ regulates synaptic vesicle recycling and PSD recruitment for modulating synaptic transmission and plasticity are unclear. Some evidence indicates that Aβ can bind to alpha7-nicotinic acetylcholine receptors (Puzzo et al., 2008; Gulisano et al., 2019) to induce presynaptic calcium entry. Overall, the evidence points to an Aβ physiological role, but it is still not clear which form of Aβ is relevant. Does Aβ40 being more abundant play a different physiological role from Aβ42? Other products of APP processing, as well as APP full length, also have synaptic physiological functions that have been recently reviewed (Ludewig and Korte, 2016).

Aβ-DIRECT IMPACT ON SYNAPTIC TRAFFICKING

There are several lines of evidence demonstrating that Aβ is synaptotoxic. In most experimental conditions, exogenous preparations of synthetic or brain-derived oligomeric Aβ were used (reviewed by Mucke and Selkoe, 2012), while other experimental conditions mimicked chronic and time-dependent Aβ accumulation with overexpression of mutant APP, with only a few assessing the contribution of intracellular Aβ. Here we will cover intracellular Aβ-dependent mechanisms focusing on trafficking dysfunction.

Aβ progressively accumulates within neurons (Gouras et al., 2000; Mochizuki et al., 2000) in the limiting membrane of late endosomes or MVBs pre- and especially postsynaptically (Takahashi et al., 2002; Willén et al., 2017; Yu et al., 2018). This intracellular Aβ can oligomerize and disrupt synapses (Takahashi et al., 2004; Pickett et al., 2016). Increased Aβ production, as a result of overexpression of exogenous APP or β-CTF in hippocampal slices, is sufficient to depress synaptic transmission, since inhibiting beta- or gamma-secretase prevented synaptic depression (Kamenetz et al., 2003).

More mechanistically, increased Aβ42 production, as a result of overexpression of APP with eFAD Swedish mutation (APPsw) in primary neurons, is enough to trigger postsynaptic dysfunction with loss of PSD-95, AMPA and NMDA glutamate receptors (Almeida et al., 2005; Snyder et al., 2005). Loss of PSD-95 and spines also occurs *in vivo* in AD mice and human AD brain (Gylys et al., 2004; Pham et al., 2010; Proctor et al., 2010; Sultana et al., 2010; Baglietto-Vargas et al., 2018). Since PSD-95 drives AMPA receptors' incorporation in the postsynaptic density, its loss may underlie the synaptic removal of these receptors (Ehrlich and Malinow, 2004). The loss of AMPA receptors likely causes the reduced AMPA receptor-mediated currents observed even when APP is overexpressed (Ting et al., 2007). Aβ42 requirement for loss of AMPA transmission was confirmed when a mutation that inhibits BACE1 cleavage (APPM596V) blocked synaptic depression (Ting et al., 2007). Indeed, Aβ-dependent synaptic endocytosis of AMPA receptors is sufficient to account for spine loss and reduced NMDA synaptic response (Hsieh et al., 2006). One interesting study found that intracellular Aβ oligomerization, induced by overexpression of APP with the Osaka mutation, reduced spines *via* dysfunction of BDNF, mitochondria, and endosomes transport (Umeda et al., 2015). Intracellular Aβ also interferes with the BDNF TrkB receptors' endosomal sorting for lysosomal degradation, which could disturb synapses (Almeida et al., 2006).

The presynaptic compartment may get affected after the postsynaptic compartment since the loss of synaptophysin, a major component of SVs, only occurred after AMPA receptor synaptic loss (Almeida et al., 2005). Indeed, the presynaptic

decrease of synaptophysin and synapsin mark AD synaptic loss. Interestingly, the presynaptic compartments of APPsw neurons are enlarged but undergo SV recycling (Almeida et al., 2005). Also, upon sustained neuronal activation of APPwt neurons, SV recycling is reduced (Ting et al., 2007). The defects in SV endocytosis could be partially due to dynamin-1 depletion induced by APPsw overexpression in eFAD mice (Kelly et al., 2005; Parodi et al., 2010). The contribution of intracellular Aβ to SV cycle dysfunction remains mostly unstudied.

Secreted Aβ can affect synapses extracellularly and by contributing to intracellular Aβ *via* endocytosis of extracellular Aβ (Lai and McLaurin, 2010). Endocytosed Aβ oligomers could translocate to synapses where interaction with the SV marker synaptophysin can be detected (Russell et al., 2012). Extracellular Aβ can also form a complex with secreted ApoE. This complex can bind to low-density lipoprotein receptor (LDLR) and LRP1, internalize, and accumulate into endosomes within synapses (Bilousova et al., 2019). It is not clear how endosomal Aβ can interact with cytosolic proteins. An answer may be provided by a study that showed that endocytosed Aβ42 could accumulate in endosomes, increasing their membrane permeability and facilitating Aβ cytosolic accumulation and neuronal toxicity (Yang et al., 1998). Moreover, a recent study demonstrated that Aβ oligomers *in vitro* could inhibit the SNARE fusion complex assembly by direct binding to syntaxin-1a (Yang et al., 2015). Besides, *in vitro*, Aβ seems to be able to block synaptophysin complex formation with VAMP2 with relevance for SV exocytosis (Russell et al., 2012). Thus, when Aβ oligomers rupture endosomes and reach the cytosol, Aβ could directly inhibit the SV cycle. This mechanism is similar to the one used by alpha-synuclein in Parkinson's disease, where cytosolic alpha-synuclein oligomerization inhibits SNARE-mediated vesicle fusion in dopaminergic neurons (Garcia-Reitböck et al., 2010; DeWitt and Rhoades, 2013).

Secreted Aβ, or exogenous synthetic Aβ, can also bind extracellularly to excitatory synapses, namely postsynaptically (Wang et al., 2017; Willén et al., 2017), increasing calcium influx, which triggers AMPA and NMDA receptor phosphorylation leading to their removal from synapses by endocytosis (Snyder et al., 2005; Liu et al., 2010; Miñano-Molina et al., 2011; Sinnen et al., 2016; Baglietto-Vargas et al., 2018). The mechanisms of disruption of glutamate receptor trafficking induced by extracellular Aβ have been extensively reviewed (Guntupalli et al., 2016). Other synaptic receptors may also be affected by exposure to Aβ oligomers, such as EphB2, the degradation of which increases upon Aβ binding (Cissé et al., 2011). EphB2 regulates NMDAR expression and currents, for long-term plasticity in the dentate gyrus, consequently regulating memory (Cissé et al., 2011). Extracellular Aβ may also contribute to spine loss *via* F-actin disassembly (Kommaddi et al., 2018). The mechanisms of SV cycle disruption by extracellular Aβ that seem to involve calcium influx have been recently reviewed (Marsh and Alifragis, 2018).

Overall, extracellular Aβ has the same targets of intracellular Aβ. While the acute treatment with Aβ oligomers promotes synaptic receptor dysfunction, chronic treatment results in abnormal spine morphology, with the induction of long thin spines that, ultimately, cause a significant decrease in spine density (Lacor et al., 2007). Alternatively, evidence indicates that extracellular Aβ depends on intracellular Aβ for synaptotoxicity as follows: Aβ binds to APP with high affinity (Lorenzo et al., 2000; Lu et al., 2003; Lacor et al., 2004; Fogel et al., 2014; Wang et al., 2017); extracellular Aβ can promote its processing and intracellular Aβ accumulation (Tampellini et al., 2009); APP enriched at synapses can be the synaptic receptor for Aβ (Laßek et al., 2013; Del Prete et al., 2014; Fanutza et al., 2015; Montagna et al., 2017); APP KO neurons are resistant to exogenous Aβ toxicity (Wang et al., 2017); and, extracellular synthetic Aβ no longer reduces PSD-95 when Aβ production is inhibited (Tampellini et al., 2009).

In vivo in normal rodent hippocampus, acute exposure to Aβ dimers extracted from the AD brain reduced dendritic spine density and potently inhibited LTP and enhanced LTD (Shankar et al., 2008). Interestingly while LTD required mGluR5, spine loss required NMDA receptors (Shankar et al., 2008). In a 3xTg-AD mouse model, the chronic accumulation of Aβ correlated with the impaired synaptic insertion of GluA1-containing AMPARs during chemical LTP stimulation (Baglietto-Vargas et al., 2018). However, in some AD models (APP/PS1), a postsynaptic reduction of AMPA receptors or spine loss was not a significant phenotype; instead, the presynaptic SV release was affected (He et al., 2019). A reduction of the phosphoinositol PtdIns(4, 5)P2 (PIP2) triggered by endogenous or exogenous Aβ oligomers could account for the presynaptic deficits (Berman et al., 2008; He et al., 2019). PIP2 is a plasma membrane phosphoinositide that binds to synaptotagmin-1 on the SV to allow for its docking and fusion (Lee et al., 2010). Selective inhibition of Aβ-induced PIP2 hydrolysis *via* presynaptic mGluR5 could rescue the presynaptic release of glutamate and restore synaptic transmission in APP/PS1 mice (He et al., 2019; Kunkle et al., 2019).

We summarized how Aβ accumulates at the synapse, as well as the earliest Aβ-dependent mechanisms of synapse dysfunction (**Figure 2**).

LOAD GENETIC RISK-DRIVEN TRAFFICKING DEFECTS IMPACT SYNAPSES INDEPENDENTLY OF Aβ

Among the 11 LOAD risk genes involved in intracellular trafficking, we will review the evidence that supports a direct synaptic (dys)function for APOE4, ABCA7, BIN1, CD2AP, PICALM, SORL1, and EPH1A.

APOE4

Apolipoprotein E gene (*APOE*) has a risk LOAD variant (*APOE4*). Two single nucleotide polymorphisms (SNPs) generate three allelic variants of the human APOE gene, ε2, ε3, and ε4 that affect the structure of the ApoE protein, as well as, the binding to lipids, receptors, and Aβ (Liu et al., 2013; Yamazaki et al., 2019). APOE ε3 is the most common allele, with a prevalence of 77.9%, the ε2 allele is the less prevalent (8.4%), and the ε4 allele has a

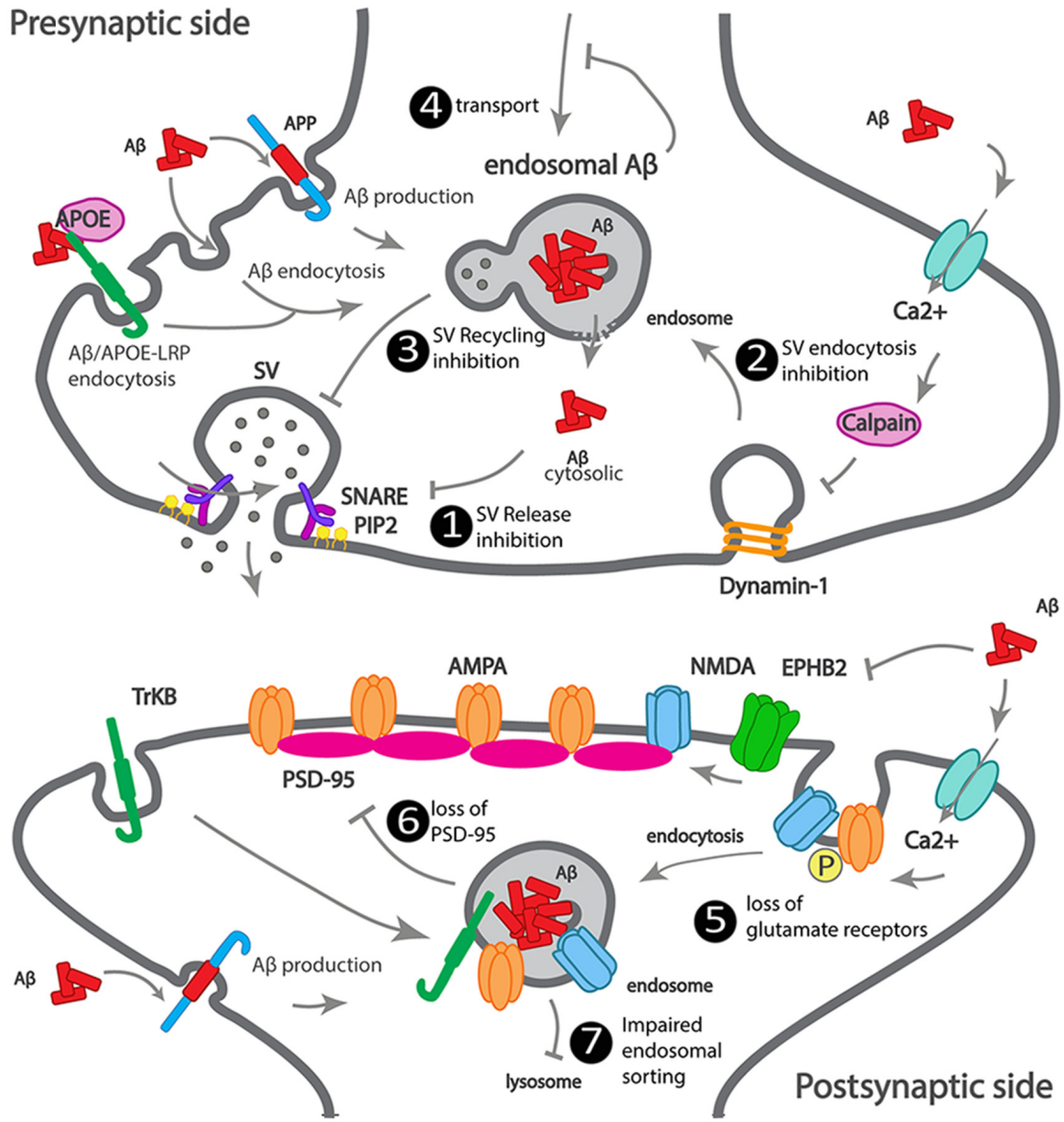

FIGURE 2 | Scheme illustrating how Aβ impacts synaptic trafficking. Scheme of a dysfunctional early-onset familial AD (eFAD) synapse. At the presynaptic terminal: 1. Synaptic vesicle release inhibition, extracellular Aβ endocytosed, alone or *via* ApoE-LRP endocytosis can accumulate at endosomes. Intracellular Aβ, produced from APP endocytosis, accumulates at endosomes. Endosomal Aβ can disrupt the endosomal membrane and reach the cytosol, where it can potentially bind to SNARE subunit syntaxin-1a, or indirectly inhibit synaptophysin or PIP2, thus inhibiting synaptic vesicles (SV) fusion and neurotransmitter release. 2. SV endocytosis inhibition, extracellular Aβ increases calcium influx, triggers calcium-dependent calpain to degrade dynamin1, reducing endocytosis. 3. SV recycling inhibition by intracellular Aβ. 4. Transport to synapses inhibition by intracellular Aβ oligomerization. At the postsynaptic terminal: 5. Increased endocytosis of AMPA and NMDA receptors, by intracellular and extracellular Aβ. 6. Loss of PSD-95 by intracellular Aβ. 7. Impaired endosomal sorting of TrkB receptor, by endosomal Aβ.

frequency of 13.7% that increases in LOAD patients (Farrer et al., 1997; Michaelson, 2014).

In the brain, ApoE is the primary lipoprotein of high-density lipoprotein (HDL), mainly secreted by astrocytes and also produced by neurons (Xu et al., 1999; Hauser et al., 2011). Secreted ApoE scavenges lipids from the local environment for cellular delivery. Upon receptor-mediated endocytosis and lipid unloading, ApoE is released from its receptor at the endosomal pH and sorted for recycling or degradation (Hauser et al., 2011).

ApoE knockdown altered the cholesterol distribution within synaptic membranes (Igbavboa et al., 1997). ApoE mediates cholesterol transport into neurons, increasing synapse formation (Mauch et al., 2001; Liu et al., 2013). Cholesterol binding to synaptophysin may enable the correct sorting of SV constituents at the plasma membrane necessary for SV recycling (Thiele et al., 2000).

ApoE4 differs from ApoE3 by one aminoacid, which is sufficient to cause ApoE4 misfolding and abnormal trafficking.

Reduced ApoE4 recycling and endosomal accumulation may lead to increased cholesterol intracellular accumulation (Heeren et al., 2004), as well as increased ApoE4 lysosomal degradation, accounting for the reduction of ApoE in the brain of APOE4 carriers (Riddell et al., 2008). ApoE4 is hypolipidated compared with ApoE3 and ApoE2, the most lipidated (Heinsinger et al., 2016). The APOE state of lipidation may be more critical than ApoE levels. There is some evidence that ApoE4 transports cholesterol into and out of neurons less efficiently (Michikawa et al., 2000; Rapp et al., 2006). Controversy exists since ApoE2 may delay AD development by reducing brain cholesterol (Oikawa et al., 2014).

APOE4 knock-in (KI) increased excitatory postsynaptic currents in human-induced neurons, suggesting enhanced SV release or synapse density (Lin et al., 2018). Importantly, APOE4 KI and APOE KO mice show reduced neuronal complexity and impaired synaptic plasticity (Trommer et al., 2004). Importantly, in APOE4 KI mice, LTP is diminished and LTP maintenance unimpaired (Trommer et al., 2004; Korwek et al., 2009).

Morphologically, APOE KO and APOE4 KI present less spine density and shorter spines (Wang et al., 2005; Dumanis et al., 2009; Rodriguez et al., 2013). Reduced spines could be due to both a delay in spine formation and increased spine elimination, as observed in APOE4 KI neurons *in vitro* (Nwabuisi-Heath et al., 2014). APOE4 KI show increased calcineurin activity (Neustadtl et al., 2017), a phosphatase that can dephosphorylate AMPA receptors, promoting their synaptic removal and increasing LTD (Zhou et al., 2004). Presynaptically, APOE4 KI show reduced production of the neurotransmitter glutamate (Dumanis et al., 2013) and glutamate transporter vGlut1 (Liraz et al., 2013).

ApoE receptors, members of the low-density lipoprotein (LDL) receptor family, include ApoE receptor 2 (ApoEr2), very low-density lipoprotein receptor (VLDLR), LDLR, and LDLR-related protein 1 (LRP1). ApoE receptors allow for its endocytosis and are also present at synapses, where they have specific functions (May et al., 2004; Bal et al., 2013; Bilousova et al., 2019). Presynaptically, ApoE receptors regulate SV release (Bal et al., 2013). Presynaptic activation of Apoer2 and VLDLR by Reelin, another ligand, leads to a rise in Ca^{2+} and SV fusion (Bal et al., 2013). The SNARE complex involved, containing VAMP7 and SNAP-25, was specifically up-regulated (Bal et al., 2013). Interestingly, SNAP-25 levels were higher in APOE ε4 carriers CSF compared to non-carriers with mild-cognitive impairment (MCI; Wang et al., 2018). Postsynaptically, LRP1 interaction with PSD-95 is disrupted upon NMDA activation to modulate NMDA receptors signaling (Bacskai et al., 2000; May et al., 2004). LRP1 regulates NMDA receptor function (May et al., 2004) and endocytosis, promoting, during development, the switch from NR2B to NR2A subunits at synapses (Maier et al., 2013). ApoER2 can get trapped in postsynaptic recycling endosomes upon ApoE4 binding, thus preventing reelin dependent activation of the NMDA receptor, decreasing calcium influx and LTP (Chen et al., 2010; Yong et al., 2014). Long-term spatial memory could require LDLR binding to ApoE4 (Johnson et al., 2014).

Interestingly, clusterin (or apolipoprotein J), another putative LOAD genetic risk factor, accumulates in synapses of human post-mortem brains of APOE4 AD carriers (Jackson et al., 2019).

Research is still needed to address if the detrimental synaptic effects of ApoE4 are independent of ApoE4 impact on Aβ brain accumulation. Importantly, genetically correcting APOE4 to APOE3 in LOAD IPSCs reduced synaptic release and synaptic density without however rescuing secreted Aβ (Lin et al., 2018). Complementarity may also exist since APOE KO or APOE4 KI can potentiate LTP inhibition induced by Aβ oligomers (Trommer et al., 2005). Also, APOE4 KI in an early onset model (5xTg mice) increases amyloid pathology and enhances age-dependent decline in cognitive function by down-regulating an NMDA receptor pathway (Liu et al., 2015).

ABCA7

ATP-binding cassette transporter A7 (ABCA7) belongs to the ABC transporter family that transports lipids, including cholesterol and lipophilic proteins, across membranes. While some ABCA7 variants increase the risk of developing AD (Carrasquillo et al., 2015; Cuyvers et al., 2015; Steinberg et al., 2015; Allen et al., 2017), others are protective (Vasquez et al., 2013). In LOAD, it is not clear whether ABCA7 expression is altered early in the disease; surprisingly, in advanced AD, ABCA7's higher expression was associated with advanced cognitive decline (Karch et al., 2012). ABCA7 knockout mice have altered brain lipid profiles, and when aged, show impaired spatial memory (Sakae et al., 2016) with more pronounced effects in female mice (Logge et al., 2012). ABCA7 knockout may accelerate amyloid pathology in some eFAD mouse models (APP/PS1; Sakae et al., 2016), but not in others (J20; Kim et al., 2013). Whether or not ABCA7 knockout impacts cognitive function needs to be studied. Suggestive of an effect on synaptic function, a recent study found that healthy ABCA7 carriers show impaired cortical connectivity (Sinha et al., 2019). Interestingly, there might be genetic interactions between APOE4 with ABCA7 that impact memory (Chang et al., 2019). ABCA7 expression in the brain is highest in neurons (Zhang et al., 2014).

BIN1

Bridging integrator-1 gene (*BIN1)* encodes for Bin1, a member of the BAR (Bin–Amphiphysin–Rvsp) superfamily (Sakamuro et al., 1996), homologous to the previously reported amphiphysin-1 (Lichte et al., 1992; Leprince et al., 1997). Bin1, with highest expression in brain and skeletal muscle (Sakamuro et al., 1996; Butler et al., 1997), undergoes alternative splicing (Tsutsui et al., 1997), originating at least 10 isoforms. The main isoforms are a longer neuronal-specific isoform with an extra clathrin binding domain (CLAP), two ubiquitous, and a muscle isoform (Ramjaun et al., 1997). All contain an N-BAR domain, through which Bin1 confers and senses membrane curvature, and a C-terminal SH3 domain that mediates Bin1 interaction with proteins involved in endocytosis, such as amphiphysin-1, dynamin (Butler et al., 1997; Leprince et al., 1997; Ramjaun et al., 1997; Wigge et al., 1997) and endophilin (Micheva et al., 1997). The brain expresses mainly the Bin1 neuronal-specific isoform

and at least one ubiquitous isoform (Prokic et al., 2014). Initially, Bin1 was detected in brain synaptosomes and was shown to localize to axon initial segments and nodes of Ranvier (Butler et al., 1997; Wigge et al., 1997; Wigge and McMahon, 1998).

Bin1 can dimerize, through its BAR domain, with itself or with amphiphysin-1 (Wigge et al., 1997). Overexpressed Bin1 inhibits clathrin-mediated endocytosis (Wigge et al., 1997). In contrast, BIN1 knockdown reduced the recycling but not endocytosis of the transferrin receptor in fibroblasts and HeLa cells (Muller et al., 2003; Pant et al., 2009). In neurons, Bin1 polarizes to axons, where its knockdown reduced BACE1 recycling and degradation but not its endocytosis (Miyagawa et al., 2016; Ubelmann et al., 2017). Mechanistically, Bin1 contributes to the scission of recycling carriers from early endosomes (Ubelmann et al., 2017). Neuronal BIN1 knockdown enlarges early endosomes by cargo accumulation or over-activation of Rab5, a small GTPase and regulator of early endosome formation, by interaction with RIN3, a Rab5 GEF and a putative risk factor for LOAD (Calafate et al., 2016).

The expression of Bin1 in the AD brain remains controversial. In AD human brains, *BIN1* transcription increases (Chapuis et al., 2013). In contrast, BIN1 protein decreases in sporadic AD human brains (Glennon et al., 2013). In eFAD models, there is BIN1 accumulation adjacent to amyloid plaques (De Rossi et al., 2019). Subsequently, a separate analysis of two Bin1 isoforms, neuronal and ubiquitous, indicated reduced neuronal *BIN1* but increased ubiquitous *BIN1* in AD human brains (Holler et al., 2014; De Rossi et al., 2016).

To investigate the impact of Bin1 overexpression, the Lambert lab generated a human BIN1 transgenic mouse (h*Bin1*-Tg; Daudin et al., 2018). The hBin1-Tg mice showed an early phenotype of neurodegeneration starting at 3 months, with structural impairment of fiber pathways and structural and functional changes in entorhinal cortex-dentate gyrus (EC-DG) pathway, the earliest brain region impacted in LOAD (Khan et al., 2014; Small, 2014). BIN1 overexpression seems to affect hippocampal physiology, even in the absence of amyloid plaques (Daudin et al., 2018). These data show that the BIN1 risk factor can be sufficient to generate phenotypic changes before the accumulation of Aβ plaques or tau aggregates.

The di Camilli lab identified a synaptic role for Bin1 (Di Paolo et al., 2002). They found Bin1 depleted in the amphiphysin-1 knockout mice. Amphiphysin-1 knockout and *Bin1* knockdown mice synaptosomes exhibited SV recycling defects, such as slower recycling and a smaller pool of SVs and irreversible seizures (Di Paolo et al., 2002). Unfortunately, BIN1 knockout mice die after birth due to muscle defects (Muller et al., 2003). In neurons, Bin1 enriched in axons (Ubelmann et al., 2017) has a presynaptic localization (Di Paolo et al., 2002) and *in vitro* binds to SV glycoprotein 2A (SV2A; Yao et al., 2010), suggesting a presynaptic role for Bin1.

Additionally, a proteomic analysis of postsynaptic compartments identified Bin1, suggesting a postsynaptic role for Bin1 (Bayés et al., 2011). Subsequently, both an increase and a decrease in Bin1 levels led to a small impact on spine morphology (Schürmann et al., 2019). BIN1 knockdown resulted in a reduction of the mean amplitude of AMPAR currents and reduced surface expression of GluA1 in spines and the dendritic shaft (Schürmann et al., 2019). Given that Bin1 is a regulator of endocytic recycling (Pant et al., 2009; Ubelmann et al., 2017), it could be necessary for GluA1 synaptic insertion, *via* recycling carriers from postsynaptic endosomes (Oku and Huganir, 2013).

CD2AP

CD2AP, CD2-associated protein, belongs to the CIN85/CD2AP protein family, contains three SH3 domains in the N-terminal, a proline-rich domain, and a coil-coiled domain in the C-terminal. CD2AP enriched in podocytes functions in kidney glomeruli (Shih et al., 1999; Dikic, 2002). In podocytes foot processes, in T-cell contacts, at the lamellipodia of migrating cells, CD2AP is at the interface between endocytic trafficking and actin cytoskeleton (Dustin et al., 1998; Li et al., 2000; Welsch et al., 2005; Zhao et al., 2013).

It is still unknown whether CD2AP has a synaptic function. Interestingly, in the kidney, CD2AP interacts with endophilin and, as CIN85, with dynamin and synaptojanin, proteins that have synaptic functions in neurons (Soda et al., 2012). In neurons, a pool of CD2AP localizes to dendritic but not axonal early endosomes (Ubelmann et al., 2017). Functionally, there is only one recent study of Cindr, CD2AP/CIN85 homolog in *Drosophila melanogaster* (Ojelade et al., 2019). Cindr localizes to presynaptic boutons. Importantly, Cindr depletion leads to the impairment of synaptic maturation and SV recycling and release. Mechanistically, Cindr forms a complex with 14–3–3, a regulator of UPS-mediated degradation, to control the levels of calcium channels and synapsin (Ojelade et al., 2019). This study suggests that CD2AP, like Cindr, could regulate neurotransmission and synaptic plasticity.

In the future, it would be imperative to understand if in AD brain CD2AP expression is altered and if its loss of function has an impact on synapses, whether if it is through presynaptic channels degradation or postsynaptic endosomal missorting.

PICALM

PICALM encodes for CALM (clathrin assembly lymphoid myeloid leukemia), a ubiquitous expressed endocytic clathrin adaptor, the paralog of the neuronal-specific AP180 (Dreyling et al., 1996; Yao et al., 2005). Both bind to membrane lipids, such as PI(4, 5)P2, through their *N*-terminal domain and interact with clathrin through their C-terminal (Yao et al., 2005). In neurons, AP180 is mostly presynaptic, while CALM is both pre- and postsynaptic (Yao et al., 2005). AP180 and CALM are involved in neuronal growth, but are not functionally redundant; AP180 controls axonal development, while CALM controls dendritic morphology (Bushlin et al., 2008). AP180 participates specifically in clathrin-mediated SV recycling (Vanlandingham et al., 2014).

At the plasma membrane, CALM sorts cargo into nascent clathrin-coated vesicles and recruits R-SNARES (Vamp2, 3, 4, 7, and 8) to endocytic vesicles allowing for fusion into early endosomes (Meyerholz et al., 2005; Sahlender et al., 2013).

Presynaptically, CALM facilitates VAMP2 synaptic endocytosis (Harel et al., 2008; Koo et al., 2011; Gimber et al., 2015). Interestingly, VAMP2 is essential for the fusion of

SVs and neurotransmitter release (Fernández-Alfonso and Ryan, 2006). CALM can also recluster associated and integral synaptic proteins, such as synaptophysin and synaptotagmin, after SV exocytosis, for sorting into endocytic vesicles for SV recycling (Gimber et al., 2015; Xu et al., 2015).

Postsynaptically, CALM can modulate the abundance of GluA2 at the postsynaptic membrane by influencing its endocytosis (Harel et al., 2011), indicating a possible role of CALM in AMPA receptor dysfunction in AD.

EPH1A

Eph receptors are a large family of receptor tyrosine kinases (RTK). Based on their structural similarity and the interaction with their ligands, the Eph family members are divided into two types, Eph type-A (EphA) and Eph type-B receptors (EphB), with nine and five members respectively. Their natural ligands are membrane-anchored molecules bound to the cell surface called ephrins. EphrinAs, with higher affinity to EphA, are ligands bound to the cell surface through a glycosylphosphatidylinositol (GPI)-linked moiety, and ephrinBs preferentially interact with transmembrane EphB (Pasquale, 2004; Héroult et al., 2006).

Ephrins also present reverse signaling properties, and Eph-ephrin binding can function in a bidirectional way between two opposing cells. Therefore, Ephs and ephrins localize both pre- or postsynaptically; their signaling can be initiated at the presynapse and move forward or reverse *via* the postsynaptic Eph receptor, and signaling can be initiated at the postsynapse and translated through a presynaptic Eph receptor (Klein, 2009).

Ephs and ephrins function in the formation and regulation of excitatory synapses is well established (Hruska and Dalva, 2012; Sloniowski and Ethell, 2012). EphA4 regulates dendritic spine morphogenesis in the hippocampus, triggering dendritic spine retraction (Bourgin et al., 2007) in a process involving actin (Zhou et al., 2012), Cdk5 (Fu et al., 2007) and integrins (Bourgin et al., 2007). Also, postsynaptic EphA4, but not axonal, is required for synaptic plasticity (Filosa et al., 2009). EphB is necessary for spine formation *via* N-WASP and Cdc42 (Irie and Yamaguchi, 2002), in an RhoA-GEF-dependent manner (Penzes et al., 2003; Margolis et al., 2010). Also, EphB is necessary for spine morphogenesis and synapse formation in the hippocampus (Henkemeyer et al., 2003), as well as for the recruitment, localization, and function of NMDA receptors (Dalva et al., 2000; Takasu et al., 2002; Nolt et al., 2011). EphBs are also crucial for synaptic plasticity (Grunwald et al., 2004).

In AD-related models, Aβ oligomers can bind to EphB2, depleting them, and consequently impairing synaptic plasticity and cognitive functions (Cissé et al., 2011).

Although the EPHA1 gene has been known as a putative risk factor since 2011 (Hollingworth et al., 2011; Naj et al., 2011), it is still unclear how EPHA1 could contribute to LOAD synapse dysfunction.

SORL1

SORL1 encodes for the sortilin-related receptor with A-type repeats (Sorla), also known as LR11, a member of the vacuolar protein sorting ten domain (VPS10) receptor family and LDLR family (Jacobsen et al., 1996; Yamazaki et al., 1996). SORL1 variants were first associated with LOAD in 2007 (Rogaeva et al., 2007), but a decrease in Sorla expression in the brain of AD patients had been already observed in 2004 by the Lah lab (Scherzer et al., 2004) and in 2005 by the Willnow lab (Andersen et al., 2005). Even in mild cognitive impairment, there is less Sorla expression (Sager et al., 2007). Sorla expression is widespread in the brain (Motoi et al., 1999) and localizes to early endosomes and Golgi compartments (Andersen et al., 2005; Offe et al., 2006) as well as pre- and postsynaptic compartments (Rohe et al., 2013; Hartl et al., 2016).

SORL1's role in synaptic function is unclear. In neurons, Sorla may function as a neuroprotective factor supported by findings that Sorla is a sorting factor for the tropomyosin-related kinase receptor B (TrkB) to facilitate trafficking between synaptic plasma membrane, postsynaptic densities, and cell soma (Rohe et al., 2013). TrkB is a receptor of brain-derived neurotrophic factor (BDNF), a growth factor involved in neuronal survival (Chao, 2003).

Presynaptically, Sorla can interact with phosphorylated synapsin, *via* 14–3–3 adaptor proteins to sort it for degradation by the protease calpain (Hartl et al., 2016). Also, supporting a role for Sorla in regulating synapsin turnover, a proteomic study of cortices and hippocampus of SORL1-deficient mice revealed an increase in synapsin 1 and 2 (Hartl et al., 2016).

Postsynaptically, Sorla interacts with the synaptic EphA4 receptor tyrosine kinase attenuating its activation by ephrinA1 (Huang et al., 2017). Interestingly, EPhA4 activation by ephrinA1 induces spine retraction (Sloniowski and Ethell, 2012). Sorla overexpression *in vivo* decreases EPhA4 activation and reduces the deficits caused by Aβ in LTP and memory (Fu et al., 2014; Huang et al., 2017). This study indicates that in LOAD, decreased Sorla may account for increased activation of spine retraction, maybe even in the absence of Aβ.

We attempted to summarize how LOAD trafficking genes may affect synapses, although direct supporting data is missing in most cases (**Figure 3**).

CONCLUSION

For many years, LOAD etiology has been a debatable topic among researchers. The amyloid hypothesis has dominated the field as the leading cause of AD. Experimental models of eFAD support this hypothesis, as well as the delay of disease onset in carriers of the AD protective mutation in APP that reduces Aβ production (Jonsson et al., 2012). It remains unclear if Aβ accumulation causes the earliest synaptic dysfunction in LOAD.

Moreover, most clinical trials targeting Aβ aggregation cleared amyloid plaques, but the cognitive improvement was limited at best. Today, clinical trials include patients early in the disease, but it is still unclear if once disease manifests, it will be possible to revert synapse damage. In the future, based on the genetic risk, it will be possible to predict the age of onset, and thus preventive therapeutic strategies targeted at the still reversible synapse dysfunction may be the solution. Now, we need to determine the targets for future preventive therapies based on the mechanisms that drive the initial synaptic dysfunction in AD.

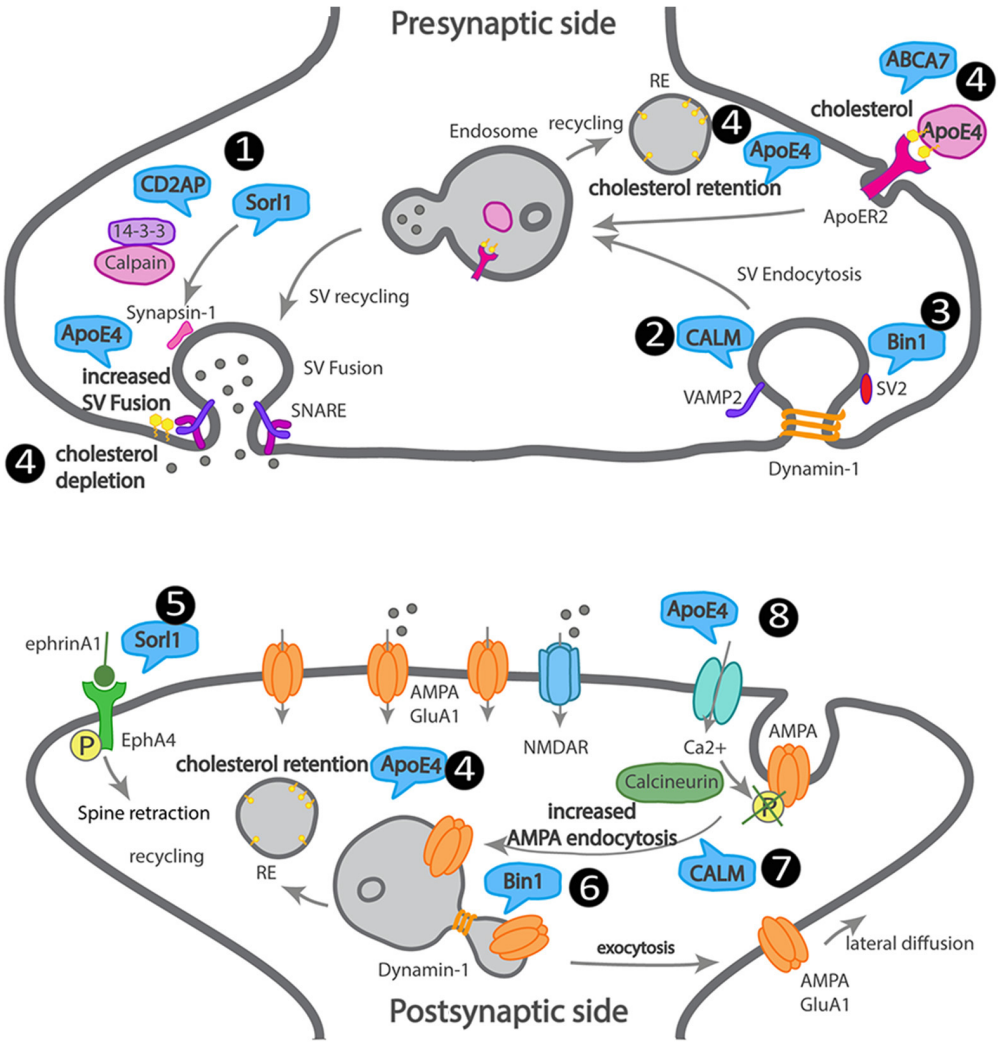

FIGURE 3 | Scheme of a dysfunctional LOAD synapse illustrating how LOAD trafficking genes impact synaptic trafficking. At the presynaptic terminal, 1. Sorl1 and Cindr (CD2AP homolog) interact with synapsin, *via* 14–3–3, and their loss of function leads to aberrant synapsin accumulation. 2. CALM mediates VAMP2 endocytosis and SNARE complex recycling. 3. Bin1 interacts with dynamin and SV2 and could play a role in SV endocytosis. 4. ApoE4 and ABCA7 alter the transport of cholesterol and other lipids into neurons, leading to cholesterol retention in recycling endosomes and depletion from the synaptic membranes. At the postsynaptic terminal, 5. Sorl1 attenuates EphA4 activation by ephrinA1, causing spine retraction. 6. Bin1 regulates GluA1 availability at synapses *via* recycling. 7. CALM regulates GluA2 availability at synapses *via* endocytosis. 8. ApoE4 regulates AMPA receptor availability at synapses *via* calcium influx, calcineurin activation, that dephosphorylates AMPA receptors triggering their endocytosis.

Here we reviewed the Aβ-dependent mechanisms of synapse function and dysfunction as well as potentially Aβ-independent mechanisms. We found evidence in the literature supporting that Aβ, at the physiological concentration (picomolar), facilitates synaptic transmission and plasticity while reducing it when at pathological levels (nanomolar). Pathological Aβ has multiple synaptic targets indicating a broad impact on synapse or a lack of specificity. Alternatively, the multiplication of Aβ targets reflects the need for an effort from the research community to improve cellular and *in vivo* models, to uniformize the experimental conditions, and to integrate individual findings. Overall, we find that presynaptically, Aβ targets the synaptic vesicle cycle and neurotransmitter release. However, the mechanism thus far identified depends on the disruption of the endosomal membrane by Aβ. Once at the cytosol, at least *in vitro*, Aβ can bind to the SV release machinery and disrupt SV release. Postsynaptically, Aβ targets spine loss and glutamate receptors endocytosis, depressing synaptic transmission; the mechanism involved seems to depend on extracellular Aβ-driven calcium influx and endosomal Aβ. However, the mechanisms by which endosomal Aβ interferes with synapses remain mostly unknown.

Moreover, the generalized use of exogenous Aβ treatments or transgenic models overexpressing APP or presenilin with eFAD mutations may disguise relevant Aβ-dependent synaptic dysfunction mechanisms, such as the ones mediated by aging or

by LOAD risk factors. So, there is an increasing need for better models to understand the physiological targets of Aβ in AD.

Regarding Aβ-independent mechanisms of synapse dysfunction, we focused on LOAD genetic risk factors linked to endocytic trafficking, given its importance for synapses. There are few studies on the impact of these genes' loss of function and even less on the effects of patient's variants. Nevertheless, it is interesting to find that most of the LOAD genes, similarly to Aβ, control the synaptic vesicle cycle and the trafficking of glutamate receptors.

Knowing the synaptic dysfunction mechanisms used by each LOAD gene will likely reveal novel targets that may be independent of Aβ. It would be essential to correlate the mechanism of each LOAD gene with the cognitive decline and the carrier genotype.

Therefore, new preclinical animal and cellular models bearing LOAD genetic risk are being established and will hopefully soon contribute to identifying early LOAD therapeutic targets and potential biomarkers. Thus, with these new medical strategies, we might approach LOAD during its prodromal phase, and we might minimize the disease burden, expanding life span with a better quality of life.

AUTHOR CONTRIBUTIONS

CP: review of presynaptic mechanisms and LOAD genetic risk factors presynaptic (dys)functions. MB: Go analysis of LOAD genes and preparation of **Figure 1**. MB and JC: introduction. MB, JC, and MA: review of Abeta synaptotoxicity. MA: review of postsynaptic mechanisms and LOAD genetic risk factors postsynaptic (dys)functions. FM: illustration of **Figures 2**, **3**. CP and FM: writing modifications and feedback. CG: supervision, writing, interpretation, and editing of the manuscript.

FUNDING

The Almeida lab has been supported by FCT-JPCOFUND/0004/2015; Alzheimer's Association Research Grant (AARG-19-618007); Maratona da Saúde; H2020 Spreading Excellence and Widening Participation, H2020-WIDESPREAD-01-2016-2017-TeamingPhase2-GA739572; iNOVA4Health (UID/Multi/04462/2019), a program financially supported by Fundação para a Ciência e Tecnologia (FCT)/Ministério da Educação e Ciência, through national funds and co-funded by FEDER under the PT2020 Partnership Agreement. CG's salary is supported by FCT-CEECIND/00410/2017. FM has been the recipient of an FCT doctoral fellowship (PD/BD/128344/2017). CP has been the recipient of an FCT doctoral fellowship (SFRH/BD/128374/2017).

ACKNOWLEDGMENTS

We acknowledge Tatiana Burrinha for critically reading the manuscript.

REFERENCES

Abramov, E., Dolev, I., Fogel, H., Ciccotosto, G. D., Ruff, E., and Slutsky, I. (2009). Amyloid-β as a positive endogenous regulator of release probability at hippocampal synapses. *Nat. Neurosci.* 12, 1567–1576. doi: 10.1038/nn.2433

Allen, M., Lincoln, S. J., Corda, M., Watzlawik, J. O., Carrasquillo, M. M., Reddy, J. S., et al. (2017). ABCA7 loss-of-function variants, expression, and neurologic disease risk. *Neurol. Genet.* 3:e126. doi: 10.1212/nxg.0000000000000126

Almeida, C. G., Takahashi, R. H., and Gouras, G. K. (2006). β-amyloid accumulation impairs multivesicular body sorting by inhibiting the ubiquitin-proteasome system. *J. Neurosci.* 26, 4277–4288. doi: 10.1523/jneurosci.5078-05.2006

Almeida, C. G., Tampellini, D., Takahashi, R. H., Greengard, P., Lin, M. T., Snyder, E. M., et al. (2005). β-amyloid accumulation in APP mutant neurons reduces PSD-95 and GluR1 in synapses. *Neurobiol. Dis.* 20, 187–198. doi: 10.1016/j.nbd.2005.02.008

Alzheimer's Association. (2019). 2019 Alzheimer's disease facts and figures. *Alzheimers Dement.* 15, 321–387. doi: 10.1016/j.jalz.2019.01.010

Andersen, O. M., Reiche, J., Schmidt, V., Gotthardt, M., Spoelgen, R., Behlke, J., et al. (2005). Neuronal sorting protein-related receptor sorLA/LR11 regulates processing of the amyloid precursor protein. *Proc. Natl. Acad. Sci. U S A* 102, 13461–13466. doi: 10.1073/pnas.0503689102

Azarnia Tehran, D., Kuijpers, M., and Haucke, V. (2018). Presynaptic endocytic factors in autophagy and neurodegeneration. *Curr. Opin. Neurobiol.* 48, 153–159. doi: 10.1016/j.conb.2017.12.018

Bacskai, B. J., Xia, M. Q., Strickland, D. K., Rebeck, G. W., and Hyman, B. T. (2000). The endocytic receptor protein LRP also mediates neuronal calcium signaling *via* N-methyl-D-aspartate receptors. *Proc. Natl. Acad. Sci. U S A* 97, 11551–11556. doi: 10.1073/pnas.200238297

Baglietto-Vargas, D., Prieto, G. A., Limon, A., Forner, S., Rodriguez-Ortiz, C. J., Ikemura, K., et al. (2018). Impaired AMPA signaling and cytoskeletal alterations induce early synaptic dysfunction in a mouse model of Alzheimer's disease. *Aging Cell* 17:e12791. doi: 10.1111/acel.12791

Bal, M., Leitz, J., Reese, A. L., Ramirez, D. M. O., Durakoglugil, M., Herz, J., et al. (2013). Reelin mobilizes a VAMP7-dependent synaptic vesicle pool and selectively augments spontaneous neurotransmission. *Neuron* 80, 934–946. doi: 10.1016/j.neuron.2013.08.024

Barry, M. F., and Ziff, E. B. (2002). Receptor trafficking and the plasticity of excitatory synapses. *Curr. Opin. Neurobiol.* 12, 279–286. doi: 10.1016/s0959-4388(02)00329-x

Bayés, A., van de Lagemaat, L. N., Collins, M. O., Croning, M. D. R., Whittle, I. R., Choudhary, J. S., et al. (2011). Characterization of the proteome, diseases and evolution of the human postsynaptic density. *Nat. Neurosci.* 14, 19–21. doi: 10.1038/nn.2719

Berman, D. E., Dall'Armi, C., Voronov, S. V., McIntire, L. B. J., Zhang, H., Moore, A. Z., et al. (2008). Oligomeric amyloid-β peptide disrupts phosphatidylinositol-4,5-bisphosphate metabolism. *Nat. Neurosci.* 11, 547–554. doi: 10.1038/nn.2100

Billings, L. M., Oddo, S., Green, K. N., McGaugh, J. L., and LaFerla, F. M. (2005). Intraneuronal Aβ causes the onset of early Alzheimer's disease-related cognitive deficits in transgenic mice. *Neuron* 45, 675–688. doi: 10.1016/j.neuron.2005.01.040

Bilousova, T., Melnik, M., Miyoshi, E., Gonzalez, B. L., Poon, W. W., Vinters, H. V., et al. (2019). Apolipoprotein E/amyloid-β complex accumulates in alzheimer disease cortical synapses *via* apolipoprotein e receptors and is enhanced by APOE4. *Am. J. Pathol.* 189, 1621–1636. doi: 10.1016/j.ajpath.2019.04.010

Bilousova, T., Miller, C. A., Poon, W. W., Vinters, H. V., Corrada, M., Kawas, C., et al. (2016). Synaptic amyloid-β oligomers precede p-Tau and differentiate high pathology control cases. *Am. J. Pathol.* 186, 185–198. doi: 10.1016/j.ajpath.2015.09.018

Bourgin, C., Murai, K. K., Richter, M., and Pasquale, E. B. (2007). The EphA4 receptor regulates dendritic spine remodeling by affecting β1-integrin signaling pathways. *J. Cell Biol.* 178, 1295–1307. doi: 10.1083/jcb.200610139

Bredt, D. S., and Nicoll, R. A. (2003). AMPA receptor trafficking at excitatory synapses. *Neuron* 40, 361–379. doi: 10.1016/s0896-6273(03)00640-8

Bushlin, I., Petralia, R. S., Wu, F., Harel, A., Mughal, M. R., Mattson, M. P., et al. (2008). Clathrin assembly protein AP180 and CALM differentially control axogenesis and dendrite outgrowth in embryonic hippocampal neurons. *J. Neurosci.* 28, 10257–10271. doi: 10.1523/jneurosci.2471-08.2008

Butler, M. H., David, C., Ochoa, G. C., Freyberg, Z., Daniell, L., Grabs, D., et al. (1997). Amphiphysin II (SH3P9; BIN1), a member of the amphiphysin/Rvs family, is concentrated in the cortical cytomatrix of axon initial segments and nodes of ranvier in brain and around T tubules in skeletal muscle. *J. Cell Biol.* 137, 1355–1367. doi: 10.1083/jcb.137.6.1355

Calafate, S., Flavin, W., Verstreken, P., and Moechars, D. (2016). Loss of bin1 promotes the propagation of tau pathology. *Cell Rep.* 17, 931–940. doi: 10.1016/j.celrep.2016.09.063

Carrasquillo, M. M., Crook, J. E., Pedraza, O., Thomas, C. S., Pankratz, V. S., Allen, M., et al. (2015). Late-onset alzheimer's risk variants in memory decline, incident mild cognitive impairment and Alzheimer's disease. *Neurobiol. Aging* 36, 60–67. doi: 10.1016/j.neurobiolaging.2014.07.042

Chanaday, N. L., Cousin, M. A., Milosevic, I., Watanabe, S., and Morgan, J. R. (2019). The synaptic vesicle cycle revisited: new insights into the modes and mechanisms. *J. Neurosci.* 39, 8209–8216. doi: 10.1523/jneurosci.1158-19.2019

Chapuis, J., Hansmannel, F., Gistelinck, M., Mounier, A., Van Cauwenberghe, C., Kolen, K. V., et al. (2013). Increased expression of BIN1 mediates Alzheimer genetic risk by modulating tau pathology. *Mol. Psychiatry* 18, 1225–1234. doi: 10.1038/mp.2013.1

Chang, Y.-T., Hsu, S.-W., Huang, S.-H., Huang, C.-W., Chang, W.-N., Lien, C.-Y., et al. (2019). ABCA7 polymorphisms correlate with memory impairment and default mode network in patients with APOEε4-associated Alzheimer's disease. *Alzheimers Res. Ther.* 11:103. doi: 10.1186/s13195-019-0563-3

Chao, M. V. (2003). Neurotrophins and their receptors: a convergence point for many signalling pathways. *Nat. Rev. Neurosci.* 4, 299–309. doi: 10.1038/nrn1078

Chen, Y., Durakoglugil, M. S., Xian, X., and Herz, J. (2010). ApoE4 reduces glutamate receptor function and synaptic plasticity by selectively impairing ApoE receptor recycling. *Proc. Natl. Acad. Sci. U S A* 107, 12011–12016. doi: 10.1073/pnas.0914984107

Cissé, M., Halabisky, B., Harris, J., Devidze, N., Dubal, D. B., Sun, B., et al. (2011). Reversing EphB2 depletion rescues cognitive functions in Alzheimer model. *Nature* 469, 47–52. doi: 10.1038/nature09635

Cuyvers, E., De Roeck, A., Van den Bossche, T., Van Cauwenberghe, C., Bettens, K., Vermeulen, S., et al. (2015). Mutations in ABCA7 in a Belgian cohort of Alzheimer's disease patients: a targeted resequencing study. *Lancet Neurol.* 14, 814–822. doi: 10.1016/S1474-4422(15)00133-7

Dalva, M. B., Takasu, M. A., Lin, M. Z., Shamah, S. M., Hu, L., Gale, N. W., et al. (2000). EphB receptors interact with NMDA receptors and regulate excitatory synapse formation. *Cell* 103, 945–956. doi: 10.1016/s0092-8674(00)00197-5

Daudin, R., Marechal, D., Wang, Q., Abe, Y., Bourg, N., Sartori, M., et al. (2018). BIN1 genetic risk factor for Alzheimer is sufficient to induce early structural tract alterations in entorhinal cortex-dentate gyrus pathway and related hippocampal multi-scale impairments. *BioRxiv* [Preprint]. doi: 10.1101/437228

Del Prete, D., Lombino, F., Liu, X., and D'Adamio, L. (2014). APP is cleaved by Bace1 in pre-synaptic vesicles and establishes a pre-synaptic interactome, *via* its intracellular domain, with molecular complexes that regulate pre-synaptic vesicles functions. *PLoS One* 9:e108576. doi: 10.1371/journal.pone.0108576

Derkach, V. A., Oh, M. C., Guire, E. S., and Soderling, T. R. (2007). Regulatory mechanisms of AMPA receptors in synaptic plasticity. *Nat. Rev. Neurosci.* 8, 101–113. doi: 10.1038/nrn2055

Derkach, V., Barria, A., and Soderling, T. R. (1999). Ca^{2+}/calmodulin-kinase II enhances channel conductance of α-amino-3-hydroxy-5-methyl-4-isoxazolepropionate type glutamate receptors. *Proc. Natl. Acad. Sci. U S A* 96, 3269–3274. doi: 10.1073/pnas.96.6.3269

De Rossi, P., Buggia-Prévot, V., Clayton, B. L., Vasquez, J. B., van Sanford, C., Andrew, R. J., et al. (2016). Predominant expression of Alzheimer's disease-associated BIN1 in mature oligodendrocytes and localization to white matter tracts. *Mol. Neurodegener.* 11:59. doi: 10.1186/s13024-016-0124-1

De Rossi, P., Andrew, R. J., Musial, T. F., Buggia-Prevot, V., Xu, G., Ponnusamy, M., et al. (2019). Aberrant accrual of BIN1 near Alzheimer's disease amyloid deposits in transgenic models. *Brain Pathol.* 29, 485–501. doi: 10.1111/bpa.12687

DeWitt, D. C., and Rhoades, E. (2013). α-synuclein can inhibit SNARE-mediated vesicle fusion through direct interactions with lipid bilayers. *Biochemistry* 52, 2385–2387. doi: 10.1021/bi4002369

Di Paolo, G., Sankaranarayanan, S., Wenk, M. R., Daniell, L., Perucco, E., Caldarone, B. J., et al. (2002). Decreased synaptic vesicle recycling efficiency and cognitive deficits in amphiphysin 1 knockout mice. *Neuron* 33, 789–804. doi: 10.1016/s0896-6273(02)00601-3

Dikic, I. (2002). CIN85/CMS family of adaptor molecules. *FEBS Lett.* 529, 110–115. doi: 10.1016/s0014-5793(02)03188-5

Dittman, J. S., and Ryan, T. A. (2019). The control of release probability at nerve terminals. *Nat. Rev. Neurosci.* 20, 177–186. doi: 10.1038/s41583-018-0111-3

Doncheva, N. T., Morris, J. H., Gorodkin, J., and Jensen, L. J. (2019). Cytoscape stringapp: network analysis and visualization of proteomics data. *J. Proteome Res.* 18, 623–632. doi: 10.1021/acs.jproteome.8b00702

Dreyling, M. H., Martinez-Climent, J. A., Zheng, M., Mao, J., Rowley, J. D., and Bohlander, S. K. (1996). The t(10;11)(p13;q14) in the U937 cell line results in the fusion of the AF10 gene and CALM, encoding a new member of the AP-3 clathrin assembly protein family. *Proc. Natl. Acad. Sci. U S A* 93, 4804–4809. doi: 10.1073/pnas.93.10.4804

Dumanis, S. B., DiBattista, A. M., Miessau, M., Moussa, C. E. H., and Rebeck, G. W. (2013). APOE genotype affects the pre-synaptic compartment of glutamatergic nerve terminals. *J. Neurochem.* 124, 4–14. doi: 10.1111/j.1471-4159.2012.07908.x

Dumanis, S. B., Tesoriero, J. A., Babus, L. W., Nguyen, M. T., Trotter, J. H., Ladu, M. J., et al. (2009). ApoE4 decreases spine density and dendritic complexity in cortical neurons *in vivo*. *J. Neurosci.* 29, 15317–15322. doi: 10.1523/jneurosci.4026-09.2009

Dustin, M. L., Olszowy, M. W., Holdorf, A. D., Li, J., Bromley, S., Desai, N., et al. (1998). A novel adaptor protein orchestrates receptor patterning and cytoskeletal polarity in T-cell contacts. *Cell* 94, 667–677. doi: 10.1016/s0092-8674(00)81608-6

Ehrlich, I., and Malinow, R. (2004). Postsynaptic density 95 controls AMPA receptor incorporation during long-term potentiation and experience-driven synaptic plasticity. *J. Neurosci.* 24, 916–927. doi: 10.1523/jneurosci.4733-03.2004

Fanutza, T., Del Prete, D., Ford, M. J., Castillo, P. E., and D'Adamio, L. (2015). APP and APLP2 interact with the synaptic release machinery and facilitate transmitter release at hippocampal synapses. *Elife* 4:e09743. doi: 10.7554/elife.09743

Farrer, L. A., Cupples, L. A., Haines, J. L., Hyman, B., Kukull, W. A., Mayeux, R., et al. (1997). Effects of age, sex, and ethnicity on the association between apolipoprotein E genotype and Alzheimer disease. A meta-analysis. APOE and Alzheimer Disease Meta Analysis Consortium. *JAMA* 278, 1349–1356. doi: 10.1001/jama.278.16.1349

Fernández-Alfonso, T., Kwan, R., and Ryan, T. A. (2006). Synaptic vesicles interchange their membrane proteins with a large surface reservoir during recycling. *Neuron* 51, 179–186. doi: 10.1016/j.neuron.2006.06.008

Fernández-Alfonso, T., and Ryan, T. A. (2006). The efficiency of the synaptic vesicle cycle at central nervous system synapses. *Trends Cell Biol.* 16, 413–420. doi: 10.1016/j.tcb.2006.06.007

Filosa, A., Paixão, S., Honsek, S. D., Carmona, M. A., Becker, L., Feddersen, B., et al. (2009). Neuron-glia communication *via* EphA4/ephrin-A3 modulates LTP through glial glutamate transport. *Nat. Neurosci.* 12, 1285–1292. doi: 10.1038/nn.2394

Fogel, H., Frere, S., Segev, O., Bharill, S., Shapira, I., Gazit, N., et al. (2014). APP homodimers transduce an amyloid-β-mediated increase in release probability at excitatory synapses. *Cell Rep.* 7, 1560–1576. doi: 10.1016/j.celrep.2014.04.024

Fu, W.-Y., Chen, Y., Sahin, M., Zhao, X.-S., Shi, L., Bikoff, J. B., et al. (2007). Cdk5 regulates EphA4-mediated dendritic spine retraction through an ephexin1-dependent mechanism. *Nat. Neurosci.* 10, 67–76. doi: 10.1038/nn1811

Fu, A. K. Y., Hung, K.-W., Huang, H., Gu, S., Shen, Y., Cheng, E. Y. L., et al. (2014). Blockade of EphA4 signaling ameliorates hippocampal synaptic dysfunctions in mouse models of Alzheimer's disease. *Proc. Natl. Acad. Sci. U S A* 111, 9959–9964. doi: 10.1073/pnas.1405803111

Garcia-Reitböck, P., Anichtchik, O., Bellucci, A., Iovino, M., Ballini, C., Fineberg, E., et al. (2010). SNARE protein redistribution and synaptic failure in a transgenic mouse model of Parkinson's disease. *Brain* 133, 2032–2044. doi: 10.1093/brain/awq132

Gatz, M., Reynolds, C. A., Fratiglioni, L., Johansson, B., Mortimer, J. A., Berg, S., et al. (2006). Role of genes and environments for explaining Alzheimer disease. *Arch. Gen. Psychiatry* 63, 168–174. doi: 10.1001/archpsyc.63.2.168

Gimber, N., Tadeus, G., Maritzen, T., Schmoranzer, J., and Haucke, V. (2015). Diffusional spread and confinement of newly exocytosed synaptic vesicle proteins. *Nat. Commun.* 6:8392. doi: 10.1038/ncomms9392

Glennon, E. B., Whitehouse, I. J., Miners, J. S., Kehoe, P. G., Love, S., Kellett, K. A., et al. (2013). BIN1 is decreased in sporadic but not familial Alzheimer's disease or in aging. *PLoS One* 8:e78806. doi: 10.1371/journal.pone.0078806

Gordon, S. L., and Cousin, M. A. (2016). The iTRAPs: guardians of synaptic vesicle cargo retrieval during endocytosis. *Front. Synaptic Neurosci.* 8:1. doi: 10.3389/fnsyn.2016.00001

Gouras, G. K., Almeida, C. G., and Takahashi, R. H. (2005). Intraneuronal Aβ accumulation and origin of plaques in Alzheimer's disease. *Neurobiol. Aging* 26, 1235–1244. doi: 10.1016/j.neurobiolaging.2005.05.022

Gouras, G. K., Tsai, J., Naslund, J., Vincent, B., Edgar, M., Checler, F., et al. (2000). Intraneuronal Aβ42 accumulation in human brain. *Am. J. Pathol.* 156, 15–20. doi: 10.1016/s0002-9440(10)64700-1

Grunwald, I. C., Korte, M., Adelmann, G., Plueck, A., Kullander, K., Adams, R. H., et al. (2004). Hippocampal plasticity requires postsynaptic ephrinBs. *Nat. Neurosci.* 7, 33–40. doi: 10.1038/nn1164

Grupe, A., Abraham, R., Li, Y., Rowland, C., Hollingworth, P., Morgan, A., et al. (2007). Evidence for novel susceptibility genes for late-onset Alzheimer's disease from a genome-wide association study of putative functional variants. *Hum. Mol. Genet.* 16, 865–873. doi: 10.1093/hmg/ddm031

Guimas Almeida, C., Sadat Mirfakhar, F., Perdigão, C., and Burrinha, T. (2018). Impact of late-onset Alzheimer's genetic risk factors on β-amyloid endocytic production. *Cell. Mol. Life Sci.* 75, 2577–2589. doi: 10.1007/s00018-018-2825-9

Gulisano, W., Melone, M., Ripoli, C., Tropea, M. R., Li Puma, D. D., Giunta, S., et al. (2019). Neuromodulatory action of picomolar extracellular Aβ42 oligomers on presynaptic and postsynaptic mechanisms underlying synaptic function and memory. *J. Neurosci.* 39, 5986–6000. doi: 10.1523/jneurosci.0163-19.2019

Guntupalli, S., Widagdo, J., and Anggono, V. (2016). Amyloid-β-induced dysregulation of AMPA receptor trafficking. *Neural Plast.* 2016:3204519. doi: 10.1155/2016/3204519

Gylys, K. H., Fein, J. A., Yang, F., Wiley, D. J., Miller, C. A., and Cole, G. M. (2004). Synaptic changes in Alzheimer's disease: increased amyloid-β and gliosis in surviving terminals is accompanied by decreased PSD-95 fluorescence. *Am. J. Pathol.* 165, 1809–1817. doi: 10.1016/s0002-9440(10)63436-0

Hanley, J. G. (2008). AMPA receptor trafficking pathways and links to dendritic spine morphogenesis. *Cell Adh. Migr.* 2, 276–282. doi: 10.4161/cam.2.4.6510

Harel, A., Mattson, M. P., and Yao, P. J. (2011). CALM, a clathrin assembly protein, influences cell surface GluR2 abundance. *Neuromolecular Med.* 13, 88–90. doi: 10.1007/s12017-010-8142-6

Harel, A., Wu, F., Mattson, M. P., Morris, C. M., and Yao, P. J. (2008). Evidence for CALM in directing VAMP2 trafficking. *Traffic* 9, 417–429. doi: 10.1111/j.1600-0854.2007.00694.x

Harold, D., Abraham, R., Hollingworth, P., Sims, R., Gerrish, A., Hamshere, M. L., et al. (2009). Genome-wide association study identifies variants at CLU and PICALM associated with Alzheimer's disease. *Nat. Genet.* 41, 1088–1093. doi: 10.1038/ng.440

Hartl, D., Nebrich, G., Klein, O., Stephanowitz, H., Krause, E., and Rohe, M. (2016). SORLA regulates calpain-dependent degradation of synapsin. *Alzheimers Dement.* 12, 952–963. doi: 10.1016/j.jalz.2016.02.008

Hauser, P. S., Narayanaswami, V., and Ryan, R. O. (2011). Apolipoprotein E: from lipid transport to neurobiology. *Prog. Lipid Res.* 50, 62–74. doi: 10.1016/j.plipres.2010.09.001

Hayashi, Y., Shi, S. H., Esteban, J. A., Piccini, A., Poncer, J. C., and Malinow, R. (2000). Driving AMPA receptors into synapses by LTP and CaMKII: requirement for GluR1 and PDZ domain interaction. *Science* 287, 2262–2267. doi: 10.1126/science.287.5461.2262

He, Y., Wei, M., Wu, Y., Qin, H., Li, W., Ma, X., et al. (2019). Amyloid β oligomers suppress excitatory transmitter release *via* presynaptic depletion of phosphatidylinositol-4,5-bisphosphate. *Nat. Commun.* 10:1193. doi: 10.1038/s41467-019-09114-z

Heeren, J., Grewal, T., Laatsch, A., Becker, N., Rinninger, F., Rye, K.-A., et al. (2004). Impaired recycling of apolipoprotein E4 is associated with intracellular cholesterol accumulation. *J. Biol. Chem.* 279, 55483–55492. doi: 10.1074/jbc.m409324200

Heinsinger, N. M., Gachechiladze, M. A., and Rebeck, G. W. (2016). Apolipoprotein E genotype affects size of apoe complexes in cerebrospinal fluid. *J. Neuropathol. Exp. Neurol.* 75, 918–924. doi: 10.1093/jnen/nlw067

Henkemeyer, M., Itkis, O. S., Ngo, M., Hickmott, P. W., and Ethell, I. M. (2003). Multiple EphB receptor tyrosine kinases shape dendritic spines in the hippocampus. *J. Cell Biol.* 163, 1313–1326. doi: 10.1083/jcb.200306033

Henley, J. M., and Wilkinson, K. A. (2016). Synaptic AMPA receptor composition in development, plasticity and disease. *Nat. Rev. Neurosci.* 17, 337–350. doi: 10.1038/nrn.2016.37

Héroult, M., Schaffner, F., and Augustin, H. G. (2006). Eph receptor and ephrin ligand-mediated interactions during angiogenesis and tumor progression. *Exp. Cell Res.* 312, 642–650. doi: 10.1016/j.yexcr.2005.10.028

Holler, C. J., Davis, P. R., Beckett, T. L., Platt, T. L., Webb, R. L., Head, E., et al. (2014). Bridging integrator 1 (BIN1) protein expression increases in the Alzheimer's disease brain and correlates with neurofibrillary tangle pathology. *J. Alzheimers Dis.* 42, 1221–1227. doi: 10.3233/jad-132450

Hollingworth, P., Harold, D., Sims, R., Gerrish, A., Lambert, J.-C., Carrasquillo, M. M., et al. (2011). Common variants at ABCA7, MS4A6A/MS4A4E, EPHA1, CD33 and CD2AP are associated with Alzheimer's disease. *Nat. Genet.* 43, 429–435. doi: 10.1038/ng.803

Hruska, M., and Dalva, M. B. (2012). Ephrin regulation of synapse formation, function and plasticity. *Mol. Cell. Neurosci.* 50, 35–44. doi: 10.1016/j.mcn.2012.03.004

Hsieh, H., Boehm, J., Sato, C., Iwatsubo, T., Tomita, T., Sisodia, S., et al. (2006). AMPAR removal underlies Aβ-induced synaptic depression and dendritic spine loss. *Neuron* 52, 831–843. doi: 10.1016/j.neuron.2006.10.035

Huang, T. Y., Zhao, Y., Jiang, L.-L., Li, X., Liu, Y., Sun, Y., et al. (2017). SORLA attenuates EphA4 signaling and amyloid β-induced neurodegeneration. *J. Exp. Med.* 214, 3669–3685. doi: 10.1084/jem.20171413

Huijbregts, R. P., Topalof, L., and Bankaitis, V. A. (2000). Lipid metabolism and regulation of membrane trafficking. *Traffic* 1, 195–202. doi: 10.1034/j.1600-0854.2000.010301.x

Igbavboa, U., Avdulov, N. A., Chochina, S. V., and Wood, W. G. (1997). Transbilayer distribution of cholesterol is modified in brain synaptic plasma membranes of knockout mice deficient in the low-density lipoprotein receptor, apolipoprotein E, or both proteins. *J. Neurochem.* 69, 1661–1667. doi: 10.1046/j.1471-4159.1997.69041661.x

Irie, F., and Yamaguchi, Y. (2002). EphB receptors regulate dendritic spine development *via* intersectin, Cdc42 and N-WASP. *Nat. Neurosci.* 5, 1117–1118. doi: 10.1038/nn964

Jackson, R. J., Rose, J., Tulloch, J., Henstridge, C., Smith, C., and Spires-Jones, T. L. (2019). Clusterin accumulates in synapses in Alzheimer's disease and is increased in apolipoprotein E4 carriers. *Brain Commun.* 1:fcz003. doi: 10.1093/braincomms/fcz003

Jacobsen, L., Madsen, P., Moestrup, S. K., Lund, A. H., Tommerup, N., Nykjaer, A., et al. (1996). Molecular characterization of a novel human hybrid-type receptor that binds the α2-macroglobulin receptor-associated protein. *J. Biol. Chem.* 271, 31379–31383. doi: 10.1074/jbc.271.49.31379

Johnson, L. A., Olsen, R. H. J., Merkens, L. S., DeBarber, A., Steiner, R. D., Sullivan, P. M., et al. (2014). Apolipoprotein E-low density lipoprotein receptor interaction affects spatial memory retention and brain ApoE levels in an isoform-dependent manner. *Neurobiol. Dis.* 64, 150–162. doi: 10.1016/j.nbd.2013.12.016

Jansen, I. E., Savage, J. E., Watanabe, K., Bryois, J., Williams, D. M., Steinberg, S., et al. (2019). Genome-wide meta-analysis identifies new loci and functional

pathways influencing Alzheimer's disease risk. *Nat. Genet.* 51, 404–413. doi: 10.1038/s41588-018-0311-9

Jonsson, T., Atwal, J. K., Steinberg, S., Snaedal, J., Jonsson, P. V., Bjornsson, S., et al. (2012). A mutation in APP protects against Alzheimer's disease and age-related cognitive decline. *Nature* 488, 96–99. doi: 10.1038/nature11283

Kakegawa, W., Tsuzuki, K., Yoshida, Y., Kameyama, K., and Ozawa, S. (2004). Input- and subunit-specific AMPA receptor trafficking underlying long-term potentiation at hippocampal CA3 synapses. *Eur. J. Neurosci.* 20, 101–110. doi: 10.1111/j.1460-9568.2004.03461.x

Kamenetz, F., Tomita, T., Hsieh, H., Seabrook, G., Borchelt, D., Iwatsubo, T., et al. (2003). APP processing and synaptic function. *Neuron* 37, 925–937. doi: 10.1016/s0896-6273(03)00124-7

Karch, C. M., Jeng, A. T., Nowotny, P., Cady, J., Cruchaga, C., and Goate, A. M. (2012). Expression of novel Alzheimer's disease risk genes in control and Alzheimer's disease brains. *PLoS One* 7:e50976. doi: 10.1371/journal.pone.0050976

Katzman, R. (1976). The prevalence and malignancy of alzheimer disease. *Arch. Neurol.* 33, 217–218. doi: 10.1001/archneur.1976.00500040001001

Kelly, B. L., Vassar, R., and Ferreira, A. (2005). β-amyloid-induced dynamin 1 depletion in hippocampal neurons. A potential mechanism for early cognitive decline in Alzheimer disease. *J. Biol. Chem.* 280, 31746–31753. doi: 10.1074/jbc.m503259200

Kessels, H. W., and Malinow, R. (2009). Synaptic AMPA receptor plasticity and behavior. *Neuron* 61, 340–350. doi: 10.1016/j.neuron.2009.01.015

Khan, U. A., Liu, L., Provenzano, F. A., Berman, D. E., Profaci, C. P., Sloan, R., et al. (2014). Molecular drivers and cortical spread of lateral entorhinal cortex dysfunction in preclinical Alzheimer's disease. *Nat. Neurosci.* 17, 304–311. doi: 10.1038/nn.3606

Kim, W. S., Li, H., Ruberu, K., Chan, S., Elliott, D. A., Low, J. K., et al. (2013). Deletion of Abca7 increases cerebral amyloid-β accumulation in the J20 mouse model of Alzheimer's disease. *J. Neurosci.* 33, 4387–4394. doi: 10.1523/jneurosci.4165-12.2013

Klein, R. (2009). Bidirectional modulation of synaptic functions by Eph/ephrin signaling. *Nat. Neurosci.* 12, 15–20. doi: 10.1038/nn.2231

Kommaddi, R. P., Das, D., Karunakaran, S., Nanguneri, S., Bapat, D., Ray, A., et al. (2018). Aβ mediates F-actin disassembly in dendritic spines leading to cognitive deficits in Alzheimer's disease. *J. Neurosci.* 38, 1085–1099. doi: 10.1523/JNEUROSCI.2127-17.2017

Kononenko, N. L., and Haucke, V. (2015). Molecular mechanisms of presynaptic membrane retrieval and synaptic vesicle reformation. *Neuron* 85, 484–496. doi: 10.1016/j.neuron.2014.12.016

Koo, S. J., Puchkov, D., and Haucke, V. (2011). AP180 and CALM: dedicated endocytic adaptors for the retrieval of synaptobrevin 2 at synapses. *Cell Logist.* 1, 168–172. doi: 10.4161/cl.1.4.18897

Korwek, K. M., Trotter, J. H., Ladu, M. J., Sullivan, P. M., and Weeber, E. J. (2009). ApoE isoform-dependent changes in hippocampal synaptic function. *Mol. Neurodegener.* 4:21. doi: 10.1186/1750-1326-4-21

Kunkle, B. W., Grenier-Boley, B., Sims, R., Bis, J. C., Damotte, V., Naj, A. C., et al. (2019). Genetic meta-analysis of diagnosed Alzheimer's disease identifies new risk loci and implicates Aβ, tau, immunity and lipid processing. *Nat. Genet.* 51, 414–430. doi: 10.1038/s41588-019-0358-2

Lacor, P. N., Buniel, M. C., Chang, L., Fernandez, S. J., Gong, Y., Viola, K. L., et al. (2004). Synaptic targeting by Alzheimer's-related amyloid β oligomers. *J. Neurosci.* 24, 10191–10200. doi: 10.1523/JNEUROSCI.3432-04.2004

Lacor, P. N., Buniel, M. C., Furlow, P. W., Clemente, A. S., Velasco, P. T., Wood, M., et al. (2007). Aβ oligomer-induced aberrations in synapse composition, shape and density provide a molecular basis for loss of connectivity in Alzheimer's disease. *J. Neurosci.* 27, 796–807. doi: 10.1523/jneurosci.3501-06.2007

Lai, A. Y., and McLaurin, J. (2010). Mechanisms of amyloid-β Peptide uptake by neurons: the role of lipid rafts and lipid raft-associated proteins. *Int. J. Alzheimers Dis.* 2011:548380. doi: 10.4061/2011/548380

Lambert, J. C., Ibrahim-Verbaas, C. A., Harold, D., Naj, A. C., Sims, R., Bellenguez, C., et al. (2013). Meta-analysis of 74,046 individuals identifies 11 new susceptibility loci for Alzheimer's disease. *Nat. Genet.* 45, 1452–1458. doi: 10.1038/ng.2802

Laßek, M., Weingarten, J., Einsfelder, U., Brendel, P., Müller, U., and Volknandt, W. (2013). Amyloid precursor proteins are constituents of the presynaptic active zone. *J. Neurochem.* 127, 48–56. doi: 10.1111/jnc.12358

Lee, H.-K., Yang, Y., Su, Z., Hyeon, C., Lee, T.-S., Lee, H.-W., et al. (2010). Dynamic Ca^{2+}-dependent stimulation of vesicle fusion by membrane-anchored synaptotagmin 1. *Science* 328, 760–763. doi: 10.1126/science.1187722

Leprince, C., Romero, F., Cussac, D., Vayssiere, B., Berger, R., Tavitian, A., et al. (1997). A new member of the amphiphysin family connecting endocytosis and signal transduction pathways. *J. Biol. Chem.* 272, 15101–15105. doi: 10.1074/jbc.272.24.15101

Li, C., Ruotsalainen, V., Tryggvason, K., Shaw, A. S., and Miner, J. H. (2000). CD2AP is expressed with nephrin in developing podocytes and is found widely in mature kidney and elsewhere. *Am. J. Physiol. Renal Physiol.* 279, F785–F792. doi: 10.1152/ajprenal.2000.279.4.f785

Lichte, B., Veh, R. W., Meyer, H. E., and Kilimann, M. W. (1992). Amphiphysin, a novel protein associated with synaptic vesicles. *EMBO J.* 11, 2521–2530. doi: 10.1002/j.1460-2075.1992.tb05317.x

Lin, Y.-T., Seo, J., Gao, F., Feldman, H. M., Wen, H.-L., Penney, J., et al. (2018). APOE4 causes widespread molecular and cellular alterations associated with Alzheimer's disease phenotypes in human iPSC-derived brain cell types. *Neuron* 98, 1141.e7–1154.e7. doi: 10.1016/j.neuron.2018.05.008

Liraz, O., Boehm-Cagan, A., and Michaelson, D. M. (2013). ApoE4 induces Aβ42, tau, and neuronal pathology in the hippocampus of young targeted replacement apoE4 mice. *Mol. Neurodegener.* 8:16. doi: 10.1186/1750-1326-8-16

Liu, S.-J., Gasperini, R., Foa, L., and Small, D. H. (2010). Amyloid-β decreases cell-surface AMPA receptors by increasing intracellular calcium and phosphorylation of GluR2. *J. Alzheimers Dis.* 21, 655–666. doi: 10.3233/jad-2010-091654

Liu, C.-C., Liu, C.-C., Kanekiyo, T., Xu, H., and Bu, G. (2013). Apolipoprotein E and Alzheimer disease: risk, mechanisms and therapy. *Nat. Rev. Neurol.* 9, 106–118. doi: 10.1038/nrneurol.2012.263

Liu, D., Pan, X., Zhang, J., Shen, H., Collins, N. C., Cole, A. M., et al. (2015). APOE4 enhances age-dependent decline in cognitive function by down-regulating an NMDA receptor pathway in EFAD-Tg mice. *Mol. Neurodegener.* 10:7. doi: 10.1186/s13024-015-0002-2

Logge, W., Cheng, D., Chesworth, R., Bhatia, S., Garner, B., Kim, W. S., et al. (2012). Role of Abca7 in mouse behaviours relevant to neurodegenerative diseases. *PLoS One* 7:e45959. doi: 10.1371/journal.pone.0045959

Lorenzo, A., Yuan, M., Zhang, Z., Paganetti, P. A., Sturchler-Pierrat, C., Staufenbiel, M., et al. (2000). Amyloid β interacts with the amyloid precursor protein: a potential toxic mechanism in Alzheimer's disease. *Nat. Neurosci.* 3, 460–464. doi: 10.1038/74833

Lu, D. C., Shaked, G. M., Masliah, E., Bredesen, D. E., and Koo, E. H. (2003). Amyloid β protein toxicity mediated by the formation of amyloid-β protein precursor complexes. *Ann. Neurol.* 54, 781–789. doi: 10.1002/ana.10761

Ludewig, S., and Korte, M. (2016). Novel insights into the physiological function of the APP (Gene) family and its proteolytic fragments in synaptic plasticity. *Front. Mol. Neurosci.* 9:161. doi: 10.3389/fnmol.2016.00161

Maier, W., Bednorz, M., Meister, S., Roebroek, A., Weggen, S., Schmitt, U., et al. (2013). LRP1 is critical for the surface distribution and internalization of the NR2B NMDA receptor subtype. *Mol. Neurodegener.* 8:25. doi: 10.1186/1750-1326-8-25

Malinow, R., and Malenka, R. C. (2002). AMPA receptor trafficking and synaptic plasticity. *Annu. Rev. Neurosci.* 25, 103–126. doi: 10.1146/annurev.neuro.25.112701.142758

Margolis, S. S., Salogiannis, J., Lipton, D. M., Mandel-Brehm, C., Wills, Z. P., Mardinly, A. R., et al. (2010). EphB-mediated degradation of the RhoA GEF Ephexin5 relieves a developmental brake on excitatory synapse formation. *Cell* 143, 442–455. doi: 10.1016/j.cell.2010.09.038

Marsh, J., and Alifragis, P. (2018). Synaptic dysfunction in Alzheimer's disease: the effects of amyloid β on synaptic vesicle dynamics as a novel target for therapeutic intervention. *Neural Regen. Res.* 13, 616–623. doi: 10.4103/1673-5374.230276

Mauch, D. H., Nägler, K., Schumacher, S., Göritz, C., Müller, E. C., Otto, A., et al. (2001). CNS synaptogenesis promoted by glia-derived cholesterol. *Science* 294, 1354–1357. doi: 10.1126/science.294.5545.1354

May, P., Rohlmann, A., Bock, H. H., Zurhove, K., Marth, J. D., Schomburg, E. D., et al. (2004). Neuronal LRP1 functionally associates with postsynaptic proteins

and is required for normal motor function in mice. *Mol. Cell. Biol.* 24, 8872–8883. doi: 10.1128/mcb.24.20.8872-8883.2004

McQuade, A., and Blurton-Jones, M. (2019). Microglia in alzheimer's disease: exploring how genetics and phenotype influence risk. *J. Mol. Biol.* 431, 1805–1817. doi: 10.1016/j.jmb.2019.01.045

Meyerholz, A., Hinrichsen, L., Groos, S., Esk, P.-C., Brandes, G., and Ungewickell, E. J. (2005). Effect of clathrin assembly lymphoid myeloid leukemia protein depletion on clathrin coat formation. *Traffic* 6, 1225–1234. doi: 10.1111/j.1600-0854.2005.00355.x

Michaelson, D. M. (2014). APOE ε4: the most prevalent yet understudied risk factor for Alzheimer's disease. *Alzheimers Dement.* 10, 861–868. doi: 10.1016/j.jalz.2014.06.015

Micheva, K. D., Ramjaun, A. R., Kay, B. K., and McPherson, P. S. (1997). SH3 domain-dependent interactions of endophilin with amphiphysin. *FEBS Lett.* 414, 308–312. doi: 10.1016/s0014-5793(97)01016-8

Michikawa, M., Fan, Q. W., Isobe, I., and Yanagisawa, K. (2000). Apolipoprotein E exhibits isoform-specific promotion of lipid efflux from astrocytes and neurons in culture. *J. Neurochem.* 74, 1008–1016. doi: 10.1046/j.1471-4159.2000.0741008.x

Milosevic, I. (2018). Revisiting the role of clathrin-mediated endoytosis in synaptic vesicle recycling. *Front. Cell. Neurosci.* 12:27. doi: 10.3389/fncel.2018.00027

Miñano-Molina, A. J., España, J., Martín, E., Barneda-Zahonero, B., Fadó, R., Solé, M., et al. (2011). Soluble oligomers of amyloid-β peptide disrupt membrane trafficking of α-amino-3-hydroxy-5-methylisoxazole-4-propionic acid receptor contributing to early synapse dysfunction. *J. Biol. Chem.* 286, 27311–27321. doi: 10.1074/jbc.M111.227504

Miyagawa, T., Ebinuma, I., Morohashi, Y., Hori, Y., Young Chang, M., Hattori, H., et al. (2016). BIN1 regulates BACE1 intracellular trafficking and amyloid-β production. *Hum. Mol. Genet.* 25, 2948–2958. doi: 10.1093/hmg/ddw146

Mochizuki, A., Tamaoka, A., Shimohata, A., Komatsuzaki, Y., and Shoji, S. (2000). Aβ42-positive non-pyramidal neurons around amyloid plaques in Alzheimer's disease. *Lancet* 355, 42–43. doi: 10.1016/s0140-6736(99)04937-5

Montagna, E., Dorostkar, M. M., and Herms, J. (2017). The role of APP in structural spine plasticity. *Front. Mol. Neurosci.* 10:136. doi: 10.3389/fnmol.2017.00136

Motoi, Y., Aizawa, T., Haga, S., Nakamura, S., Namba, Y., and Ikeda, K. (1999). Neuronal localization of a novel mosaic apolipoprotein E receptor, LR11, in rat and human brain. *Brain Res.* 833, 209–215. doi: 10.1016/s0006-8993(99)01542-5

Mucke, L., and Selkoe, D. J. (2012). Neurotoxicity of amyloid β-protein: synaptic and network dysfunction. *Cold Spring Harb. Perspect. Med.* 2:a006338. doi: 10.1101/cshperspect.a006338

Muller, A. J., Baker, J. F., DuHadaway, J. B., Ge, K., Farmer, G., Donover, P. S., et al. (2003). Targeted disruption of the murine Bin1/Amphiphysin II gene does not disable endocytosis but results in embryonic cardiomyopathy with aberrant myofibril formation. *Mol. Cell. Biol.* 23, 4295–4306. doi: 10.1128/mcb.23.12.4295-4306.2003

Naj, A. C., Jun, G., Beecham, G. W., Wang, L.-S., Vardarajan, B. N., Buros, J., et al. (2011). Common variants at MS4A4/MS4A6E, CD2AP, CD33 and EPHA1 are associated with late-onset Alzheimer's disease. *Nat. Genet.* 43, 436–441. doi: 10.1038/ng.801

Naj, A. C., Jun, G., Reitz, C., Kunkle, B. W., Perry, W., Park, Y. S., et al. (2014). Effects of multiple genetic loci on age at onset in late-onset Alzheimer disease: a genome-wide association study. *JAMA Neurol.* 71, 1394–1404. doi: 10.1001/jamaneurol.2014.1491

Neustadtl, A. L., Winston, C. N., Parsadanian, M., Main, B. S., Villapol, S., and Burns, M. P. (2017). Reduced cortical excitatory synapse number in APOE4 mice is associated with increased calcineurin activity. *Neuroreport* 28, 618–624. doi: 10.1097/wnr.0000000000000811

Newpher, T. M., and Ehlers, M. D. (2008). Glutamate receptor dynamics in dendritic microdomains. *Neuron* 58, 472–497. doi: 10.1016/j.neuron.2008.04.030

Nolt, M. J., Lin, Y., Hruska, M., Murphy, J., Sheffler-Colins, S. I., Kayser, M. S., et al. (2011). EphB controls NMDA receptor function and synaptic targeting in a subunit-specific manner. *J. Neurosci.* 31, 5353–5364. doi: 10.1523/JNEUROSCI.0282-11.2011

Nwabuisi-Heath, E., Rebeck, G. W., Ladu, M. J., and Yu, C. (2014). ApoE4 delays dendritic spine formation during neuron development and accelerates loss of mature spines *in vitro*. *ASN Neuro* 6:e00134. doi: 10.1042/an20130043

Offe, K., Dodson, S. E., Shoemaker, J. T., Fritz, J. J., Gearing, M., Levey, A. I., et al. (2006). The lipoprotein receptor LR11 regulates amyloid β production and amyloid precursor protein traffic in endosomal compartments. *J. Neurosci.* 26, 1596–1603. doi: 10.1523/JNEUROSCI.4946-05.2006

Oikawa, N., Hatsuta, H., Murayama, S., Suzuki, A., and Yanagisawa, K. (2014). Influence of APOE genotype and the presence of Alzheimer's pathology on synaptic membrane lipids of human brains. *J. Neurosci. Res.* 92, 641–650. doi: 10.1002/jnr.23341

Ojelade, S. A., Lee, T. V., Giagtzoglou, N., Yu, L., Ugur, B., Duraine, L., et al. (2019). *cindr*, the *Drosophila* homolog of the *cd2ap* Alzheimer's disease susceptibility gene, is required for synaptic transmission and proteostasis. *Cell Rep.* 28, 1799.e5–1813.e5. doi: 10.1016/j.celrep.2019.07.041

Oku, Y., and Huganir, R. L. (2013). AGAP3 and Arf6 regulate trafficking of AMPA receptors and synaptic plasticity. *J. Neurosci.* 33, 12586–12598. doi: 10.1523/JNEUROSCI.0341-13.2013

Pant, S., Sharma, M., Patel, K., Caplan, S., Carr, C. M., and Grant, B. D. (2009). AMPH-1/Amphiphysin/Bin1 functions with RME-1/Ehd1 in endocytic recycling. *Nat. Cell Biol.* 11, 1399–1410. doi: 10.1038/ncb1986

Parodi, J., Sepúlveda, F. J., Roa, J., Opazo, C., Inestrosa, N. C., and Aguayo, L. G. (2010). β-amyloid causes depletion of synaptic vesicles leading to neurotransmission failure. *J. Biol. Chem.* 285, 2506–2514. doi: 10.1074/jbc.m109.030023

Pasquale, E. B. (2004). Eph-ephrin promiscuity is now crystal clear. *Nat. Neurosci.* 7, 417–418. doi: 10.1038/nn0504-417

Penzes, P., Beeser, A., Chernoff, J., Schiller, M. R., Eipper, B. A., Mains, R. E., et al. (2003). Rapid induction of dendritic spine morphogenesis by trans-synaptic ephrinB-EphB receptor activation of the Rho-GEF kalirin. *Neuron* 37, 263–274. doi: 10.1016/s0896-6273(02)01168-6

Pham, E., Crews, L., Ubhi, K., Hansen, L., Adame, A., Cartier, A., et al. (2010). Progressive accumulation of amyloid-β oligomers in Alzheimer's disease and in amyloid precursor protein transgenic mice is accompanied by selective alterations in synaptic scaffold proteins. *FEBS J.* 277, 3051–3067. doi: 10.1111/j.1742-4658.2010.07719.x

Pickett, E. K., Koffie, R. M., Wegmann, S., Henstridge, C. M., Herrmann, A. G., Colom-Cadena, M., et al. (2016). Non-fibrillar oligomeric amyloid-β within synapses. *J. Alzheimers Dis.* 53, 787–800. doi: 10.3233/JAD-160007

Proctor, D. T., Coulson, E. J., and Dodd, P. R. (2010). Reduction in post-synaptic scaffolding PSD-95 and SAP-102 protein levels in the Alzheimer inferior temporal cortex is correlated with disease pathology. *J. Alzheimers Dis.* 21, 795–811. doi: 10.3233/jad-2010-100090

Prokic, I., Cowling, B. S., and Laporte, J. (2014). Amphiphysin 2 (BIN1) in physiology and diseases. *J. Mol. Med.* 92, 453–463. doi: 10.1007/s00109-014-1138-1

Puzzo, D., Privitera, L., Leznik, E., Fà, M., Staniszewski, A., Palmeri, A., et al. (2008). Picomolar amyloid-β positively modulates synaptic plasticity and memory in hippocampus. *J. Neurosci.* 28, 14537–14545. doi: 10.1523/JNEUROSCI.2692-08.2008

Rajendran, L., and Paolicelli, R. C. (2018). Microglia-mediated synapse loss in Alzheimer's disease. *J. Neurosci.* 38, 2911–2919. doi: 10.1523/JNEUROSCI.1136-17.2017

Ramjaun, A. R., Micheva, K. D., Bouchelet, I., and McPherson, P. S. (1997). Identification and characterization of a nerve terminal-enriched amphiphysin isoform. *J. Biol. Chem.* 272, 16700–16706. doi: 10.1074/jbc.272.26.16700

Rapp, A., Gmeiner, B., and Hüttinger, M. (2006). Implication of apoE isoforms in cholesterol metabolism by primary rat hippocampal neurons and astrocytes. *Biochimie* 88, 473–483. doi: 10.1016/j.biochi.2005.10.007

Riddell, D. R., Zhou, H., Atchison, K., Warwick, H. K., Atkinson, P. J., Jefferson, J., et al. (2008). Impact of apolipoprotein E (ApoE) polymorphism on brain ApoE levels. *J. Neurosci.* 28, 11445–11453. doi: 10.1523/JNEUROSCI.1972-08.2008

Rodriguez, G. A., Burns, M. P., Weeber, E. J., and Rebeck, G. W. (2013). Young APOE4 targeted replacement mice exhibit poor spatial learning and memory, with reduced dendritic spine density in the medial entorhinal cortex. *Learn. Mem.* 20, 256–266. doi: 10.1101/lm.030031.112

Rogaeva, E., Meng, Y., Lee, J. H., Gu, Y., Kawarai, T., Zou, F., et al. (2007). The neuronal sortilin-related receptor SORL1 is genetically associated with Alzheimer disease. *Nat. Genet.* 39, 168–177. doi: 10.1038/ng1943

Rohe, M., Hartl, D., Fjorback, A. N., Klose, J., and Willnow, T. E. (2013). SORLA-mediated trafficking of TrkB enhances the response of neurons to BDNF. *PLoS One* 8:e72164. doi: 10.1371/journal.pone.0072164

Russell, C. L., Semerdjieva, S., Empson, R. M., Austen, B. M., Beesley, P. W., and Alifragis, P. (2012). Amyloid-β acts as a regulator of neurotransmitter release disrupting the interaction between synaptophysin and VAMP2. *PLoS One* 7:e43201. doi: 10.1371/journal.pone.0043201

Sager, K. L., Wuu, J., Leurgans, S. E., Rees, H. D., Gearing, M., Mufson, E. J., et al. (2007). Neuronal LR11/sorLA expression is reduced in mild cognitive impairment. *Ann. Neurol.* 62, 640–647. doi: 10.1002/ana.21190

Sahlender, D. A., Kozik, P., Miller, S. E., Peden, A. A., and Robinson, M. S. (2013). Uncoupling the functions of CALM in VAMP sorting and clathrin-coated pit formation. *PLoS One* 8:e64514. doi: 10.1371/journal.pone.0064514

Sakae, N., Liu, C.-C., Shinohara, M., Frisch-Daiello, J., Ma, L., Yamazaki, Y., et al. (2016). ABCA7 deficiency accelerates Amyloid-β generation and Alzheimer's neuronal pathology. *J. Neurosci.* 36, 3848–3859. doi: 10.1523/JNEUROSCI.3757-15.2016

Sakamuro, D., Elliott, K. J., Wechsler-Reya, R., and Prendergast, G. C. (1996). BIN1 is a novel MYC-interacting protein with features of a tumour suppressor. *Nat. Genet.* 14, 69–77. doi: 10.1038/ng0996-69

Scherzer, C. R., Offe, K., Gearing, M., Rees, H. D., Fang, G., Heilman, C. J., et al. (2004). Loss of apolipoprotein E receptor LR11 in Alzheimer disease. *Arch. Neurol.* 61, 1200–1205. doi: 10.1001/archneur.61.8.1200

Schürmann, B., Bermingham, D. P., Kopeikina, K. J., Myczek, K., Yoon, S., Horan, K. E., et al. (2019). A novel role for the late-onset Alzheimer's disease (LOAD)-associated protein Bin1 in regulating postsynaptic trafficking and glutamatergic signaling. *Mol. Psychiatry* doi: 10.1038/s41380-019-0407-3 [Epub ahead of print].

Schwarz, L. A., Hall, B. J., and Patrick, G. N. (2010). Activity-dependent ubiquitination of GluA1 mediates a distinct AMPA receptor endocytosis and sorting pathway. *J. Neurosci.* 30, 16718–16729. doi: 10.1523/JNEUROSCI.3686-10.2010

Selkoe, D. J., and Hardy, J. (2016). The amyloid hypothesis of Alzheimer's disease at 25 years. *EMBO Mol. Med.* 8, 595–608. doi: 10.15252/emmm.201606210

Shankar, G. M., Li, S., Mehta, T. H., Garcia-Munoz, A., Shepardson, N. E., Smith, I., et al. (2008). Amyloid-β protein dimers isolated directly from Alzheimer's brains impair synaptic plasticity and memory. *Nat. Med.* 14, 837–842. doi: 10.1038/nm1782

Sheng, M., and Hyoung Lee, S. (2003). AMPA receptor trafficking and synaptic plasticity: major unanswered questions. *Neurosci. Res.* 46, 127–134. doi: 10.1016/s0168-0102(03)00040-3

Shepherd, J. D., and Huganir, R. L. (2007). The cell biology of synaptic plasticity: AMPA receptor trafficking. *Annu. Rev. Cell Dev. Biol.* 23, 613–643. doi: 10.1146/annurev.cellbio.23.090506.123516

Shih, N. Y., Li, J., Karpitskii, V., Nguyen, A., Dustin, M. L., Kanagawa, O., et al. (1999). Congenital nephrotic syndrome in mice lacking CD2-associated protein. *Science* 286, 312–315. doi: 10.1126/science.286.5438.312

Sinha, N., Reagh, Z. M., Tustison, N. J., Berg, C. N., Shaw, A., Myers, C. E., et al. (2019). ABCA7 risk variant in healthy older African Americans is associated with a functionally isolated entorhinal cortex mediating deficient generalization of prior discrimination training. *Hippocampus* 29, 527–538. doi: 10.1002/hipo.23042

Sinnen, B. L., Bowen, A. B., Gibson, E. S., and Kennedy, M. J. (2016). Local and use-dependent effects of β-amyloid oligomers on NMDA receptor function revealed by optical quantal analysis. *J. Neurosci.* 36, 11532–11543. doi: 10.1523/JNEUROSCI.1603-16.2016

Sloniowski, S., and Ethell, I. M. (2012). Looking forward to EphB signaling in synapses. *Semin. Cell Dev. Biol.* 23, 75–82. doi: 10.1016/j.semcdb.2011.10.020

Small, S. A. (2014). Isolating pathogenic mechanisms embedded within the hippocampal circuit through regional vulnerability. *Neuron* 84, 32–39. doi: 10.1016/j.neuron.2014.08.030

Snyder, E. M., Nong, Y., Almeida, C. G., Paul, S., Moran, T., Choi, E. Y., et al. (2005). Regulation of NMDA receptor trafficking by amyloid-β. *Nat. Neurosci.* 8, 1051–1058. doi: 10.1038/nn1503

Soda, K., Balkin, D. M., Ferguson, S. M., Paradise, S., Milosevic, I., Giovedi, S., et al. (2012). Role of dynamin, synaptojanin, and endophilin in podocyte foot processes. *J. Clin. Invest.* 122, 4401–4411. doi: 10.1172/jci65289

Steinberg, S., Stefansson, H., Jonsson, T., Johannsdottir, H., Ingason, A., Helgason, H., et al. (2015). Loss-of-function variants in ABCA7 confer risk of Alzheimer's disease. *Nat. Genet.* 47, 445–447. doi: 10.1038/ng.3246

Stocker, H., Möllers, T., Perna, L., and Brenner, H. (2018). The genetic risk of Alzheimer's disease beyond APOE ε4: systematic review of Alzheimer's genetic risk scores. *Transl. Psychiatry* 8:166. doi: 10.1038/s41398-018-0221-8

Strittmatter, W. J., Saunders, A. M., Schmechel, D., Pericak-Vance, M., Enghild, J., Salvesen, G. S., et al. (1993). Apolipoprotein E: high-avidity binding to β-amyloid and increased frequency of type 4 allele in late-onset familial Alzheimer disease. *Proc. Natl. Acad. Sci. U S A* 90, 1977–1981. doi: 10.1073/pnas.90.5.1977

Südhof, T. C. (2013). Neurotransmitter release: the last millisecond in the life of a synaptic vesicle. *Neuron* 80, 675–690. doi: 10.1016/j.neuron.2013.10.022

Sultana, R., Banks, W. A., and Butterfield, D. A. (2010). Decreased levels of PSD95 and two associated proteins and increased levels of BCl2 and caspase 3 in hippocampus from subjects with amnestic mild cognitive impairment: insights into their potential roles for loss of synapses and memory, accumulation of Aβ, and neurodegeneration in a prodromal stage of Alzheimer's disease. *J. Neurosci. Res.* 88, 469–477. doi: 10.1002/jnr.22227

Takahashi, R. H., Almeida, C. G., Kearney, P. F., Yu, F., Lin, M. T., Milner, T. A., et al. (2004). Oligomerization of Alzheimer's β-amyloid within processes and synapses of cultured neurons and brain. *J. Neurosci.* 24, 3592–3599. doi: 10.1523/JNEUROSCI.5167-03.2004

Takahashi, R. H., Milner, T. A., Li, F., Nam, E. E., Edgar, M. A., Yamaguchi, H., et al. (2002). Intraneuronal Alzheimer Aβ42 accumulates in multivesicular bodies and is associated with synaptic pathology. *Am. J. Pathol.* 161, 1869–1879. doi: 10.1016/s0002-9440(10)64463-x

Takahashi, R. H., Nagao, T., and Gouras, G. K. (2017). Plaque formation and the intraneuronal accumulation of β-amyloid in Alzheimer's disease. *Pathol. Int.* 67, 185–193. doi: 10.1111/pin.12520

Takasu, M. A., Dalva, M. B., Zigmond, R. E., and Greenberg, M. E. (2002). Modulation of NMDA receptor-dependent calcium influx and gene expression through EphB receptors. *Science* 295, 491–495. doi: 10.1126/science.1065983

Tampellini, D., and Gouras, G. K. (2010). Synapses, synaptic activity and intraneuronal Aβ in Alzheimer's disease. *Front. Aging Neurosci.* 2:13. doi: 10.3389/fnagi.2010.00013

Tampellini, D., Rahman, N., Gallo, E. F., Huang, Z., Dumont, M., Capetillo-Zarate, E., et al. (2009). Synaptic activity reduces intraneuronal Aβ, promotes APP transport to synapses and protects against Aβ-related synaptic alterations. *J. Neurosci.* 29, 9704–9713. doi: 10.1523/JNEUROSCI.2292-09.2009

Thiele, C., Hannah, M. J., Fahrenholz, F., and Huttner, W. B. (2000). Cholesterol binds to synaptophysin and is required for biogenesis of synaptic vesicles. *Nat. Cell Biol.* 2, 42–49. doi: 10.1038/71366

Ting, J. T., Kelley, B. G., Lambert, T. J., Cook, D. G., and Sullivan, J. M. (2007). Amyloid precursor protein overexpression depresses excitatory transmission through both presynaptic and postsynaptic mechanisms. *Proc. Natl. Acad. Sci. U S A* 104, 353–358. doi: 10.1073/pnas.0608807104

Tracy, T. E., and Gan, L. (2018). Tau-mediated synaptic and neuronal dysfunction in neurodegenerative disease. *Curr. Opin. Neurobiol.* 51, 134–138. doi: 10.1016/j.conb.2018.04.027

Trommer, B. L., Shah, C., Yun, S. H., Gamkrelidze, G., Pasternak, E. S., Stine, W. B., et al. (2005). ApoE isoform-specific effects on LTP: blockade by oligomeric amyloid-β1–42. *Neurobiol. Dis.* 18, 75–82. doi: 10.1016/j.nbd.2004.08.011

Trommer, B. L., Shah, C., Yun, S. H., Gamkrelidze, G., Pasternak, E. S., Ye, G. L., et al. (2004). ApoE isoform affects LTP in human targeted replacement mice. *Neuroreport* 15, 2655–2658. doi: 10.1097/00001756-200412030-00020

Tsutsui, K., Maeda, Y., Tsutsui, K., Seki, S., and Tokunaga, A. (1997). cDNA cloning of a novel amphiphysin isoform and tissue-specific expression of its multiple splice variants. *Biochem. Biophys. Res. Commun.* 236, 178–183. doi: 10.1006/bbrc.1997.6927

Tucker, W. C., Weber, T., and Chapman, E. R. (2004). Reconstitution of Ca^{2+}-regulated membrane fusion by synaptotagmin and SNAREs. *Science* 304, 435–438. doi: 10.1126/science.1097196

Ubelmann, F., Burrinha, T., Salavessa, L., Gomes, R., Ferreira, C., Moreno, N., et al. (2017). Bin1 and CD2AP polarise the endocytic generation of β-amyloid. *EMBO Rep.* 18, 102–122. doi: 10.15252/embr.201642738

Umeda, T., Ramser, E. M., Yamashita, M., Nakajima, K., Mori, H., Silverman, M. A., et al. (2015). Intracellular amyloid β oligomers impair organelle transport and induce dendritic spine loss in primary neurons. *Acta Neuropathol. Commun.* 3:51. doi: 10.1186/s40478-015-0230-2

Van Acker, Z. P., Bretou, M., and Annaert, W. (2019). Endo-lysosomal dysregulations and late-onset Alzheimer's disease: impact of genetic risk factors. *Mol. Neurodegener.* 14:20. doi: 10.1186/s13024-019-0323-7

Vanlandingham, P. A., Barmchi, M. P., Royer, S., Green, R., Bao, H., Reist, N., et al. (2014). AP180 couples protein retrieval to clathrin-mediated endocytosis of synaptic vesicles. *Traffic* 15, 433–450. doi: 10.1111/tra.12153

Vasquez, J. B., Fardo, D. W., and Estus, S. (2013). ABCA7 expression is associated with Alzheimer's disease polymorphism and disease status. *Neurosci. Lett.* 556, 58–62. doi: 10.1016/j.neulet.2013.09.058

Waites, C. L., Craig, A. M., and Garner, C. C. (2005). Mechanisms of vertebrate synaptogenesis. *Annu. Rev. Neurosci.* 28, 251–274. doi: 10.1146/annurev.neuro.27.070203.144336

Wang, J., Gossing, M., Fang, P., Zimmermann, J., Li, X., von Mollard, G. F., et al. (2011). Epsin N-terminal homology domains bind on opposite sides of two SNAREs. *Proc. Natl. Acad. Sci. U S A* 108, 12277–12282. doi: 10.1073/pnas.1013101108

Wang, Z., Jackson, R. J., Hong, W., Taylor, W. M., Corbett, G. T., Moreno, A., et al. (2017). Human brain-derived Aβ oligomers bind to synapses and disrupt synaptic activity in a manner that requires APP. *J. Neurosci.* 37, 11947–11966. doi: 10.1523/JNEUROSCI.2009-17.2017

Wang, C., Wilson, W. A., Moore, S. D., Mace, B. E., Maeda, N., Schmechel, D. E., et al. (2005). Human apoE4-targeted replacement mice display synaptic deficits in the absence of neuropathology. *Neurobiol. Dis.* 18, 390–398. doi: 10.1016/j.nbd.2004.10.013

Wang, S., Zhang, J., Pan, T., and for Alzheimer's Disease Neuroimaging Initiative. (2018). APOE ε4 is associated with higher levels of CSF SNAP-25 in prodromal Alzheimer's disease. *Neurosci. Lett.* 685, 109–113. doi: 10.1016/j.neulet.2018.08.029

Welsch, T., Endlich, N., Gökce, G., Doroshenko, E., Simpson, J. C., Kriz, W., et al. (2005). Association of CD2AP with dynamic actin on vesicles in podocytes. *Am. J. Physiol. Renal Physiol.* 289, F1134–F1143. doi: 10.1152/ajprenal.00178.2005

Wigge, P., Köhler, K., Vallis, Y., Doyle, C. A., Owen, D., Hunt, S. P., et al. (1997). Amphiphysin heterodimers: potential role in clathrin-mediated endocytosis. *Mol. Biol. Cell* 8, 2003–2015. doi: 10.1091/mbc.8.10.2003

Wigge, P., and McMahon, H. T. (1998). The amphiphysin family of proteins and their role in endocytosis at the synapse. *Trends Neurosci.* 21, 339–344. doi: 10.1016/s0166-2236(98)01264-8

Willén, K., Sroka, A., Takahashi, R. H., and Gouras, G. K. (2017). Heterogeneous association of Alzheimer's disease-linked amyloid-β and amyloid-β protein precursor with synapses. *J. Alzheimers Dis.* 60, 511–524. doi: 10.3233/JAD-170262

Xu, P. T., Gilbert, J. R., Qiu, H. L., Ervin, J., Rothrock-Christian, T. R., Hulette, C., et al. (1999). Specific regional transcription of apolipoprotein E in human brain neurons. *Am. J. Pathol.* 154, 601–611. doi: 10.1016/s0002-9440(10)65305-9

Xu, W., Tan, L., and Yu, J.-T. (2015). The role of PICALM in alzheimer's disease. *Mol. Neurobiol.* 52, 399–413. doi: 10.1007/s12035-014-8878-3

Yamazaki, H., Bujo, H., Kusunoki, J., Seimiya, K., Kanaki, T., Morisaki, N., et al. (1996). Elements of neural adhesion molecules and a yeast vacuolar protein sorting receptor are present in a novel mammalian low density lipoprotein receptor family member. *J. Biol. Chem.* 271, 24761–24768. doi: 10.1074/jbc.271.40.24761

Yamazaki, Y., Zhao, N., Caulfield, T. R., Liu, C.-C., and Bu, G. (2019). Apolipoprotein E and Alzheimer disease: pathobiology and targeting strategies. *Nat. Rev. Neurol.* 15, 501–518. doi: 10.1038/s41582-019-0228-7

Yang, A. J., Chandswangbhuvana, D., Margol, L., and Glabe, C. G. (1998). Loss of endosomal/lysosomal membrane impermeability is an early event in amyloid Aβ1–42 pathogenesis. *J. Neurosci. Res.* 52, 691–698. doi: 10.1002/(sici)1097-4547(19980615)52:6<691::aid-jnr8>3.0.co;2-3

Yang, Y., Kim, J., Kim, H. Y., Ryoo, N., Lee, S., Kim, Y., et al. (2015). Amyloid-β oligomers may impair SNARE-mediated exocytosis by direct binding to syntaxin 1a. *Cell Rep.* 12, 1244–1251. doi: 10.1016/j.celrep.2015.07.044

Yao, J., Nowack, A., Kensel-Hammes, P., Gardner, R. G., and Bajjalieh, S. M. (2010). Cotrafficking of SV2 and synaptotagmin at the synapse. *J. Neurosci.* 30, 5569–5578. doi: 10.1523/JNEUROSCI.4781-09.2010

Yao, P. J., Petralia, R. S., Bushlin, I., Wang, Y., and Furukawa, K. (2005). Synaptic distribution of the endocytic accessory proteins AP180 and CALM. *J. Comp. Neurol.* 481, 58–69. doi: 10.1002/cne.20362

Yong, S.-M., Lim, M.-L., Low, C.-M., and Wong, B.-S. (2014). Reduced neuronal signaling in the ageing apolipoprotein-E4 targeted replacement female mice. *Sci. Rep.* 4:6580. doi: 10.1038/srep06580

Yu, Q., Wang, Y., Du, F., Yan, S., Hu, G., Origlia, N., et al. (2018). Overexpression of endophilin A1 exacerbates synaptic alterations in a mouse model of Alzheimer's disease. *Nat. Commun.* 9:2968. doi: 10.1038/s41467-018-04389-0

Zhang, Y., Chen, K., Sloan, S. A., Bennett, M. L., Scholze, A. R., O'Keeffe, S., et al. (2014). An RNA-sequencing transcriptome and splicing database of glia, neurons, and vascular cells of the cerebral cortex. *J. Neurosci.* 34, 11929–11947. doi: 10.1523/JNEUROSCI.1860-14.2014

Zhang, X., Fu, Z., Meng, L., He, M., and Zhang, Z. (2018). The early events that initiate β-amyloid aggregation in Alzheimer's disease. *Front. Aging Neurosci.* 10:359. doi: 10.3389/fnagi.2018.00359

Zhao, J., Bruck, S., Cemerski, S., Zhang, L., Butler, B., Dani, A., et al. (2013). CD2AP links cortactin and capping protein at the cell periphery to facilitate formation of lamellipodia. *Mol. Cell. Biol.* 33, 38–47. doi: 10.1128/mcb.00734-12

Zhou, Q., Homma, K. J., and Poo, M. (2004). Shrinkage of dendritic spines associated with long-term depression of hippocampal synapses. *Neuron* 44, 749–757. doi: 10.1016/j.neuron.2004.11.011

Zhou, L., Jones, E. V., and Murai, K. K. (2012). EphA signaling promotes actin-based dendritic spine remodeling through slingshot phosphatase. *J. Biol. Chem.* 287, 9346–9359. doi: 10.1074/jbc.m111.302802

Conflict of Interest: The authors declare that the research was conducted in the absence of any commercial or financial relationships that could be construed as a potential conflict of interest.

frontiers in Neuroscience

ORIGINAL RESEARCH
published: 18 June 2020
doi: 10.3389/fnins.2020.00614

Microglial Sirtuin 2 Shapes Long-Term Potentiation in Hippocampal Slices

Joana Sa de Almeida[1,2,3], Mariana Vargas[2,3], João Fonseca-Gomes[2,3], Sara Ramalho Tanqueiro[2,3], Rita F. Belo[2,3], Catarina Miranda-Lourenço[2,3], Ana M. Sebastião[2,3], Maria José Diógenes[2,3]† and Teresa F. Pais[4]*†*

[1] Division of Development and Growth, Department of Woman, Child and Adolescent, University Hospitals of Geneva, Geneva, Switzerland, [2] Instituto de Farmacologia e Neurociências, Faculdade de Medicina, Universidade de Lisboa, Lisbon, Portugal, [3] Instituto de Medicina Molecular João Lobo Antunes, Faculdade de Medicina, Universidade de Lisboa, Lisbon, Portugal, [4] Instituto Gulbenkian de Ciência, Oeiras, Portugal

OPEN ACCESS

Edited by:
Einar M. Sigurdsson, New York University, United States

Reviewed by:
Zemin Wang, Harvard Medical School, United States
Wendy Noble, King's College London, United Kingdom

***Correspondence:**
Maria José Diógenes
diogenes@medicina.ulisboa.pt
Teresa F. Pais
mtpais@igc.gulbenkian.pt; tfariapais@gmail.com

† These authors have contributed equally to this work

Specialty section:
This article was submitted to Neurodegeneration, a section of the journal Frontiers in Neuroscience

Received: *29 December 2019*
Accepted: *18 May 2020*
Published: *18 June 2020*

Citation:
Sa de Almeida J, Vargas M, Fonseca-Gomes J, Tanqueiro SR, Belo RF, Miranda-Lourenço C, Sebastião AM, Diógenes MJ and Pais TF (2020) Microglial Sirtuin 2 Shapes Long-Term Potentiation in Hippocampal Slices. Front. Neurosci. 14:614. doi: 10.3389/fnins.2020.00614

Microglial cells have emerged as crucial players in synaptic plasticity during development and adulthood, and also in neurodegenerative and neuroinflammatory conditions. Here we found that decreased levels of Sirtuin 2 (Sirt2) deacetylase in microglia affects hippocampal synaptic plasticity under inflammatory conditions. The results show that long-term potentiation (LTP) magnitude recorded from hippocampal slices of wild type mice does not differ between those exposed to lipopolysaccharide (LPS), a pro-inflammatory stimulus, or BSA. However, LTP recorded from hippocampal slices of microglial-specific Sirt2 deficient ($Sirt2^{-}$) mice was significantly impaired by LPS. Importantly, LTP values were restored by memantine, an antagonist of N-methyl-D-aspartate (NMDA) receptors. These results indicate that microglial Sirt2 prevents NMDA-mediated excitotoxicity in hippocampal slices in response to an inflammatory signal such as LPS. Overall, our data suggest a key-protective role for microglial Sirt2 in mnesic deficits associated with neuroinflammation.

Keywords: sirtuin 2, long-term potentiation, microglia, neuroinfalmmation, memantine

INTRODUCTION

Neuroinflammation generally refers to the noxious effects caused by immunological activation of microglia and astrocytes in various diseases of the central nervous system (CNS) and also in aging (Streit et al., 2004).

Microglia are primary innate immune cells, the resident macrophages of the CNS that constantly survey the microenvironment. They are known to play an important role in regulating brain development and in synaptic plasticity, controlling synapse formation, function and elimination during development and adulthood (Lenz and Nelson, 2018; Lee and Chung, 2019). Additionally, abnormal microglial activation, through the activation of the transcription factor NF-κB (Glass et al., 2010), a master regulator of the inflammatory and neurotoxic gene response (Streit et al., 2004; Glass et al., 2010), contributes to the initiation and progression of various neurodegenerative

diseases (Glass et al., 2010). Once the delicate neuro-glial interactive balance is compromised, CNS synaptic transmission, plasticity and memory are also affected (Streit et al., 2004; Bains and Oliet, 2007; Di Filippo et al., 2008). Indeed, the release of pro-inflammatory molecules such as IL-1β may result in synaptic dysfunction. Accordingly, there are evidences that both peripheral and central inflammation are associated with impairments of synaptic plasticity in particular of hippocampal CA1 long-term potentiation (LTP) which is dependent on glutamate NMDA receptors activation (Di Filippo et al., 2013). LTP is considered an electro-physiological model for the basic mechanisms involved in learning and memory formation (Bliss and Collingridge, 1993; Martin and Shapiro, 2000) known to be impaired in models of neurodegenerative diseases characterized by mnesic deficits (Martin and Shapiro, 2000; Lynch, 2004).

Sirtuins are a seven-member (SIRT1-SIRT7) family of NAD^+-dependent lysine deacetylases in humans and other mammals that can act on different substrates and regulate a variety of cellular functions, comprising genome maintenance, longevity and metabolism (Westphal et al., 2007; Yamamoto et al., 2007; Vassilopoulos et al., 2011). They have been shown to hold protective effects against age-related diseases such as: cancer, diabetes, cardiovascular and neurodegenerative diseases, including Alzheimer's disease (AD) and Parkinson's disease (PD) (Donmez and Outeiro, 2013). Sirtuins interfere with multiple key processes of neurodegeneration, namely by preventing the accumulation of toxic protein aggregates and restoring protein homeostasis (Donmez and Outeiro, 2013), by increasing transcription of important genes for learning and memory with an impact in neural plasticity (Herskovits and Guarente, 2014), by reducing oxidative stress through activation of mitochondrial functions (Osborne et al., 2016) and by suppressing sustained chronic inflammation via inhibition of NF-κB and through epigenetic modifications (Han, 2009; Min et al., 2013).

Sirt2 is the most abundant sirtuin in the brain (Maxwell et al., 2011). It is primarily a cytoplasmic protein that can transiently shuttle into the nucleus during mitosis but little is known about its precise function (Harting and Knoll, 2010; de Oliveira et al., 2012). An increasing number of studies have reported that Sirt2 is involved in the regulation of inflammatory diseases (Yu et al., 2016; Yuan et al., 2016). In particular, Sirt2 has been shown to be a potential regulator of brain inflammatory responses mediated by microglia, holding a key inhibitory role in microglia−mediated inflammation and neurotoxicity (Pais et al., 2013). Upon pro-inflammatory stimuli, to counteract microglial overactivation, Sirt2 is dephosphorylated, which enhances its deacetylase activity. Sirt2 deacetylates NF-κB (which is found hyperacetylated in the absence of Sirt2), inhibiting thus NF-κB-dependent pro-inflammatory cytokine expression and preventing, this way, excessive transcription of genes that are related to aging and inflammation (Pais et al., 2013; Lo Sasso et al., 2014; Rothgiesser et al., 2019). Therefore, Sirt2 might function as a "gatekeeper," preventing excessive microglial activation and restraining its deleterious effects through NF-κB deacetylation. Indeed, it has been shown that intra-cortical injection of LPS decreases Sirt2 levels in the brain of wild type mice and is associated with increased nitrotyrosination, neurotoxicity and neuronal cell death in Sirt2 deficient mice (Fernandes et al., 2012; Kim et al., 2013; Pais et al., 2013).

Additionally, Sirt2 was shown to alleviate neuropathic pain (Zhang and Chi, 2018) and traumatic brain injury (Yuan et al., 2016) associated with inhibition of NF-κB signaling and neuroinflammation. On the other hand, deletion of Sirt2 resulted in depressive-like behaviors and impaired hippocampal neurogenesis (Liu et al., 2015).

Given that Sirt2 plays a key role in microglia-mediated inflammation, and that LTP can be affected by neuroinflammation, we aimed to investigate the impact of microglial-Sirt2 deficiency on hippocampal LTP. Our findings revealed that, upon LPS inflammatory stimulus, Sirt2-deficiency in microglia leads to an LTP impairment in hippocampal slices, which can be reversed by prior exposition of hippocampal slices to memantine, an antagonist of NMDA receptor. Our results suggest that microglial Sirt2 prevents NMDA-mediated excitotoxicity in hippocampal slices stimulated with LPS, revealing thus a key-protective role for microglial Sirt2 in mnesic deficits associated with neuroinflammation.

MATERIALS AND METHODS

Animals

Myeloid-specific Sirt2 deficient mice, $LysM^{Cre/wt}Sirt2^{flox/flox}$, were generated at Instituto de Medicina Molecular João Lobo Antunes (IMM) by crossing $LysM^{Cre/wt}$ mice (The Jackson Laboratory) with $Sirt2^{flox/flox}$ mice (Dr. Auwerx, Laboratory of Integrative and Systems Physiology, Ecole Polytechnique de Lausanne (EPFL), Switzerland). $LysM^{wt/wt}Sirt2^{flox/flox}$ mice were used as control. The experimental animals were 2–6 months old.

All experiments were performed according to institutional and national guidelines, with local ethical approval in accordance with the recommendations of "Directive 2010/63/EU."

Microglia

Primary microglial cell cultures were prepared from individual newborn $LysM^{Cre/wt}Sirt2^{flox/flox}$ and control $LysM^{wt/wt}Sirt2^{flox/flox}$ mice as described before with a purity >90% (Pais et al., 2008). Briefly, after removal of the meninges, brains were mechanically disrupted in cold Hank's balanced salt solution (HBSS). Cells were cultured in high-glucose Dulbecco's Modified Eagle Medium (DMEM) containing Glutamax (Invitrogen) and supplemented with 10% FBS (Endotoxin <10 EU/ml), 5 μg/ml insulin (Sigma), 2.0 mg/ml L-glucose (Sigma), 0.25 ng/ml Granulocyte-macrophage colony-stimulating factor (GM−CSF) (Peprotech) and 1% Penicillin-Streptomycin 50 mM (Invitrogen) for 10 days. Medium was changed after 3 days and at day 6, an equal amount of medium was added to the culture. The confluent mixed glial cell cultures were shaken for 2 h at 250 r.p.m. and microglial cells obtained from the supernatant after centrifugation.

Adult microglia were obtained from brains of $LysM^{Cre/wt}Sirt2^{flox/flox}$ and control $LysM^{wt/wt}Sirt2^{flox/flox}$ mice (8 weeks old) perfused with 30 ml of PBS via the left ventricle of the heart as described before (Pais and Chatterjee, 2005). Brains

were removed and homogenized in HBSS containing collagenase VIII (0.2 mg/ml) (Sigma). After incubation for 45 min at 37°C, the digested tissue was minced, strained trough a nylon cell strainer of 100 μm (BD Falcon^{TM}) and centrifuged. The pellet was ressuspended in 30% Percoll (Amersham Biosciences AB, Upssala, Sweden) in PBS and centrifuged at 515 *g* for 30 min at room temperature. Microglial cells were obtained after MACS Cell separation of the pelleted cells incubated with CD11b (Microglia) MicroBeads (Milteny Biotec) according to manufacturer's instructions. The purity of isolated microglial cells by MACS assessed by CD11b staining and flow cytometry analysis is within 80–90%.

Western Blot Analysis

Western blot analysis was performed to confirm that microglial expression of Sirt2 was decreased in primary cultures and in adult microglia isolated from LysM$^{Cre/wt}$Sirt2$^{flox/flox}$ in comparison with cells obtained from control LysM$^{wt/wt}$Sirt2$^{flox/flox}$ mice (**Supplementary Figure 1**). Primary microglial cells and brain adult microglia extracts were prepared in NP-40 lysis buffer (150 mM NaCl, 50 mM Tris–HCl, 1% NP-40 for cell culture; 50 mM Tris, 1 mM EDTA, 5 mM MgCl2, 1% Triton X-100 for brain tissue) containing protease and phosphatase inhibitors (Roche Diagnostics GmbH) and resolved in 12% SDS gels. Proteins were transferred onto nitrocellulose membranes (Bio−Rad) and incubated with primary antibodies against Sirt2 (Sigma) and β-actin (Applied Biosystems) or NF-κB p65 (acetyl K310) (Abcam) followed by incubation with horseradish peroxidase-conjugated secondary antibodies (GE Healthcare). The immunoreactivity was detected with an Immobilon Western Chemiluminescent HRP Substrate (Millipore).

Hippocampal Slice Preparation

LysM$^{Cre/wt}$Sirt2$^{flox/flox}$ and control LysM$^{wt/wt}$Sirt2$^{flox/flox}$ mice were sacrificed under sevoflurane anaesthesia (Merial, Harlow, United Kingdom) and brains rapidly removed. The skull was exposed by cutting the skin at the top of the head, the cerebrum bisected along the midline, separating the two hemispheres, and both hippocampi dissected in ice-cold, oxygenated (95% O_2, 5% CO_2) Kreb's solution (artificial cerebrospinal fluid, aCSF) containing (in mM): 124 NaCl, 3 KCl, 1.25 NaH_2PO_4, 26 $NaHCO_3$, 1 $MgSO_4$, 2 $CaCl_2$, and 10 mM glucose, pH 7,4. Hippocampal slices (400 μm thick) were cut perpendicularly to the long axis of the hippocampus using a McIlwain tissue chopper, and incubated in a submerged resting chamber, with Kreb's solution, at room temperature, for at least 1 h prior to experimentation, for functional and energetic recovery.

Hippocampal slices, after resting for 1 h at room temperature, were incubated at room temperature, either with LPS (10 μg/ml; Escherichia coli serotype 055:B5, Sigma) or with control BSA (0,002%; Bovine serum albumin) for 20 min.

To assess the role of NMDA receptors activation (namely the extra-synaptic ones), the hippocampal slices were incubated, after resting, first with memantine (1 μM, for 60 min). After this first incubation step, the hippocampal slices from LysM$^{Cre/wt}$Sirt2$^{flox/flox}$ and control LysM$^{wt/wt}$Sirt2$^{flox/flox}$ mice were subsequently exposed either to LPS or control BSA.

Ex vivo Microelectrophysiological Recordings: LTP Induction, Registration and Quantification

Slices were transferred to a recording chamber for submerged slices and continuously superfused at 3 ml/min with Kreb's solution at 32°C, gassed with 5% CO_2 and 95% O_2.

Recordings were obtained with an Axoclamp 2B amplifier and digitized (Axon Instruments, Foster City, CA, United States). Individual responses were monitored, and averages of six consecutive responses were continuously stored on a personal computer with the LTP program (Anderson and Collingridge, 2001). Field excitatory post-synaptic potentials (fEPSPs) were recorded through microelectrode (2–6 MΩ resistance) placed in the stratum radiatum of the CA1 area. Recording electrodes were pulled from borosilicate glass capillary tubes (Harvard Apparatus, United States) and filled with aCSF.

In LTP experiments, stimulation (rectangular 0.1 ms pulses, once every 10 s) was delivered alternatively to two independent pathways through two bipolar concentric electrodes placed on the Shaffer collateral/commissural fibers in the stratum radiatum. The intensity of the stimulus was adjusted to obtain a fEPSP slope within 50% of the maximum slope recorded and having minimal contamination with population spikes.

A stable baseline of at least 20 min was recorded prior to application of theta-burst stimulation (TBS) protocol, which consisted of 10 bursts of 4 stimuli at 100 Hz, separated by 200 ms. The intensity of the stimulus was never changed during these induction protocols. LTP was quantified as the % of change in the average slope of the fEPSP taken from 50 to 60 min after LTP induction in relation to the average slope of the fEPSP measured during the 10 min that preceded the induction of LTP.

Data were acquired using WinLTP 2.01 M,X-Series software and are presented graphically as mean percentage EPSP slope ± standard error of the mean (SEM).

Input-Output Curve

Input–output curves (I/O) in slices from different genotype groups were performed to ensure that modifications in LTP magnitude were not due to changes in basal synaptic transmission. After obtaining a stable baseline for at least 15 min, the stimulus delivered to the slice (rectangular 0.1 ms pulses, once every 15 s) was decreased until disappearance of the fEPSPs. The stimuli delivered to the slice were then progressively increased by steps of 20 mA. For each stimulation condition, data from three consecutive averaged fEPSP (each averaged fEPSP is the computerized mean of six individual fEPSP) were stored. The range of all inputs delivered to the slice was typically from 60 mA to supra-maximum stimulation amplitude of 300 mA. The input–output curve was plotted as the relationship of fEPSP slope vs stimulus intensity, providing a measure of synaptic efficiency. The max slope (Emax) values were obtained by extrapolation upon nonlinear fitting of the I/O curve.

Statistical Analysis

Values are reported as mean ± standard deviation (SD). Significant differences between different genotypes and

treatments were assessed by means of two-way ANOVA with Bonferroni's post-hoc correction using IBM SPSS Statistics for Macintosh, Version 25.0. Armonk, NY: IBM Corp. Values of $p < 0.05$ were considered to represent statistically significant differences.

RESULTS

LPS Induces LTP Impairment in Hippocampal Slices Deficient in Microglial Sirt2

Theta-burst-stimulation (TBS) reliably induced a robust and reproducible LTP in both hippocampal slices of mice deficient in microglial Sirt2 (Sirt2$^-$) and control mice (Ctr) when incubated either with BSA as a control or with LPS (**Figures 1A,B**). Two-way analysis of variance revealed a significant main effect for treatment, $F(1,20) = 23.23$, $p < 0.0001$, and a significant interaction between treatment and group, $F(1,20) = 12.56$, $p < 0.0001$. Bonferroni post hoc test was conducted and evidenced a statistically significantly LTP magnitude decrease in slices from Sirt2$^-$ mice when incubated with LPS in comparison to BSA (LTP-Sirt2$^-_{LPS}$ = 27.43 ± 10.26 %, $n = 6$ vs LTP-Sirt2$^-_{BSA}$ = 92.65 ± 24.07 %, $n = 6$; $p = 0.001$), while there was no significant difference between LPS and BSA-incubated slices of Ctr mice ($p > 0.05$) (**Figure 1C**). Therefore, lower levels of Sirt2 in microglia strongly reduced the LTP magnitude of hippocampal slices incubated with LPS (**Figure 1B**). Additionally, LTP magnitude was significantly increased in BSA-treated slices from Sirt2$^-$ mice in comparison to slices from Ctr mice (LTP-Sirt2$^-_{BSA}$ = 92.65 ± 24.07 %, $n = 6$ vs LTP-Ctr$_{BSA}$ = 64.44 ± 18.57 %, $n = 6$; $p = 0.019$) (**Figure 1C**). Moreover, LTP magnitude recorded in hippocampal slices from Sirt2$^-$ mice exposed to LPS was significantly reduced when compared to LTP magnitude recorded in similar conditions in hippocampal slices from Ctr mice (LTP-Sirt2$^-_{LPS}$ = 27.43 ± 10.26 %, $n = 6$ vs LTP-Ctr$_{LPS}$ = 54.49 ± 20,75 %, $n = 6$; $p = 0.023$) (**Figure 1C**).

I/O curves confirmed that, using slices taken from the same animals and exposed to LPS in the same conditions of those used in LTP recordings, the alterations detected in LTP magnitude were not attributed to changes in baseline synaptic efficiency (**Figure 1D**).

Although the I/O curve of hippocampal slices deficient in microglial Sirt2 and exposed to LPS revealed a slight deviation from the other curves, fEPSP values (taken as a measure of the strength of the post-synaptic response) were similar for the four different conditions at the maximum stimulation (Emax): LTP-Ctr$_{BSA}$ = 1.021 ± 0.262, $n = 4$; LTP-Sirt2$^-_{BSA}$ = 1.028 ± 0.261, $n = 4$; LTP-Ctr$_{LPS}$ = 1.116 ± 0.262, $n = 5$; LTP-Sirt2$^-_{LPS}$ = 0.909 ± 0.261, $n = 3$. Two-way analysis of variance revealed no significant differences in Emax obtained from slices taken from the different groups. There was no significant main effect of the group, $F(1,10) = 0.001$, $p = 0.981$, neither of treatment, $F(1,10) = 0.001$, $p = 0.981$, nor of the interaction effect between the two $F(1,10) = 0.838$, $p = 0.381$.

Importantly, we attested that the basal stimulation was adjusted to obtain 50% of the maximum fEPSP slope. Therefore, we have used the following intensities for LTP recording: LTP-Ctr$_{BSA}$ = 187 mA; LTP-Sirt2$^-_{BSA}$ = 184 mA; LTP-Ctr$_{LPS}$ = 182 mA; LTP-Sirt2$^-_{LPS}$ = 235 mA. Accordingly, the LTP was induced in each hippocampal slice when similar values of fEPSP slope were obtained by adjusting the initial intensity of stimulation. The intensity of the stimulus was maintained during the induction protocol. Therefore, the slices from LTP-Sirt2$^-_{LPS}$ were stimulated in a range of mA out from the range of stimulation where a decreased response was detected, avoiding therefore any possible influence in LTP induction. Indeed, two-way analysis of variance did not show significant differences between groups regarding the fEPSP slope values corresponding to 50% of the maximum fEPSP slope ($p > 0.05$).

Memantine Reverts the LTP Decline Induced by LPS in Microglial-Specific Sirt2 Deficient Hippocampal Slices

NMDA receptors are critical for CA1 hippocampal LTP induction and expression (Bliss and Collingridge, 1993; Collingridge et al., 2004). However, excessive or prolonged activation of NMDA receptors can be involved in pathological processes (Rothman and Olney, 1995; Parsons et al., 1998). Accordingly, numerous attempts to reduce glutamate-induced excitotoxicity by antagonizing NMDA receptors have been tested (Sun et al., 2019). However, due to the important physiological role of NMDA receptor activation, most NMDA receptor antagonists produce undesired effects on LTP and memory (Frankiewicz et al., 2000). One of the drugs that has been used to selectively block the pathological activation of NMDA receptors, whilst leaving their physiological functions intact, is memantine (for review see Danysz et al., 1997; Parsons et al., 1999; Danysz and Parsons, 2003; Wenk, 2006). Therefore, in order to investigate the putative role of NMDA receptors in the alterations observed in LTP magnitude in hippocampal slices from microglial-specific Sirt2 deficient mice exposed to LPS, hippocampal slices were pre-incubated with memantine (1 μM, for 60 min) prior to the incubation with LPS or BSA.

We found that pre-incubation with memantine before LPS exposure restored the LTP of LPS-stimulated hippocampal slices to levels similar do the BSA condition (Sirt2$^-_{BSA}$ = 105.3 ± 18.04%, $n = 4$ vs LTP-Sirt2$^-_{Memantine+LPS}$ = 77.6 ± 16.97%, $n = 8$; $p > 0.05$). In fact, the LTP magnitude of the hippocampal slices from Sirt2$^-$ mice incubated with memantine and LPS, was significantly increased when compared to LTP magnitude of hippocampal slices incubated with LPS alone (LTP-Sirt2$^-_{Memantine+LPS}$ = 77.6 ± 16.97%, $n = 8$ vs LTP-Sirt2$^-_{LPS}$ = 27.8 ± 10.30%, $n = 6$; $p < 0.001$). The pre-incubation of hippocampal slices from Sirt2$^-$ mice with memantine followed by BSA incubation did not affect LTP magnitude when compared to BSA incubation alone.

There were no statistically significant differences regarding LTP magnitude between the four different conditions (BSA, LPS,

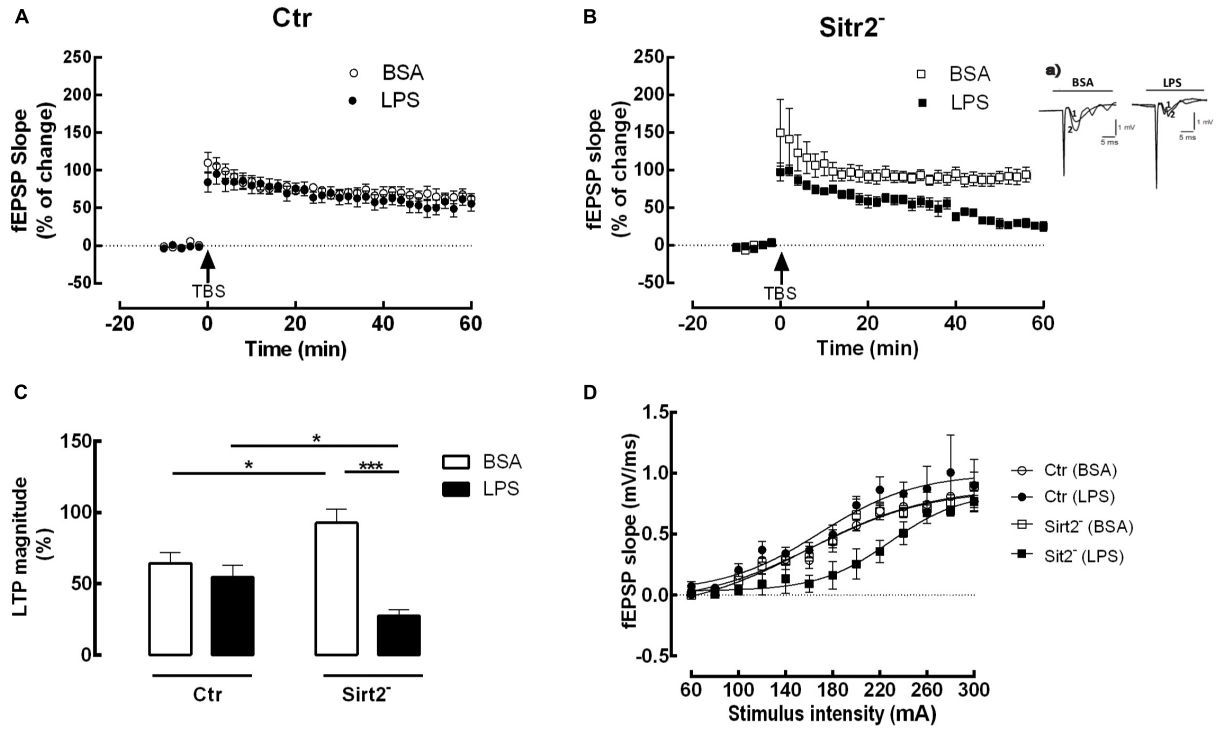

FIGURE 1 | Impaired LTP in microglial Sirt2-deficient hippocampal slices incubated with LPS. Changes in fEPSP slope induced by TBS in hippocampal slices from Ctr **(A)** or Sirt2^{-} **(B)** mice pre-treated for 20 min with either vehicle BSA (n = 6, ○ and □) or LPS (n = 6, ● and ■). Arrow indicates TBS. **(Ba)** shows traces obtained in a representative experiment in **(B)**; each trace is the average of six consecutive responses obtained immediately before (1) and after (2) TBS, and is composed of the stimulus artifact, followed by the presynaptic volley and the fEPSP. **(C)** LTP magnitude % of change, resulting from the difference between the fEPSP slope of LTP induced by TBS during the last 50–60 min of the experiment, in relation to pre-theta-burst values from the experiments shown in **(A)** and **(B)**. Lines indicate statistical significant differences between groups, using two-away ANOVA between-groups with Bonferroni's post-hoc correction. All values are mean ± SEM, $^{*}p < 0.05$; $^{****}p < 0.001$. **(D)** I/O curves of hippocampal slices stimulated or not with LPS. I/O curves were performed in the presence of either BSA or LPS in hippocampal slices deficient in Sirt2 (BSA, n = 4, □; LSP, n = 3, ■) and control slices (BSA, n = 4, ○; LSP, n = 5, ●).

Memantine+BSA, Memantine+LPS) recorded in hippocampal slices prepared from Ctr mice ($p > 0.05$) (**Figure 2**).

DISCUSSION

In the present study, we show a significant impairment on LTP magnitude in hippocampal slices from microglia-specific Sirt2 deficient mice pre-exposed to the general inflammatory stimulus LPS.

Sirt2 has already been shown to hold a key-inhibitory role in microglia-mediated inflammation (Pais et al., 2013). In the current study, we propose that Sirt2 may also take part in protective mechanisms that ensure CNS synaptic transmission and plasticity under an inflammatory environment.

Microglia processes are driven by neuronal activity and can simultaneously interact with both presynaptic and postsynaptic elements (Wake et al., 2009). In response to inflammatory stimuli, microglia are activated, releasing key regulatory molecules, such as TNF-α, IL-1β, IL-6, and IL-8, prostaglandin E2, as well as glutamate, reactive oxygen and nitrogen species, that are known to be highly upregulated during CNS inflammation and to control synaptic transmission and plasticity (Milner and Campbell, 2003; Di Filippo et al., 2008; Dilger and Johnson, 2008; Gomes-Leal, 2012). However, whether and how microglia influence physiological synaptic transmission is still unclear. Nevertheless, there is evidence that under pathological conditions, activation of microglia, which is the primary stage of neuroinflammation, is a common early feature of most brain diseases, followed by synaptic alterations (Cagnin, 2001; Dekosky and Marek, 2003).

According to our published work, microglia not expressing Sirt2, upon an inflammatory stimulus like LPS, become over-activated due to the absence of NF-κB inhibition by Sirt2 (Pais et al., 2013). This leads to overproduction of pro-inflammatory cytokines, such as TNF-α, IL-6, and reactive oxygen and nitrogen species (Pais et al., 2013), all known to have a key role in synaptic plasticity and to mediate LTP impairment (Wang et al., 2015; Rizzo et al., 2018).

To induce deletion of the floxed Sirt2 in microglia, we have used the Cre under the LysM promoter that has been shown to induce a limited recombination in microglia (∼40%) when compared to the CX3CR1 promoter (∼90%) (Goldmann and Prinz, 2013). Although we observed a partial decrease in microglial Sirt2 levels (**Supplementary Figure 1**) it would be interesting to perform the LTP experiments in hippocampal slices

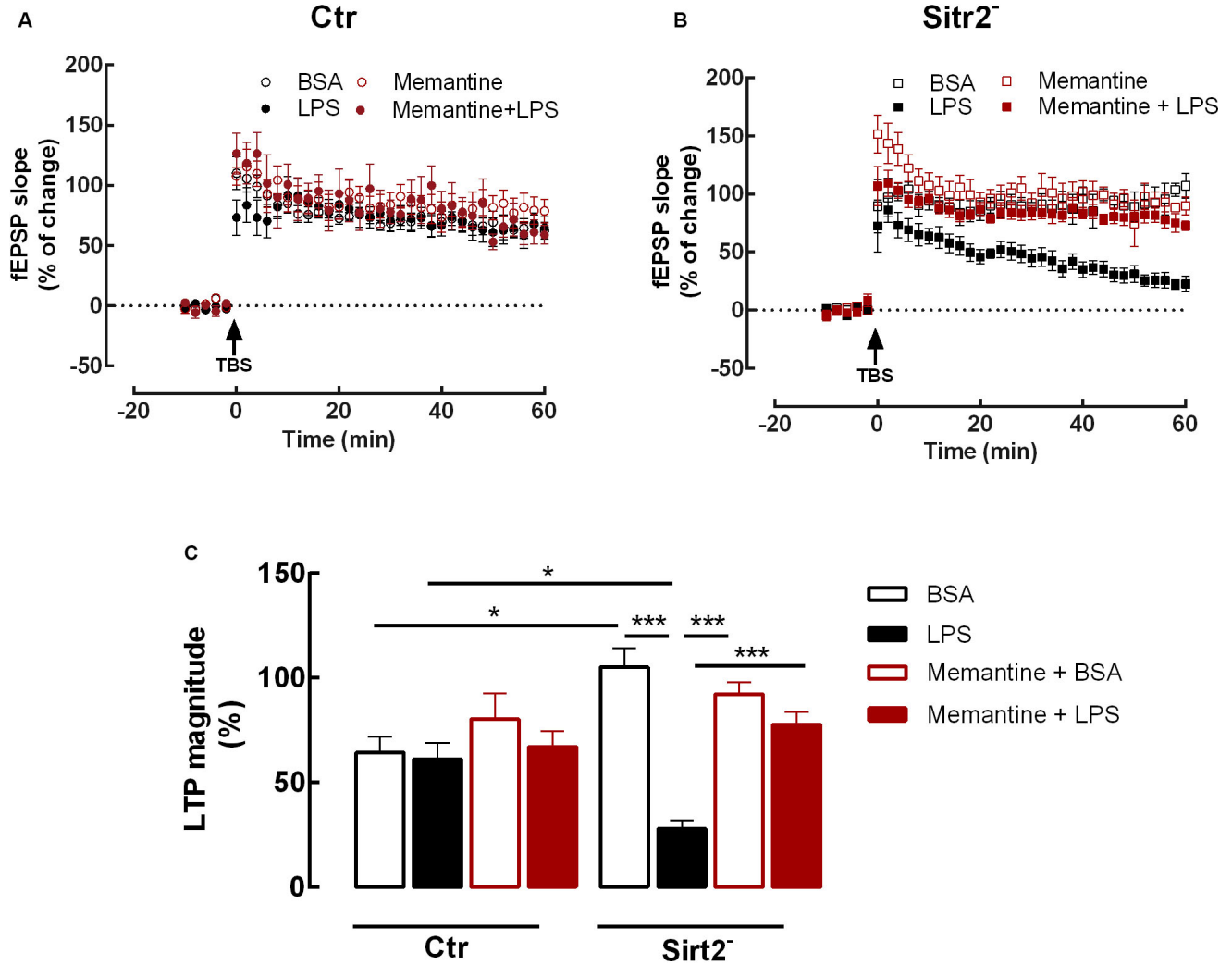

FIGURE 2 | Memantine rescues LTP impairment in microglial Sirt2 deficient hippocampal slices. Changes in fEPSP slope induced by TBS in hippocampal slices from Ctr **(A)** or Sirt2^{-} **(B)** mice pre-treated for 20 min with either vehicle BSA (n = 6, ○ and n = 4, □) or LPS (n = 8, ● and n = 6, ■) or for 60 min of memantine followed by 20 min with either vehicle BSA (n = 7, ○ and n = 6, □) or LPS (n = 4, ● and n = 8, ■). Arrow indicates TBS. **(C)** Plot of LTP magnitude % of change, resulting from the difference between the fEPSP slope of LTP induced by TBS during the last 50–60 min of the experiment, in relation to pre-theta-burst values from the experiments shown in **(A)** and **(B)**, as indicated below the columns. All values are mean ± SEM. Lines indicate statistical significant differences between groups, using two-away ANOVA between-groups with Bonferroni's post-hoc correction. *p < 0.05; ***p < 0.001.

of CX3CR1$^{Cre/wt}$Sirt2$^{flox/flox}$ mice which will probably have a stronger *Sirt2* gene deletion.

We found an increased LTP magnitude in hippocampal slices from microglial Sirt2 deficient mice under control conditions. A possible explanation might be that, in microglia-specific Sirt2 deficient mice, in absence of Sirt2, hippocampal microglia become "primed," being able to easily liberate and produce important factors for synaptic plasticity. Although these might be beneficial at a certain level, when overproduced, as it may happen after LPS stimulation they may contribute to LTP decrease. This seems the case of IL-1β, which has a dual role in LTP, being required for LTP under physiological conditions, but inhibiting LPT when at higher doses, as encountered in pathological conditions (Ross et al., 2003). Our finding contrasts, however, with the results of a recent study that has shown that whole-body Sirt2 knockout (KO) mice present an LTP reduction in hippocampal slices without any inflammatory stimulation, which is accompanied by impairments in long-term memory and is likely result from enhanced acetylation and surface expression of AMPA receptors in neurons (Wang et al., 2017). Future work will investigate whether our observation is due to selective deficiency of Sirt2 in microglia.

Here we show that the absence of Sirt2 specifically in microglia is responsible for an LTP impairment under inflammatory conditions. Interestingly, the I/O curve of

hippocampal slices deficient in microglial Sirt2 and exposed to LPS revealed a slight deviation from the others, which may suggest a certain latency in achieving maximal synaptic response. However, there were no significant differences regarding fEPSP slope values between groups, neither for the initial intensity of stimulation before LTP induction, neither for the obtained maximal synaptic responses between slices (Emax). This finding is supported by a previous study that has also proved that loss of Sirt2 did not cause changes in basal synaptic properties compared to Ctr mice (Wang et al., 2017).

Rescue of LTP impairment with memantine in LPS stimulated microglial Sirt2-deficient hippocampal slices strongly suggests the involvement of extra-synaptic NMDA receptors. Although CA1 LTP depends upon synaptic NMDA receptors activation (Fox et al., 2006), extra-synaptic NMDA receptors activation are well-known for mediating toxic effects (Viviani et al., 2006; Xia et al., 2010). Extra-synaptic NMDARs are enriched in GluN2B-containing heterodimers (GluN2B-NMDARs) and its activity has been associated with neuronal death, in particular in neurodegenerative disorders such as Huntington's or Alzheimer's disease (Papouin and Oliet, 2014). In fact, memantine is an antagonist of the NMDA receptors, and at the concentration used in this study particularly inhibits extra-synaptic NMDA receptors (Xia et al., 2010). These extra-synaptic NMDA receptors are generally activated by pro-inflammatory and neurotoxic factors produced by activated microglia, such as IL-1β, TNF and glutamate (Barger and Basile, 2001; Viviani et al., 2003; Floden et al., 2005; Gardoni et al., 2011). Both IL-1β and TNF were shown to decrease LTP (Cunningham et al., 1996; Coogan and OConnor, 1997; Murray and Lynch, 1998; Ross et al., 2003). Several studies have reported a cross-talk between activation of IL-1β and NMDA receptors (Viviani et al., 2003; Yang et al., 2005; Gardoni et al., 2011). In fact, IL-1RI (interleukin-1 receptor type I) colocalizes with the GluN2B subunit of NMDA extra-synaptic receptors in hippocampal neurons (Gardoni et al., 2011). Importantly, pre-treatment of hippocampal neurons with IL-1β enhance NMDA-induced $[Ca^{2+}]i$ through activation of the Src family of kinases, which increase tyrosine phosphorylation of the NR2A/B subunits (Viviani et al., 2003). IL-1β may have a similar effect during LTP induction as it also involves Src kinase activation (Salter, 1998). Although it is clear that IL-1β and other inflammatory factors interfere with NMDA receptors, the effect in calcium influxes may be dose dependent and have different outcomes in physiological and pathological conditions. We have previously shown that Sirt2-deficent microglia become overactivated by LPS stimulation. Therefore, we hypothesize that LPS-incubated hippocampal slices of microglial-specific Sirt2 deficient mice overproduce inflammatory mediators such as IL-1β, TNF and glutamate enhancing NMDA-induced neuronal death. Future investigation of the specific mechanisms underlying the decreased LTP will be needed to identify the precise factors released by Sirt2-deficient microglia in stimulated hippocampal slices. Moreover, we cannot exclude an anti-inflammatory effect of memantine. Besides being an antagonist of the NMDA receptors, memantine has also been shown to inhibit microglial activation by LPS (Rosi et al., 2006; Wu et al., 2009).

Given the crucial role of microglia in neuroinflammation, the fact that Sirt2 is able to regulate the inflammatory response in the CNS through microglial cells, with an impact in synaptic plasticity, makes it a potential therapeutic target to prevent cognitive decline associated to neuroinflammation. Although development of new drugs for the prevention of neurodegenerative diseases has been an area of intense activity, little progress has been observed. Interestingly, various potent small-molecule modulators of sirtuins have shown efficacy in preclinical models of neurodegenerative and inflammatory diseases, holding promise for drug discovery efforts in multiple therapeutic areas (Lavu et al., 2008; Langley and Sauve, 2013; Min et al., 2013). Our data reinforces this possibility and, in particular, point toward microglial Sirt2 as a potential therapeutic target to prevent cognitive decline associated to neuroinflammation.

CONCLUSION

The results obtained show that, in the absence of microglial Sirt2, inflammatory stimuli significantly impair NMDA-mediated synaptic plasticity. This reveals a key-protective role for microglial Sirt2 in neuroinflammation.

By showing neuroprotective effects, Sirt2 emerges as a potential target for therapeutic intervention in an array of neurological disorders, playing a vital role in all conditions where microglial activation and neuroinflammation may have a major importance in the disease process, like neurodegenerative diseases. This matter is of great importance, since the comprehension of the molecular mechanisms underlying sirtuins activity may help us find new therapeutic targets for these diseases.

DATA AVAILABILITY STATEMENT

The raw data supporting the conclusions of this article will be made available by the authors, without undue reservation, to any qualified researcher upon request.

ETHICS STATEMENT

The animal study was reviewed and approved by by the iMM's Institutional Animal Welfare Body – ORBEA-iMM and the National Competent Authority – DGAV (Direção-Geral de Alimentação e Veterinária).

AUTHOR CONTRIBUTIONS

TP, MD, and AS contributed conception and design of the study. JS and MV performed the main experiments. JF-G, ST, RB, and CM-L contributed to the experimental work. JS, TP, and

MD wrote the manuscript. All authors read and approved the submitted version.

FUNDING

This study was supported by Santa Casa da Misericórdia de Lisboa (MB37-2017), GAPIC Research Program of the University of Lisbon Medical School (n° 2014002 and n° 2015028) and the following doctoral grants: PD/BD/128091/2016, SFRH/BD/118238/2016, PD/BD/114337/2016, and PD/BD/1144-41/2016.

ACKNOWLEDGMENTS

The authors thank Sebastião lab for helpful discussions and technical support.

SUPPLEMENTARY MATERIAL

The Supplementary Material for this article can be found online at: https://www.frontiersin.org/articles/10.3389/fnins.2020.00614/full#supplementary-material

REFERENCES

Anderson, W. W., and Collingridge, G. L. (2001). The LTP program: a data acquisition program for on-line analysis of long-term potentiation and other synaptic events. *J. Neurosci. Meth.* 108, 71–83. doi: 10.1016/s0165-0270(01)00374-0

Bains, J. S., and Oliet, S. H. R. (2007). Glia: they make your memories stick! *Trends Neurosci.* 30, 417–424. doi: 10.1016/j.tins.2007.06.007

Barger, S. W., and Basile, A. S. (2001). Activation of microglia by secreted amyloid precursor protein evokes release of glutamate by cystine exchange and attenuates synaptic function. *J. Neurochem.* 76, 846–854. doi: 10.1046/j.1471-4159.2001.00075.x

Bliss, T. V. P., and Collingridge, G. L. (1993). A synaptic model of memory – long-term potentiation in the *Hippocampus*. *Nature* 361, 31–39. doi: 10.1038/361031a0

Cagnin, A. (2001). In-vivo measurement of activated microglia in dementia. *Lancet* 358, 766–766.

Collingridge, G. L., Isaac, J. T. R., and Wang, Y. T. (2004). Receptor trafficking and synaptic plasticity. *Nat. Rev. Neurosci.* 5, 952–962.

Coogan, A., and OConnor, J. J. (1997). Inhibition of NMDA receptor-mediated synaptic transmission in the rat dentate gyrus in vitro by IL-1 beta. *Neuroreport* 8, 2107–2110. doi: 10.1097/00001756-199707070-00004

Cunningham, A. J., Murray, C. A., O'Neill, L. A., Lynch, M. A., and O'Connor, J. J. (1996). Interleukin-1 beta (IL-1 beta) and tumour necrosis factor (TNF) inhibit long-term potentiation in the rat dentate gyrus in vitro. *Neurosci. Lett.* 203, 17–20. doi: 10.1016/0304-3940(95)12252-4

Danysz, W., and Parsons, C. G. (2003). The NMDA receptor antagonist memantine as a symptomatological and neuroprotective treatment for Alzheimer's disease: preclinical evidence. *Int. J. Geriatr. Psychol.* 18, S23–S32.

Danysz, W., Parsons, C. G., Kornhuber, J., Schmidt, W. J., and Quack, G. (1997). Aminoadamantanes as NMDA receptor antagonists and antiparkinsonian agents – Preclinical studies. *Neurosci. Biobehav. R.* 21, 455–468. doi: 10.1016/s0149-7634(96)00037-1

de Oliveira, R. M., Sarkander, J., Kazantsev, A. G., and Outeiro, T. F. (2012). SIRT2 as a therapeutic target for age-related disorders. *Front. Pharmacol.* 3:82. doi: 10.3389/fphar.2012.00082

Dekosky, S. T., and Marek, K. (2003). Looking backward to move forward: early detection of neurodegenerative disorders. *Science* 302, 830–834. doi: 10.1126/science.1090349

Di Filippo, M., Chiasserini, D., Gardoni, F., Viviani, B., Tozzi, A., Giampà, C., et al. (2013). Effects of central and peripheral inflammation on hippocampal synaptic plasticity. *Neurobiol. Dis.* 52, 229–236.

Di Filippo, M., Sarchielli, P., Picconi, B., and Calabresi, P. (2008). Neuroinflammation and synaptic plasticity: theoretical basis for a novel, immune-centred, therapeutic approach to neurological disorders. *Trends Pharmacol. Sci.* 29, 402–412. doi: 10.1016/j.tips.2008.06.005

Dilger, R. N., and Johnson, R. W. (2008). Aging, microglial cell priming, and the discordant central inflammatory response to signals from the peripheral immune system. *J. Leukocyte Biol.* 84, 932–939. doi: 10.1189/jlb.0208108

Donmez, G., and Outeiro, T. F. (2013). SIRT1 and SIRT2: emerging targets in neurodegeneration. *EMBO Mol. Med.* 5, 344–352. doi: 10.1002/emmm.201302451

Fernandes, C. A., Fievez, L., Neyrinck, A. M., Delzenne, N. M., Bureau, F., and Vanbever, R. (2012). Sirtuin inhibition attenuates the production of inflammatory cytokines in lipopolysaccharide-stimulated macrophages. *Biochem. Biophys. Res. Commun.* 420, 857–861. doi: 10.1016/j.bbrc.2012.03.088

Floden, A. M., Li, S. S., and Combs, C. K. (2005). beta-Amyloid-stimulated microglia induce neuron death via synergistic stimulation of tumor necrosis factor alpha and NMDA receptors. *J. Neurosci.* 25, 2566–2575. doi: 10.1523/jneurosci.4998-04.2005

Fox, C. J., Russell, K. I., Wang, Y. T., and Christie, B. R. (2006). Contribution of NR2A and NR2B NMDA subunits to bidirectional synaptic plasticity in the hippocampus in vivo. *Hippocampus* 16, 907–915. doi: 10.1002/hipo.20230

Frankiewicz, T., Pilc, A., and Parsons, C. G. (2000). Differential effects of NMDA-receptor antagonists on long-term potentiation and hypoxic/hypoglycaemic excitotoxicity in hippocampal slices. *Neuropharmacology* 39, 631–642. doi: 10.1016/s0028-3908(99)00168-9

Gardoni, F., Boraso, M., Zianni, E., Corsini, E., Galli, C. L., Cattabeni, F., et al. (2011). Distribution of interleukin-1 receptor complex at the synaptic membrane driven by interleukin-1 beta and NMDA stimulation. *J. Neuroinflamm.* 8:14. doi: 10.1186/1742-2094-8-14

Glass, C. K., Saijo, K., Winner, B., Marchetto, M. C., and Gage, F. H. (2010). Mechanisms underlying inflammation in neurodegeneration. *Cell* 140, 918–934. doi: 10.1016/j.cell.2010.02.016

Goldmann, T., and Prinz, M. (2013). Role of microglia in CNS autoimmunity. *Clin. Dev. Immunol.* 2013:208093.

Gomes-Leal, W. (2012). Microglial physiopathology: how to explain the dual role of microglia after acute neural disorders? *Brain Behav.* 2, 345–356. doi: 10.1002/brb3.51

Han, S. H. (2009). Potential role of sirtuin as a therapeutic target for neurodegenerative diseases. *J. Clin. Neurol.* 5, 120–125.

Harting, K., and Knoll, B. (2010). SIRT2-mediated protein deacetylation: an emerging key regulator in brain physiology and pathology. *Eur. J. Cell Biol.* 89, 262–269. doi: 10.1016/j.ejcb.2009.11.006

Herskovits, A. Z., and Guarente, L. (2014). SIRT1 in neurodevelopment and brain senescence. *Neuron* 81, 471–483. doi: 10.1016/j.neuron.2014.01.028

Kim, M. J., Kim, D. W., Park, J. H., Kim, S. J., Lee, C. H., Yong, J. I., et al. (2013). PEP-1-SIRT2 inhibits inflammatory response and oxidative stress-induced cell death via expression of antioxidant enzymes in murine macrophages. *Free Radic. Biol. Med.* 63, 432–445. doi: 10.1016/j.freeradbiomed.2013.06.005

Langley, B., and Sauve, A. (2013). Sirtuin deacetylases as therapeutic targets in the nervous system. *Neurotherapeutics* 10, 605–620. doi: 10.1007/s13311-013-0214-5

Lavu, S., Boss, O., Elliott, P. J., and Lambert, P. D. (2008). Sirtuins - novel therapeutic targets to treat age-associated diseases. *Nat. Rev. Drug Discov.* 7, 841–853. doi: 10.1038/nrd2665

Lee, E., and Chung, W. S. (2019). Glial control of synapse number in healthy and diseased brain. *Front. Cell. Neurosci.* 13:42. doi: 10.3389/fncel.2019.00042

Lenz, K. M., and Nelson, L. H. (2018). Microglia and beyond: innate immune cells as regulators of brain development and behavioral function. *Front. Immunol.* 9:698. doi: 10.3389/fimmu.2018.00698

Liu, R., Dang, W., Du, Y., Zhou, Q., Jiao, K., and Liu, Z. H. (2015). SIRT2 is involved in the modulation of depressive behaviors. *Sci. Rep.* 5:8415.

Lo Sasso, G., Menzies, K. J., Mottis, A., Piersigilli, A., Perino, A., Yamamoto, H., et al. (2014). SIRT2 deficiency modulates macrophage polarization and susceptibility to experimental colitis. *PLos One* 9:e103573. doi: 10.1371/journal.pone.0103573

Lynch, M. A. (2004). Long-term potentiation and memory. *Physiol. Rev.* 84, 87–136.

Martin, P. D., and Shapiro, M. L. (2000). Disparate effects of long-term potentiation on evoked potentials and single CA1 neurons in the hippocampus of anesthetized rats. *Hippocampus* 10, 207–212. doi: 10.1002/1098-1063(2000)10:3<207::aid-hipo1>3.0.co;2-s

Maxwell, M. M., Tomkinson, E. M., Nobles, J., Wizeman, J. W., Amore, A. M., Quinti, L., et al. (2011). The Sirtuin 2 microtubule deacetylase is an abundant neuronal protein that accumulates in the aging CNS. *Hum. Mol. Genet.* 20, 3986–3996. doi: 10.1093/hmg/ddr326

Milner, R., and Campbell, I. L. (2003). The extracellular matrix and cytokines regulate microglial integrin expression and activation. *J. Immunol.* 170, 3850–3858. doi: 10.4049/jimmunol.170.7.3850

Min, S. W., Sohn, P. D., Cho, S. H., Swanson, R. A., and Gan, L. (2013). Sirtuins in neurodegenerative diseases: an update on potential mechanisms. *Front. Aging Neurosci.* 5:53. doi: 10.3389/fnagi.2013.00053

Murray, C. A., and Lynch, M. A. (1998). Evidence that increased hippocampal expression of the cytokine interleukin-1 beta is a common trigger for age- and stress-induced impairments in long-term potentiation. *J. Neurosci.* 18, 2974–2981. doi: 10.1523/jneurosci.18-08-02974.1998

Osborne, B., Bentley, N. L., Montgomery, M. K., and Turner, N. (2016). The role of mitochondrial sirtuins in health and disease. *Free Radic. Biol. Med.* 100, 164–174. doi: 10.1016/j.freeradbiomed.2016.04.197

Pais, T. F., and Chatterjee, S. (2005). Brain macrophage activation in murine cerebral malaria precedes accumulation of leukocytes and CD8+ T cell proliferation. *J. Neuroimmunol.* 163, 73–83. doi: 10.1016/j.jneuroim.2005.02.009

Pais, T. F., Figueiredo, C., Peixoto, R., Braz, M. H., and Chatterjee, S. (2008). Necrotic neurons enhance microglial neurotoxicity through induction of glutaminase by a MyD88-dependent pathway. *J. Neuroinflamm.* 5:43. doi: 10.1186/1742-2094-5-43

Pais, T. F., Szego, E. M., Marques, O., Miller-Fleming, L., Antas, P., Guerreiro, P., et al. (2013). The NAD-dependent deacetylase sirtuin 2 is a suppressor of microglial activation and brain inflammation. *EMBO J.* 32, 2603–2616. doi: 10.1038/emboj.2013.200

Papouin, T., and Oliet, S. H. R. (2014). Organization, control and function of extrasynaptic NMDA receptors. *Philos. Trans. R. Soc. Lond. B Biol. Sci.* 369:20130601. doi: 10.1098/rstb.2013.0601

Parsons, C. G., Danysz, W., and Quack, G. (1998). Glutamate in CNS disorders as a target for drug development: an update. *Drug News Perspect.* 11, 523–569.

Parsons, C. G., Danysz, W., and Quack, G. (1999). Memantine is a clinically well tolerated N-methyl-D-aspartate (n.d.) receptor antagonist - a review of preclinical data. *Neuropharmacology* 38, 735–767. doi: 10.1016/s0028-3908(99)00019-2

Rizzo, F. R., Musella, A., De Vito, F., Fresegna, D., Bullitta, S., Vanni, V., et al. (2018). Tumor necrosis factor and interleukin-1 beta modulate synaptic plasticity during neuroinflammation. *Neural Plast.* 2018:8430123.

Rosi, S., Vazdarjanova, A., Ramirez-Amaya, V., Worley, P. F., Barnes, C. A., and Wenk, G. L. (2006). Memantine protects against LPS-induced neuroinflammation, restores behaviorally-induced gene expression and spatial learning in the rat. *Neuroscience* 142, 1303–1315. doi: 10.1016/j.neuroscience.2006.08.017

Ross, F. M., Allan, S. M., Rothwell, N. J., and Verkhratsky, A. (2003). A dual role for interleukin-1 in LTP in mouse hippocampal slices. *J. Neuroimmunol.* 144, 61–67. doi: 10.1016/j.jneuroim.2003.08.030

Rothgiesser, K. M., Erener, S., Waibel, S., Luscher, B., and Hottiger, M. O. (2019). SIRT2 regulates NF-kappa B-dependent gene expression through deacetylation of p65 Lys310. *J. Cell Sci.* 123(Pt 24), 4251–4258. doi: 10.1242/jcs.073783

Rothman, S. M., and Olney, J. W. (1995). Excitotoxicity and the NMDA receptor – still lethal after 8 years. *Trends Neurosci.* 18, 57–58. doi: 10.1016/0166-2236(95)93869-y

Salter, M. W. (1998). Src, N-methyl-D-aspartate (n.d.) receptors, and synaptic plasticity. *Biochem. Pharmacol.* 56, 789–798. doi: 10.1016/s0006-2952(98)00124-5

Streit, W. J., Mrak, R. E., and Griffin, W. S. T. (2004). Microglia and neuroinflammation: a pathological perspective. *J. Neuroinflamm.* 1:14.

Sun, Y. J., Feng, X., Ding, Y., Li, M. T., Yao, J., Wang, L., et al. (2019). Phased treatment strategies for cerebral ischemia based on glutamate receptors. *Front. Cell. Neurosci.* 13:168. doi: 10.3389/fncel.2019.00168

Vassilopoulos, A., Fritz, K. S., Petersen, D. R., and Gius, D. (2011). The human sirtuin family: evolutionary divergences and functions. *Hum. Genomics* 5, 485–496.

Viviani, B., Bartesaghi, S., Gardoni, F., Vezzani, A., Behrens, M. M., Bartfai, T., et al. (2003). Interleukin-1 beta enhances NMDA receptor-mediated intracellular calcium increase through activation of the Src family of kinases. *J. Neurosci.* 23, 8692–8700. doi: 10.1523/jneurosci.23-25-08692.2003

Viviani, B., Gardoni, F., Bartesaghi, S., Corsini, E., Facchi, A., Galli, C. L., et al. (2006). Interleukin-1 beta released by gp120 drives neural death through tyrosine phosphorylation and trafficking of NMDA receptors. *J. Biol. Chem.* 281, 30212–30222.

Wake, H., Moorhouse, A. J., Jinno, S., Kohsaka, S., and Nabekura, J. (2009). Resting microglia directly monitor the functional state of synapses in vivo and determine the fate of ischemic terminals. *J. Neurosci.* 29, 3974–3980.

Wang, G., Li, S. M., Gilbert, J., Gritton, H. J., Wang, Z. M., Li, Z., et al. (2017). Crucial roles for SIRT2 and AMPA receptor acetylation in synaptic plasticity and memory. *Cell Rep.* 20, 1335–1347.

Wang, W. Y., Tan, M. S., Yu, J. T., and Tan, L. (2015). Role of pro-inflammatory cytokines released from microglia in Alzheimer's disease. *Ann. Transl. Med.* 3:136.

Wenk, G. L. (2006). Neuropathologic changes in Alzheimer's disease: potential targets for treatment. *J. Clin. Psychiatry* 67, 3–7.

Westphal, C. H., Dipp, M. A., and Guarente, L. (2007). A therapeutic role for sirtuins in diseases of aging? *Trends Biochem. Sci.* 32, 555–560.

Wu, H. M., Tzeng, N. S., Qian, L., Wei, S. J., Hu, X. M., Chen, S.-H., et al. (2009). Novel neuroprotective mechanisms of memantine: increase in neurotrophic factor release from astroglia and anti-inflammation by preventing microglial activation. *Neuropsychopharmacology* 34, 2344–2357.

Xia, P., Chen, H. S. V., Zhang, D. X., and Lipton, S. A. (2010). Memantine preferentially blocks extrasynaptic over synaptic NMDA receptor currents in hippocampal autapses. *J. Neurosci.* 30, 11246–11250.

Yamamoto, H., Schoonjans, K., and Auwerx, J. (2007). Sirtuin functions in health and disease. *Mol. Endocrinol.* 21, 1745–1755.

Yang, S., Liu, Z. W., Wen, L., Qiao, H. F., Zhou, W. X., Zhang, Y. X. (2005). Interleukin-1β enhances NMDA receptor-mediated current but inhibits excitatory synaptic transmission. *Brain Res.* 1034, 172–179.

Yu, J. W., Wu, Y. Q., and Yang, P. X. (2016). High glucose-induced oxidative stress represses sirtuin deacetylase expression and increases histone acetylation leading to neural tube defects. *J. Neurochem.* 137, 371–383.

Yuan, F., Xu, Z. M., Lu, L. Y., Nie, H., Ding, J., Ying, W.-H., et al. (2016). SIRT2 inhibition exacerbates neuroinflammation and blood-brain barrier disruption in experimental traumatic brain injury by enhancing NF-kappaB p65 acetylation and activation. *J. Neurochem.* 136, 581–593.

Zhang, Y., and Chi, D. (2018). Overexpression of SIRT2 alleviates neuropathic pain and neuroinflammation through deacetylation of transcription factor nuclear factor-kappa B. *Inflammation* 41, 569–578.

Conflict of Interest: The authors declare that the research was conducted in the absence of any commercial or financial relationships that could be construed as a potential conflict of interest.

frontiers in Molecular Neuroscience

BRIEF RESEARCH REPORT
published: 06 July 2020
doi: 10.3389/fnmol.2020.00119

hiPSC-Based Model of Prenatal Exposure to Cannabinoids: Effect on Neuronal Differentiation

*Cláudia C. Miranda[1], Tiago Barata[1], Sandra H. Vaz[2], Carla Ferreira[3,4], Alexandre Quintas[3,4] and Evguenia P. Bekman[1,2,5]**

[1]*Department of Bioengineering and iBB—Institute for Bioengineering and Biosciences, Instituto Superior Técnico, Universidade de Lisbon, Lisbona, Portugal,* [2]*Instituto de Medicina Molecular, João Lobo Antunes, Faculdade de Medicina da Universidade de Lisboa, Lisbon, Portugal,* [3]*Molecular Pathology and Forensic Biochemistry Laboratory, CiiEM, Campus Universitário Quinta da Granja, Monte da Caparica, Caparica, Portugal,* [4]*Forensic and Psychological Sciences Laboratory Egas Moniz, Campus Universitário Quinta da Granja, Monte da Caparica, Caparica, Portugal,* [5]*The Discoveries Centre for Regenerative and Precision Medicine, Lisbon, Portugal*

Phytocannabinoids are psychotropic substances of cannabis with the ability to bind endocannabinoid (eCB) receptors that regulate synaptic activity in the central nervous system (CNS). Synthetic cannabinoids (SCs) are synthetic analogs of Δ^9-tetrahydrocannabinol (Δ^9-THC), the psychotropic compound of cannabis, acting as agonists of eCB receptor CB_1. SC is an easily available and popular alternative to cannabis, and their molecular structure is always changing, increasing the hazard for the general population. The popularity of cannabis and its derivatives may lead, and often does, to a child's exposure to cannabis both *in utero* and through breastfeeding by a drug-consuming mother. Prenatal exposure to cannabis has been associated with an altered rate of mental development and significant changes in nervous system functioning. However, the understanding of mechanisms of its action on developing the human CNS is still lacking. We investigated the effect of continuous exposure to cannabinoids on developing human neurons, mimicking the prenatal exposure by drug-consuming mother. Two human induced pluripotent stem cells (hiPSC) lines were induced to differentiate into neuronal cells and exposed for 37 days to cannabidiol (CBD), Δ^9-THC, and two SCs, THJ-018 and EG-018. Both Δ^9-THC and SC, at 10 μM, promote precocious neuronal and glial differentiation, while CBD at the same concentration is neurotoxic. Neurons exposed to Δ^9-THC and SC show abnormal functioning of voltage-gated calcium channels when stimulated by extracellular potassium. In sum, all studied substances have a profound impact on the developing neurons, highlighting the importance of thorough research on the impact of prenatal exposure to natural and SC.

Keywords: phytocannabinoids, synthetic cannabinoids, hiPSC, neuronal differentiation, Δ^9-THC, CBD, EG-018, THJ-018

OPEN ACCESS

Edited by:
Cláudia Guimas Almeida, New University of Lisbon, Portugal

Reviewed by:
Ismael Galve-Roperh, Complutense University of Madrid, Spain
Bruno Miguel Fonseca, University of Porto, Portugal

****Correspondence:***
Evguenia P. Bekman
evguenia.bekman@tecnico.ulisboa.pt

Received: *02 February 2020*
Accepted: *09 June 2020*
Published: *06 July 2020*

Citation:
Miranda CC, Barata T, Vaz SH, Ferreira C, Quintas A and Bekman EP (2020) hiPSC-Based Model of Prenatal Exposure to Cannabinoids: Effect on Neuronal Differentiation. Front. Mol. Neurosci. 13:119. doi: 10.3389/fnmol.2020.00119

INTRODUCTION

Phytocannabinoids, such as Δ^9-THC, are substances found in cannabis that can bind to the endocannabinoid (eCB) system receptors, which regulate a variety of physiological processes in the human body, such as synaptic activity in the central nervous system (CNS), and analgesic and metabolic effects in the peripheric nervous system, PNS (Pertwee, 2008; Wu et al., 2011; Metz and Stickrath, 2015). Cannabinoid receptors 1 (CB_1) and 2 (CB_2), are expressed in the developing brain and there is growing evidence supporting the role of these receptors in neural progenitor proliferation and modulation of neuronal maturation and specification (Galve-Roperh et al., 2013). The expression of these receptors in the fetal and adult human brain was also reported (reviewed in Galve-Roperh et al., 2009). Prenatal exposure to cannabinoids acting as agonists of CB_1 and CB_2 receptors can produce long-lasting effects on eCB signaling affecting motor activity, verbal development, nociception, drug-seeking behavior and other processes (reviewed in Broyd et al., 2016; Richardson et al., 2016; Grant et al., 2018). Due to their lipophilic nature, phytocannabinoids can easily permeate cellular membranes passing from drug-consuming mothers' bloodstream into foetal tissues (Grotenhermen, 2003). Prenatal exposure to cannabis has been associated with lower weight at birth and a higher risk of newborn morbidity (Hurd et al., 2005; Metz and Stickrath, 2015). In two extended cohort studies, altered rate of mental development and significant changes in nervous system functioning were consistently found (Fried, 2002; Smith et al., 2004; Gray et al., 2005). However, the cellular mechanisms underlying cannabinoid effects on human neural development are still poorly known. Thus, there is an urgent need for a better understanding of the impact of these substances on human brain development, especially due to the contemporary trend of increasing cannabis use.

Besides this trend, a new problem has emerged in the form of synthetic analogs of Δ^9-tetrahydrocannabinol (Δ^9-THC). Synthetic cannabinoids (SCs) are a group of Novel Psychoactive Substances with similar properties to Δ^9-THC that appeared on the drug market usually sold as herbal blends (United Nations Office on Drugs and Crime, The Challenge of New Psychoactive Substances; 2013). The SCs usually show a higher affinity to the CB_1 receptor and elicit a stronger and long-lasting effect on brain cells when compared to Δ^9-THC. Also, many of these substances are easily available on the internet and thus escape the control of authorities. SCs use is associated with more severe side effects and intoxications, with both neurologic symptoms and acute organ toxicity observed (Schoeder et al., 2018). Two SCs used in this study are derivatives of JWH-018, the first indole-based potent CB_1, and CB_2 receptor agonist (Atwood et al., 2010) with a toxicity profile diverging from that of Phyto-CBs (Grant et al., 2018). THJ-018 is a 2nd generation SC, with CB_1 binding affinity of 5.84 nM and a CB_2 binding affinity of 4.57 nM (Hess et al., 2016). EG-018 is a 3rd generation SC, which replaced THJ-018, with an affinity to CB_1 of 7.17 nM and CB_2 of 2.22 nM (Schoeder et al., 2018). This study aims to address the impact of SCs with higher affinity than Δ^9-THC for CB_1 and/or CB_2 on developing human brain cells using neural differentiation of human-induced pluripotent stem cells (hiPSCs). The effect of the non-psychotropic component of cannabis, CBD, that binds the CB_2 receptor and was shown to act as a negative allosteric modulator of CB_1 (Laprairie et al., 2015) was also evaluated. Controlled aggregation of hiPSCs in neural-inducing medium allows recapitulating the initial steps of the self-organizing neural tube and subsequent progenitor proliferation and production of neurons of forebrain identity (Shi et al., 2012; Miranda et al., 2015). This system represents a simple and reproducible *in vitro* model that allows assessing the effect of continuous exposure to cannabinoid on the development of human brain cells at molecular, cellular, and functional levels. Two hiPSC lines were induced into neural differentiation and treated with CBD, Δ^9-THC and two synthetic Δ^9-THC analogues, THJ-018 and EG-18. Our results indicate that all four substances have profound impact on the differentiation, maturation and functioning of developing CNS neurons, providing a new evidence for the importance of thorough research of the impact of prenatal exposure to cannabis and its synthetic analogues.

MATERIALS AND METHODS

Maintenance of Human iPSCs

Human-induced pluripotent stem cells (hiPSCs), Gibco® Human Episomal iPSC line derived from $CD34^+$ cord blood (iPSC6.2, Burridge et al., 2011) and F002.1A.13 (TCLab—Tecnologias Celulares para Aplicação Médica, Unipessoal, Lda.) were routinely cultured on Matrigel™ (1:100, Corning)-coated plates using mTeSR™1 medium (StemCell Technologies). Cells were passaged 1:5 using EDTA every 5 days (Beers et al., 2012).

Neural Commitment and Differentiation

hiPSCs were induced towards neural commitment as 3D aggregates using a modified dual SMAD inhibition protocol (Miranda et al., 2015) and allowed to achieve functional differentiation using the recently described BrainPhys medium (Bardy et al., 2015). Briefly, cells were incubated with 10 μM ROCK inhibitor (ROCKi, Y-27632, StemGent) for 1 h at 37°C and then treated with accutase for 5 min at 37°C. Cells were seeded in microwell plates (AggreWell™, StemCell Technologies) at a density of 1.0×10^6 cells/ml to generate aggregates averaging a diameter of 150 μm using mTeSR™1 supplemented with 10 μM ROCKi for 24 h. After 24 h of culture inside microwells, mTeSR1 medium was replaced by 1:1 N2 and B27 medium, as previously described (Shi et al., 2012). The medium was replaced daily and supplemented with 10 μM SB431542 (SB, Sigma) and 100 nM LDN193189 (LDN, StemGent) for 9 days, followed by a 3-day period without SB431542 and LDN19318.

On day 12 aggregates were recovered from the microwells, gently dissociated with EDTA, and plated onto poly-L-ornithine (15 μg/ml, Sigma) and Laminin (20 μg/ml, Sigma)-coated plates at a density of 200,000 cells/cm^2 in N2B27 medium. Twenty-four hours after replating, the medium was replaced by N2B27 supplemented with 20 ng/ml bFGF from day 13 to day

15 of differentiation. From day 15 onwards, the medium was changed every other day without bFGF supplementation.

Exposure to Cannabinoids and Neuronal Maturation

On day 19 of the differentiation protocol, cells were gently detached from the plates and re-plated with 1:3 splitting in the same conditions, for neuronal differentiation and drug treatment. From day 19 to day 30 of differentiation CBD, Δ^9-THC and two different SCs, EG-018 and THJ-018 were added to the medium at every medium change at a concentration of 10 μM in ethanol, except CBD, which was added at a 1–10 μM concentration. Untreated and vehicle (0.01% ethanol)-treated cultures were used as a control. At day 30 gentle replating was performed once again and the cultures were allowed to mature in complete BrainPhys™ Neuronal Medium (StemCell Technologies)—supplemented with NeuroCult™ SM1 Neuronal Supplement (StemCell Technologies), N2 Supplement-A (StemCell Technologies), Recombinant Human Brain-Derived Neurotrophic Factor (BDNF, PeproTech, 20 ng/ml), Recombinant Human Glial-Derived Neurotrophic Factor (GDNF, PeproTech, 20 ng/ml), dibutyryl cAMP (1 mM, Sigma), and ascorbic acid (200 nM, Sigma). One-third of the medium volume was changed every 3 days.

Immunostaining

Cells were fixed with 4% (v/v) paraformaldehyde (PFA; Sigma) and stained according to a previously described protocol (Miranda et al., 2015). MAP2 (Sigma, 1:500), glial fibrillary acidic protein (GFAP, Abcam, 1:200), Synaptophysin (SYN; Abcam, 1:200), ZO-1 (Novex, 1:100), SOX2 (R&D, 1:200), PAX6 (Covance, 1:400), NESTIN (R&D, 1:400), Ki-67 (Abcam, 1:100), HuC/D (Thermo Fischer Scientific, 1:100), activated CASPASE3 (pCASP3, Cell Signaling, 1:400), were used as primary antibodies whereas goat anti-mouse IgG Alexa Fluor–488 or 546 (1:500, Invitrogen), goat anti-rabbit IgG Alexa Fluor–488 or 546 (1:500, Invitrogen) were used as secondary antibodies. Fluorescence images were acquired with Zeiss LSM 710 Confocal Laser Point-Scanning Microscope using 20× and 63× objectives and integrated density were calculated for each channel using ImageJ software. The ratio between integrated density for the marker of interest and nuclear counterstaining with DAPI was calculated for each image. For each staining, the same acquisition settings were applied for all images.

Real-Time (RT)-PCR

For quantitative analysis, total RNA was extracted at different time-points of differentiation and treatments using the High Pure RNA Isolation Kit (Roche), according to the manufacturer's instructions. Total RNA was converted into complementary cDNA with Transcriptor High Fidelity cDNA Synthesis Kit (Roche) using 500 ng of RNA. Relative gene expression was evaluated using 10 ng of cDNA and 250 μM of each primer.

Expression levels were analyzed using SYBR® green chemistry, with primers for *GAPDH, PAX6, MAP2, NESTIN, GFAP, GAD67*, and *VGLUT1* from Silva et al. (2020). Primers for *CNR1* and *CNR2* were from Stanslowsky et al. (2017).

All PCR reactions were done in triplicate, using the ViiA™ 7 RT-PCR Systems (Applied BioSystems). Fold change was calculated using the $2^{-\Delta Ct}$ method, using GAPDH as the reference gene. Log2 normalized expression values of the average fold-change were used for ClustVis analysis of pluripotency and neural genes (Metsalu and Vilo, 2015).

Single-Cell Calcium Imaging

To analyze the intracellular variations of Ca^{2+} by single-cell calcium imaging (SCCI), cells were re-plated on Glass Bottom Cell Culture Dish (Nest) previously coated with poly-L-ornithine (15 μg/ml, Sigma) and Laminin (20 μg/ml, Sigma). Calcium indicator Fura-2, a fluorescent dye that switches its excitation peak from 340 to 380 nm when bound to calcium, allows the concentration of intracellular calcium to be determined based on the ratio of fluorescence emission after sequential excitation at 340 and 380 nm (Grienberger and Konnerth, 2012). Cells were preloaded with 5 μM Fura-2 AM (Invitrogen) in Krebs solution (132 mM NaCl, 4 mM KCl, 1.4 mM $MgCl_2$, 2.5 mM $CaCl_2$, 6 mM glucose, 10 mM HEPES, pH 7.4) for 45 min at 37°C in an incubator with 5% CO_2 and 95% atmospheric air. Dishes were washed in Krebs solution and then mounted on an inverted microscope with epifluorescence optics (Axiovert 135TV, Zeiss). Cells were continuously perfused with Krebs solution and stimulated by applying high-potassium Krebs solution (containing 10–100 mM KCl, isosmotic substitution with NaCl), or 100 μM histamine. Ratio images were obtained from image pairs acquired every 200 ms by exciting the cells at 340 nm and 380 nm. Excitation wavelengths were changed through a high-speed switcher (Lambda DG4, Sutter Instrument, Novato, CA, United States). The emission fluorescence was recorded at 510 nm by a cooled CDD camera (Photometrics CoolSNAP fx). Images were processed and analyzed using the software MetaFluor (Universal Imaging, West Chester, PA, USA). Regions of interest were defined manually.

Heatmaps

For hierarchical clustering, ClustVis analysis software[1] was used with the rows clustered using correlation distance and average linkage (Metsalu and Vilo, 2015).

Statistical Analysis

Statistical analysis was done in Graphpad. Error bars represent the standard error of the mean (SEM). When appropriate, statistical analysis was done using a two-tailed *t*-student test for independent samples, and a *p*-value of less than 0.05 was considered statistically significant.

RESULTS

Efficient Neural Commitment of hiPSCs and Exposure to Cannabinoids

Neural differentiation of hiPSCs was achieved by controlled aggregation in serum-free medium N2B27 in the presence of SB431542, an inhibitor of TGFβ signaling, and LDN193189, an

[1] http://biit.cs.ut.ee/clustvis

inhibitor of BMP signaling, both necessary for the acquisition of neuroepithelial identity (Chambers et al., 2009). Aggregates were cultured in non-adherent conditions until day 12 and then re-plated on laminin-coated plates to allow for the proliferation of neuroepithelial progenitors, further supported by the addition of bFGF between days 13 and 15, as depicted on the scheme of the experiment (**Supplementary Figure S1**). More than 1,000-fold increase in the expression of neural progenitor gene *PAX6* was consistently registered from day 12 on (**Figure 1B**). On day 16, an efficient neural commitment was evidenced by the presence of numerous neural rosettes (**Figure 1Ci**), typical morphology of neural precursors growing in 2D conditions (Abranches et al., 2009). By day 19 these cultures reached confluency and were gently replated, without dissociation of individual rosettes. Further neuronal differentiation led to the expression of neuronal-specific gene MAP2 from day 19 on (**Figure 1B**) and to the appearance of glutamatergic VGLUT1 and GABAergic GAD67 markers on day 56 (**Supplementary Figures S2A,B**). On day 30 cultures contained numerous $SOX2^+/PAX6^+$ neural rosettes (**Figures 1Cii,iii**). that were still present at day 56 surrounded by $MAP2^+$ neurons and very rare occasional $GFAP^+$ glial cells (**Figures 1Civ–vii**).

After replating on day 19, and to mimic continuous prenatal exposure of developing CNS cells to cannabinoids, solutions of CBD, Δ^9-THC, EG-018, and THJ-018 in EtOH were added to culture media at every medium change, to a final concentration of 10 μM, except CBD, which was added to a final concentration of 1 and 10 μM. The culture medium containing these substances was changed every other day between days 19 and 30. Cannabinoids were added to the cultures at every medium change until day 56, and at this point, all cultures were processed for analyses. EtOH-treated cultures (0.01%, vehicle control, **Figures 1Ciii,v,vii**, **1Dii,viii**) showed some increase in neuronal marker MAP2 staining as compared with the untreated cells (**Figures 1Cii,iv,vi,Di,vii**) although this increase, also detected by qRT-PCR, was not significant and was not accompanied by changes in progenitor parker PAX6 (**Figure 1B**).

Neurotoxicity of CBD at 10 μM Concentration

In two independent experiments, the addition of CBD at 10 μM concentration showed massive cell death upon second medium change, between days 21–22 in culture. In all further experiments, 1 μM of CBD was used. At this concentration, CBD-treated cultures did not differ from the controls by cell morphology and the presence of neural progenitor and neuronal markers (**Figure 1D**) although the density of CBD-treated cultures was systematically lower than in other conditions indicating a possible negative effect on proliferation and/or survival of neuronal progenitors and differentiated neurons.

Exposure to Δ^9-THC and SCs Promotes Neuronal Differentiation

By day 30 all six conditions showed expression of progenitor parker PAX6 and neuron-specific microtubule-associated protein 2 (MAP2; **Figure 1D**). Δ^9-THC, EG-018, and THJ-018 -treated cultures showed decreased staining for the PAX6 neural rosette marker that was not reflected at the transcriptional level (**Supplementary Figure S2C**) suggesting a possible decrease of progenitor pool and exit for differentiation. However, transcript levels for neuron-specific gene *MAP2* showed a significant increase by day 30 only in THJ-018 condition (**Supplementary Figure S2D**) and immunostaining for this marker even decreased in EG-018-treated cultures (**Supplementary Figure S3**). To quantify better this effect, we performed immunostaining for HuC/D protein marker that is expressed earlier in differentiating CNS neurons (**Figure 2A**; Okano and Darnell, 1997; Abranches et al., 2009) and counted the percentage of cells expressing this antigen. Our data show that the decrease in the PAX6 staining (**Figure 2Ci**) is accompanied by the trend for an increased percentage of HuC/D^+ cells upon exposure to all cannabinoids, with statistical significance in the case of THJ-018 (p-value < 0.0275; **Figure 2Cii**). In parallel, all CB-treated cultures exhibited elevated levels of apoptosis marker cleaved CASPASE3 (**Figure 2Ciii**), while there were no significant differences in the number of Ki-67^+ proliferative cells (data not shown). Together, these results indicate that both Δ^9-THC and two SCs lead to premature differentiation of rosette progenitors that seems to be more pronounced in the case of THJ-018, possibly due to lower neuronal survival upon exposure to Δ^9-THC and EG-018. One of the reasons for lower neuronal survival could be a functional impairment or inability to achieve functional maturation.

Exposure to Cannabinoids Leads to the Formation of Functionally Impaired Neurons

After detecting an increase in the number of differentiating neurons upon continuous exposure to cannabinoids we next questioned if these neurons were able to achieve functional maturation. For this goal, all cultures were maintained in BrainPhys™ neuronal maturation medium for 16 days, with 1/3 medium volume change three times per week and continuous exposure to cannabinoids. Immunofluorescent staining for mature synaptic protein SYN of Δ^9-THC and EG-018-treated day 56 cultures revealed decreased staining intensity (**Figures 2B,Di**) suggesting a lower density of mature synaptic puncta. Additionally, an increase in glial acidic fibrillary protein (GFAP) staining was visible in both conditions (**Figure 2E**), indicating premature glial differentiation, which is detectable in untreated cultures only around day 80 (not shown) and was found to be increased in Δ^9-THC and SCs-exposed cultures (**Figure 2Dii**). To further evaluate both the neuron-glia ratio and the functionality of these cultures we performed SCCI. Control and CB-treated cultured cells were sequentially stimulated by exposure to KCl and histamine. Differentiated functional neurons are expected to open voltage-sensitive calcium channels in response to KCl, resulting in a massive influx of calcium to the cytoplasm (Ambrósio et al., 2000; Macías et al., 2001). Immature neurons, neural progenitors and glial cells express functional histamine receptors, which stimulation also increases intracellular calcium concentration. Indeed, histamine/KCl

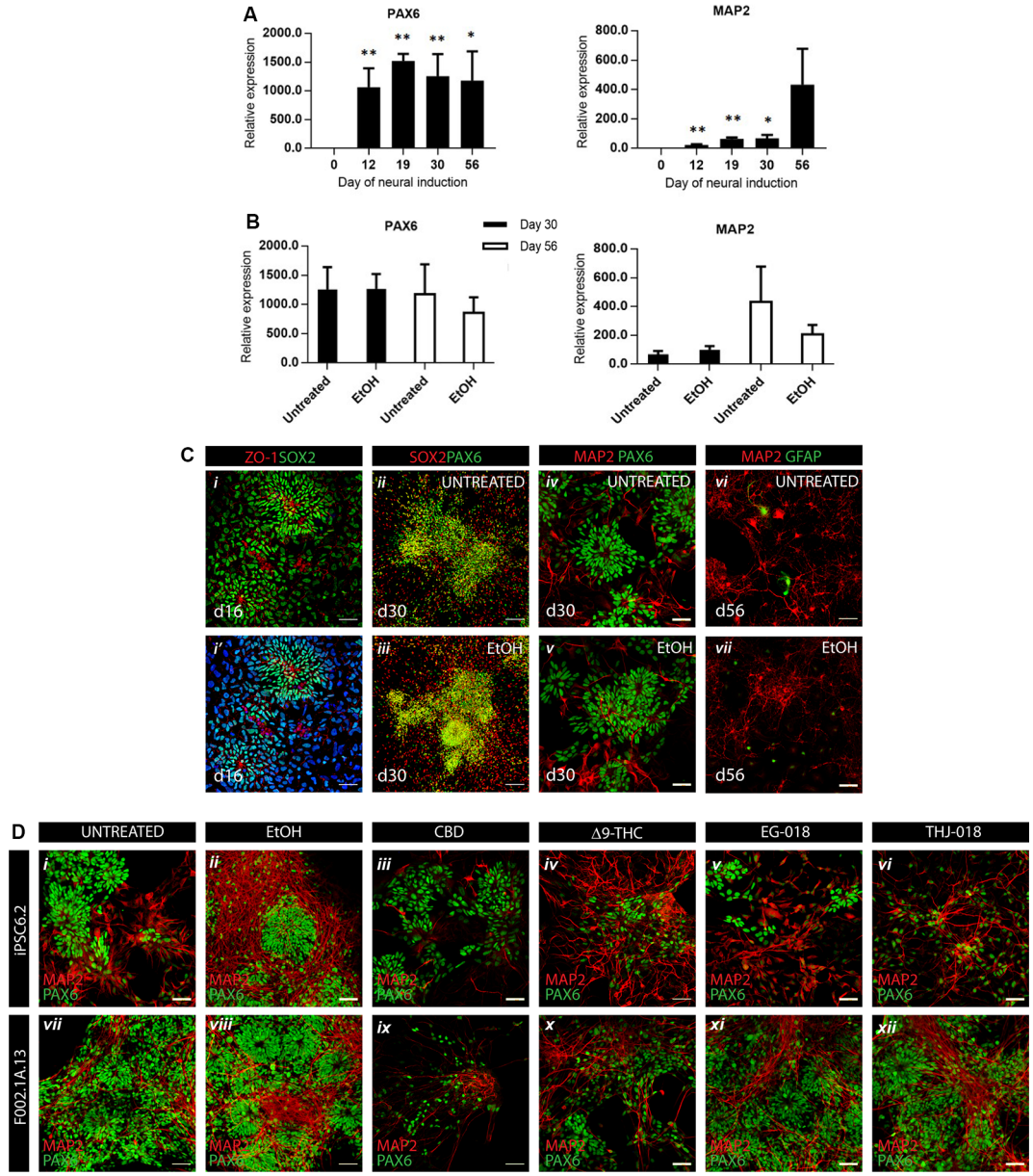

FIGURE 1 | Efficient neural differentiation of hiPSCs and the effect of cannabinoid exposure. **(A)** qRT-PCR analysis of neural progenitor (*PAX6*) and neuronal (*MAP2*) mRNA expression levels relative to *GAPDH* at indicated timepoints. Data were analyzed by unpaired *t*-test, $*p < 0.05$, $**p < 0.01$; error bars represent standard error of the mean (SEM). **(B)** qRT-PCR analysis of *PAX6* and *MAP2* mRNA levels in untreated vs. vehicle-treated (0.01% EtOH) cultures showing no significant differences by unpaired *t*-test. Data in panels **(A,B)** were obtained from four independent experiments using iPSC6.2 cells. **(C)** Immunofluorescence for neural progenitor, neural and glial markers at different timepoints showing efficient neural commitment and differentiation of hiPSCs. Scale bars in panels **(i,i')**, 100 μm. Scale bars in panels **(ii–vii)**, 50 μm. **(D)** Immunofluorescence at day 30 for neural progenitor marker PAX6 and neuron-specific microtubule-associated protein MAP2 in untreated (i, vii), vehicle-treated (ii, viii), and exposed to cannabinoids from day 19 to day 30 cultures (iii–vi, ix–xii), in two different iPSC lines, iPCS6.2 (male donor) and F002.1A.13 (female donor). Scale bars: 50 μm.

ratios can be used to evaluate the proportion of mature/immature neurons in these cultures (Agasse et al., 2008; Rodrigues et al., 2017).

Upon KCl stimulation, a sharp increase in cytosolic calcium concentration was observed in both controls and CBD-treated cultures (**Figures 3A,D**), with an average fold change of fluorescence intensity around two in all three conditions (**Figure 3B**, **Supplementary Figure S2I**). In contrast, very few cells responded to histamine in these cultures, and the few responding cells exhibited fold change below 1.5 (**Figure 3B**, **Supplementary Figures S2J,K**), indicating that most of the cells in these cultures are excitable neurons, with a small proportion

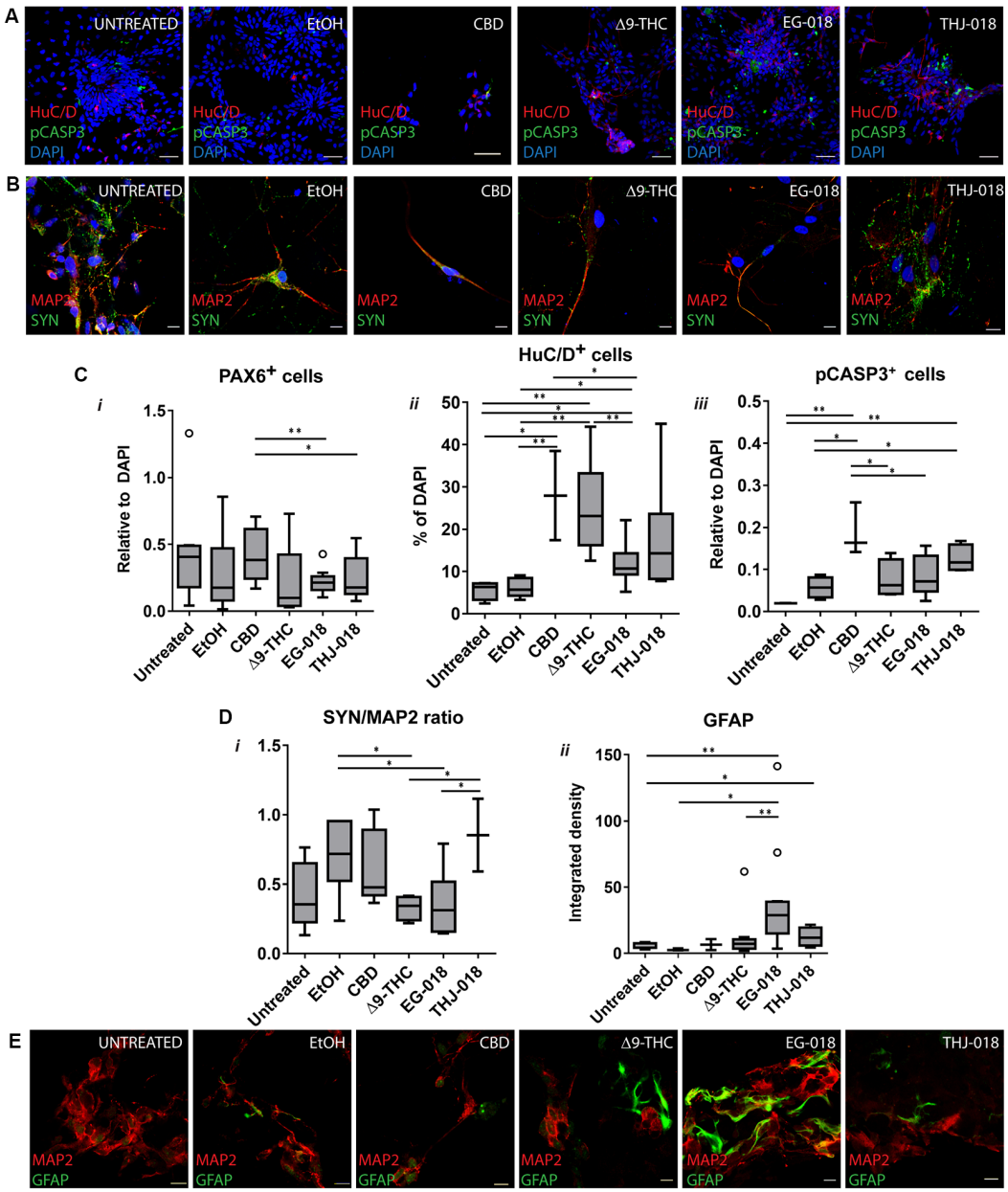

FIGURE 2 | Effect of cannabinoid exposure on day 30 and 56 of neural differentiation. **(A)** Immunofluorescence for newborn neuronal marker HuC/D and apoptosis marker pCASPASE3 (pCASP3) at day 30 showing an increase in HuC/D staining and apoptotic cells in s cannabinoid-treated cultures. Scale bars: 15 μm. **(B)** Immunofluorescence for neuronal (MAP2) and synaptic protein synaptophysin (SYN) in cultures continuously exposed to cannabinoids from day 19 to day 56. Scale bars: 15 μm. **(C)** Quantification of PAX6$^+$ **(i)**, HuC/D$^+$ **(ii)** and pCASP3$^+$ **(iii)** cells at day 30, relative to DAPI. Results for three independent experiments. **(D)** Quantification of the ratio of fluorescence intensity of SYN and MAP2 in day 56 cultures **(i)**, and of integrated fluorescence density for GFAP **(ii)**. Data from three independent experiments, 3–10 images per condition. Data in **(C)** and **(D)** analyzed by unpaired *t*-test; $^*p < 0.05$, $^{**}p < 0.01$; error bars represent SEM. Tukey's range test was applied to determine outlier data points (open circles). **(E)** Immunofluorescence for glial (GFAP) marker and MAP2 in cultures continuously exposed to cannabinoids from day 19 to day 56. Scale bars: 15 μm.

of neural progenitors/glia. These results agree with very rare occasional GFAP staining detected in both control cultures at this stage, contrasting with numerous GFAP$^+$ cells in Δ^9-THC and SC-treated cultures.

Exposure to CBD has a small but statistically significant effect on the functionality of differentiating neuronal cells, with a lower amplitude of response to KCl stimulation compared with the controls (**Figure 3A**, **Supplementary Figure S2I**). In sheer contrast to this, the exposure to both Δ^9-THC and SCs severely impaired the ability to differentiate neurons to respond to both KCl and histamine stimulation (**Figures 3A,B**). Δ^9-THC-treated cells showed delayed (85 s vs. 28–35 s in control

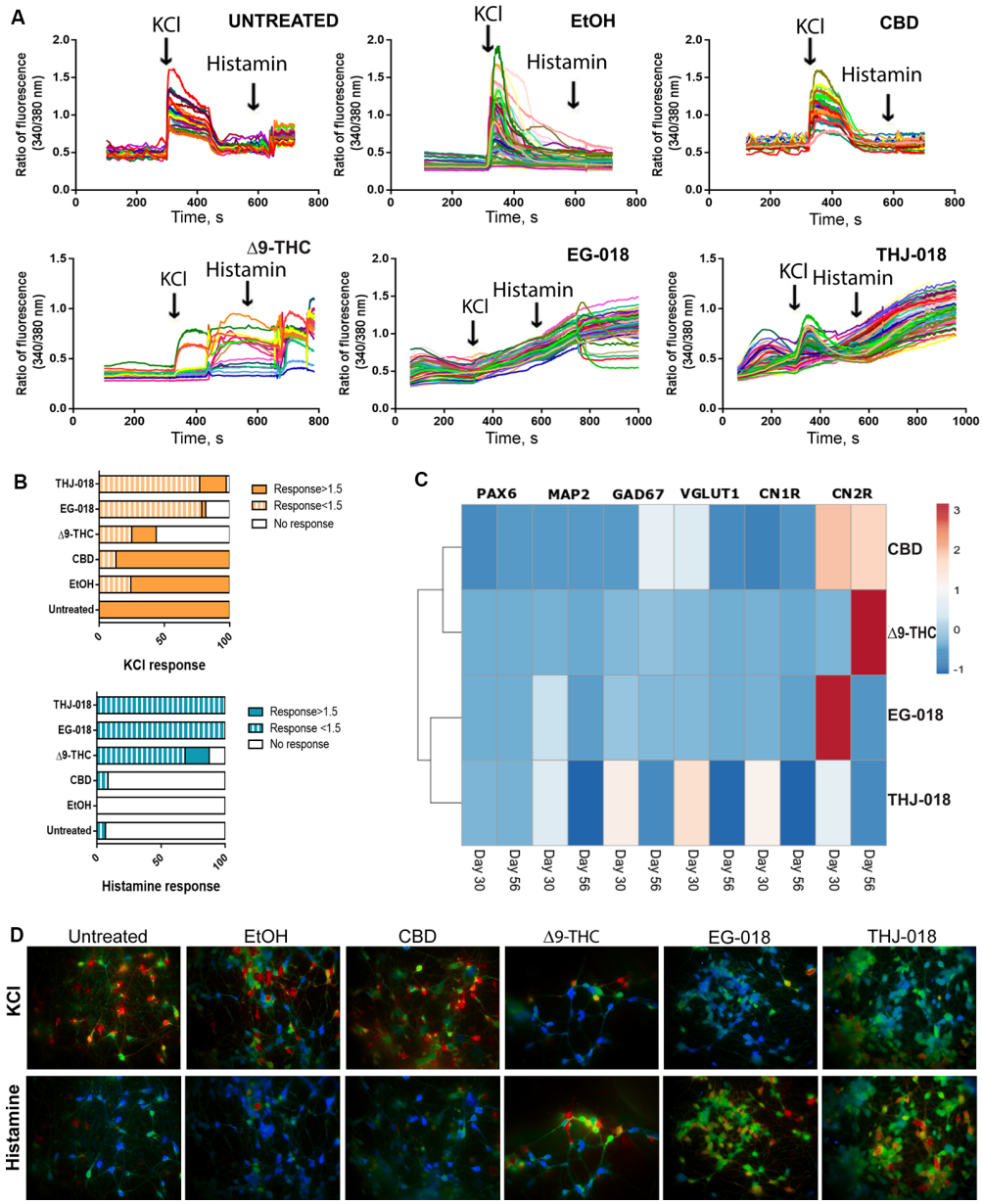

FIGURE 3 | Functional assessment of cannabinoid-treated cultures on day 56. **(A)** Single-cell calcium imaging (SCCI) analysis of day 56 cultures showing abnormal response to KCl and histamine stimuli by Δ^9-THC, EG-018, and THJ-018-treated neuronal cells. **(B)** Summary of SCCI analyses presented as percentage of responding and non-responding cells for KCl and histamine stimulation. The timepoint of response corresponds to the peak seen in the graph in panel **(A)**, and the ratio of fluorescence value for this timepoint over baseline level >1 was considered as a response. For EG-018 and THJ-018 conditions, the last time point before washing was used to calculate the response to histamine stimulation. **(C)** Hierarchical clustering illustrates relative expression levels of different genes at day 30 and 56 of neural differentiation. *PAX6, MAP2, GAD67, VGLUT1, CNR1*, and *CNR2* were analyzed by qRT-PCR. Rows are centered; unit variance scaling is applied to rows. Rows are clustered using correlation distance and average linkage. Corresponding qRT-PCR data are presented in **Supplementary Figure S2**. **(D)** Single-cell calcium imaging. Representative ratio images for different culture conditions on day 56. Images were taken immediately after cells received the indicated stimulus (KCl or histamine).

conditions) response to KCl, with 56.3% of non-responding cells contrasting with the absence of non-responding cells in both controls (**Supplementary Figure S2K**). As the majority of KCl-responding cells either responded too late or were unable to return to baseline intracellular calcium levels upon KCl stimulation, it is impossible to determine the exact proportion of cells that responded to histamine. Therefore, the higher proportion of histamine-responding cells (87.5% vs. 6.9% in untreated control and 0% in EtOH-treated cultures, **Supplementary Figure S2K**) most probably corresponds to

a mixture of functionally impaired neuronal cells showing abnormal response to KCl stimulation with some glia-like $GFAP^+$ cells that are also more abundant in this condition.

In comparison to Δ^9-THC, THJ-018 has a slightly less severe effect on the functionality of neuronal cells, with less pronounced delay in response to KCl, 51 s vs. 28–35 s in control conditions. The percentage of KCl-responding cells is similar to the controls, 97.2%, however, the majority of responses, 76.9%, are below 1.5x fold increase (**Supplementary Figure S2**). Moreover, only 8.7% of cells exhibit a well-defined peak of response to KCl while 88.5% of cells show continuously increasing Ca^{2+} levels, being unable to return to baseline levels after washout of KCl-containing medium. The percentage of histamine-responding cells in this condition is even higher than that of Δ^9-THC, reaching 100% of all assayed cells (**Figure 3A**, **Supplementary Figure S2K**), however, it is not supported by the increase in $GFAP^+$ cells and includes almost all cells that already responded to KCl. Therefore, this response to histamine most probably represents that of functionally impaired neurons with very slow kinetics of KCl response, rather than that of neural progenitors or immature neurons expressing both voltage-gated calcium channels and histamine receptors (in the latter case, the well-defined peak of histamine response should also be present).

EG-018-treated cells represent the most severely affected condition (**Figures 3A,B**), with no discernible peak of KCl response and the highest percentage of cells with weak (<1.5x) or no response to KCl (78.8% and 18.2%, respectively, **Supplementary Figure S2K**). Like the THJ-018-treated cells, 100% of EG-018-treated cells seemingly responded to histamine, however, instead of a well-defined peak of the response, a continuous increase in intracellular Ca^{2+} was also observed in this case (**Figure 3A**). These data might indicate that exposure to EG-018 leads to an even greater delay in the cellular response to KCl stimulation. This conclusion is further supported by the absence of a well-defined peak of histamine response despite the abundance of $GFAP^+$ cells in this condition (**Figures 2Dii,E**).

RT-PCR Analysis of the Expression of Cannabinoid Receptors 1 and 2 and Neural Markers

qRT-PCR expression data for all four cannabinoids were normalized to EtOH condition (**Supplementary Figures S2C–H**) and analyzed by hierarchical clustering (**Figure 3C**). The most pronounced fold changes of expression levels were detected for the genes encoding cannabinoid receptors 1 and 2, *CNR1*, and *2*. Exposure to CBD, Δ^9-THC, EG-018, and a less extent, THJ-018 led to a significant increase in the expression levels of *CNR2* (**Figure 3C**). Interestingly, levels of *CNR1* were slightly increased after exposure to Δ^9-THC and two SCs by day 30 and decreased by day 56 (**Figure 3C**, **Supplementary Figure S2G**) probably reflecting the long-term downregulation of CB_1 levels, similarly to what was reported to occur at both protein and mRNA level in a response to chronic exposure to Δ^9-THC (Oviedo et al., 1993; Romero et al., 1997; Villares, 2007). However, both SCs and THJ-018 in particular were able to elicit a stronger effect than Δ^9-THC.

Curiously, THJ-018 and CBD, which were found to cause less functional impairment on neuronal cells according to SCCI data, led to more pronounced changes in gene expression levels in both neural markers and CB receptor genes. Thus, the effect of exposure to these two substances requires further examination by different techniques than those used in this study, to uncover the nature of the cellular response to these substances.

DISCUSSION

The recreational use of cannabis is being legalized in an increasing roll of countries and as many as 57% of adults in the USA favor this tendency (Harris and Okorie, 2017). Not surprisingly, the rates of cannabis use show a consistent increase over past years, inclusively in pregnant and non-pregnant women (Brown et al., 2017; Harris and Okorie, 2017). Alarmingly, in a recent study, 19% of 18–24-year aged pregnant women screened positive for marihuana, showing a trend to increase in the last decade (Young-Wolff et al., 2017). The outcome of prenatal exposure to cannabinoids on human neurodevelopment can be evaluated only retrogradely, after several years or even decades, through the assessment of cognitive, motor, and behavioral scores. A plethora of other intervening factors introduces huge variations of the outcome, making it difficult to conclude which are the direct consequences of prenatal exposure to cannabis (reviewed in Wu et al., 2011; Scheyer et al., 2019). In this work, we propose a simplified system that reproduces the initial steps of neural differentiation from human pluripotent cells, where we expose neural cells to cannabinoids in a continuous way, mimicking the regular, three-times per week usage. The concentration of 10 μM used for Δ^9-THC, THJ-018, and EG-018, corresponds to 314, 342, and 391 ng/ml, respectively. As an example, smoking a joint with 3, 55% of Δ^9-THC leads to a plasma peak concentration of 150 ng/ml after 10 min (Huestis, 2007). However, the Δ^9-THC concentration of current marijuana can reach 20% which can lead to a plasma peak concentration of Δ^9-THC higher than 800 ng/ml. Thus, the concentration of Δ^9-THC used in this work is similar to smoking a joint with 7% of Δ^9-THC, corresponding to the CB_1 saturation level of 70–80%. In our system, the addition of 10 μM CBD was neurotoxic, while 1 μM concentration consistently yielded low culture densities possibly also due to neurotoxicity. However, exposure to 1 μM CBD led to an increase in GABAergic and decrease in glutamatergic markers expression levels (**Figure 3C**, **Supplementary Figures S2E,F**) hinting at a possible disbalance between the number of excitatory and inhibitory neurons that needs to be further investigated. CBD concentrations between 1 μM and 14 μM were found not to be cytotoxic to HUVEC cells (Solinas et al., 2012), while 10 μM CBD showed no toxicity for human breast carcinoma (Namdar et al., 2019). The same concentration of CBD was neurotoxic in our model. The neurotoxicity of CBD is of particular concern given that CBD content can reach 25% in several legally available cannabis preparations with reported blood concentration reaching 82.6 ng/ml (0.263 μM) after

chronic use (Meier et al., 2018), which is a just a small fraction of the total CBD concentration in the body of these users. The ratio between the concentration of a lipophilic drug in the fat tissue and plasma at a steady-state can reach a value of 3–4 digits undermining the measured drug concentration found by blood analysis. Δ^9-THC is a partial agonist of CB_1 and many of its effects on CNS were shown to be mediated by CB_1 (Pertwee, 2008). CB_1 antagonist SR1411716 was shown to increase neuronal differentiation (Rueda et al., 2002), while CB_1 KO decreased progenitor proliferation (Aguado et al., 2005). In our study, chronic exposure to Δ^9-THC promoted neuronal (**Figures 1D**, **2C**, **Supplementary Figure S2**) and glial (**Figures 2Dii,E**) differentiation, resembling the effect of CB_1 antagonist. However, the mRNA levels of *CNR1* decreased only slightly in this condition (**Supplementary Figure S2G**), while those of *CNR2* increased (**Supplementary Figure S2H**). The interplay of CB_1 and CB_2 was implicated in the modulation of postnatal neurogenesis in rodents (Rodrigues et al., 2017). In our study, exposure to Δ^9-THC and SCs differentially impacted the expression levels of *CNR1* and *CNR2* also supporting the view that both receptors might be involved in the neurogenesis. In a recent study, RNA transcriptomic analyses of hiPSC-derived neurons exposed both acutely and chronically (for 7 days) to 1 μM Δ^9-THC revealed significant changes in genes associated with intellectual disability, autism and psychiatric disorders (Guennewig et al., 2018). Interestingly, they showed that chronic Δ^9-THC exposure resulted in the downregulation of several histone-binding genes including *MECP2*, Rett syndrome causing genes. The lack of this gene results in precocious neuronal and glial differentiation in a forebrain organoid model of the disease, similarly to our results of chronic exposure to Δ^9-THC. A different study employed continuous exposure to eCB AEA and Δ^9-THC in dopaminergic neuronal differentiation from hiPSCs (Stanslowsky et al., 2017). These authors show that 10 μM concentrations of both cannabinoids impaired neuronal function by reducing voltage-gated sodium and potassium currents, action potential amplitudes and spontaneous synaptic activity. Our data further support functional impairment induced by exposure to Δ^9-THC, EG-018 and THJ-018, by demonstrating the inability of CB-treated neurons to increase their intracellular Ca^{2+} levels in response to KCl stimulus. SCs used in this study are Novel Psychoactive substances with properties similar to Δ^9-THC exhibiting considerably higher binding affinities to CB receptors (Hess et al., 2016; Schoeder et al., 2018). THJ-018 is 2nd generation SC behaving as a slightly better than Δ^9-THC partial agonist of both CB_1 and CB_2 in cAMP accumulation essay (Hess et al., 2016). In contrast, EG-018 was shown to activate CB_1 more than full agonist CP55, 940, having much less activity on CB_2 (Schoeder et al., 2018). This differential receptor activation capacity of the two SCs might explain some of the differences observed in this study. Generally stronger effect of EG-018 exposure might be due to its higher capacity to activate CB_1. However, experiments using selective receptor agonists and antagonists should be conducted to unveil the mechanisms of EG-018 action.

The observed functional impairment induced by chronic exposure to Δ^9-THC, EG-018, and THJ-018 during neuronal differentiation and formation of functional neuronal circuitry might help to explain the observed link between prenatal exposure to cannabis and psychiatric disorders. Δ^9-THC-treated neurons displayed synaptic and glutamate signaling alterations resembling those observed in schizophrenia patient iPSC-derived neurons (Guennewig et al., 2018). Another interesting avenue to explore in future studies is the observed difference in CB-induced phenotype severity between two iPSC lines, with male cell line iPSC6.2 being more affected by Δ^9-THC and SCs than the female F002.1A.13 (**Figure 1D**). Sex-dependent susceptibility to Δ^9-THC has been reported before and in a recent study using a mouse model of prenatal exposure male offspring was particularly affected showing pronounced hippocampal interneuronopathy (de Salas-Quiroga et al., 2020).

In conclusion, our data show that continuous exposure to both Δ^9-THC and SCs can induce functional impairment to newborn neurons during the formation of the human CNS, which is able to produce a deep and lasting impact on the overall brain structure and functioning. By showing this impairment, our data contribute to support the observations of long-lasting alterations in neural activity in adolescents subjected to prenatal marihuana exposure (Smith et al., 2004; Wu et al., 2011; Grant et al., 2018).

DATA AVAILABILITY STATEMENT

All datasets generated for this study are included in the article/**Supplementary Materials**.

AUTHOR CONTRIBUTIONS

EB and AQ outlined the general framework of this study. CM, EB, AQ, and CF designed the experiments. CM, EB, SV, and TB performed the experiments. CF and AQ provided the unique reagents. CM and EB analyzed the data. EB and CM wrote the manuscript.

FUNDING

This work was supported by the Fundação para a Ciência e a Tecnologia (FCT), Portugal (SFRH/BPD/81627/2011 to SV), by iBB — Institute for Bioengineering and Biosciences — project UIDB/04565/2020, and by Egas Moniz Higher Institute of Health Science (Egas Moniz, CRL). Funding was also received from the European Union's Horizon 2020 Research and Innovation programme, under the Grant Agreement number 739572—The Discoveries Centre for Regenerative and Precision Medicine H2020-WIDESPREAD-01-2016-2017 to EB.

ACKNOWLEDGMENTS

We thank Professor Joaquim M.S. Cabral for supporting this research, Teresa P. Silva for insightful discussions, and Ismael Galve-Roperh and Bruno Miguel Fonseca for critical review. We are grateful to the members of the bioimaging facility at iMM for helping with confocal microscopy and to our colleagues from

CiiEM, Professor Isabel Barahona and Susana Bandarra for their help at cell culture facility.

SUPPLEMENTARY MATERIAL

The Supplementary Material for this article can be found online at: https://www.frontiersin.org/articles/10.3389/fnmol.2020.00119/full#supplementary-material.

FIGURE S1 | A scheme representing culture procedure to induce neural differentiation of hiPSCs showing culture media and supplements used as well as cell morphologies observed at different time points. Individual experiments, cell lines, and substances used are depicted below the scheme. Solid green boxes represent total medium change every other day, while striped green boxes show the 1/3 medium change three times a week.

FIGURE S2 | (A,B) qRT-PCR analysis of *GAPDH*-normalized expression levels of GABAergic neuronal marker *GAD67* **(A)** and glutamatergic marker *GLUT1* **(B)** along with the differentiation in untreated cultures. **(C–H)** qRT-PCR analysis of relative expression levels of neural progenitor (*PAX6*, **C**), neuronal (*MAP2*, **D**), GABAergic (*GAD67*, **E**) and glutamatergic (*GLUT1*, **F**), and CB receptors *CNR1* **(G)** and CNR2 **(H)**. *GAPDH*-normalized expression levels were further normalized against EtOH (vehicle) condition. All qRT-PCR data analyzed by unpaired *t*-test; $^{*}p < 0.05$, $^{**}p < 0.01$; error bars represent SEM. **(I–J)** Quantification of the SCCI data regarding the strength of the response to KCl **(I)** and histamine **(J)**. The value of the response was considered at the time point corresponding to the peak seen in the graph in **Figure 3A**, and the ratio of fluorescence value for this timepoint over baseline level was calculated for each responding cell. For EG-018 and THJ-018 conditions, the last time point before washing was used to calculate the response to histamine stimulation. Data analyzed by unpaired *t*-test; $^{*}p < 0.05$, $^{**}p < 0.01$; error bars represent SEM. **(K)** Values used for building the graphs in **Figure 3B**. Percentages calculated as described in the legend for **Figure 3**.

FIGURE S3 | Quantification of $MAP2^{+}$ cells at day 30, relative to DAPI. Results from three independent experiments. Tukey's range test was applied to determine outlier data points (open circles). Data analyzed by unpaired *t*-test; $^{*}p < 0.05$, $^{**}p < 0.01$; error bars represent SEM.

REFERENCES

Abranches, E., Silva, M., Pradier, L., Schulz, H., Hummel, O., Henrique, D., et al. (2009). Neural differentiation of embryonic stem cells *in vitro*: a road map to neurogenesis in the embryo. *PLoS One* 4:e6286. doi: 10.1371/journal.pone.0006286

Agasse, F., Bernardino, L., Silva, B., Ferreira, R., Grade, S., and Malva, J. O. (2008). Response to histamine allows the functional identification of neuronal progenitors, neurons, astrocytes and immature cells in subventricular zone cell cultures. *Rejuvenation Res.* 11, 187–200. doi: 10.1089/rej.2007.0600

Aguado, T., Monory, K., Palazuelos, J., Stella, N., Cravatt, B., Lutz, B., et al. (2005). The endocannabinoid system drives neural progenitor proliferation. *FASEB J.* 19, 1704–1706. doi: 10.1096/fj.05-3995fje

Ambrósio, A. F., Silva, A. P., Malva, J. O., Mesquita, J. F., Carvalho, A. P., and Carvalho, C. M. (2000). Role of desensitization of AMPA receptors on the neuronal viability and on the $[Ca^{2+}]$i changes in cultured rat hippocampal neurons. *Eur. J. Neurosci.* 12, 2021–2031. doi: 10.1046/j.1460-9568.2000.00091.x

Atwood, B. K., Huffman, J., Straiker, A., and Mackie, K. (2010). JWH018, a common constituent of 'Spice' herbal blends, is a potent and efficacious cannabinoid CB1receptor agonist. *Br. J. Pharmacol.* 160, 585–593. doi: 10.1111/j.1476-5381.2009.00582.x

Bardy, C., van den Hurk, M., Eames, T., Marchand, C., Hernandez, R. V., Kellogg, M., et al. (2015). Neuronal medium that supports basic synaptic functions and activity of human neurons *in vitro*. *Proc. Natl. Acad. Sci. U S A* 112, E2725–E2734. doi: 10.1073/pnas.1504393112

Beers, J., Gulbranson, D. R., George, N., Siniscalchi, L. I., Jones, J., Thomson, J. A., et al. (2012). Passaging and colony expansion of human pluripotent stem cells by enzyme-free dissociation in chemically defined culture conditions. *Nat. Protoc.* 7, 2029–2040. doi: 10.1038/nprot.2012.130

Brown, Q. L., Sarvet, A. L., Shmulewitz, D., Martins, S. S., Wall, M. M., and Hasin, D. S. (2017). Trends in marijuana use among pregnant and nonpregnant reproductive-aged women, 2002–2014. *JAMA* 317, 207–209. doi: 10.1001/jama.2016.17383

Broyd, S. J., van Hell, H. H., Beale, C., Yücel, M., and Solowij, N. (2016). Acute and chronic effects of cannabinoids on human cognition—a systematic review. *Biol. Psychiatry* 79, 557–567. doi: 10.1016/j.biopsych.2015.12.002

Burridge, P. W., Thompson, S., Millrod, M. A., Weinberg, S., Yuan, X., Peters, A., et al. (2011). A universal system for highly efficient cardiac differentiation of human induced pluripotent stem cells that eliminates interline variability. 6:e18293. doi: 10.1371/journal.pone.0018293

Chambers, S. M., Fasano, C. A., Papapetrou, E. P., Tomishima, M., Sadelain, M., and Studer, L. (2009). Highly efficient neural conversion of human ES and iPS cells by dual inhibition of SMAD signaling. *Nat. Biotechnol.* 27, 275–280. doi: 10.1038/nbt.1529

de Salas-Quiroga, A., García-Rincón, D., Gómez-Domínguez, D., Valero, M., Simón-Sánchez, S., Paraíso-Luna, J., et al. (2020). Long-term hippocampal interneuronopathy drives sex-dimorphic spatial memory impairment induced by prenatal THC exposure. *Neuropsychopharmacology* 45, 877–886. doi: 10.1038/s41386-020-0621-3

Fried, P. A. (2002). Conceptual issues in behavioral teratology and their application in determining long-term sequelae of prenatal marihuana exposure. *J. Child Psychol. Psychiatry* 43, 81–102. doi: 10.1111/1469-7610.00005

Galve-Roperh, I., Chiurchiù, V., Díaz-Alonso, J., Bari, M., Guzmán, M., and Maccarrone, M. (2013). Cannabinoid receptor signaling in progenitor/stem cell proliferation and differentiation. *Prog. Lipid Res.* 52, 633–650. doi: 10.1016/j.plipres.2013.05.004

Galve-Roperh, I., Palazuelos, J., Aguado, T., and Guzmán, M. (2009). The endocannabinoid system and the regulation of neural development: potential implications in psychiatric disorders. *Eur. Arch. Psychiatry Clin. Neurosci.* 259, 371–382. doi: 10.1007/s00406-009-0028-y

Grant, K. S., Petroff, R., Isoherranen, N., Stella, N., and Burbacher, T. M. (2018). Cannabis use during pregnancy: pharmacokinetics and effects on child development. *Pharmacol. Ther.* 182, 133–151. doi: 10.1016/j.pharmthera.2017.08.014

Gray, K. A., Day, N. L., Leech, S., and Richardson, G. A. (2005). Prenatal marijuana exposure: effect on child depressive symptoms at ten years of age. *Neurotoxicol. Teratol.* 27, 439–448. doi: 10.1016/j.ntt.2005.03.010

Grienberger, C., and Konnerth, A. (2012). Imaging calcium in neurons. *Neuron* 73, 862–885. doi: 10.1016/j.neuron.2012.02.011

Grotenhermen, F. (2003). Pharmacokinetics and pharmacodynamics of cannabinoids. *Clin. Pharmacokinet.* 42, 327–360. doi: 10.2165/00003088-200342040-00003

Guennewig, B., Bitar, M., Obiorah, I., Hanks, J., O'Brien, E. A., Kaczorowski, D. C., et al. (2018). THC exposure of human iPSC neurons impacts genes associated with neuropsychiatric disorders. *Transl. Psychiatry* 8:89. doi: 10.1038/s41398-018-0137-3

Harris, A. L., and Okorie, C. S. (2017). Assessing marijuana use during pregnancy. *Nurs. Womens Health* 21, 207–216. doi: 10.1016/j.nwh.2017.04.001

Hess, C., Schoeder, C. T., Pillaiyar, T., Madea, B., and Müller, C. E. (2016). Pharmacological evaluation of synthetic cannabinoids identified as constituents of spice. *Forensic Toxicol.* 34, 329–343. doi: 10.1007/s11419-016-0320-2

Huestis, M. A. (2007). Human cannabinoid pharmacokinetics. *Chem. Biodivers.* 4, 1770–1804. doi: 10.1002/cbdv.200790152

Hurd, Y. L., Wang, X., Anderson, V., Beck, O., Minkoff, H., and Dow-Edwards, D. (2005). Marijuana impairs growth in mid-gestation fetuses. *Neurotoxicol. Teratol.* 27, 221–229. doi: 10.1016/j.ntt.2004.11.002

Laprairie, R. B., Bagher, A. M., Kelly, M. E. M., and Denovan-Wright, E. M. (2015). Cannabidiol is a negative allosteric modulator of the cannabinoid CB1 receptor. *Br. J. Pharmacol.* 172, 4790–4805. doi: 10.1111/bph.13250

Macías, W., Carlson, R., Rajadhyaksha, A., Barczak, A., and Konradi, C. (2001). Potassium chloride depolarization mediates CREB phosphorylation in striatal neurons in an NMDA receptor-dependent manner. *Brain Res.* 890, 222–232. doi: 10.1016/s0006-8993(00)03163-2

Meier, U., Dussy, F., Scheurer, E., Mercer-Chalmers-Bender, K., and Hangartner, S. (2018). Cannabinoid concentrations in blood and urine after smoking cannabidiol joints. *Forensic Sci. Int.* 291, 62–67. doi: 10.1016/j.forsciint.2018.08.009

Metsalu, T., and Vilo, J. (2015). ClustVis: a web tool for visualizing clustering of multivariate data using Principal Component Analysis and heatmap. *Nucleic Acids Res.* 43, W566–W570. doi: 10.1093/nar/gkv468

Metz, T. D., and Stickrath, E. H. (2015). Marijuana use in pregnancy and lactation: a review of the evidence. *Am. J. Obstet. Gynecol.* 213, 761–778. doi: 10.1016/j.ajog.2015.05.025

Miranda, C. C., Fernandes, T. G., Pascoal, J. F., Haupt, S., Brüstle, O., Cabral, J. M. S., et al. (2015). Spatial and temporal control of cell aggregation efficiently directs human pluripotent stem cells towards neural commitment. *Biotechnol. J.* 10, 1612–1624. doi: 10.1002/biot.201400846

Namdar, D., Voet, H., Ajjampura, V., Nadarajan, S., Mayzlish-Gati, E., Mazuz, M., et al. (2019). Terpenoids and phytocannabinoids co-produced in *cannabis sativa* strains show specific interaction for cell cytotoxic activity. *Molecules* 24:3031. doi: 10.3390/molecules24173031

Okano, H. J., and Darnell, R. B. (1997). A hierarchy of hu RNA binding proteins in developing and adult neurons. *J. Neurosci.* 17, 3024–3037. doi: 10.1523/JNEUROSCI.17-09-03024.1997

Oviedo, A., Glowa, J., and Herkenham, M. (1993). Chronic cannabinoid administration alters cannabinoid receptor binding in rat brain: a quantitative autoradiographic study. *Brain Res.* 616, 293–302. doi: 10.1016/0006-8993(93)90220-h

Pertwee, R. G. (2008). The diverse CB1and CB2receptor pharmacology of three plant cannabinoids: Δ9-tetrahydrocannabinol, cannabidiol and Δ9-tetrahydrocannabivarin. *Br. J. Pharmacol.* 153, 199–215. doi: 10.1038/sj.bjp.0707442

Richardson, K. A., Hester, A. K., and McLemore, G. L. (2016). Prenatal cannabis exposure—the "first hit" to the endocannabinoid system. *Neurotoxicol. Teratol.* 58, 5–14. doi: 10.1016/j.ntt.2016.08.003

Rodrigues, R. S., Ribeiro, F. F., Ferreira, F., Vaz, S. H., Sebastiao, A. M., and Xapelli, S. (2017). Interaction between cannabinoid type 1 and type 2 receptors in the modulation of subventricular zone and dentate gyrus neurogenesis. *Front. Pharmacol.* 8:516. doi: 10.3389/fphar.2017.00516

Romero, J., Garcia-Palomero, E., Castro, J. G., Garcia-Gil, L., Ramos, J. A., and Fernandez-Ruiz, J. J. (1997). Effects of chronic exposure to Δ9-tetrahydrocannabinol on cannabinoid receptor binding and mRNA levels in several rat brain regions. *Mol. Brain Res.* 46, 100–108. doi: 10.1016/s0169-328x(96)00277-x

Rueda, D., Navarro, B., Martinez-Serrano, A., Guzman, M., and Galve-Roperh, I. (2002). The endocannabinoid anandamide inhibits neuronal progenitor cell differentiation through attenuation of the Rap1/B-Raf/ERK pathway. *J. Biol. Chem.* 277, 46645–46650. doi: 10.1074/jbc.m206590200

Scheyer, A. F., Melis, M., Trezza, V., and Manzoni, O. J. J. (2019). Consequences of perinatal cannabis exposure. *Trends Neurosci.* 42, 871–884. doi: 10.1016/j.tins.2019.08.010

Schoeder, C. T., Hess, C., Madea, B., Meiler, J., and Müller, C. E. (2018). Pharmacological evaluation of new constituents of "Spice": synthetic cannabinoids based on indole, indazole, benzimidazole and carbazole scaffolds. *Forensic Toxicol.* 36, 385–403. doi: 10.1007/s11419-018-0415-z

Shi, Y., Kirwan, P., Smith, J., Robinson, H. P., and Livesey, F. J. (2012). Human cerebral cortex development from pluripotent stem cells to functional excitatory synapses. *Nat. Neurosci.* 15, 477–486, S1. doi: 10.1038/nn.3041

Silva, T. P., Bekman, E., Fernandes, T. G., Vaz, S. H., Rodrigues, C. A., Diogo, M. M., et al. (2020). Maturation of human pluripotent stem cell-derived cerebellar neurons in the absence of co-culture. *Front. Bioeng. Biotechnol.* 14:70. doi: 10.3389/fbioe.2020.00070

Smith, A. M., Fried, P. A., Hogan, M. J., and Cameron, I. (2004). Effects of prenatal marijuana on response inhibition: an fMRI study of young adults. *Neurotoxicol. Teratol.* 26, 533–542. doi: 10.1016/j.ntt.2004.04.004

Solinas, M., Massi, P., Cantelmo, A., Cattaneo, M., Cammarota, R., Bartolini, D., et al. (2012). Cannabidiol inhibits angiogenesis by multiple mechanisms. *Br. J. Pharmacol.* 167, 1218–1231. doi: 10.1111/j.1476-5381.2012.02050.x

Stanslowsky, N., Jahn, K., Venneri, A., Naujock, M., Haase, A., Martin, U., et al. (2017). Functional effects of cannabinoids during dopaminergic specification of human neural precursors derived from induced pluripotent stem cells. *Addict. Biol.* 22, 1329–1342. doi: 10.1111/adb.12394

Villares, J. (2007). Chronic use of marijuana decreases cannabinoid receptor binding and mRNA expression in the human brain. *Neuroscience* 145, 323–334. doi: 10.1016/j.neuroscience.2006.11.012

Wu, C. S., Jew, C. P., and Lu, H. C. (2011). Lasting impacts of prenatal cannabis exposure and the role of endogenous cannabinoids in the developing brain. *Future Neurol.* 6, 459–480. doi: 10.2217/fnl.11.27

Young-Wolff, K. C., Tucker, L.-Y., Alexeeff, S., Armstrong, M. A., Conway, A., Weisner, C., et al. (2017). Trends in self-reported and biochemically tested marijuana use among pregnant females in california from 2009–2016. *JAMA* 318, 2490–2491. doi: 10.1001/jama.2017.17225

Conflict of Interest: The authors declare that the research was conducted in the absence of any commercial or financial relationships that could be construed as a potential conflict of interest.

frontiers in Molecular Neuroscience

BRIEF RESEARCH REPORT
published: 05 August 2020
doi: 10.3389/fnmol.2020.00146

Non-genomic Actions of Methylprednisolone Differentially Influence GABA and Glutamate Release From Isolated Nerve Terminals of the Rat Hippocampus

*Rafael Neiva[1,2], Ana Caulino-Rocha[1,2], Fátima Ferreirinha[1,2], Maria Graça Lobo[1,2] and Paulo Correia-de-Sá[1,2]**

[1] Laboratório de Farmacologia e Neurobiologia – Departamento de Imuno-Fisiologia e Farmacologia, Instituto de Ciências Biomédicas de Abel Salazar (ICBAS), Universidade do Porto (UP), Porto, Portugal, [2] Center for Drug Discovery and Innovative Medicines (MedInUP), Instituto de Ciências Biomédicas de Abel Salazar (ICBAS), Universidade do Porto (UP), Porto, Portugal

Corticosteroids exert a dual role in eukaryotic cells through their action via (1) intracellular receptors (slow genomic responses), or (2) membrane-bound receptors (fast non-genomic responses). Highly vulnerable regions of the brain, like the hippocampus, express high amounts of corticosteroid receptors, yet their actions on ionic currents and neurotransmitters release are still undefined. Here, we investigated the effect of methylprednisolone (MP) on GABA and glutamate (Glu) release from isolated nerve terminals of the rat hippocampus. MP favored both spontaneous and depolarization-evoked [^{14}C]Glu release from rat hippocampal nerve terminals, without affecting [^{3}H]GABA outflow. Facilitation of [^{14}C]Glu release by MP is mediated by a Na^{+}-dependent Ca^{2+}-independent non-genomic mechanism relying on the activation of membrane-bound glucocorticoid (GR) and mineralocorticoid (MR) receptors sensitive to their antagonists mifepristone and spironolactone, respectively. The involvement of Na^{+}-dependent high-affinity EAAT transport reversal was inferred by blockage of MP-induced [^{14}C]Glu release by DL-TBOA. Depolarization-evoked [^{3}H]GABA release in the presence of MP was partially attenuated by the selective P2X7 receptor antagonist A-438079, but this compound did not affect the release of [^{14}C]Glu. Data indicate that MP differentially affects GABA and glutamate release from rat hippocampal nerve terminals via fast non-genomic mechanisms putatively involving the activation of membrane-bound corticosteroid receptors. Facilitation of Glu release strengthen previous assumptions that MP may act as a cognitive enhancer in rats, while crosstalk with ATP-sensitive P2X7 receptors may promote a therapeutically desirable GABAergic inhibitory control during paroxysmal epileptic crisis that might be particularly relevant when extracellular Ca^{2+} levels decrease below the threshold required for transmitter release.

Keywords: methylprednisolone, glucocorticoid receptors, mineralocorticoid receptors, synchronous GABA and glutamate release, hippocampal nerve terminals

OPEN ACCESS

Edited by:
Sara Xapelli,
University of Lisbon, Portugal

Reviewed by:
Peter Illes,
Leipzig University, Germany
Ricardo J. Rodrigues,
University of Coimbra, Portugal

***Correspondence:**
Paulo Correia-de-Sá
farmacol@icbas.up.pt;
pcorreiasa@mail.telepac.pt

Received: *04 August 2019*
Accepted: *14 July 2020*
Published: *05 August 2020*

Citation:
Neiva R, Caulino-Rocha A, Ferreirinha F, Lobo MG and Correia-de-Sá P (2020) Non-genomic Actions of Methylprednisolone Differentially Influence GABA and Glutamate Release From Isolated Nerve Terminals of the Rat Hippocampus. Front. Mol. Neurosci. 13:146. doi: 10.3389/fnmol.2020.00146

HIGHLIGHTS

- Methylprednisolone (MP) favors the spontaneous and depolarization-evoked release of Glu from rat hippocampal nerve terminals, without affecting GABA outflow;
- Facilitation of Glu release by MP is mediated by a Na^+-dependent Ca^{2+}-independent fast non-genomic mechanism altering high-affinity Glu transport through the plasma membrane;
- Depolarization-evoked GABA release in the presence of MP depends on activation of ATP-sensitive P2X7 receptors.

INTRODUCTION

Glucocorticoids (GRs) are steroid hormones that are responsible for countless important regulatory functions in the human body (Joëls and Ronald de Kloet, 1994; Zhang et al., 2007; Groeneweg et al., 2012). Among the lifesaving corticosteroid drugs widely prescribed, methylprednisolone (MP) is used since 1955 and is listed as an Essential Medicine by the World Health Organization for the treatment of chronic inflammatory conditions, autoimmune diseases and allergic reactions, including several neurological disorders (Gumy et al., 2008; Kajiyama et al., 2010; Nicolaides et al., 2010). The usual daily dosing regimens indicated for MP vary significantly (from 15 to 20 mg to 120 mg) depending on the underlying disease condition. Higher dosing regimens of MP (e.g., 30 mg/kg IV, followed by repeated injections or continuous perfusions during 24 to 48 h) have been advocated in life-threatening edematous conditions, acute spinal cord injuries, and autoimmune rheumatic diseases. Although MP safety margin is high and side effects relatively rare (Bast et al., 2014; Tauheed et al., 2014), it may be detrimental for certain neurological conditions (reviewed in Parissis et al., 2017).

The hippocampus is a major structure of the human brain, which has been implicated in a variety of different functions, including declarative memory consolidation and formation of spatial memories. Like other limbic structures, the hippocampus is highly enriched in corticosteroid receptors, both GR and mineralocorticoid (MR) receptors (Joëls et al., 2012). This brain region is affected in several types of dementia and it is highly sensitive to pathological insults (e.g., hypoxia/ischemia, epileptic crisis, post-traumatic stress). Regarding the effects of GRs in the hippocampus, decreases in the number of interneurons in hippocampal CA3 and dentate gyrus have been observed after MP use for brain injury (Zhang et al., 2011). High doses of GRs are known to affect the induction of hippocampal long-term potentiation (LTP; Krugers et al., 2005; Maggio and Segal, 2007) and block synaptic strength and the formation of new synapses between CA3 and CA1 regions (Saito et al., 2016). Contrariwise, low to moderate doses of corticosterone may enhance LTP (Diamond et al., 1992). Recently, our group proposed MP (5–30 mg/kg, i.p., for 10 days) as a cognitive enhancer *in vivo* because it favored aversive memory persistence in adult rats, without any effect on exploring behavior, locomotor activity, anxiety levels and pain perception (de Vargas et al., 2017).

Despite the high number of studies in the literature aiming at exploring the effects of corticosteroids in the brain, their role is still controversial (Bartholome et al., 2004; Song and Buttgereit, 2006; Zhang et al., 2007; Rickard and Young, 2009; Groeneweg et al., 2012; Oliveira et al., 2015; Russo et al., 2016). The reason for this disparity may be attributed to insufficient knowledge about the exact molecular mechanism(s) of action of corticosteroids in the nervous tissue. Corticosteroids exert a dual role in eukaryotic cells acting via activation of (i) cytosolic receptors mediating slow genomic responses, and/or (ii) plasma membrane-bound receptors, resulting in fast changes in neuronal signaling, ion channel conductance and neurotransmitters release (non-genomic mechanisms). In a recent publication, we demonstrated that amplification of the neuromuscular transmission by MP (300 μM) involves activation of pre-synaptic facilitatory A_{2A} receptors by endogenous adenosine generated from ATP released by motor nerve terminals under resting conditions, leading to subsequent synaptic vesicles redistribution that favors acetylcholine exocytosis during high-frequency neuronal activation (Oliveira et al., 2015). In the hippocampus, data suggest that corticosteroids rapidly increase the mobility of post-synaptic membrane-bound glutamate receptors and facilitate the glutamate release probability from pre-synaptic neurons, thus strengthening the glutamatergic neurotransmission (Karst et al., 2005; Groc et al., 2008; Olijslagers et al., 2008; Wang and Wang, 2009; Zheng, 2009; Groeneweg et al., 2012). These findings are, however, far from being consensual, along with the fact that experimental studies addressing the effects of corticosteroids on inhibitory GABAergic neurotransmission are surprisingly lacking in literature.

Thus, this study was designed to investigate in parallel and under the same experimental conditions the mechanisms underlying the effect MP on resting and depolarization-evoked [^{3}H]GABA and [^{14}C]Glu release from isolated nerve terminals of the hippocampus of adult rats.

EXPERIMENTAL PROCEDURES

Drugs and Solutions

2′(3′)-*O*-(4-Benzoylbenzoyl)adenosine 5′-triphosphate triethylammonium salt (BzATP), dexamethasone, GABA (γ-aminobutyric acid), mifepristone, spironolactone, NMDG (*N*-methyl-D-glucamine), EGTA (ethylene glycol-bis(2-aminoethylether)-*N*,*N*,*N*′,*N*′-tetraacetic acid) and aminooxyacetic acid were obtained from Sigma-Aldrich (St. Louis, MO, United States). L-Glutamic acid, A-438079 (3-[[5-(2,3-dichlorophenyl)-1*H*-tetrazol-1-yl] methyl]pyridine

Abbreviations: A-438079, 3-[[5-(2,3-dichlorophenyl)-1*H*-tetrazol-1-yl] methyl]pyridine hydrochloride; BzATP, 2′(3′)-*O*-(4-benzoylbenzoyl)adenosine 5′-triphosphate triethylammonium salt; CNS, central nervous system; CPMs, counts per minute; DL-TBOA, DL-*threo*-β-benzyloxyaspartic acid; DPMs, disintegrations per minute; EAATs, excitatory amino-acid transporters; EGTA, ethylene glycol-bis(2-aminoethylether)-*N*,*N*,*N*′,*N*′-tetraacetic acid; GABA, γ-aminobutyric acid; Glu, glutamate (glutamic acid); HEPES, 2-[4-(2-hydroxyethyl)piperazin-1-yl]ethanesulfonic acid; NMDG, *N*-methyl-D-glucamine; SKF-89976A, 1-(4,4-diphenyl-3-butenyl)-3-piperidinecarboxylic acid hydrochloride; VT, veratridine.

hydrochloride), DL-TBOA (DL-*threo*-β-benzyloxyaspartic acid), and VT were obtained from Tocris Bioscience (Bristol, United Kingdom). 1-(4,4-Diphenyl-3-butenyl)-3-piperidinecarboxylic acid hydrochloride (SKF-89976A) was obtained from Abcam (Cambridge, United Kingdom). MP was obtained from Pfizer (Puurs, Belgium). [^{14}C]Glu and [^{3}H]GABA were from American Radiolabeled Chemicals, Inc. (St. Louis, MO, United States). Stock solutions were stored as frozen aliquots. Dilutions of stock solutions were made daily and appropriate solvent controls were done. No statistically significant differences were observed in control experiments made with solvents at maximal concentrations compared to the physiological buffer.

Animals

Hippocampi were obtained from Wistar Han rats of both genders (2–5 months old, Charles River™, Barcelona, Spain). Animal care and experimental procedures were performed in consonance with the United Kingdom Animals (Scientific Procedures) Act 1986 and followed the European Communities Council Directive of 24 November 1986 (86/609/EEC) and the National Institutes of Health Guide for Care and Use of Laboratory animals (NIH Publications No. 80-23) revised 1996. All studies involving animals are reported in accordance with the ARRIVE guidelines for reporting experiments involving animals. The study was approved by the Ethics Committee and the Animal Welfare Responsible Organism of ICBAS-UP (Decision no 224/2017). Wistar rats were kept at a constant temperature (21°C) and a regular light (06.30–19.30 h)–dark (19.30–06.30 h) cycle, with food and water *ad libitum*. All efforts were made to minimize animal suffering and to reduce the number of animals used.

Isolation of Nerve Terminals From the Rat Hippocampus

Nerve terminals were isolated as previously described (Helme-Guizon et al., 1998; modified in Bancila et al., 2009; Barros-Barbosa et al., 2015). Briefly, brain hemispheres were separated and hippocampi were dissected out and gently homogenized in cold oxygenated (95% O_2 and 5% CO_2) Krebs solution (in mM: glucose 5.5, NaCl 136, KCl 3, $MgCl_2$ 1.2, Na_2HPO_4 1.2, $NaHCO_3$ 16.2, $CaCl_2$ 0.5, pH 7.40). Homogenates were filtered through a nylon filter (mesh size 100 μm). The filtrate was left to sit during 30–45 min until formation of a pellet, which was re-suspended into Krebs solution and left at room temperature. Protein concentration determined by the bicinchoninic acid method (Pierce™ bicinchoninic acid protein assay, Thermo Scientific, Rockford, IL, United States) was adjusted to 6.25 mg protein mL^{-1}.

Re-sealed nerve terminal membranes isolated from the rat hippocampus using this methodology allows processing larger amounts of tissue compared to synaptosomal preparations, while taking up and release [^{3}H]GABA and [^{14}C]glutamate via Na^+-dependent high-affinity transporters with a similar kinetics. This method is relevant in order to take full advantage of scarce human brain tissue (from cadaveric samples and surgical resections of epileptic foci) often tested in parallel by our group (see Barros-Barbosa et al., 2015, 2016, 2018).

[^{3}H]GABA and [^{14}C]Glu Release Experiments

Isolated nerve terminals were incubated with [^{3}H]GABA (0.25 μCi mL^{-1}; 70 Ci mmol^{-1}; 0.5 μM) and [^{14}C]Glu (0.25 μCi mL^{-1}; 0.270 Ci mmol^{-1}; 10 μM), for 10 min at 37°C, and their release was measured simultaneously. Aliquots of nerve terminals suspension were layered onto glass fiber filters (Merck Millipore, Cork, Ireland), which were mounted in 365 μL chambers of a semi-automated 12-sample superfusion system (SF-12 Suprafusion 1000, Brandel, Gaithersburg, MD, United States). The filters containing the sample were superfused at a flow rate of 0.5 mL min^{-1}, at 37°C, with a physiological solution containing (in mM): NaCl 128, $MgCl_2$ 1.2, KCl 3, glucose 10, HEPES–Na 10 (pH = 7.4), $CaCl_2$ 2.2, and aminooxyacetic acid 0.01, an inhibitor of tissue GABA breakdown by 4-aminobutyrate aminotransferase (GABA-T). After a 26 min equilibration period, 2-min fractions were automatically collected, using the SF-12 suprafusion system. Eight (S1) and twenty-six (S2) min after starting samples collection, isolated nerve terminals were depolarized with a solution containing high KCl (15 mM) or VT (5 μM, a Na^+ channel activator) during 2 min; this was done by changing the inlet tube from one flask to another containing the depolarizer agent. High KCl and VT are the most common strategies to depolarize the plasma membrane of isolated nerve terminals as they allow to differentiate between pre-synaptic Na^+ channel-mediated responses (Adam-Vizi and Ligeti, 1986; Costa et al., 2006). VT acts as a neurotoxin through binding to site 2 of voltage-gated sodium channels resulting in their persistent activation.

Methylprednisolone was added 15 min before S2. Solutions without Ca^{2+} or Na^+ and containing drug modifiers (e.g., transport inhibitors, receptor antagonists) were applied from the beginning of samples collection, so that they were present throughout the testing period including S1 and S2; under such conditions, the normalized [^{3}H]GABA and [^{14}C]Glu release in S2 compared to S1 was not different ($P > 0.05$) from that obtained in control conditions (with no drugs added). The radioactive content of collected fractions and that remaining in the filters at the end of the protocol was measured by liquid scintillation spectrometry (TriCarb2900TR, Perkin Elmer, Boston, MA, United States).

SDS–PAGE and Western Blot Analysis

Total membrane lysates and nerve terminals isolated from the rat hippocampus were homogenized in Radio Immuno Precipitation Assay (RIPA) buffer containing: Tris–HCl (pH 7.6) 25 mM, NaCl 150 mM, sodium deoxycholate 1%, triton-X-100 1%, SDS 0.1%, EDTA 5 mM and a protease inhibitor cocktail (Sigma-Aldrich, St. Louis, MO, United States). The protein content of the samples was evaluated using the BCA method. Samples were solubilized at 70°C in SDS reducing buffer [Tris–HCl (pH 6.8) 125 mM, SDS 4%, bromophenol blue 0.005%, glycerol 20%, and 2-mercaptoethanol 5%] for 10 min,

subjected to electrophoresis in 12.5% SDS–polyacrylamide gels and electrotransferred onto PVDF membranes (Merck MilliPore, Temecula, CA, United States). Membranes were blocked for 1 h in Tris-buffered saline [TBS; in mM: Tris–HCl 10 (pH 7.6), NaCl 150] containing Tween 20 0.05% and BSA 5% and, subsequently, incubated overnight, at 4°C, with primary antibodies: mouse anti-synaptophysin (1:1000, Chemicon, Temecula, CA, United States) and mouse anti-GFAP (1:500, Chemicon, Temecula, CA, United States). Membranes were washed three times for 10 min in 0.05% Tween 20 in TBS and then incubated with horseradish anti-rabbit or anti-mouse peroxidase-conjugated secondary antibodies for 120 min, at room temperature. The antigen–antibody complexes were visualized by chemiluminescence with the Immun-Star WesternC Kit (Bio-Rad Laboratories, Hercules, CA, United States) using the ChemiDoc MP imaging system (Bio-Rad Laboratories, Hercules, CA, United States). Gel band image densities were quantified with ImageJ (National Institute of Health, United States).

Immunofluorescence Confocal Microscopy

Immunofluorescent staining and confocal microscopy analysis was performed as previously described (Barros-Barbosa et al., 2015, 2016). Brain samples were fixed in 4% paraformaldehyde in phosphate-buffered saline (PBS; in mM: NaCl 137, KCl 2.6, Na_2HPO_4 4.3, KH_2PO_4 1.5; pH = 7.4) for about 48 h (4°C), cryopreserved in 30% sucrose in PBS and stored in a tissue freezing medium at −80°C. Free-floating 30-μm brain slices were incubated for 1 h, at room temperature, with blocking buffer I (fetal bovine serum 10%, BSA 1%, triton X-100 0.5%, NaN_3 0.05%) and subsequently incubated overnight, at 4°C, with the following primary antibodies: rabbit anti-P2X7 receptor (1:50, #APR004, Alomone, Jerusalem, Israel), mouse anti-GFAP (1:350, Chemicon, Temecula, CA, United States), goat anti-VAMP-1 (1:20, R&D Systems, Minneapolis, MN, United States) diluted in blocking buffer II (fetal bovine serum 5%, BSA 0.5%, triton X-100 0.5%, NaN_3 0.05% in PBS). Sections were rinsed in PBS supplemented with triton X-100 0.5% (three cycles of 10 min) and incubated for 120 min with species-specific secondary antibodies conjugated with fluorescent dyes (donkey anti-rabbit IgG Alexa Fluor 488, donkey anti-mouse IgG Alexa Fluor 568; donkey anti-goat Alexa 633) diluted in blocking buffer II, at room temperature. After rinsing in PBS, slices were mounted on optical-quality glass slides using VectaShield (Vector Labs, Peterborough, United Kingdom) as mounting media. Observations were performed with a laser scanning confocal microscopy (Olympus FV1000, Tokyo, Japan). Controls were performed by following the same procedure but replacing the primary antibodies with the same volume of blocking buffer II. Images were analyzed using the Olympus Fluoview 4.2 Software (Olympus FV1000, Tokyo, Japan). Co-localization was assessed by calculating the staining overlap and the Pearson's coefficient (ρ) for each confocal micrograph stained with two fluorescent dyes. Overlap between two stainings gives a value between +1 and 0 inclusive, where 1 is total overlap and 0 is no overlap. ρ is a measure of the linear correlation between two variables (stainings), giving a value between +1 and −1 inclusive, where 1 is total positive correlation, 0 is no correlation, and −1 is total negative correlation.

Data Presentation and Statistical Analysis

[^{14}C]Glu and [^{3}H]GABA release by isolated nerve terminals was obtained as CPMs in function of time (min) obtained by the digital conversion of the intensity of radiation emitted by β particles detected by the liquid scintillation analyzer in channels 1 and 2, which correspond to the specific range of β energies (counting windows) for [^{14}C] and [^{3}H], respectively. Correction for efficiency and background are needed to convert CPMs into DPMs, the number of decay events that actually occurred; this was done using the expressions 1 and 2 presented below.

$$C = \frac{N_1 - N_2(h_1/h_2)}{c_1 - c_2(h_1/h_2)} \quad (1)$$

$$H = \frac{N_2 - N_1(c_2/c_1)}{h_2 - h_1(c_2/c_1)} \quad (2)$$

C = *carbon DPMs in sample*
H = *tritium DPMs in sample*
c_1 = *carbon-14 efficiency in channel 1*
c_2 = *carbon-14 efficiency in channel 2*
h_1 = *tritium efficiency in channel 1*
h_2 = *tritium efficiency in channel 2*
N_1 = *CPMs in channel 1*
N_2 = *CPMs in channel 2*

The area of the peak corresponding to the release of [^{3}H]GABA and [^{14}C]Glu was calculated as the sum of the differences between the total radioactivity present in 2–3 samples collected after stimulus (e.g., KCl, VT) application and the basal leakage of the corresponding isotope. Baseline values during stimulus influence were inferred by linear regression of the radioactivity decay immediately before stimulus and after its return to baseline. Thus, the action of test drugs on evoked [^{3}H]GABA and [^{14}C]Glu release during S2 was normalized by the effect of the depolarizing conditions alone obtained in S1 of the same experiment (S2/S1 ratios).

The results are expressed as mean ± SEM, with n (showed in graphs) indicating the number of animals. Statistical analysis of data was carried out using GraphPad Prism 7.05 software (La Jolla, CA, United States). One-way ANOVA (uncorrected Fisher's Least Significant Difference or Tukey's multiple comparison test, with single pooled variance) or two-way ANOVA (followed by the Dunnett's multicomparison test) were used when appropriate. Unpaired Student's t-test was used to compare the ratios between GFAP and synaptophysin protein densities (immunoblots) in total cell lysates and isolated nerve terminals obtained from the same hippocampus in three different animals. $P < 0.05$ (two tailed) values were considered to show significant differences between means.

RESULTS

Nerve Terminals Isolated From Rat Hippocampal Homogenates Are Highly Enriched in the Presynaptic Marker, Synaptophysin, With No Contamination by Glial Subcellular Particles

The method used for nerve terminals isolation described by Helme-Guizon et al. (1998; modified in Bancila et al., 2009; Barros-Barbosa et al., 2015) yields greater amounts of nerve terminals from rat hippocampal homogenates with very little (if at all) contamination by glial subcellular particles (gliosomes). This was demonstrated by the high density of synaptophysin (a typical nerve terminal marker) compared to the astrocytic glial fibrillary acidic protein (GFAP) content detected in the nerve terminals fraction *vis a vis* that found in total hippocampal cell lysates by Western blot analysis (**Figure 1**).

Methylprednisolone Increases the Resting and Depolarization-Evoked Release of Glu From Hippocampal Nerve Terminals via Fast Non-genomic Mechanisms, Without Affecting the GABA Outflow

Figures 2A, **3A** show the time course of synchronous [^{3}H]GABA and [^{14}C]Glu outflow from rat hippocampal nerve terminals depolarized with high KCl (15 mM) or VT (5 μM), respectively. The depolarizing agents were applied twice (S1 and S2) during 2 min either in the absence or in the presence of MP (300 μM), which contacted with rat hippocampal isolated nerve terminals for at least 15 min before S2. Immediately after application, MP (300 μM) progressively increased the basal release of [^{14}C]Glu, without affecting [^{3}H]GABA outflow (**Figures 2A**, **3A**; see **Figure 2D** for more detail). MP (300 μM) could still further increase depolarization-evoked [^{14}C]Glu release by about three-fold compared to control conditions, but the same was not observed regarding the release of [^{3}H]GABA (**Figures 2B**, **3B**). The facilitatory effect of MP on KCl-induced [^{14}C]Glu release was concentration-dependent (10–300 μM; with effects ranging from 16 to 336%, n = 5–6) and mimicked by the long-acting corticosteroid, dexamethasone, applied at an approximate equivalent concentration (60 μM, n = 5), but it was independent of the depolarizing agent, either high KCl (**Figure 2B**) or VT (**Figure 3B**).

The hippocampus expresses high amounts of corticosteroid receptors (de Vargas et al., 2017), but so far no attempt has been made to discriminate the effect of GR (low affinity) and MR (high affinity) receptors on transmitters release in this brain region. Pre-treatment of hippocampal nerve terminals either with mifepristone (500 nM) or with spironolactone (500 nM) to block GR and MR, respectively, prevented the facilitatory effect of MP (300 μM) on evoked [14C]Glu release independently of the depolarizing agent being used, either high KCl (**Figure 2Bii**) or VT (**Figure 3Bii**). Mifepristone (500 nM) blocked more efficiently than spironolactone (500 nM) the enhancing effect of MP (300 μM) on the resting [14C]Glu outflow (**Figure 2Di**), thus suggesting that GRs may have a predominant effect over the MR in the resting release of [^{14}C]Glu. Unexpectedly, MP (300 μM) decreased KCl-induced [^{3}H]GABA release in the presence of mifepristone (500 nM), and even more when spironolactone (500 nM) was used (**Figure 2Bi**), but no such effect was observed when VT was used to depolarize hippocampal nerve terminals (**Figure 3Bi**).

It is worth noting that, on their own, mifepristone (500 nM) and spironolactone (500 nM) did not significantly ($P > 0.05$) affect [^{3}H]GABA and [^{14}C]Glu outflow from rat hippocampal nerve terminals, both during resting conditions and following plasma membrane depolarization with high KCl (**Figure 2B**) or VT (**Figure 3B**). The S2/S1 ratio of KCl-induced [^{3}H]GABA release in the presence of mifepristone (500 nM) and spironolactone (500 nM) applied 15 min before S2 was 0.63 ± 0.14 (n = 6) and 0.58 ± 0.03 (n = 5) vs. 0.60 ± 0.06 in control conditions ($P > 0.05$); likewise, these drugs also did not significantly modify ($P > 0.05$) the S2/S1 ratio regarding the release of [^{14}C]Glu measured in the same samples (0.85 ± 0.16, n = 6 and 0.73 ± 0.09, n = 5, respectively), compared to the control situation when no drugs were added to the incubation fluid (0.78 ± 0.13, n = 7).

Influence of External Ca^{2+} on Methylprednisolone-Induced Changes in Glu and GABA Outflow From Hippocampal Nerve Terminals

Performing experiments in Ca^{2+}-free solutions (plus the Ca^{2+} chelator, EGTA 0.1 mM) restrain vesicular transmitter exocytosis and aim at mimicking conditions of paroxysmal neuronal activity verified during and after physiological and pathological brain events (such as epileptic seizures) where extracellular Ca^{2+} may fall up to 90% of the initial levels (Engelborghs K. et al., 2000; Engelborghs S. et al., 2000).

In Ca^{2+}-free media (plus EGTA 0.1 mM), MP (300 μM) could still progressively increase the release of [^{14}C]Glu from resting hippocampal nerve terminals (**Figures 4Aiii,D**), without affecting the basal [^{3}H]GABA outflow. Removal of Ca^{2+} from the incubation solution (plus EGTA 0.1 mM) also failed to affect MP (300 μM)-induced facilitation of [^{14}C]Glu release evoked by high KCl (15 mM) depolarization (**Figures 4Aiii,vi**), but it significantly diminished the facilitatory effect of the corticosteroid when VT (5 μM) was used as depolarizing agent (**Figure 4Bii**). In Ca^{2+}-free conditions (plus EGTA 0.1 mM), MP (300 μM) facilitated the release of [^{3}H]GABA from hippocampal nerve terminals depolarized with high KCl (15 mM) [**Figures 4Ai,v**], but not when VT (5 μM) was used instead (**Figure 4Bi**).

The facilitatory effect of MP (300 μM) on high KCl-induced [^{3}H]GABA and [^{14}C]Glu release in Ca^{2+}-free media (plus EGTA 0.1 mM) was abrogated by the GR antagonist, mifepristone (500 nM) (**Figures 2Ci,ii**, respectively), while pre-treatment with spironolactone (500 nM) only significantly ($P < 0.05$) decreased MP (300 μM)-induced facilitation of [^{14}C]Glu release

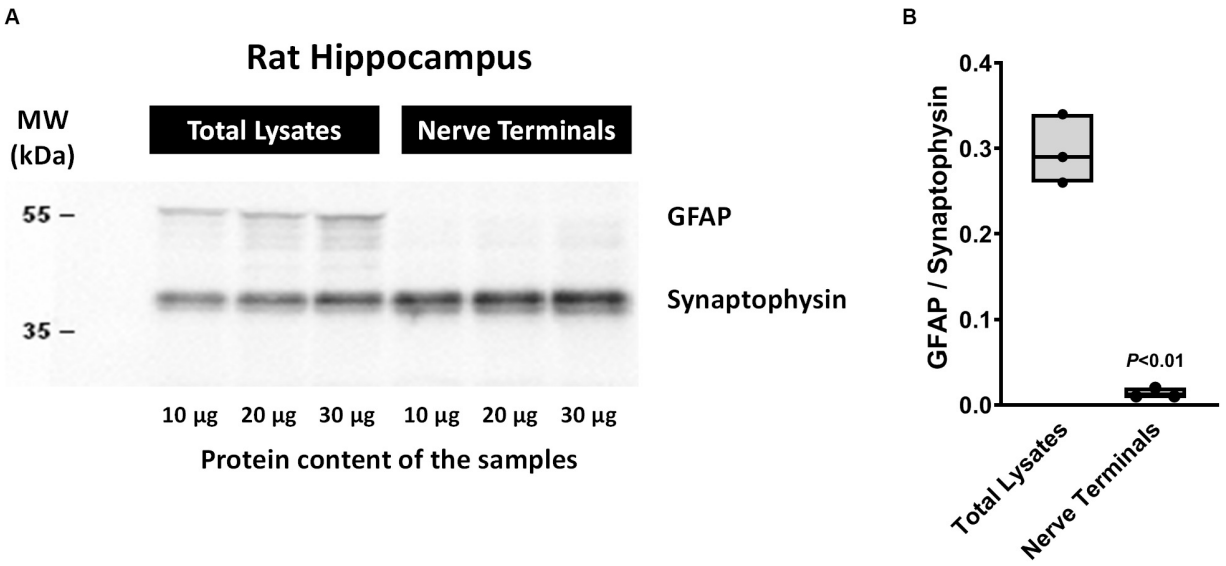

FIGURE 1 | Western blot analysis of synaptophysin and glial fibrillary acidic protein (GFAP) contents in total cell lysates and isolated nerve terminals of the rat hippocampus by the method of Helme-Guizon et al. (1998; method modified in Bancila et al., 2009). Panel **(A)** shows representative immunoblots of three distinct animals loaded with different protein amounts (10, 20, and 30 μg). In panel **(B)** shown are floating bars (min to max, line at median) representing the ratios between GFAP and synaptophysin protein densities obtained in total cell lysates and isolated nerve terminals of three distinct animals. $P < 0.05$ (unpaired Student's *t*-test) represents a significant difference compared to total cell lysates. Please note that under the present experimental conditions synaptophysin-immunoreactivity indicates that rat hippocampal cell fractions are highly enriched in nerve terminals, whereas the lack of GFAP immunoreactivity denotes very little (if at all) contamination by glial subcellular particles (gliosomes).

(**Figure 2Cii**) with a minor effect on [^{3}H]GABA outflow (**Figure 2Ci**). Like that observed in normal Ca^{2+} conditions (**Figure 2Di**), mifepristone (500 nM) blocked more efficiently than spironolactone (500 nM) the basal [^{14}C]Glu outflow promoted by MP (300 μM) in Ca^{2+}-free media (**Figure 2Dii**).

Dissipation of the Na^+ Gradient Across the Plasma Membrane Prevents Facilitation of KCl-Evoked Glu Release by Methylprednisolone, Without Affecting the GABA Outflow

The transmembrane Na^+ gradient is required to take up GABA and Glu from the extracellular milieu by high-affinity amino-acid transporters (GAT1 and EAATs). Substitution of Na^+ with NMDG (128 mM) in the incubation medium transiently increased [^{3}H]GABA and [^{14}C]Glu outflow by rat cortical synaptosomes (see e.g., Wu et al., 2006). Previously, we showed that disruption of the transmembrane Na^+ gradient leading to a reversal of amino-acid transporters to operate in the releasing mode can affect differentially the outflow of [^{3}H]GABA and [^{14}C]Glu (Barros-Barbosa et al., 2018).

Replacement of extracellular Na^+ with NMDG (128 mM) failed to affect KCl-induced [^{3}H]GABA release in the presence of MP (300 μM) (**Figures 4Aii,v**), but it fully prevented the facilitatory effect of the corticosteroid on [^{14}C]Glu outflow, both under resting conditions (**Figures 4Aiv,D**) and during depolarization of hippocampal nerve terminals with high KCl (15 mM) (**Figures 4Aiv,vi**). Taking this into account, we questioned whether blockage of high-affinity EAAT transporters working in the reverse mode with DL-TBOA (100 μM) could also prevent MP (300 μM)-induced facilitation of [^{14}C]Glu release from rat hippocampal nerve terminals. As a matter of fact, DL-TBOA (100 μM) significantly ($P < 0.05$) attenuated the facilitatory effect of MP (300 μM) on [^{14}C]Glu release, both under resting conditions (**Figure 4D**) and during depolarization of rat hippocampal nerve terminals with high KCl (15 mM) (**Figure 4Cii**), a situation that mimicked the effect observed by replacing Na^+ with NMDG (128 mM) in the incubation medium (**Figure 4Avi**). No changes in the coincidental release of [^{3}H]GABA were observed under the latter experimental conditions (**Figures 4Av,Ci**).

Blockade of the ATP-Sensitive P2X7 Receptor Decreases Depolarization-Evoked [^{3}H]GABA Release From Hippocampal Nerve Terminals in the Presence of Methylprednisolone, Without Affecting the Release of [^{14}C]Glu

Previously, our group demonstrated that MP (300 μM) favors the release of ATP from resting motor nerve terminals (Oliveira et al., 2015) and the nucleotide acting via ionotropic P2X7 receptors can differentially affect GABA and Glu release (and uptake) from isolated nerve terminals of the rat cerebral cortex (Barros-Barbosa et al., 2015, 2018). Confocal micrographs depicted in **Figure 5** show that the fairly

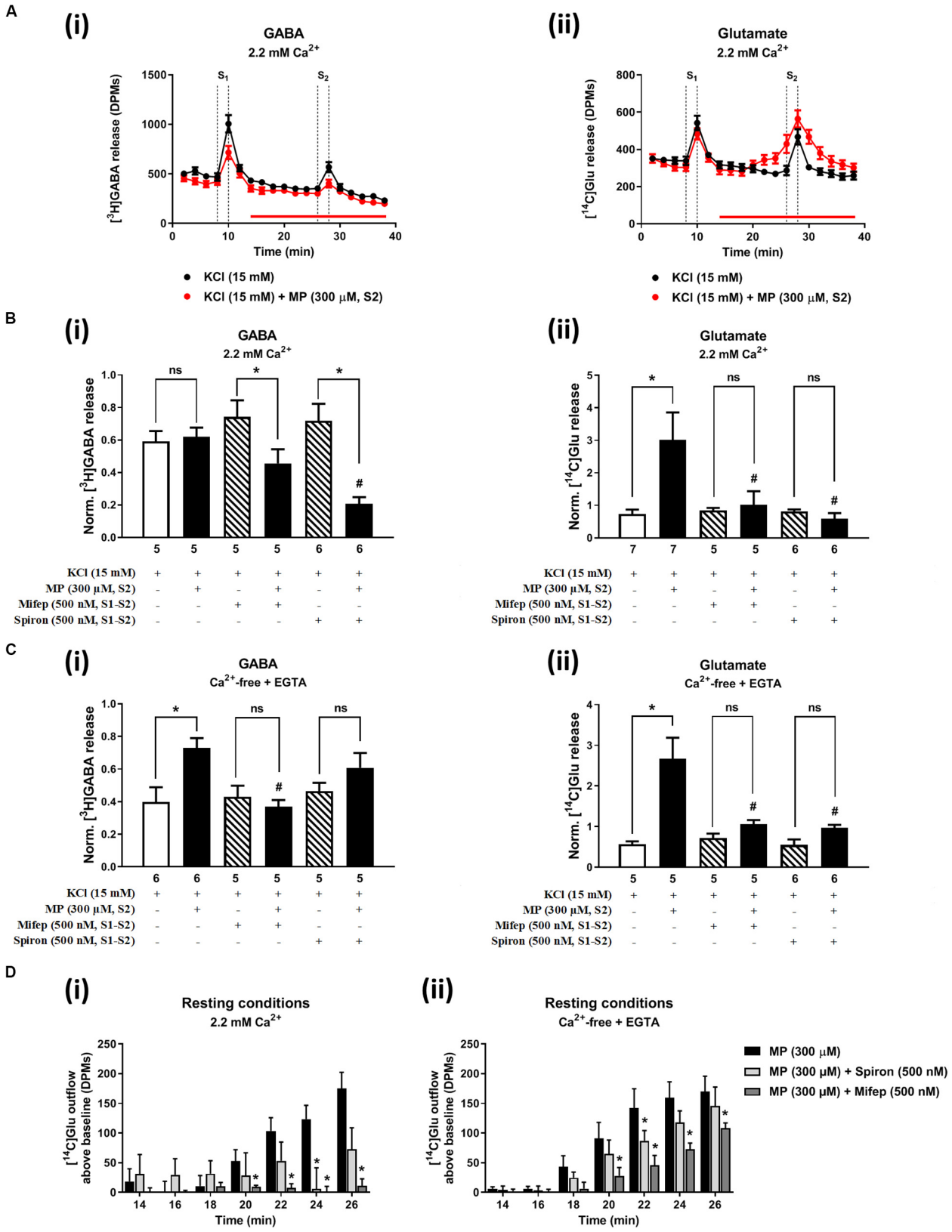

FIGURE 2 | Continued

FIGURE 2 | Methylprednisolone (MP) increases the resting and high KCl-evoked release of [^{14}C]Glu from isolated nerve terminals of the rat hippocampus, without affecting the [^{3}H]GABA outflow. Panel **(A)** shows [^{3}H]GABA **(Ai)** and [^{14}C]glutamate **(Aii)** outflow from rat hippocampal nerve terminals over time; nerve terminals were depolarized twice (S1 and S2) with high KCl (15 mM) applied for 2 min (dotted vertical lines). In panels **(B,C)**, ordinates represent the normalized [^{3}H]GABA **(Bi,Ci)** and [^{14}C]Glu **(Bii,Cii)** release (S2/S1 ratios) from hippocampal nerve terminals depolarized with high KCl (15 mM) in normal Ca^{2+} (2.2 mM, **B**) and in Ca^{2+}-free (plus EGTA, 1 mM, **C**) conditions. MP (300 μM) was applied to the superfusion fluid 15 min before S2 (red horizontal line) either in the absence or in the presence of mifepristone (Mifep, 500 nM) and spironolactone (Spiron, 500 nM); corticosteroid receptor antagonists were present throughout the assay, including S1 and S2. Panel **(D)** illustrates the outflow of [^{14}C]Glu above baseline over time caused by MP (300 μM) in the absence and in the presence of mifepristone (Mifep, 500 nM) or spironolactone (Spiron, 500 nM) in normal Ca^{2+} (2.2 mM, **Di**) and in Ca^{2+}- free (plus EGTA, 1 mM, **Dii**) conditions. The results are expressed as mean ± SEM; the *n*, number of individual experiments per condition is shown below each bar. In panels **(B,C)**, $^{*}P < 0.05$ and $^{\#}P < 0.05$ (one-way ANOVA, uncorrected Fisher's LSD with single pooled variance) represent significant differences compared to control conditions (i.e., drugs in S1 and S2) and to the effect of MP alone, respectively; ns, non-significant; the computed *F* ratios were 5.40 **(Bi)**, 4.05 **(Bii)**, 13.19 **(Ci)** and 6.59 **(Cii)**. In panel **(D)**, $^{*}P < 0.05$ (two-way ANOVA, followed by the Dunnett's multicomparison test) represent significant differences as compared to the effect of MP alone; the computed F ratios for rows (baseline variation) and columns (test groups) were 2.72 and 11.72 for **(Di)** and 26.24 and 12.66 for **(Dii)**, respectively.

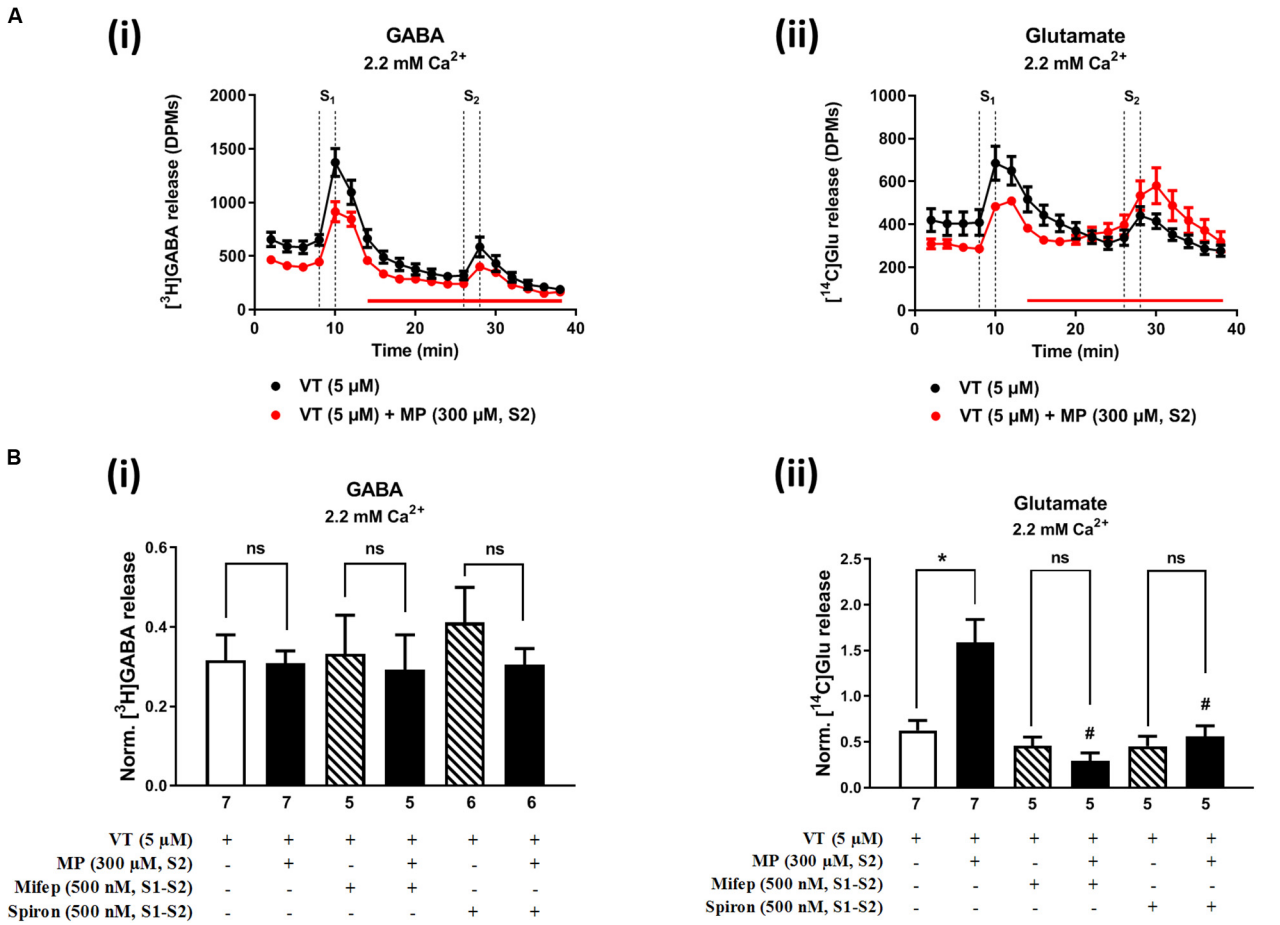

FIGURE 3 | Methylprednisolone (MP) increases VT-evoked release of [^{14}C]Glu from isolated nerve terminals of the rat hippocampus, without affecting the [^{3}H]GABA outflow. Panel **(A)** shows [^{3}H]GABA **(Ai)** and [^{14}C]glutamate **(Aii)** outflow from rat hippocampal nerve terminals over time; nerve terminals were depolarized twice (S1 and S2) with VT (5 μM) applied for 2 min (dotted vertical lines). In panel **(B)**, ordinates represent the normalized [^{3}H]GABA **(Bi)** and [^{14}C]Glu **(Bii)** release (S2/S1 ratio) from hippocampal nerve terminals depolarized with VT (5 μM). MP (300 μM) was applied to the superfusion fluid 15 min before S2 (red horizontal line) either in the absence or in the presence of mifepristone (Mifep, 500 nM) and spironolactone (Spiron, 500 nM); corticosteroid receptor antagonists were present throughout the assay, including S1 and S2. The results are expressed as mean ± SEM; the *n*, number of individual experiments per condition is shown below each bar. In panel **(B)**, $^{*}P < 0.05$ and $^{\#}P < 0.05$ (one-way ANOVA, uncorrected Fisher's LSD with single pooled variance) represent significant differences compared to control conditions (i.e., drugs in S1 and S2) and to the effect of MP alone, respectively; ns, non-significant; the computed *F* ratios were 0.44 **(Bi)** and 10.51 **(Bii)**.

specific antibody against the C-terminal of the rat P2X7 receptor (#APR-004) co-localizes extensively with the synaptic nerve terminal marker, VAMP-1, but no color merge was detected in GFAP-positive astrocytic cells of the rat hippocampus. The co-localization scores assessed by calculating the staining overlap and the Pearson's coefficient (ρ) for each confocal micrograph are

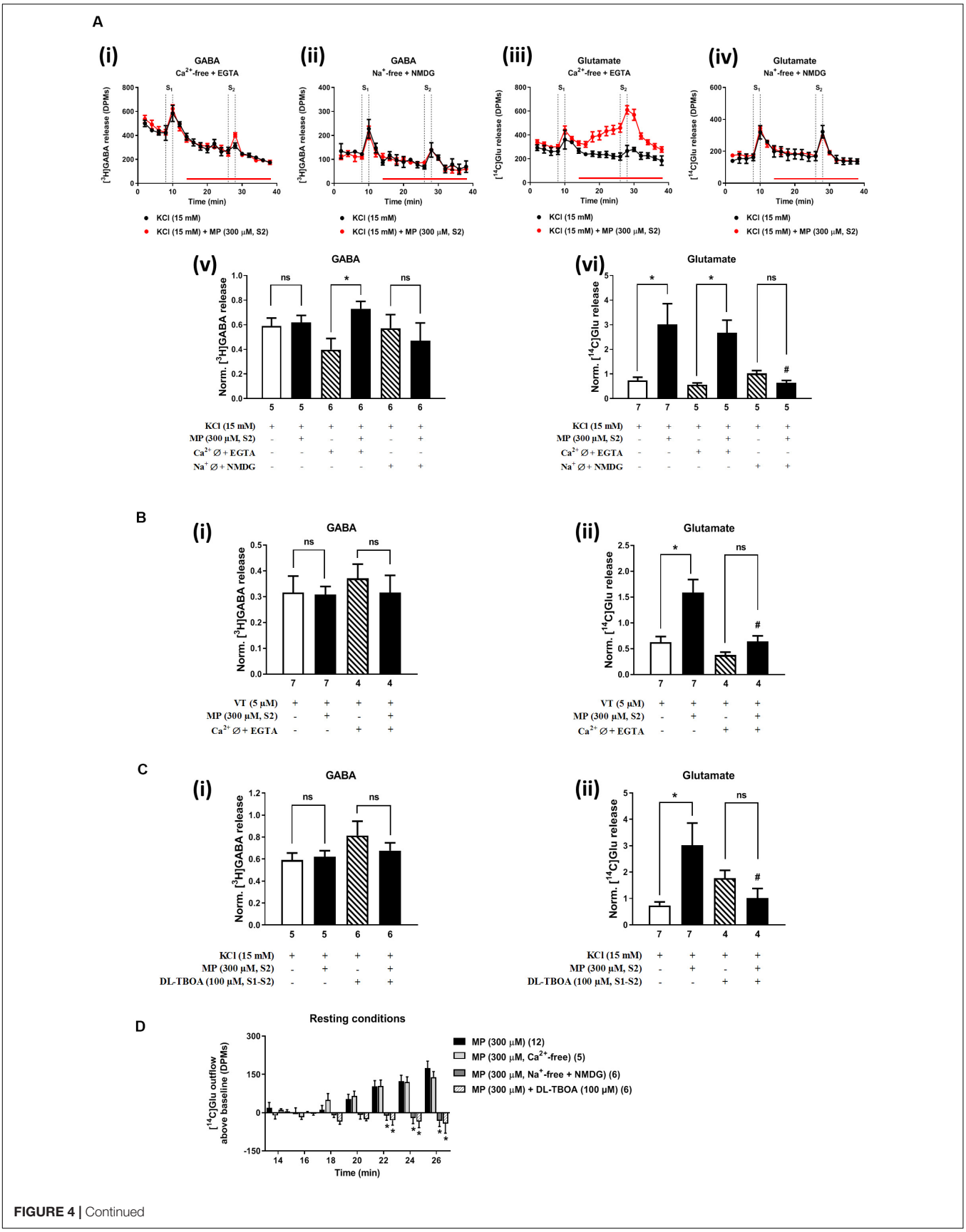

FIGURE 4 | Continued

FIGURE 4 | Influence of Ca^{2+} and Na^{+} withdrawal from the incubation fluid on the facilitatory effect of methylprednisolone (MP) on [^{3}H]GABA and [^{14}C]Glu release from resting and depolarized nerve terminals of the rat hippocampus. In panels **(A–C)**, ordinates represent the normalized [^{3}H]GABA **(i)** and [^{14}C]Glu **(ii)** release (S2/S1 ratio) from hippocampal nerve terminals depolarized with high KCl (15 mM, **A,C**) or VT (5 μM, **B**). MP (300 μM) was applied to the superfusion fluid 15 min before S2; solutions without Ca^{2+} (plus EGTA, 1 mM) or Na^{+} (which was replaced by NMDG, 128 mM) and containing DL-TBOA (100 μM) were applied from the beginning of sample collection, so that they were present throughout the assay, including S1 and S2. Panel **(D)** illustrates the outflow of [^{14}C]Glu above baseline over time caused by MP (300 μM) in the absence and in the presence of superfusion solutions containing no added Ca^{2+} (plus EGTA, 1 mM), no added Na^{+} (replaced by NMDG, 128 mM) and DL-TBOA (100 μM). The results are expressed as mean ± SEM; the *n*, number of individual experiments per condition is shown below each bar. In panels **(A–C)**, $^{*}P < 0.05$ and $^{\#}P < 0.05$ (one-way ANOVA, uncorrected Fisher's LSD with single pooled variance) represent significant differences compared to control conditions (i.e., Ca^{2+}-/Na^{+}-free conditions or DL-TBOA in S1 and S2) and to the effect of MP alone, respectively; ns, non-significant; the computed *F* ratios were 1.01 **(Av)**, 4.36 **(Avi)**, 0.36 **(Bi)**, 12.67 **(Bii)**, 1.22 **(Ci)** and 3.25 **(Cii)**. In panel **(D)**, $^{*}P < 0.05$ (two-way ANOVA, followed by the Dunnett's multicomparison test) represent significant differences as compared to the effect of MP in control conditions; the computed F ratios for rows (baseline variation) and columns (test groups) were 3.51 and 26.14, respectively.

in agreement with our findings in the rat cerebral cortex (Barros-Barbosa et al., 2015), thus confirming that the P2X7 receptor is present on nerve terminals of the various sub-regions of the rat hippocampus, namely CA1, CA2, CA3 and dentate gyrus (**Figure 5**). This prompted us to test the effect of MP (300 μM) on [^{3}H]GABA and [^{14}C]Glu release measured synchronously from isolated nerve terminals of the rat hippocampus in the presence of a selective P2X7 receptor antagonist, A-438079.

On its own, A-438079 (3 μM) was unable to modify ($P > 0.05$) the release of [^{3}H]GABA and [^{14}C]Glu from isolated nerve terminals depolarized with VT (5 μM) (**Figure 6A**) and high KCl (15 mM) (**Figure 6B**); the S2/S1 ratio of KCl-induced [^{3}H]GABA and [^{14}C]Glu release when A-438079 (3 μM) was applied 15 min before S2 was 0.52 ± 0.05 (vs. a control of 0.59 ± 0.08, $n = 6$; $P > 0.05$) and 0.78 ± 0.15 (vs. a control of 0.72 ± 0.15, $n = 6$; $P > 0.05$), respectively. Blockage of the P2X7 receptor with A-438079 (3 μM) attenuated ($P < 0.05$) VT- and high KCl-induced [^{3}H]GABA release from hippocampal nerve terminals challenged with MP (300 μM), without affecting the coincidental release of [^{14}C]Glu (**Figures 6A,B**, respectively). More interestingly, pre-treatment with A-438079 (3 μM) abolished MP (300 μM)-induced facilitation of [^{3}H]GABA release from KCl-depolarized nerve terminals in Ca^{2+}-free conditions (**Figure 6Ci**), without affecting the facilitatory effect of the corticoid on [^{14}C]Glu release, both under resting conditions (**Figure 6D**) and during depolarization of rat hippocampal nerve terminals with high KCl (15 mM) (**Figure 6Cii**).

The P2X7 receptor agonist, 2′(3′)-*O*-(4-benzoylbenzoyl)ATP (BzATP, 300 μM), increased from 0.86 ± 0.07 to 1.16 ± 0.08 ($n = 6$, $P < 0.05$) the release of [^{3}H]GABA from hippocampal nerve terminals depolarized with high KCl in normal external Ca^{2+} conditions, but this effect was not observed regarding the release of [^{14}C]Glu (data not shown). The facilitatory effect of BzATP (300 μM) on KCl-induced [^{3}H]GABA release was prevented by A-438079 (3 μM, 0.78 ± 0.08, $n = 6$), thus confirming the involvement of ATP-sensitive P2X7 receptors.

In a previous study, we demonstrated (1) that the facilitatory action of the ionotropic P2X7 receptor is enhanced after removal of Ca^{2+} from incubation media (like that observed here with MP; see **Figures 2Ci**, **4Av**), and (2) that under Ca^{2+}-free conditions the release of [^{3}H]GABA results mainly from the collapse of the transmembrane Na^{+} gradient and, subsequent, reversal of the GAT-1-mediated transport (Barros-Barbosa et al., 2018). **Figure 7** shows that inhibition of GAT-1 with SKF 89976A (40 μM) significantly ($P < 0.05$) attenuated BzATP (300 μM)-induced facilitation of [^{3}H]GABA release from KCl-depolarized hippocampal nerve terminals in Ca^{2+}-free conditions (**Figures 7Ai,Bi**), without affecting facilitation of [^{14}C]Glu release by the nucleotide (**Figures 7Aii,Bii**). SKF 89976A (40 μM) mimicked the inhibitory effect of the P2X7 receptor antagonist, A-438079 (3 μM), on MP (300 μM)-induced facilitation of [^{3}H]GABA release under similar experimental conditions (**Figures 7Ai,Bi**).

DISCUSSION

Data show here for the first time that MP favors the release of [^{14}C]Glu both from resting as well as from depolarized nerve terminals of the adult rat hippocampus, with no effect on the coincidental release of [^{3}H]GABA under physiological conditions. The mechanism underlying facilitation of [^{14}C]Glu release by MP has several important features. First, it involves the putative activation of membrane-bound corticosteroid receptors sensitive to mifepristone and spironolactone. Second, MP causes a progressive increase in [^{14}C]Glu outflow starting immediately (within a few minutes) after application of the corticosteroid, which is compatible with a fast non-genomic effect. Third, facilitation of evoked [^{14}C]Glu release is relatively independent of the depolarizing agent, either high KCl or VT. Fourth, MP-induced [^{14}C]Glu release is abrogated by dissipation of the Na^{+} gradient across the plasma membrane, but is little affected by changes in extracellular Ca^{2+}, suggesting that it results from non-vesicular release operated by Na^{+}-sensitive high-affinity EAAT transporters working in the reverse mode. The molecular mechanism responsible for this new working hypothesis has no parallel in the literature and certainly deserve to be explored in future studies. Regarding depolarization-evoked [^{3}H]GABA release in the presence of MP, data indicate that it may involve a yet unraveled (direct or indirect) interplay between low affinity GR and P2X7 receptors activation taking into consideration the inhibitory effects obtained with mifepristone and A-438079, respectively, and the fact that it is relatively sensitive to removal of Ca^{2+}, but not Na^{+}, from the incubation medium.

Corticosteroid alterations of neuronal excitability throughout the brain have been mostly attributed to fast non-genomic effects (Di et al., 2003, 2005, 2009; Karst et al., 2005; Groc et al., 2008; Groeneweg et al., 2012). This theory is supported

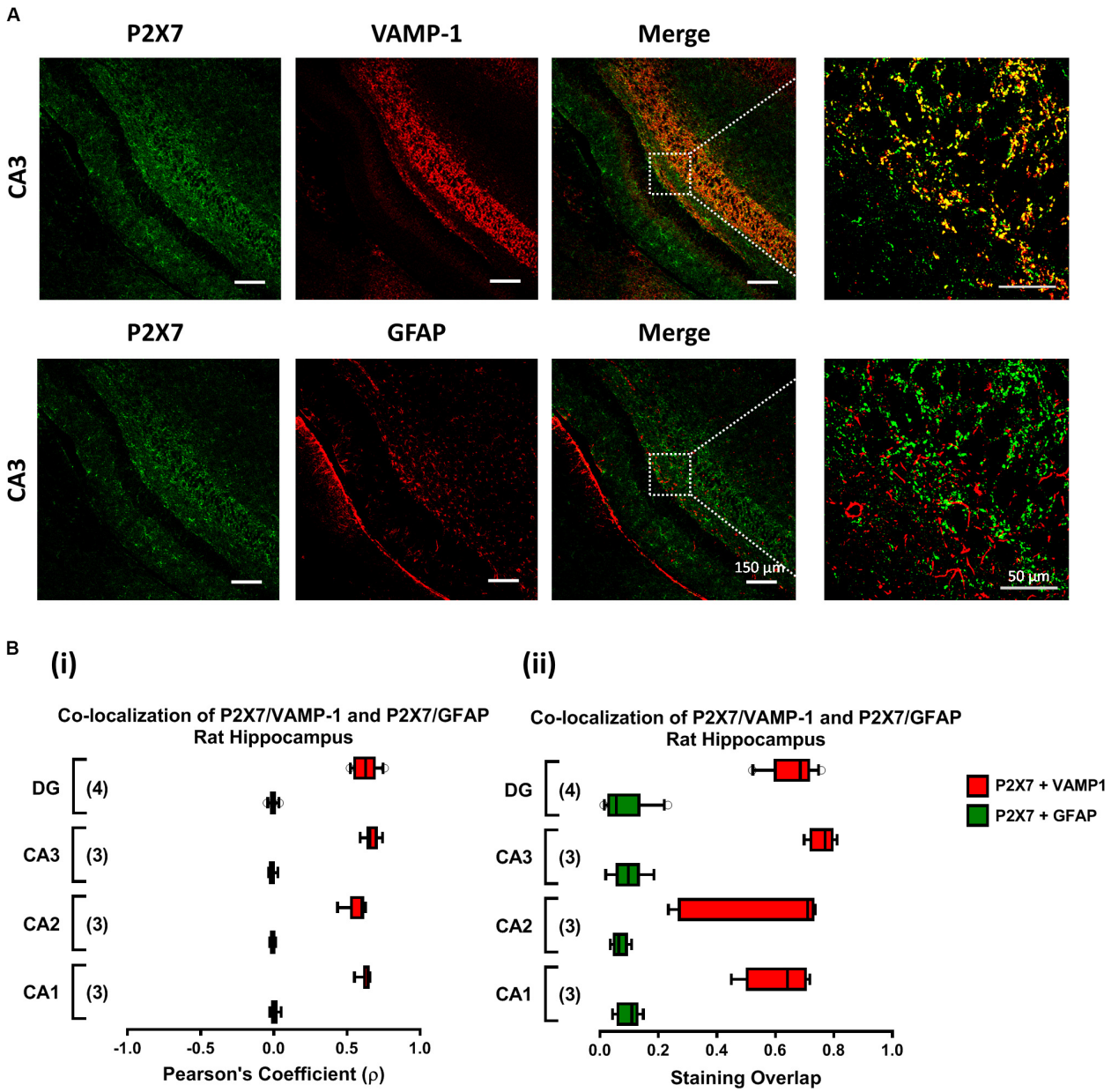

FIGURE 5 | The P2X7 receptor is present predominantly on nerve terminals of the rat hippocampus. Panel **(A)** shows the immunolocalization of the P2X7 receptor in confocal micrographs of the CA3 region of rat hippocampal slices (scale bar = 150 μm); right hand-side panels show higher magnification images zoomed from the indicated regions (scale bar = 50 μm). Synaptic nerve terminals are stained with the vesicle-associated membrane protein 1 (VAMP-1 or synaptobrevin 1) and astrocytes are labeled with the glial fibrillary acidic protein (GFAP). Data show that the P2X7 receptor (green) localizes predominantly in VAMP-1-positive synaptic nerve terminals (upper panels), but not in cells positively staining with GFAP (lower panels); yellow staining denotes co-localization of P2X7 receptors (green) and type-specific cell markers (red). In panel **(B)**, fluorescence intensity scatter plots were used to estimate staining co-localization by calculating the Pearson's Coefficient (ρ, **Bi**) and the staining overlap **(Bii)** scores; represented are "box-and-whiskers" graphs plotting data from three to four individuals performed in triplicate. These parameters were automatically calculated per image and were used to quantify the colocalization of the P2X7 receptor either with VAMP-1 or with GFAP (yellow staining) in different hippocampal subregions, namely CA1, CA2, CA3 and dentate gyrus (DG).

by our data considering (1) the (min) timescale required to observe changes in [^{14}C]Glu release and (2) the fact that we have used synaptophysin-enriched isolated nerve terminals remaining after rejecting the nucleated neuronal cell bodies and GFAP-positive glial cells of the rat hippocampus, which otherwise can confound data interpretation in whole cell preparations. The involvement of plasma membrane-bound GR and MR is highly likely because these receptors can be blocked by mifepristone and spironolactone, respectively, and both receptors were previously identified by electron microscopy in synaptosomal extracts and

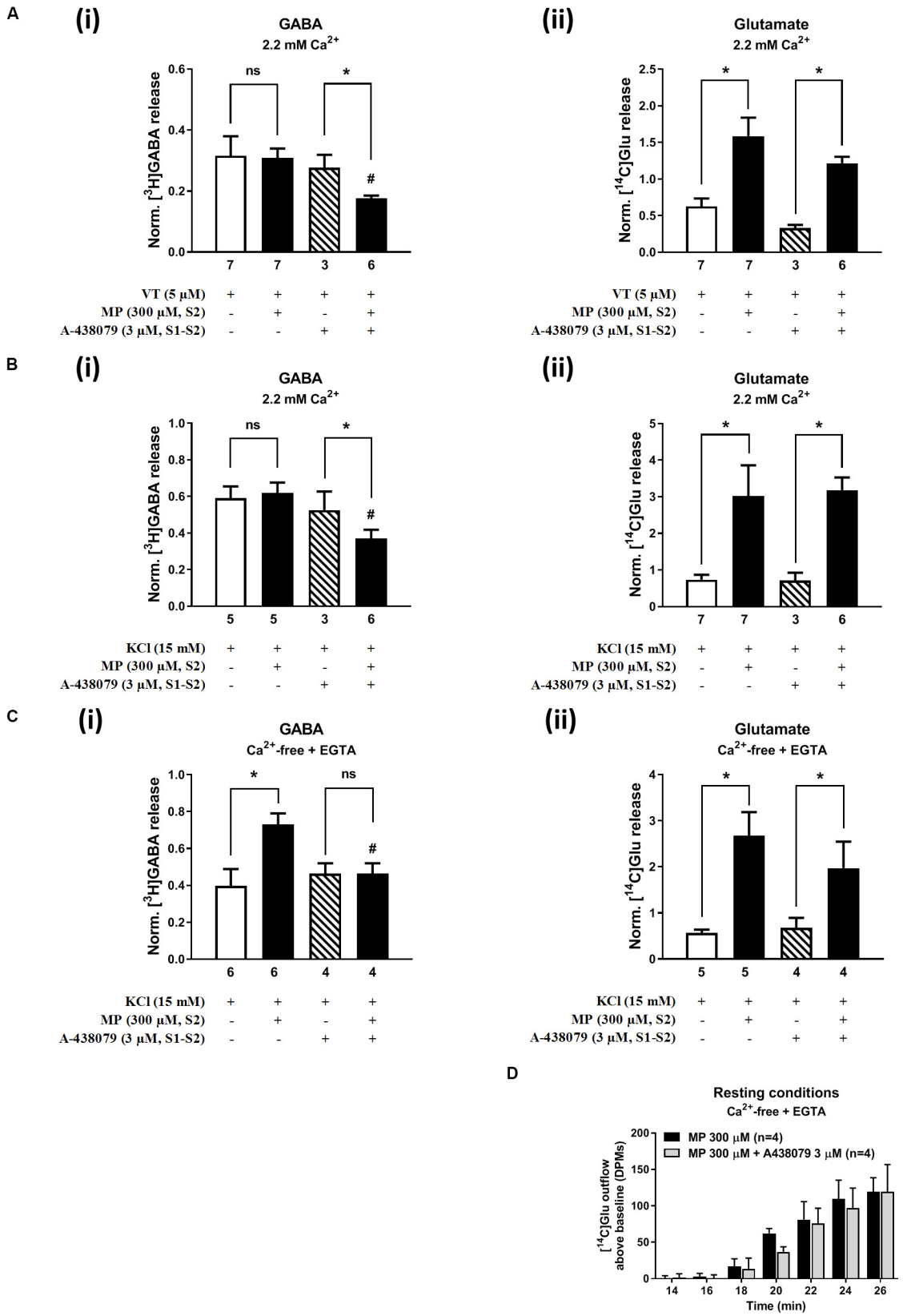

FIGURE 6 | Continued

FIGURE 6 | Blockage of the ATP-sensitive P2X7 receptor decreases depolarization-evoked [^{3}H]GABA release from hippocampal nerve terminals in the presence of methylprednisolone (MP), without affecting the release of [^{14}C]Glu. In panels **(A–C)**, ordinates represent the normalized [^{3}H]GABA **(i)** and [^{14}C]Glu **(ii)** release (S2/S1 ratio) from hippocampal nerve terminals depolarized with VT (5 μM, **A**) and high KCl (15 mM) applied in normal Ca^{2+} (2.2 mM, **B**) conditions and after removing Ca^{2+} (plus EGTA, 1 mM, **C**) from the incubation medium. MP (300 μM) was applied to the superfusion fluid 15 min before S2; the P2X7 receptor antagonist, A-438079 (3 μM), was present throughout the assay, including S1 and S2. Panel **(D)** illustrates the outflow of [^{14}C]Glu above baseline over time caused by MP (300 μM) in the absence and in the presence of A-438079 (3 μM) in Ca^{2+}-free (plus EGTA, 1 mM) conditions. The results are expressed as mean ± SEM; the n number of individual experiments per condition is shown below each bar. In panels **(A–C)**, $^*P < 0.05$ and $^{\#}P < 0.05$ (one-way ANOVA, uncorrected Fisher's LSD with single pooled variance) represent significant differences compared to control conditions (i.e., drugs in S1 and S2) and to the effect of MP alone, respectively; ns, non-significant; the computed *F* ratios were 2.35 **(Ai)**, 3.35 **(Aii)**, 2.27 **(Bi)**, 12.39 **(Bii)**, 4.26 **(Ci)**, and 8.94 **(Cii)**. In panel **(D)**, $^*P < 0.05$ (unpaired Student's *t*-test, corrected for multiple comparisons using the Holm–Sidak method) represent significant differences as compared to the effect of MP alone.

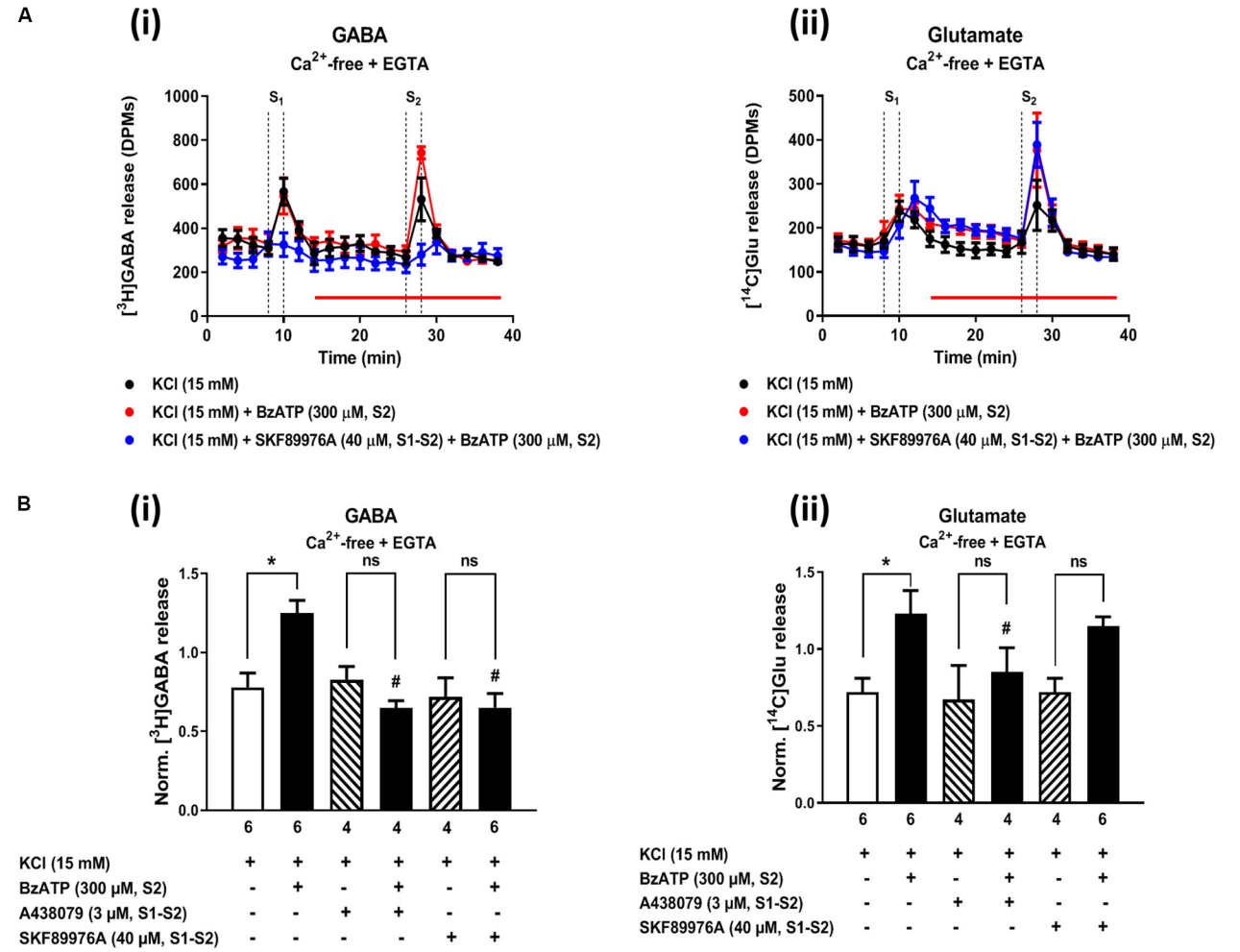

FIGURE 7 | Activation of the P2X7 receptor with BzATP increases KCl-evoked [^{3}H]GABA and [^{14}C]Glu release from hippocampal nerve terminals in Ca^{2+}-free conditions. Panel **(A)** shows [^{3}H]GABA **(Ai)** and [^{14}C]Glu **(Aii)** outflow from rat hippocampal nerve terminals over time in Ca^{2+}-free (plus EGTA, 1 mM) conditions; nerve terminals were depolarized twice (S1 and S2) with high KCl (15 mM) applied for 2 min (dotted vertical lines). BzATP (300 μM) was applied to the superfusion fluid 15 min before S2 (red horizontal line) either in the absence or in the presence of the GAT-1 transport inhibitor, SKF 89976A (40 μM), or the P2X7 receptor antagonist, A-438079 (3 μM), which were present throughout the assay, including S1 and S2. In panel **(B)**, ordinates represent the normalized [^{3}H]GABA **(Bi)** and [^{14}C]Glu **(Bii)** release (S2/S1 ratio) from depolarized hippocampal nerve terminals in Ca^{2+}-free conditions (plus EGTA, 1 mM). The results are expressed as mean ± SEM; the *n*, number of individual experiments per condition is shown below each bar. $^*P < 0.05$ and $^{\#}P < 0.05$ (one-way ANOVA, uncorrected Fisher's LSD with single pooled variance) represent significant differences compared to control conditions (i.e., drugs in S1 and S2) and to the effect of BzATP alone, respectively; ns, non-significant; the computed *F* ratios were 7.19 **(Bi)** and 3.94 **(Bii)**.

neuronal membranes of several brain regions (Johnson et al., 2005; Groeneweg et al., 2012), including the rat hippocampus (Wang and Wang, 2009). In keeping with our assumption, others have found that the facilitatory effect of corticosterone (and its cell impermeable conjugate with bovine serum albumin) on depolarization-induced [^{14}C]Glu release in the hippocampus

was also blocked by mifepristone (Karst et al., 2005; Wang and Wang, 2009), as well as by spironolactone (Groc et al., 2008). Notwithstanding these facts, the presence of functional GR receptors in the plasma membrane have been questioned mostly because these receptors have not yet been cloned and their downstream signaling pathways are still unknown.

In our hands, MP-induced increase in basal [^{14}C]Glu release was mimicked by the five-fold more potent GR agonist, dexamethasone, and it was more sensitive to blockage with mifepristone than with spironolactone, suggesting a predominant role of low affinity GRs on adult rat hippocampal nerve terminals acting to facilitate glutamate release (see also e.g., Wang and Wang, 2009). Prevention of MP-induced facilitation of [^{14}C]Glu release from depolarized nerve terminals by both corticosteroid antagonists raises questions about the selectivity of spironolactone (500 nM) for high affinity MR and whether it can also perturb the action of coexisting low affinity GR that more likely facilitate hippocampal glutamate transmission (Groc et al., 2008). The way GRs activation might cause reversal of DL-TBOA-sensitive Na^+-dependent EAAT transporters in order to release [^{14}C]Glu from pre-synaptic nerve terminals is still unknown, but it certainly deserves attention in future studies.

To the best of our knowledge, this is the first study reporting effects of corticosteroids, namely MP, on [^{3}H]GABA release from hippocampal nerve terminals measured in parallel and under the same experimental conditions as those used to quantify the release of [^{14}C]Glu. However, in contrast to the more straightforward excitatory effect of MP on [^{14}C]Glu outflow, MP-induced facilitation of [^{3}H]GABA release was only evident when rat hippocampal nerve terminals were depolarized with high KCl (but not VT) in external Ca^{2+}-free conditions (see **Figures 2C**, **4Av**), a situation that is very similar to that verified after paroxysmal neuronal activity (e.g., epileptic crises) where the extracellular concentration of Ca^{2+} falls by more than 90% (Engelborghs K. et al., 2000; Engelborghs S. et al., 2000). Although under normal Ca^{2+} conditions MP failed to affect GABA outflow, unexpectedly the amount of [^{3}H]GABA released during depolarization of hippocampal nerve terminals in the presence of MP was significantly reduced upon blocking either MRs with spironolactone or ATP-sensitive ionotropic P2X7 receptors with A-438079. We have so far no reasonable explanation to these experimental findings, but somehow blockage of MR and P2X7 receptors may unbalance depolarization-induced [^{3}H]GABA release in the presence of the corticoid decreasing the transmitter release probability when external Ca^{2+} is available, but not in stressful (low Ca^{2+}) conditions. One may hypothesize that MP might favor opening of the ATP-sensitive P2X7 receptor pore by a yet unknown mechanism leading to Na^+ influx into hippocampal nerve terminals and, subsequent, disruption of the transmembrane Na^+ gradient differentially affecting GABA and Glu release, as previously demonstrated (Barros-Barbosa et al., 2018). The preferring effect of the P2X7 receptor on [^{3}H]GABA release was confirmed using the ATP analog, BzATP, and might involve reversal of the neuronal GAT1 transporter sensitive to SKF 89976A (see e.g., Sperlágh et al., 2002), a situation that is much more likely to occur in the absence of external Ca^{2+} (Barros-Barbosa et al., 2018). The higher sensitivity for GABA than for Glu release under low Ca^{2+} conditions is probably because the GAT1 reversal potential is close to the resting potential of the neuronal membrane (Zerangue and Kavanaugh, 1996; Richerson and Wu, 2003; Allen et al., 2004; Wu et al., 2006).

Although it is generally assumed that low extracellular Ca^{2+} reduces vesicular exocytosis of neurotransmitters, an inverse correlation between Ca^{2+} concentration in the extracellular fluid and depolarization-evoked amino-acid transmitters release may be observed (see e.g., Levi et al., 1980; Cunningham and Neal, 1981; Minc-Golomb et al., 1988; Santos and Rodriguez, 1992; Rassner et al., 2016; Barros-Barbosa et al., 2018). While [^{3}H]GABA release may be operated by a Ca^{2+}-dependent pathway when extracellular Ca^{2+} is available, this mechanism may shift toward the reversal of the GAT1 transporter in low Ca^{2+} conditions (Barros-Barbosa et al., 2018; see also **Figure 7**) and, thus, became potentiated by GRs activation with MP. A different scenario is verified regarding the release of [^{14}C]Glu, since the facilitatory effect of MP was consistently verified both in the absence and in the presence of external Ca^{2+}, except when hippocampal nerve terminals were depolarized by the Na^+ channel activator, VT, which keeps the channel pore persistently opened.

This new vision regarding the molecular mechanisms underlying the differential role of corticosteroids, namely MP, on amino-acid transmitters release, together with the fact that hippocampal neurons abundantly express both MRs and GRs (Karst et al., 2005; Joëls et al., 2012), may impact on the rationale for designing new strategies for better treatment of pathological conditions affecting the hippocampus, specifically drug-refractory epilepsy, post-traumatic stress, memory deficits and neurodegenerative diseases. In a recent study from our group, it was proposed that low doses of MP given for a short period of time favored *in vivo* aversive memory persistence and this was correlated with significant gains in *in vitro* hippocampal LTP (de Vargas et al., 2017). Hippocampal LTP is highly dependent on neuronal plasticity phenomena that are commonly associated with glutamatergic neurotransmission strengthening. We demonstrate here that MP significantly increases the neuronal release of [^{14}C]Glu, both during resting and upon depolarization of hippocampal nerve terminals, without significantly affecting the release of the inhibitory neurotransmitter. Fast (non-genomic) onset enhancement of glutamatergic neurotransmission has also been observed in the CA1 hippocampal area (Karst et al., 2005). Strengthening of glutamatergic synaptic potentiation by reversibly increasing AMPA receptor-mediated miniature excitatory postsynaptic current (mEPSC) frequency was also verified by other authors upon application of corticosterone (and its membrane-impermeable conjugate with bovine serum albumin) to CA1 pyramidal neurons (Groc et al., 2008; see also Karst et al., 2005). Likewise, low nanomolar concentrations of corticosterone rapidly increased GluR2-AMPAR surface diffusion at the post-synaptic region also favoring glutamatergic synaptic potentiation.

Data from the present study clearly indicate that MP increased the release of [^{14}C]Glu both under resting conditions and during depolarization of hippocampal nerve terminals from adult rats. The closest mention we could found about spontaneous glutamate release induced by steroid hormones was in few reports showing that pregnenolone sulfate (PREGS; a neuroactive steroid hormone) dose-dependently increased the frequency of mEPSCs in immature neurons of the hippocampus (Meyer et al., 2002; Chen and Sokabe, 2005; Mameli et al., 2005), yet no direct assessment to glutamate release has been reported in the hippocampus of adult animals. Evidence that resting [^{14}C]Glu release induced by MP is Na^+-dependent, yet Ca^{2+}-independent, is in favor of the participation of DL-TBOA-sensitive Na^+-dependent high-affinity EAAT membrane transporters operating in the reverse mode, which is a novelty provided by our study.

Our group demonstrated that at the cholinergic neuromuscular synapse MP facilitates acetylcholine release indirectly by increasing ATP release and, subsequent, adenosine formation resulting in increased activation of facilitatory A_{2A} receptors (Oliveira et al., 2015). On its own, steroids may induce rapid (non-genomic) gating of several ionotropic receptors, including ATP-sensitive P2X receptors (Codocedo et al., 2009). Interestingly, synthetic testosterone derivatives have been shown to positively modulate the activity of P2X2 and P2X4, but not P2X7, receptors in heterologous systems (see e.g., Sivcev et al., 2019). It remains, however, to be elucidated whether (1) MP can allosteric modulate ATP-induced P2X7 receptor gating, and if (2) the putative allosteric binding site for MP at the P2X7 receptor pore is specifically inhibited by GR antagonists. We are also aware that steroids may activate plasma membrane receptors coupled to G proteins (Mizota et al., 2005; Schiess and Partridge, 2005), which may directly or indirectly modify ATP-gated P2X receptor currents via downstream intracellular signaling pathways. Notwithstanding the fact that we did not prove that MP induced the release of ATP, which by acting via low affinity ionotropic P2X7 receptors may favor transmitters outflow from rat hippocampal nerve terminals, the P2X7 receptor antagonist, A-438079, significantly attenuated depolarization-evoked [^{3}H]GABA, but not [^{14}C]Glu, release in the presence of MP. This result is in keeping with previous findings in nerve terminals of the rat cerebral cortex showing that the P2X7 receptor activation unbalances GABAergic vs. glutamatergic neurotransmission by differentially affecting high affinity [^{3}H]GABA and [^{14}C]Glu uptake (Barros-Barbosa et al., 2015) and release (Barros-Barbosa et al., 2018) in an extracellular Ca^{2+}-sensitive manner. Under the present experimental conditions, isolated nerve terminals of the rat hippocampus are the only possible source of endogenous ATP required to activate P2X7 receptors in the presence of MP.

Despite activation of hippocampal P2X7 receptor has been implicated in physiological processes, such as learning and memory, it may gain a different meaning under pathological conditions, such as meso-temporal lobe epilepsy, where the expression of this receptor is upregulated (Jimenez-Pacheco et al., 2013; Barros-Barbosa et al., 2016). Thus, strengthening the inhibitory GABAergic neurotransmission, without significantly affecting Glu release, by P2X7 receptor activation triggered by corticosteroid receptors may become apparent during paroxysmal neuronal firing where extracellular Ca^{2+} is low (Engelborghs K. et al., 2000; Engelborghs S. et al., 2000). We foresee that these previously unpredicted differential roles of corticosteroids on GABA and glutamate release may change our therapeutic approach to improve cognition and to avoid detrimental neuroexcitotoxicity in drug-refractory epilepsy and other neurological conditions. Thus, facilitation of Glu release strengthen previous assumptions that MP may act as a cognitive enhancer, while crosstalk with overexpressed ATP-sensitive P2X7 receptors may provide therapeutic benefits by increasing the GABAergic inhibitory drive during paroxysmal epileptic crisis and/or neuroinflammatory insults of the adult brain.

DATA AVAILABILITY STATEMENT

All datasets generated for this study are included in the article/supplementary material.

ETHICS STATEMENT

The animal study was reviewed and approved by the Ethics Committee and the Animal Welfare Responsible Organism of ICBAS-UP (Decision no 224/2017).

AUTHOR CONTRIBUTIONS

PC-d-S supervised the project. RN, ML, and PC-d-S designed the experiments. RN and PC-d-S wrote the manuscript. RN, AC-R, FF, and ML carried out the experimental work. RN, AC-R, FF, ML, and PC-d-S interpreted data and commented on the manuscript at all stages. All authors contributed to the article and approved the submitted version.

FUNDING

This work was supported by Foundation for Science and Technology (FCT) (P2020 - LISBOA-01-0145-FEDER-028311, UID/BIM/4308/2016, UID/BIM/4308/2019, and UIDP/04308/2020). The funders had no role in study design, data collection and analysis, decision to publish, or preparation of the manuscript.

ACKNOWLEDGMENTS

The authors acknowledge the participation of Ms. Tatiana Ventura and Aurora Barros-Barbosa in some of the experiments. They also thank Mrs. Helena Costa e Silva, Belmira Silva, and Helena Oliveira for their valuable technical assistance.

REFERENCES

Adam-Vizi, V., and Ligeti, E. (1986). Calcium uptake of rat brain synaptosomes as a function of membrane potential under different depolarizing conditions. *J. Physiol.* 372, 363–377. doi: 10.1113/jphysiol.1986.sp016013

Allen, N. J., Karádóttir, R., and Attwell, D. (2004). Reversal or reduction of glutamate and GABA transport in CNS pathology and therapy. *Pflug. Arch.* 449, 132–142. doi: 10.1007/s00424-004-1318-x

Bancila, V., Cordeiro, J. M., Bloc, A., and Dunant, Y. (2009). Nicotine-induced and depolarisation-induced glutamate release from hippocampus mossy fibre synaptosomes: two distinct mechanisms. *J. Neurochem.* 110, 570–580. doi: 10.1111/j.1471-4159.2009.06169.x

Barros-Barbosa, A. R., Fonseca, A. L., Guerra-Gomes, S., Ferreirinha, F., Santos, A., Rangel, R., et al. (2016). Up-regulation of P2X7 receptor-mediated inhibition of GABA uptake by nerve terminals of the human epileptic neocortex. *Epilepsia* 57, 99–110. doi: 10.1111/epi.13263

Barros-Barbosa, A. R., Lobo, M. G., Correia-de-s, P., and Cordeiro, J. M. (2018). Under stressful conditions activation of the ionotropic P2X7 receptor differentially regulates GABA and glutamate release from nerve terminals of the rat cerebral cortex. *Neurochem. Int.* 112, 81–95. doi: 10.1016/j.neuint.2017.11.005

Barros-Barbosa, A. R., Lobo, M. G., Ferreirinha, F., Correia-de-Sá, P., and Cordeiro, J. M. (2015). P2X7 receptor activation downmodulates Na+-dependent high-affinity GABA and glutamate transport into rat brain cortex synaptosomes. *Neuroscience* 306, 74–90. doi: 10.1016/j.neuroscience.2015.08.026

Bartholome, B., Spies, C. M., Gaber, T., Schuchmann, S., Berki, T., Kunkel, D., et al. (2004). Membrane glucocorticoid receptors (mGCR) are expressed in normal human peripheral blood mononuclear cells and up-regulated after in vitro stimulation and in patients with rheumatoid arthritis. *FASEB J.* 18, 70–80. doi: 10.1096/fj.03-0328com

Bast, T., Richter, S., Ebinger, F., Rating, D., Wiemer-kruel, A., and Schubert-bast, S. (2014). Efficacy and tolerability of methylprednisolone pulse therapy in childhood epilepsies other than infantile spasms. *Neuropediatrics* 45, 378–385. doi: 10.1055/s-0034-1387817

Chen, L., and Sokabe, M. (2005). Presynaptic modulation of synaptic transmission by pregnenolone sulfate as studied by optical recordings. *J. Neurophysiol.* 94, 4131–4144. doi: 10.1152/jn.00755.2004

Codocedo, J. F., Rodríguez, F. E., and Huidobro-Toro, J. P. (2009). Neurosteroids differentially modulate P2X ATP-gated channels through non-genomic interactions. *J, Neurochem.* 110, 734–744. doi: 10.1111/j.1471-4159.2009.06166.x

Costa, J., Lobo, M. G., and Correia-de-Sá, P. (2006). Paradoxical nifedipine facilitation of 45Ca uptake into rat hippocampal synaptosomes. *Eur. J. Pharmacol.* 544, 39–48. doi: 10.1016/j.ejphar.2006.06.040

Cunningham, J., and Neal, M. J. (1981). On the mechanism by which veratridine causes a calcium-dependent release of gamma-aminobutyric acid from brain slices. *Br. J. Pharmac.* 73, 655–667. doi: 10.1111/j.1476-5381.1981.tb16801.x

de Vargas, L., da, S., Gonçalves, R., Lara, M. V. S., Costa-Ferro, Z. S. M., Salamoni, S. D., et al. (2017). Methylprednisolone as a memory enhancer in rats: effects on aversive memory, long-term potentiation and calcium influx. *Brain Res.* 1670, 44–51. doi: 10.1016/j.brainres.2017.06.007

Di, S., Malcher-Lopes, R., Halmos, K. C., and Tasker, J. G. (2003). Nongenomic glucocorticoid inhibition via endocannabinoid release in the hypothalamus: a fast feedback mechanism. *J. Neurosci.* 23, 4850–4857. doi: 10.1523/jneurosci.23-12-04850.2003

Di, S., Malcher-Lopes, R., Marcheselli, V. L., Bazan, N. G., and Tasker, J. G. (2005). Rapid glucocorticoid-mediated endocannabinoid release and opposing regulation of glutamate and γ-aminobutyric acid inputs to hypothalamic magnocellular neurons. *Endocrinology* 146, 4292–4301. doi: 10.1210/en.2005-0610

Di, S., Maxson, M. M., Franco, A., and Tasker, J. G. (2009). Glucocorticoids regulate glutamate and GABA synapse-specific retrograde transmission via divergent non-genomic signaling pathways. *J. Neurosci.* 29, 393–401. doi: 10.1523/jneurosci.4546-08.2009

Diamond, D. M., Bennett, M. C., Fleshner, M., and Rose, G. M. (1992). Inverted-U relationship between the level of peripheral corticosterone and the magnitude of hippocampal primed burst potentiation. *Hippocampus* 2, 421–430. doi: 10.1002/hipo.450020409

Engelborghs, K., Haseldonckx, M., Reempts, J., Van Rossem, K., Van Wouters, L., and Borgers, M. (2000). Impaired autoregulation of cerebral blood flow in an experimental model of traumatic brain injury. *J. Neurotrauma* 17, 667–677. doi: 10.1089/089771500415418

Engelborghs, S., D'Hooge, R., and Deyn, P. P. (2000). Pathophysiology of epilepsy. *Acta Neurol. Belg.* 100, 201–213.

Groc, L., Choquet, D., and Chaouloff, F. (2008). The stress hormone corticosterone conditions AMPAR surface trafficking and synaptic potentiation. *Nat. Neurosci.* 11, 868–870. doi: 10.1038/nn.2150

Groeneweg, F. L., Karst, H., de Kloet, E. R., and Joëls, M. (2012). Mineralocorticoid and glucocorticoid receptors at the neuronal membrane, regulators of nongenomic corticosteroid signalling. *Mol. Cell. Endocrinol.* 350, 299–309. doi: 10.1016/j.mce.2011.06.020

Gumy, C., Chandsawangbhuwana, C., Dzyakanchuk, A. A., Kratschmar, D. V., Baker, M. E., and Odermatt, A. (2008). Dibutyltin disrupts glucocorticoid receptor function and impairs glucocorticoid-induced suppression of cytokine production. *PLoS One* 3:e3545. doi: 10.1371/journal.pone.0003545

Helme-Guizon, A., Davis, S., Israel, M., Lesbats, B., Mallet, J., Laroche, S., et al. (1998). Increase in syntaxin 1B and glutamate release in mossy fibre terminals following induction of LTP in the dentate gyrus: a candidate molecular mechanism underlying transsynaptic plasticity. *Eur. J. Neurosci.* 10, 2231–2237. doi: 10.1046/j.1460-9568.1998.00232.x

Jimenez-Pacheco, A., Mesuret, G., Sanz-Rodriguez, A., Tanaka, K., Mooney, C., Conroy, R., et al. (2013). Increased neocortical expression of the P2X7 receptor after status epilepticus and anticonvulsant effect of P2X7 receptor antagonist A-438079. *Epilepsia* 54, 1551–1561. doi: 10.1111/epi.12257

Joëls, M., and Ronald de Kloet, E. (1994). Mineralocorticoid and glucocorticoid receptors in the brain. Implications for ion permeability and transmitter systems. *Prog. Neurobiol.* 43, 1–36. doi: 10.1016/0301-0082(94)90014-0

Joëls, M., Sarabdjitsingh, R. A., and Karst, H. (2012). Unraveling the time domains of corticosteroid hormone influences on brain activity: rapid, slow, and chronic modes. *Pharmacol. Rev.* 64, 901–938. doi: 10.1124/pr.112.005892

Johnson, L. R., Farb, C., Morrison, J. H., McEwen, B. S., and LeDoux, J. E. (2005). Localization of glucocorticoid receptors at postsynaptic membranes in the lateral amygdala. *Neuroscience* 136, 289–299. doi: 10.1016/j.neuroscience.2005.06.050

Kajiyama, Y., Iijima, Y., Chiba, S., Furuta, M., Ninomiya, M., Izumi, A., et al. (2010). Prednisolone causes anxiety- and depression-like behaviors and altered expression of apoptotic genes in mice hippocampus. *Prog. Neuro. Psychopharmacol. Biol. Psychiatr.* 34, 159–165. doi: 10.1016/j.pnpbp.2009.10.018

Karst, H., Berger, S., Turiault, M., Tronche, F., Schutz, G., and Joels, M. (2005). Mineralocorticoid receptors are indispensable for nongenomic modulation of hippocampal glutamate transmission by corticosterone. *Proc. Natl. Acad. Sci. U.S.A.* 102, 19204–19207. doi: 10.1073/pnas.0507572102

Krugers, H. J., Alfarez, D. N., Karst, H., Parashkouhi, K., van Gemert, N., and Joëls, M. (2005). Corticosterone shifts different forms of synaptic potentiation in opposite directions. *Hippocampus* 15, 697–703. doi: 10.1002/hipo.20092

Levi, G., Gallo, V., and Raiteri, M. (1980). A reevaluation of veratridine as a tool for studying the depolarization-induced release of neurotransmitters from nerve endings. *Neurochem. Res.* 5, 281–295. doi: 10.1007/bf00964616

Maggio, N., and Segal, M. (2007). Striking variations in corticosteroid modulation of long-term potentiation along the septotemporal axis of the hippocampus. *J. Neurosci.* 27, 5757–5765. doi: 10.1523/jneurosci.0155-07.2007

Mameli, M., Carta, M., Partridge, L. D., and Valenzuela, C. F. (2005). Neurosteroid-induced plasticity of immature synapses via retrograde modulation of presynaptic NMDA Receptors. *J. Neurosci.* 25, 2285–2294. doi: 10.1523/jneurosci.3877-04.2005

Meyer, D. A., Carta, M., Partridge, L. D., Covey, D. F., and Valenzuela, C. F. (2002). Neurosteroids enhance spontaneous glutamate release in hippocampal neurons. Possible role of metabotropic sigma1-like receptors. *J. Biol. Chem.* 277, 28725–28732. doi: 10.1074/jbc.m202592200

Minc-Golomb, D., Eimerl, S., Levy, Y., and Schramm, M. (1988). Release of d-[3H]aspartate and [14C]GABA in rat hippocampus slices: effects of fatty acid-free bovine serum albumin and Ca2+ withdrawal. *Brain Res.* 457, 205–211. doi: 10.1016/0006-8993(88)90687-7

Mizota, K., Yoshida, A., Uchida, H., Fujita, R., and Ueda, H. (2005). Novel type of Gq/11 protein-coupled neurosteroid receptor sensitive to endocrine disrupting chemicals in mast cell line (RBL-2H3). *Br. J. Pharmacol.* 145, 545–550. doi: 10.1038/sj.bjp.0706213

Nicolaides, N. C., Galata, Z., Kino, T., Chrousos, G. P., and Charmandari, E. (2010). The human glucocorticoid receptor: molecular basis of biologic function. *Steroids* 75, 1–12. doi: 10.1016/j.steroids.2009.09.002

Olijslagers, J. E., Kloet, E. R., De, Elgersma, Y., Woerden, G. M., Van Joëls, M., et al. (2008). Rapid changes in hippocampal CA1 pyramidal cell function via pre- as well as postsynaptic membrane mineralocorticoid receptors. *Eur. J. Neurosci.* 27, 2542–2550. doi: 10.1111/j.1460-9568.2008.06220.x

Oliveira, L., Noronha-Matos, J. B., Costa, A. C., Corrado, A. P., Belo, C. A. D., Ambiel, C. R., et al. (2015). Neuropharmacology Ampli fi cation of neuromuscular transmission by methylprednisolone involves activation of presynaptic facilitatory adenosine A 2A receptors and redistribution of synaptic vesicles. *Neuropharmacology* 89, 64–76. doi: 10.1016/j.neuropharm.2014.09.004

Parissis, D., Syntila, S. A., and Ioannidis, P. (2017). Corticosteroids in neurological disorders: the dark side. *J. Clin. Neurosci.* 44, 1–5. doi: 10.1016/j.jocn.2017.05.040

Rassner, M. P., Moser, A., Follo, M., Joseph, K., van Velthoven-Wurster, V., and Feuerstein, T. J. (2016). Neocortical GABA release at high intracellular sodium and low extracellular calcium: an anti-seizure mechanism. *J. Neurochem.* 137, 177–189. doi: 10.1111/jnc.13555

Richerson, G. B., and Wu, Y. (2003). Dynamic equilibrium of neurotransmitter transporters: not just for reuptake anymore. *J. Neurophysiol.* 90, 1363–1374. doi: 10.1152/jn.00317.2003

Rickard, A. J., and Young, M. J. (2009). Corticosteroid receptors, macrophages and cardiovascular disease. *J. Mol. Endocrinol.* 42, 449–459. doi: 10.1677/jme-08-0144

Russo, M. F., Ah Loy, S. R., Battle, A. R., and Johnson, L. R. (2016). Membrane associated synaptic mineralocorticoid and glucocorticoid receptors are rapid regulators of dendritic spines. *Front. Cell. Neurosci.* 10:161. doi: 10.3389/fncel.2016.00161

Saito, S., Kimura, S., Adachi, N., Numakawa, T., Ogura, A., and Tominaga-Yoshino, K. (2016). An in vitro reproduction of stress-induced memory defects: effects of corticoids on dendritic spine dynamics. *Nature* 6, 1–10.

Santos, M. S., and Rodriguez, R. (1992). Effect of depolarizing agents on the Ca2+-independent and Ca2+-dependent release of [3H]GABA from sheep brain synaptosomes. *Biochem. Pharmacol.* 44, 301–308. doi: 10.1016/0006-2952(92)90013-9

Schiess, A. R., and Partridge, L. D. (2005). Pregnenolone sulfate acts through a G-protein-coupled sigma1-like receptor to enhance short term facilitation in adult hippocampal neurons. *Eur. J. Pharmacol.* 518, 22–29. doi: 10.1016/j.ejphar.2005.06.007

Sivcev, S., Slavikova, B., Rupert, M., Ivetic, M., Nekardova, M., Kudova, E., et al. (2019). Synthetic testosterone derivatives modulate rat P2X2 and P2X4 receptor channel gating. *J. Neurochem.* 150, 28–43. doi: 10.1111/jnc.14718

Song, I. H., and Buttgereit, F. (2006). Non-genomic glucocorticoid effects to provide the basis for new drug developments. *Mol. Cell. Endocrinol.* 246, 142–146. doi: 10.1016/j.mce.2005.11.012

Sperlágh, B., Köfalvi, A., Deuchars, J., Atkinson, L., Milligan, C., Buckley, N., et al. (2002). Involvement of P2X7 receptors in the regulation of neurotransmitter release in the rat hippocampus. *J. Neurochem.* 81, 1196–1211. doi: 10.1046/j.1471-4159.2002.00920.x

Tauheed, N., Usmani, H., and Siddiqui, A. (2014). A comparison of the analgesic efficacy of transforaminal methylprednisolone alone and with low doses of clonidine in lumbo-sacral radiculopathy. *Saudi J. Anaesth.* 8, 51–58.

Wang, C.-C., and Wang, S.-J. (2009). Modulation of presynaptic glucocorticoid receptors on glutamate release from rat hippocampal nerve terminals. *Synapse* 63, 745–751. doi: 10.1002/syn.20654

Wu, Y., Wang, W., and Richerson, G. B. (2006). The transmembrane sodium gradient influences ambient GABA concentration by altering the equilibrium of GABA transporters. *J. Neurophysiol.* 96, 2425–2436. doi: 10.1152/jn.00545.2006

Zerangue, N., and Kavanaugh, M. (1996). Flux coupling in a neuronal glutamate transporter. *Nature* 383, 634–637. doi: 10.1038/383634a0

Zhang, B., Chen, X., Lin, Y., Tan, T., Yang, Z., Dayao, C., et al. (2011). Impairment of synaptic plasticity in hippocampus is exacerbated by methylprednisolone in a rat model of traumatic brain injury. *Brain Res.* 1382, 165–172. doi: 10.1016/j.brainres.2011.01.065

Zhang, S., Jonklaas, J., and Danielsen, M. (2007). The glucocorticoid agonist activities of mifepristone (RU486) and progesterone are dependent on glucocorticoid receptor levels but not on EC50values. *Steroids* 72, 600–608. doi: 10.1016/j.steroids.2007.03.012

Zheng, P. (2009). Progress in neurobiology neuroactive steroid regulation of neurotransmitter release in the CNS: action, mechanism and possible significance. *Prog. Neurobiol.* 89, 134–152. doi: 10.1016/j.pneurobio.2009.07.001

Conflict of Interest: The authors declare that the research was conducted in the absence of any commercial or financial relationships that could be construed as a potential conflict of interest.

frontiers in Molecular Neuroscience

ORIGINAL RESEARCH
published: 07 August 2020
doi: 10.3389/fnmol.2020.00111

ATP Signaling Controlling Dyskinesia Through P2X7 Receptors

*Analu A. Fonteles[1], Julliana C. S. Neves[1], Ana Paula F. Menezes[1], Juliana F. Pereira[2], Ana Thais A. Silva[1], Rodrigo A. Cunha[3,4] and Geanne M. Andrade[1,2]**

[1]*Post-Graduate Program in Pharmacology, Department of Physiology and Pharmacology, Federal University of Ceará, Fortaleza, Brazil,* [2]*Post-Graduate Program in Medical Sciences, Department of Medicine, Faculty of Medicine, Center for Research and Drug Development (NPDM), Federal University of Ceará, Fortaleza, Brazil,* [3]*CNC-Center for Neuroscience and Cell Biology, Coimbra, Portugal,* [4]*Faculty of Medicine, University of Coimbra, Coimbra, Portugal*

Dopamine replacement therapy with L-3,4-dihydroxyphenylalanine (L-DOPA) is the only temporary therapy for Parkinson's disease (PD), but it triggers dyskinesia over time. Since dyskinesia is associated with increased neuronal firing that bolsters purinergic signaling, we now tested whether the selective and blood-brain barrier-permeable P2X7 receptor antagonist Brilliant Blue-G (BBG, 22.5–45 mg/kg ip) attenuated behavioral, neurochemical and biochemical alterations in rats turned hemiparkinsonian upon unilateral striatal injection of 6-hydroxydopamine (6-OHDA) and treated daily with L-DOPA (30 mg/kg by gavage) for 22 days. The blockade of P2X7 receptors decreased L-DOPA-induced dyskinesia and motor incoordination in hemiparkinsonian rats. In parallel, BBG treatment rebalanced the altered dopamine D1 and D2 receptor density and signaling as well as some neuroinflammation-associated parameters in the striatum and substantia nigra. These findings herald a hitherto unrecognized role for purinergic signaling in the etiopathology of dyskinesia and prompt P2X7 receptor antagonists as novel candidate anti-dyskinesia drugs.

Keywords: Parkinson's disease, dyskinesia, P2X7 receptor, neuroinflammation, dopamine D1 receptor, striatum, microglia, astrocyte

OPEN ACCESS

Edited by:
Maria José Diógenes, University of Lisbon, Portugal

Reviewed by:
Enric I. Canela, University of Barcelona, Spain
Karen Jaunarajs, University of Alabama at Birmingham, United States

****Correspondence:***
Geanne M. Andrade
gmatos@ufc.br

Received: *29 December 2019*
Accepted: *29 May 2020*
Published: *07 August 2020*

Citation:
Fonteles AA, Neves JCS, Menezes APF, Pereira JF, Silva ATA, Cunha RA and Andrade GM (2020) ATP Signaling Controlling Dyskinesia Through P2X7 Receptors. Front. Mol. Neurosci. 13:111. doi: 10.3389/fnmol.2020.00111

HIGHLIGHTS

- A P2X7 receptor (P2X7R) antagonist prevents L-DOPA-induced dyskinesia (LID)
- P2X7R blockade prevents LID-induced striatal D1 receptor upregulation
- P2X7R blockade dampens LID-induced DARPP-32 overactivation in striatum and nigra
- P2X7R blockade lowers LID-induced microgliosis and inflammation in striatum and nigra

Abbreviations: AIMs, abnormal involuntary movements; BBG, Brilliant Blue-G; CD11b, cluster of differentiation 11b; COX-2, cyclooxygenase-2; DARPP-32, dopamine- and cAMP-regulated neuronal phosphoprotein; DAT, dopamine transporters; GFAP, glial fibrillary acidic protein; IL1β, interleukin-1β; L-DOPA, L-3,4-dihydroxyphenylalanine; LID, L-DOPA-induced dyskinesia; 6-OHDA, 6-hydroxydopamine; P2X7R, P2X7 receptor; PD, Parkinson's disease; p-DARPP32, DARPP32 phosphorylated in residue threonine-34; TH, tyrosine hydroxylase.

INTRODUCTION

Parkinson's disease (PD) is a neurodegenerative disease mainly characterized by bradykinesia resulting from dopamine deficits in the striatum and loss of dopamine neurons in the *substantia nigra*. Dopamine replacement therapy with L-3,4-dihydroxyphenylalanine (L-DOPA) temporarily alleviates PD motor symptoms, although it is accompanied by evolving adverse side effects, namely the development of abnormal involuntary movements known as L-DOPA-induced dyskinesia (LID), occurring in up to 80% of patients within 5 years of treatment (Bastide et al., 2015). LID involves maladaptive changes of dopamine receptors typified by upregulation of dopamine D1 receptor signaling in the striatum (Heumann et al., 2014), altered patterns of synaptic plasticity at corticostriatal synapses (Wang and Zhang, 2016), together with glia deregulation and a heightened profile of neuroinflammation in nigra and striatum (Carta et al., 2017). Thus, dyskinesia resulting from L-DOPA treatment in Parkinsonian rodents triggers an increased firing rate and synaptic potentiation in D1 receptor-containing medium spiny neurons, accompanied by a decreased excitability of D2 receptor-containing medium spiny neurons in the striatum (e.g., Thiele et al., 2014; Suarez et al., 2016), coupled with disrupted excitability and synchronization in both intra- and inter-basal ganglia nuclei and the cerebral cortex. Indeed, the average firing rate of striatal medium spiny neurons increases as axial dyskinesia develops with increased delta power in the striatum (Alberico et al., 2017), hyperexcitability in the subthalamic nucleus (Aristieta et al., 2016), enhanced firing rate in the substantia nigra pars reticulata (Meissner et al., 2006) and overactivation of premotor and motor cortical areas (reviewed in Donzuso et al., 2020).

Notably, increased neuronal firing (Wieraszko et al., 1989; Cunha et al., 1996), as well as increased inflammation (Gourine et al., 2007) and microglia-mediated neuroinflammation (George et al., 2015) are associated with an augmented release of ATP, which acts as a danger signal in the brain (Rodrigues et al., 2015). Accordingly, in different animal models of PD, the blockade of ATP-activated P2X7 receptor (P2X7R) attenuates motor dysfunction (Marcellino et al., 2010; Carmo et al., 2014; Ferrazoli et al., 2017; Wang et al., 2017). This likely involves an ability of P2X7R blockade to attenuate neuroinflammation (reviewed in Volonté et al., 2012; Bartlett et al., 2014; Jimenez-Mateos et al., 2019) and neurodegeneration (e.g., Zhang et al., 2005; Arbeloa et al., 2012; Nishida et al., 2012; Gandelman et al., 2013), in particular, dopaminergic dysfunction (Jun et al., 2007; Carmo et al., 2014; Kumar et al., 2017). The combined evidence that P2X7R controls neuroinflammation and abnormal dopaminergic signaling, and the implication of these two mechanisms to generate LID led us to post the new hypothesis that P2X7R may be involved in LID pathophysiology. The relevance of this aim is best heralded by the current inexistence of therapeutic strategies to manage LID. Thus, based on the previous observations that the blood-brain barrier permeable and selective P2X7R antagonist, brilliant blue G (BBG), attenuated motor incoordination in a model of Huntington's disease (Díaz-Hernández et al., 2009), we now evaluated if this P2X7R antagonist alleviates LID in a rat model.

MATERIALS AND METHODS

Animals and Drug Treatments

Male *Wistar* rats weighing 250–300 g (n = 64) were obtained from the Animal House of the Physiology and Pharmacology Department of Federal University of Ceará. All procedures followed the ARRIVE guidelines (McGrath et al., 2010) and were approved by the ethics committee of the Federal University of Ceará (107/14). Animals were housed four per cage under a 12 h light/dark cycle and behavioral tests were performed between 9:00 AM and 5:00 PM.

The analysis of rotational behavior was carried out using 16 animals, eight for each group. Another pool of 48 animals was used to assess the pattern of AIMs and was divided into six groups: (i) sham-operated rats receiving ascorbate (0.01% in saline; Sigma) intra-striatally; (ii) BBG-treated sham-operated rats (sham+BBG45) receiving ascorbate (0.01% in saline; Sigma) intra-striatally and BBG (45 mg/kg, ip; Sigma); (iii) hemiparkinsonian (6-OHDA) rats receiving an intra-striatal unilateral injection of 6-hydroxydopamine (6-OHDA, 18 μg/3 μl; Sigma), as previously described (Carmo et al., 2014); (iv) dyskinetic (6-OHDA+L-DOPA) rats receiving 6-OHDA as above and L-DOPA (30 mg/kg; Hoffman-Laroche) by gavage daily for 22 days; (v) BBG-treated (6-OHDA+L-DOPA+BBG 22.5) rats receiving 6-OHDA, L-DOPA and BBG 22.5 mg/kg ip; and (vi) BBG-treated (6-OHDA+L-DOPA+BBG 45) rats receiving 6-OHDA, L-DOPA and BBG 45 mg/kg ip for 22 days. After completing an AIMs analysis, four animals of each of these six groups (24 in total) were subjected to the rotarod test, and their brains were dissected and used for western blot analysis; additionally, four animals of each of the six groups (24 in total) were used for immunohistochemical analysis, as depicted in **Figure 1**. Note that the animals subjected to L-DOPA and/or BBG treatment were previously subjected to apomorphine tests because only animals with recognized striatal lesions caused by 6-OHDA could be used in the following protocols (all except three animals reached this criterium).

The dose range of BBG used in the present study has previously been shown to yield a brain concentration of 200–220 nM (Díaz-Hernández et al., 2012), which is within the effective and selective range of BBG towards central P2X7R (Donnelly-Roberts and Jarvis, 2007). Accordingly, this dose range of BBG has previously been shown to afford robust neuroprotection in different animal models of brain disease (Ryu and McLarnon, 2008; Díaz-Hernández et al., 2009; Arbeloa et al., 2012; Kimbler et al., 2012; Carmo et al., 2014).

Behavioral Analysis

Rotational behavior was tested with apomorphine (1.0 mg/kg) 14 days after 6-OHDA injection, as previously described (Carmo et al., 2014). Abnormal involuntary movements (AIMs) were quantified as ALO AIMs (summing axial AIMs, limb AIMs, and

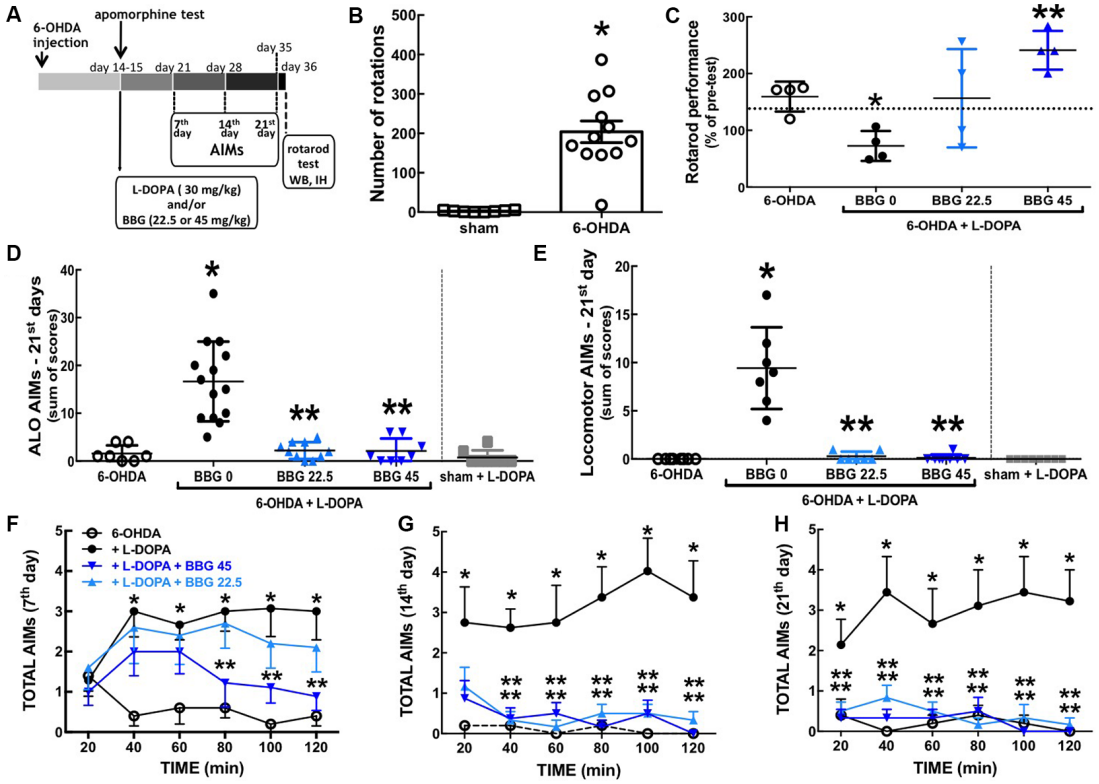

FIGURE 1 | The P2X7R antagonist, brilliant blue G (BBG), prevented L-DOPA-induced dyskinesia and motor incoordination in 6-OHDA-induced hemiparkinsonian rats. **(A)** Schematic overview of the experimental schedule. **(B)** Fourteen days after intra-striatal unilateral injections of 6-OHDA (18 μg/3 μl), rats displayed a sharp increase of apomorphine (1 mg/kg, IP)-induced contralateral rotations counted for 60 min; values are mean ± SEM; $^{*}p < 0.05$ vs. sham-operated, analysis of variance (ANOVA) followed by a Tukey test ($n = 8$). **(C)** BBG (22.5 or 45 mg/kg, IP) prevents the decreased performance in the rotarod with constant speed (20 rpm) after 22 days of L-DOPA-treatment of hemiparkinsonian rats; the test is specifically designed to evaluate the impact of L-DOPA since the performance is scored as the relative time in the rod 1 h after L-DOPA (30 mg/kg, vo) or saline administration compared to a pre-test done 1 h before L-DOPA (or saline). With all animals trained daily during the 3 days preceding the test in an accelerated version of the rotarod (16–38 rpm during 300 s); the dashed line is the median performance of sham-operated rats; values are medians and spreading intervals; $^{*}p < 0.05$ vs. 6-OHDA and $^{**}p < 0.05$ vs. 6-OHDA + L-DOPA, Mann–Whitney test ($n = 4$). **(D,E)** BBG (22.5 or 45 mg/kg, ip) prevents the development of both axial, limb and orolingual (ALO) abnormal involuntary movements (AIMs; **D**) and locomotor AIMs **(E)** after 21 days of daily treatment with L-DOPA of 6-OHDA-induced hemiparkinsonian rats; ALO AIMs (rating as a contralateral side of the lesion; limb AIMs: repetitive, rhythmic jerky movements or dystonic posturing of the forelimb on the contralateral side of the lesion; orolingual AIMs: tongue protusion without the presence of food or other objects) and locomotor AIMs (rating locomotion to the contralateral side of the lesion) were scored as (0), absent; (1), present for less than half of the observation time; (2), present for more than half of the observation time; (3), continuous but interrupted by strong sensory stimuli; (4), continuous, not interrupted by strong sensory stimuli; AIMs were scored as the sum of AIMs observed during 2 min every 20 min, starting 20 min after L-DOPA administration for a total time of 2 h. **(F–H)** Time courses of onset and evolution of total AIMs (sum of locomotor AIMs and ALO AIMs) after the administration of the last L-DOPA dose at 7 days **(F)**, 14 days **(G)** and 21 days of treatment **(H)**. $^{*}p < 0.05$ vs. 6-OHDA and $^{**}p < 0.05$ vs. 6-OHDA + L-DOPA using a Kruskal–Wallis test followed by a Dunn's test ($n = 8$).

orolingual AIMs) that are distinguished from locomotor AIMs, and were scored (Lundblad et al., 2002) for 2 min every 20 min during 2 h periods on the 21st, 28th and 36th days after 6-OHDA injection, i.e., 1–3 weeks after the apomorphine test, and during the treatment with L-DOPA without or with BBG. ALO AIMs (rating axial AIMs: contralateral torsions of the neck and body; limb AIMs: repetitive, rhythmic jerky movements or dystonic posturing of the forelimb on the contralateral side of the lesion; orolingual AIMs: tongue protrusion without the presence of food or other objects) and locomotor AIMs (rating locomotion to the contralateral side of the lesion) were scored as: (0), absent; (1), present for less than half of the observation time; (2), present for more than half of the observation time; (3), continuous but interrupted by strong sensory stimuli; and (4), continuous, not interrupted by strong sensory stimuli.

Motor coordination and balance were tested using an accelerated rotarod (Gonçalves et al., 2017), on the 37th day after 6-OHDA injection. Animals were pre-trained two sections a day, 3 days before the test in an accelerated version of the rotarod (16–38 rpm during 300 s). Twenty days after L-DOPA-treatment, each animal was tested 1 and 2 h after L-DOPA (30 mg/kg, v.o.) or saline administration with constant speed (20 rpm) and two consecutive latencies were recorded for each animal up to a maximum of 300 s. Performance was scored as the percentage of the average latency time spent on the rod, 1 and 2 h after L-DOPA, in relation to the average latency time spent in

the pre-test performed 30 min before L-DOPA administration. Thus, this protocol is specifically designed to estimate L-DOPA-induced motor incoordination in Parkinsonian models (Padovan-Neto et al., 2009) rather than the impact of 6-OHDA on motor incoordination.

Histochemical Analysis

After behavioral analysis, four rats from each group were processed as previously described (see Carmo et al., 2014) for tyrosine hydroxylase (TH; 1:800, Sigma) immunohistochemistry and FluoroJade-C staining to evaluate neuronal damage, as well as astrogliosis (GFAP immunoreactivity; 1:1,000, Sigma), microgliosis (CD11b immunoreactivity; 1:200, Serotec), and immunoreactivity for cyclooxygenase-2 (COX-2; 1:200, Santa Cruz Biotechnology, Dallas, TX, USA) and dopamine transporters (DAT; 1:500, Santa Cruz Biotechnology, Dallas, TX, USA). Coronal brain sections (50 μm thick) were collected in three series with an inter-series interval of 300 μm from the beginning to the end of the striatum (approximately 0.96 mm to −0.92 mm from bregma; Paxinos and Watson, 2005) and from the beginning to the end of the substantia nigra (approximately −4.44 mm to −6.19 mm from bregma; Paxinos and Watson, 2005). The stainings were carried out in triplicate using one-in-six free-floating sections. The stained sections were visualized using confocal microscopy (LSM510, Zeiss) and two photographs were collected per section, with care to maintain the conditions of acquisition as constant and without any digital manipulation of the acquired data. After a freehand selection of a 50 × 50 μm region of interest in the striata or nigra (ipsilateral and contralateral), we measured total fluorescence (for TH, GFAP, CD11b or FluoroJade-C) or counted the number of positively-stained elements (for COX-2) using a densitometric analysis based on the ImageJ software (Carmo et al., 2014).

Western Blot Analysis

After behavioral analysis, four rats from each group were processed for Western blot analysis (Shen et al., 2013), to measure dopamine D1 receptors (1:500, Abcam), dopamine D2 receptors (1:800, Abcam) or interleukin-1β (IL1β, 1:500, Santa Cruz Biotechnology, Dallas, TX, USA), followed by re-probing with α-tubulin (1:500, Santa Cruz Biotechnology, Dallas, TX, USA), and phospho-threonine-34 DARPP-32 (p-DARPP-32, 1:1,500, Santa Cruz Biotechnology, Dallas, TX, USA) followed by total DARPP-32 (1:1,500, Cell Signaling) re-probing (Shen et al., 2013).

Statistical Analysis

All statistical comparisons were performed using Graphpad Prism 6.0 software, with a significance level of 95%. Rotational test performance, D1 and D2 receptors, DARPP-32 and IL-1β Western-blot analysis, and COX-2 immunohistochemical analysis are represented as mean ± SEM and statistical differences were estimated using one-way analysis of variance (ANOVA), followed by a Tukey's test. The analysis of AIMs and of rotarod performance, as well as TH, DAT, GFAP and CD11b immunohistochemical results are presented as median (interquartile range) and were analyzed with Kruskal-Wallis tests followed by Mann–Whitney U-tests to compare pairs of groups.

RESULTS

Intra-striatal 6-OHDA injection triggered dopamine depletion and super-sensitization, as heralded by the sharp increase of apomorphine-induced contralateral rotations 14 days after 6-OHDA ($F_{(2,25)}$ = 10.99, $p < 0.0001$; **Figure 1B**). Chronic L-DOPA (30 mg/kg) treatment of 6-OHDA-lesioned rats significantly increased axial, limb and orolingual AIMs ($F_{(4,39)}$ = 20.61, p = 0.0005; **Figure 1D**) as well as locomotor AIMs ($F_{(5,38)}$ = 17.63, p = 0.0020; **Figure 1E**). No AIMs were observed in sham-operated animals after receiving chronic L-DOPA treatment or vehicle (**Figures 1D,E**).

Blockade of P2X7R Attenuated L-DOPA-Induced Dyskinesia

Chronic treatment with the selective P2X7R antagonist, BBG (45 mg/kg) diminished AIMs' scores 21 days after L-DOPA treatment of hemiparkinsonian rats (**Figures 1D,E**; $F_{(4,14)}$ = 19.51; p = 0.0006 and $F_{(4,17)}$ = 19.56; p = 0.0004, respectively), as also occurred 7–14 days after L-DOPA treatment (**Figures 1F,G**). BBG (45 mg/kg) decreased AIMs' scores within 80 min after L-DOPA injection on day 7, within 40 min on day 14, and within 20 min on day 21 (**Figures 1F–H**). A lower dose of BBG (22.5 mg/kg) also attenuated AIMs' scores (**Figures 1D,E**; $F_{(4,14)}$ = 18.02; p = 0.0007 and $F_{(4,12)}$ = 17.07; p = 0.0048, respectively). We have previously reported that the tested doses of BBG are devoid of motor effects in control rats (Carmo et al., 2014).

Blockade of P2X7R Attenuated LID-Induced Motor Incoordination

Chronic L-DOPA treatment decreased motor coordination of hemiparkinsonian rats on the rota-rod test ($F_{(4,16)}$ = 5.249; p = 0.0068), which was prevented by BBG (45 mg/kg; $F_{(4,16)}$ = 6.477; p = 0.025; **Figure 1C**). No alterations were observed in sham-operated animals chronically treated with L-DOPA or vehicle (not shown) and the impact of BBG on 6-OHDA-treated rats was previously described (Carmo et al., 2014).

Blockade of P2X7R Dampened Dopamine Aberrant Signaling Associated With LID

Rats with 6-OHDA lesions exhibited a greater than 70% reduction (p = 0.0286) of the immunodensity of the dopamine markers tyrosine hydroxylase (TH; **Figures 2A,B**) and of dopamine transporters (DAT; p = 0.0009; **Figures 2C,D**) only in the ipsilateral striatum (**Figures 2A,C**) and contralateral substantia nigra (**Figures 2B,D**; p = 0.0286 and p = 0.0286, respectively) compared to the sham-operated group; this was not affected by chronic treatment with L-DOPA and/or BBG (**Figure 2**). As expected when beginning BBG treatment after establishing dopamine neuronal lesions, there was no change of FluoroJade-C staining (degenerating neurons) in the striatum or nigra between the different groups (data not shown).

Western blot analysis revealed a selective increase of dopamine D1 receptor density in the striatum (**Figure 3A**,

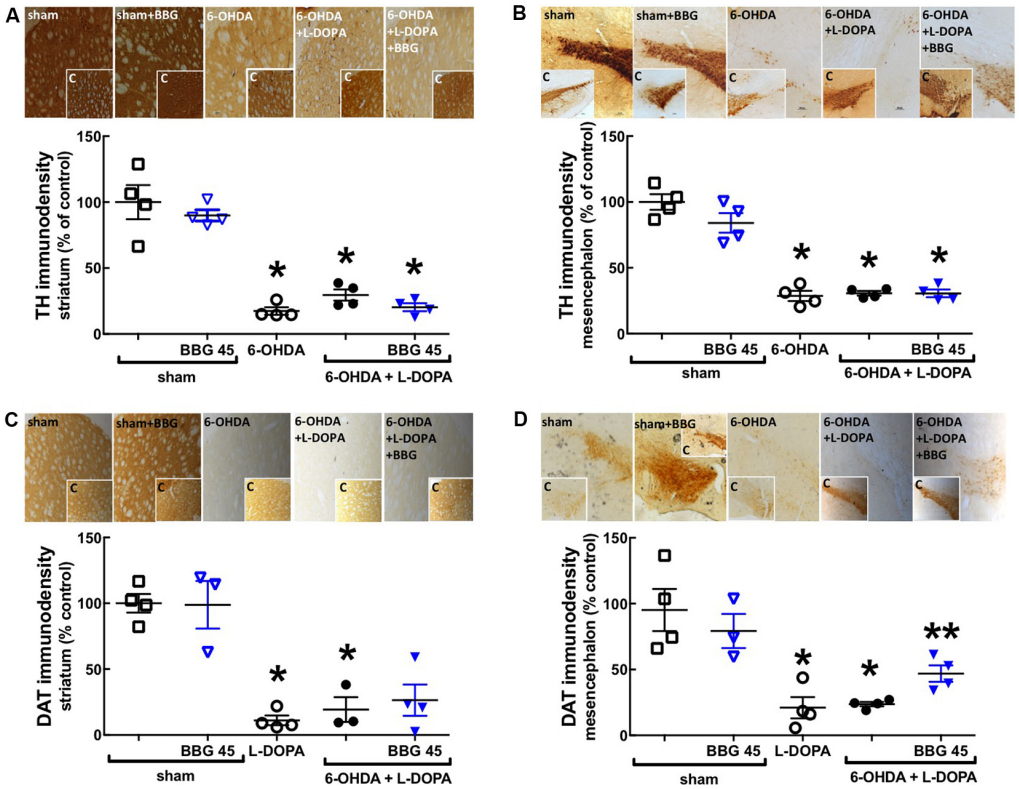

FIGURE 2 | The P2X7R antagonist, brilliant blue G (BBG), applied after L-DOPA-induced dyskinesia, did not recover the 6-OHDA-induced dopaminergic lesion in the striatum and nigra. Rats were either sham-operated or challenged with 6-OHDA (unilateral striatal injection of 18 μg/3 μl) and later treated either with saline (PARK) or L-DOPA (30 mg/kg, v.o. daily) or L-DOPA plus BBG (45 mg/kg, IP daily, 30 min before L-DOPA), before being sacrificed for preparation of coronal brain sections (30 μm) to be immunohistochemically stained with the dopaminergic markers tyrosine hydroxylase (TH) or dopamine transporter (DAT). The treatment during 21 days of L-DOPA and/or BBG does not affect the 6-OHDA-induced dopaminergic lesion in the ipsilateral striatum **(A,C)** and in the contralateral substantia nigra **(B,D)**, assessed by immunohistochemical analysis of either TH **(A,B)** or dopamine transporters (DAT; **C,D**); the photographs in each panel are representative stainings ordered as the columns and the inserts are photographs from the other hemisphere (as internal controls); the values in the bar graphs are mean ± SEM of four rats per group; $^{*}p < 0.05$ vs. sham-operated using a Mann–Whitney test. $^{**}p < 0.05$ vs. 6-OHDA + L-DOPA using a Mann-Whitney test.

$p = 0.0159$) with no alteration in the nigra (**Figure 3B**, $p = 0.2119$), whereas dopamine D2 receptor density decreased in the nigra (**Figure 3D**, $p = 0.0085$), but not in the striatum (**Figure 3C**, $p = 0.9982$) of LID rats (i.e., treated with 6-OHDA and then with L-DOPA) compared to PD rats (i.e., treated only with 6-OHDA). This resulted in an abnormally increased dopaminergic signaling in both the striatum (**Figure 3E**, $p = 0.0102$) and nigra (**Figure 3F**, $p = 0.0106$), as testified by an increased ratio of threonine-34-phosphorylated/total DARPP-32 in LID vs. PD rats. Notably, BBG (45 mg/kg) prevented these changes in striatal D1 (**Figure 3A**, $p = 0.0304$) and nigra D2 receptors (**Figure 3D**, $p = 0.0159$), normalizing dopamine signaling through DARPP-32 in both the striatum ($p = 0.0297$) and nigra ($p = 0.0596$) of LID rats (**Figures 3E,F**).

Blockade of P2X7R Prevented Some Glia-Associated Neuroinflammation Markers Upon LID

GFAP (astrocytic marker) and CD11b (microglia/macrophage marker) immunoreactivities were increased in the striatum (**Figures 4C,E**) and nigra (**Figures 4D,F**) of 6-OHDA-treated rats and further increased upon LID; this suggests the presence upon LID of astrogliosis and microgliosis, as concluded from the quantification of the total immunoreactivities of GFAP and CD11b (scatter plots in **Figure 4**), as well as the alteration of the morphology of the elements stained with either GFAP or CD11b (insert photos in **Figure 4**). These alterations were prevented by BBG (45 mg/kg), more evidently in the nigra than in the striatum (**Figure 4**). Accordingly, LID increased COX-2 immunoreactivity (**Figures 5A,B**; Bortolanza et al., 2015b) and interleukin-1β levels in the striatum and nigra (**Figures 5C,D**), which was prevented by BBG more evidently in the striatum (**Figures 5A,C**) than in the nigra (**Figures 5B,D**). Altogether, these findings are indicative of the ability of P2X7R to control neuroinflammation, although BBG displays a different ability to control glial cell markers and neurochemical features of neuroinflammation in the striatum and in the nigra. This might be due to the greater density of microglia in the nigra than elsewhere in the brain (Lawson et al., 1990; Sharaf et al., 2013), the different contribution of different players to mount a neuroinflammatory response in the striatum and in the nigra (Walker et al., 2016) or to the scar caused by the injection of 6-OHDA in the striatum.

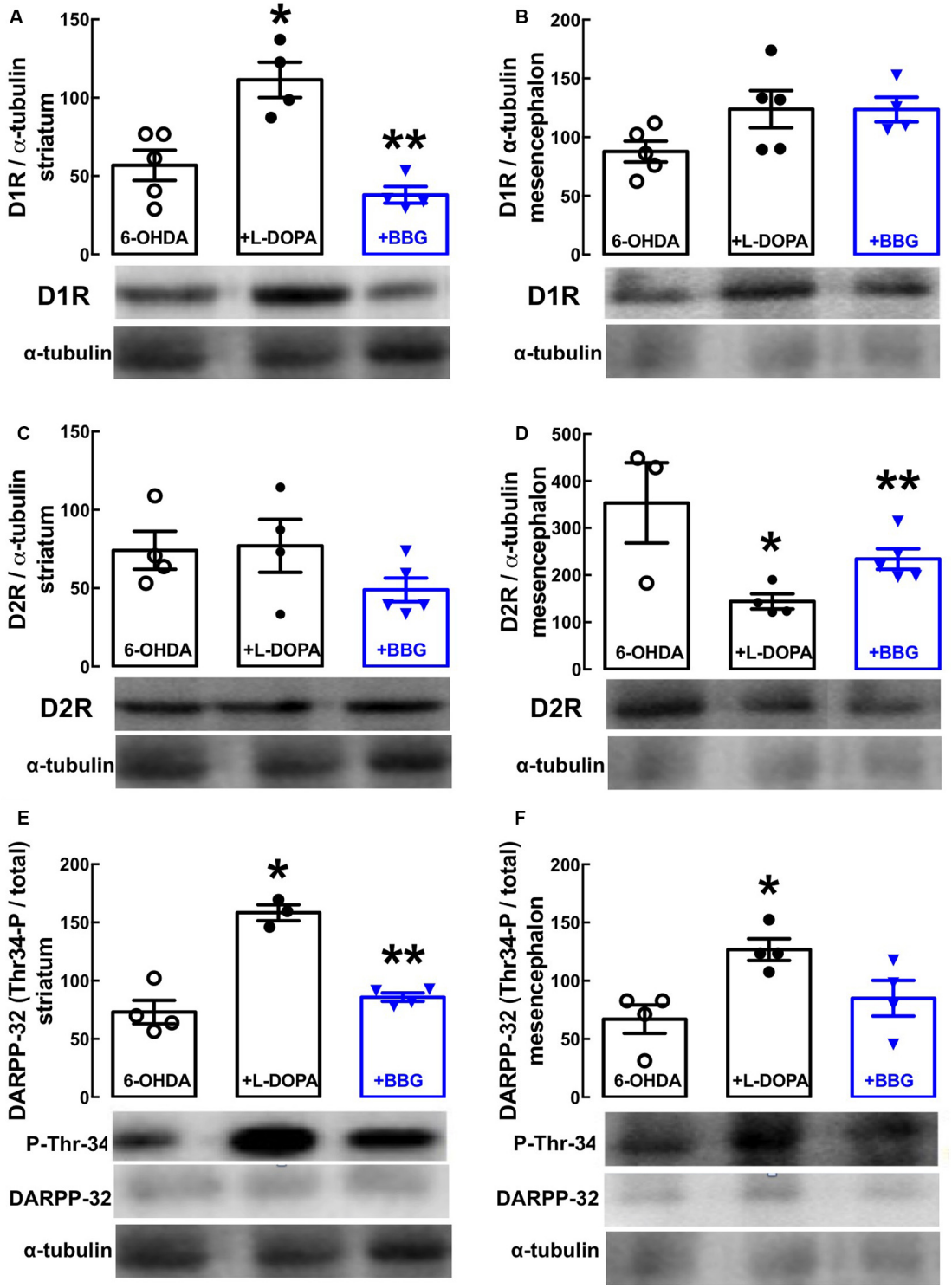

FIGURE 3 | The P2X7R antagonist, brilliant blue G (BBG), prevents the alterations of the dopaminergic signaling associated with the altered density of dopamine D1 and D2 receptors in the striatum and substantia nigra of hemiparkinsonian rats suffering from L-DOPA-induced dyskinesia. Rats were challenged with 6-OHDA (unilateral striatal injection of 18 μg/3 μl) and either saline (6-OHDA) or L-DOPA (30 mg/kg, v.o. daily, +L-DOPA) or L-DOPA plus BBG (45 mg/kg, IP daily, 30 min before L-DOPA; +BBG), and were sacrificed for preparation of extracts from the striatum or substantia nigra for Western blot analysis. **(A,B)** D1 receptor immunodensity in the striatum **(A)** and nigra **(B)**. **(C,D)** D2 receptor immunodensity in the striatum **(C)** and nigra **(D)**. **(E,F)** Threonine-34-phosphorylated DARPP-32 immunodensity in the striatum **(E)** and nigra **(F)**. All data are mean ± SEM of four rats per group; $^{*}p < 0.05$ vs. sham-operated, $^{**}p < 0.05$ vs. PARK+L-DOPA, using an ANOVA followed by a Tukey's test.

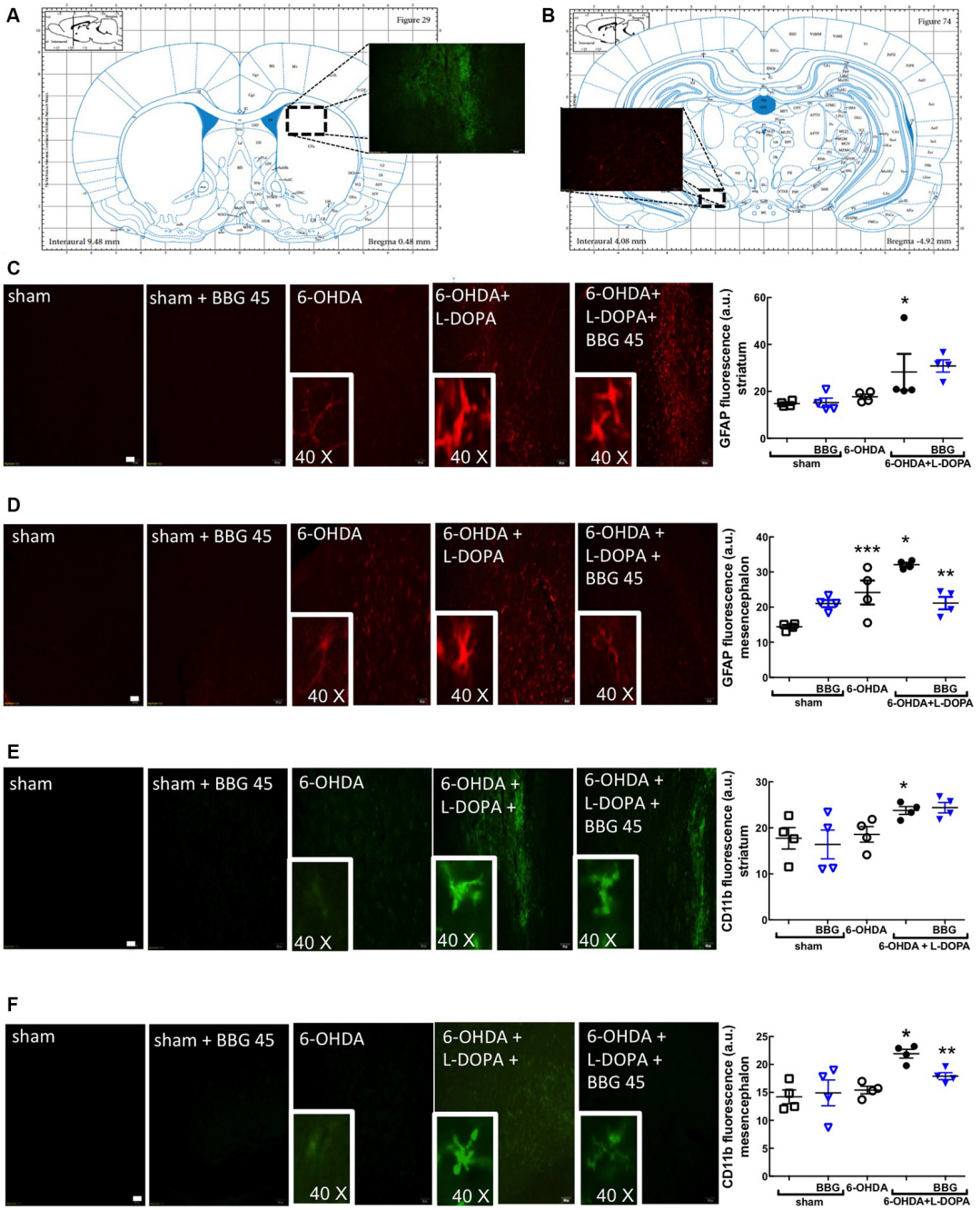

FIGURE 4 | The P2X7R antagonist, brilliant blue G (BBG), prevented astrocytic and microglial alterations in the striatum **(A)** and substantia nigra **(B)** of hemiparkinsonian rats suffering from L-DOPA-induced dyskinesia. Rats were either sham-operated or challenged with 6-OHDA (unilateral striatal injection of 18 μg/3 μl) and later treated either with saline or L-DOPA (30 mg/kg, v.o. daily) or L-DOPA plus BBG (45 mg/kg, IP daily, 30 min before L-DOPA), before being sacrificed for preparation of either coronal brain sections (50 μm thick) or extracts from the striatum or substantia nigra for Western blot analysis. **(A)** Representation from the rat brain Atlas of Paxinos and Watson (2005) at 0.48 mm from bregma, illustrating the site of a collection of striatal sections (50 μm thick) in three series of six sections around the three 6-OHDA injection sites and **(B)** representation at −4.92 mm from bregma, illustrating the site of a collection of nigral sections (50 μm thick) in three series of six sections; the insert photograph shows an example of a striatal **(A)** and nigral regions **(B)** stained for CD11b from a 6-OHDA + L-DOPA treated rat. **(C,D)** Representative photographs (ordered as indicated in the bar graph showing the average staining values) of the immunohistochemical detection of the astrocyte marker, GFAP in the striatum **(C)** and nigra **(D)**, where the inserts are the amplification of individually stained elements; bar values are medians and spreading intervals; $^{*}p < 0.05$ vs. sham-operated, $^{**}p < 0.05$ vs. 6-OHDA and $^{***}p < 0.05$ vs. 6-OHDA + L-DOPA, Mann–Whitney test ($n = 4$). **(E,F)** Representative photographs (ordered as indicated in the bar graph showing the average staining values) of the immunohistochemical detection of the microglia marker, CD11b in the striatum **(E)** and nigra **(F)**, where the inserts are the amplification of individually stained elements; bar values are medians and spreading intervals; $^{*}p < 0.05$ vs. sham-operated, $^{**}p < 0.05$ vs. 6-OHDA and $^{***}p < 0.05$ vs. 6-OHDA + L-DOPA, Mann–Whitney test ($n = 4$). Scale bar: 100 μm.

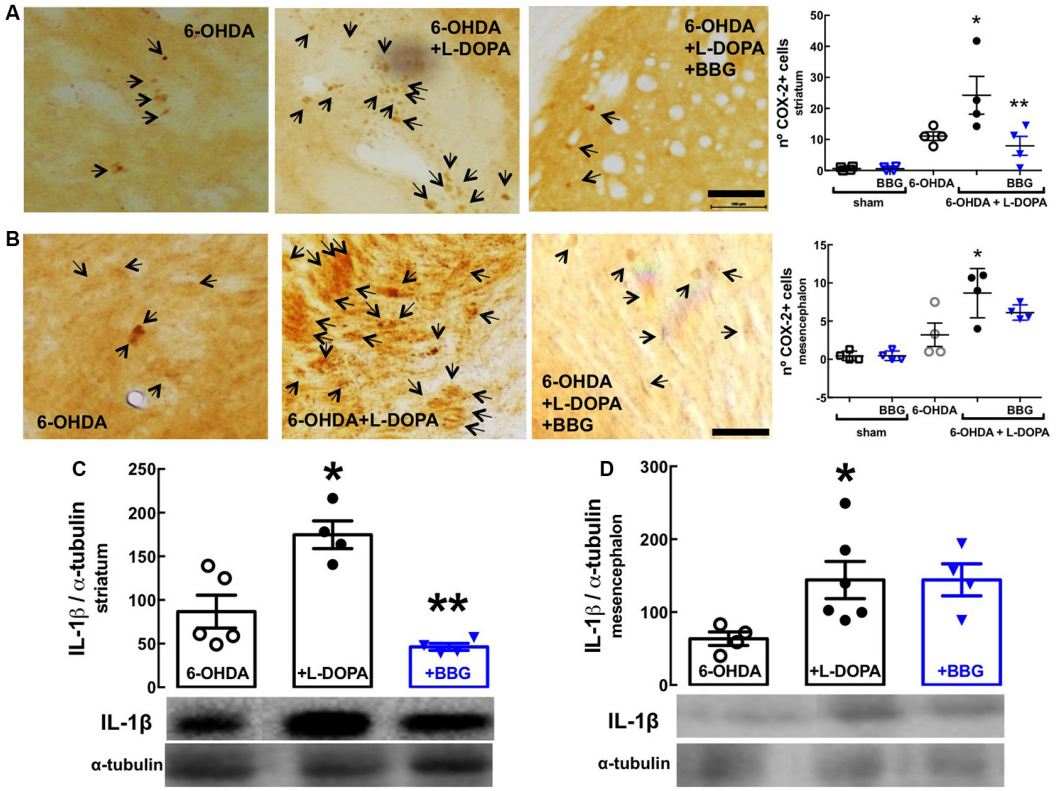

FIGURE 5 | The P2X7R antagonist, brilliant blue G (BBG), prevented alterations associated with neuroinflammation in the striatum and substantia nigra of hemiparkinsonian rats suffering from L-DOPA-induced dyskinesia. Rats were either sham-operated or challenged with 6-OHDA (unilateral striatal injection of 18 μg/3 μl) and later treated either with saline or L-DOPA (30 mg/kg, v.o. daily) or L-DOPA plus BBG (45 mg/kg, IP daily, 30 min before L-DOPA), before being sacrificed for preparation of either coronal brain sections (50 μm thick) or extracts from the striatum or substantia nigra for Western blot analysis. **(A,B)** The average immunohistochemical density of cyclooxygenase-2 (COX-2) in the striatum **(A)** and nigra **(B)**; bar values are mean ± SEM of four rats per group; $^{*}p < 0.05$ vs. 6-OHDA, $^{**}p < 0.05$ vs. 6-OHDA + L-DOPA, using an ANOVA followed by a Tukey's test. **(C,D)** Immunodensity of interleukin-1β determined by Western blot analysis in the striatum **(C)** and nigra **(D)**; bar values are mean ± SEM of four rats per group; $^{*}p < 0.05$ vs. 6-OHDA, $^{**}p < 0.05$ vs. 6-OHDA + L-DOPA, using an ANOVA followed by a Tukey's test. Scale bar: 100 μm.

DISCUSSION

Dopamine replacement therapy with L-DOPA is the main temporary therapy for PD but it triggers dyskinesia (LID) over time. We used a commercially available, brain permeable and selective P2X7R antagonist, Brillant Blue G (BBG), to show its ability to prevent LID in a rat model. We confirmed that a unilateral 6-OHDA injection caused a loss of dopamine neurons (TH, DAT staining) in the striatum and nigra, impairing motor responses (apomorphine-induced rotations) consistent with a hemiparkinsonian condition. Chronic L-DOPA administration triggered locomotor, postural, and orofacial dyskinetic movements together with motor incoordination, without altering 6-OHDA-induced dopaminergic degeneration, thus confirming the face validity of the model (Bastide et al., 2015). BBG prevented the development of the critical behavior alterations of LID, namely dyskinesia and motor incoordination. Since the two tested doses of BBG selectively target P2X7R (Donnelly-Roberts and Jarvis, 2007; Díaz-Hernández et al., 2012), having effects similar to other selective P2X7R antagonists and P2X7R knockout in different models of brain diseases (Melani et al., 2006; Díaz-Hernández et al., 2009, 2012; Kimbler et al., 2012; Carmo et al., 2014; Jimenez-Pacheco et al., 2016), the effects of BBG imply the likely involvement of P2X7R.

The pathophysiological changes underlying LID remain poorly understood. One defined neurochemical basis of LID is the imbalance of the nigrostriatal dopaminergic system due to the loss of pulsatile dopamine signaling replaced by a continuous L-DOPA-derived dopamine generation (Heumann et al., 2014). Accordingly, our LID model revealed an increased D1 receptor density, without alteration of the D2 receptor density in the striatum, together with a decreased D2 receptor density without alteration of the D1 receptor density in the nigra. This resulted in abnormal dopaminergic signaling in both structures, as indicated by the increase of DARPP-32 phosphorylation in threonine-34, which is associated with dopaminergic signaling (Svenningsson et al., 2004). BBG prevented all these LID-associated dopaminergic alterations, which might eventually result from direct effects of P2X7R located in dopamine cells (Heine et al., 2007) and striatal dopamine terminals (Carmo et al., 2014). However, although the presence of P2X7R mRNA and protein in the striatum and

substantia nigra is established (Amadio et al., 2007; Kaczmarek-Hajek et al., 2018; Crabbé et al., 2019; Gentile et al., 2019) and there is evidence for an increased P2X7R density in the striatum upon decreasing dopaminergic innervation (Ferrazoli et al., 2017; Crabbé et al., 2019), the cellular localization of P2X7R is essentially unknown, and there is no data currently available to ascribe the presence of P2X7R to different neuronal populations (e.g., D1R or D2R) in nigrostriatal pathways.

A concurrent mechanism of action of P2X7R to dampen LID results from the ability of BBG to prevent the alterations of astrocytes and microglia and the putative neuroinflammation suggested by the increased COX-2 and interleukin-1β levels in the striatum and nigra of LID mice. Indeed, neuroinflammation involving microglia and astrocytes critically controls LID (Bortolanza et al., 2015a; Mulas et al., 2016; Carta et al., 2017) and P2X7R are well-established to control neuroinflammation (Rodrigues et al., 2015; Illes et al., 2017), being most abundant in microglia (Melani et al., 2006; Bhattacharya and Biber, 2016; Kaczmarek-Hajek et al., 2018) and astrocytes (Oliveira et al., 2011). We observed that BBG displayed a different efficiency to prevent neuroinflammation-associated neurochemical alterations rather than alterations of glial cells in the striatum and neuroinflammation-associated glial cell alterations rather than neurochemical alterations in the nigra, probably due to the contribution of different players in mounting neuroinflammatory responses in the nigra and striatum (Walker et al., 2016) or as a consequence of the striatal scar caused by 6-OHDA administration. However, some parameters associated with neuroinflammation were attenuated by BBG in the striatum and nigra. Notably, several studies have proposed that the P2X7R-mediated control of neuroinflammation is actually responsible to control neuronal function (Hu et al., 2015; Bernardino et al., 2008) and recent studies identified P2X7R in microglia as paramount to mediate behavioral alterations upon repeated stress (Iwata et al., 2016; Yue et al., 2017). Further studies should exploit this observed robust ability of P2X7R to control dyskinesia as a new window of opportunity to disentangle the relative importance of the control of neuroinflammation and of the maladaptive dopaminergic alterations for the development of LID.

Although we propose that P2X7R might mainly modulate striatal and nigra dopaminergic function and neuroinflammation to control dyskinesia, it is important to note that our results do not allow a definition of the brain area (striatum, nigra or cerebral cortex) where P2X7R might play the more prominent role to control dyskinesia. The time course evaluation of the effects of BBG on dyskinesia also prompted the suggestion that the beneficial effects of BBG seem to increase with time, i.e., they seem more robust after 14 and 21 days of treatment compared to shorter periods of exposure to BBG (7 days). Future studies will be required to explore the apparent time-dependent increase of the efficiency of BBG and potential relation to an increased released of ATP, an upregulation of P2X7R, and/or increased efficiency of P2X7R action in altered cellular networks upon the evolution of a dyskinetic phenotype.

In conclusion, the present study provides the first demonstration for the involvement of the purinergic system in the development of LID and prompts considering P2X7R antagonists as novel candidate anti-dyskinesia drugs.

DATA AVAILABILITY STATEMENT

The datasets generated for this study will not be made publicly available; videos and lab books can only be scrutinized in loco at the University of Ceará.

ETHICS STATEMENT

The animal study was reviewed and approved by the ethics committee of the Federal University of Ceará (107/14).

AUTHOR CONTRIBUTIONS

AF, JN, AM, JP, and AS carried out the experimental manipulations and analyzed the data. AF, GA, and RC planned the experiments. AF, GA, and RC wrote the manuscript.

FUNDING

This work was supported by National Council for Scientific and Technological Development (Conselho Nacional de Desenvolvimento Científico e Tecnológico, CNPq). RC acknowledges CAPES-FCT, La Caixa Foundation (LCF/PR/HP17/52190001), Centro 2020 (CENTRO-01-0145-FEDER-000008:BrainHealth 2020 and CENTRO-01-0246-FEDER-000010) and Fundação para a Ciência e a Tecnologia (FCT; POCI-01-0145-FEDER-03127).

ACKNOWLEDGMENTS

We thank Matthew Janega for kindly revising the English grammar.

REFERENCES

Alberico, S. L., Kim, Y. C., Lence, T., and Narayanan, N. S. (2017). Axial levodopa-induced dyskinesias and neuronal activity in the dorsal striatum. *Neuroscience* 343, 240–249. doi: 10.1016/j.neuroscience.2016.11.046

Amadio, S., Montilli, C., Picconi, B., Calabresi, P., and Volonté, C. (2007). Mapping P2X and P2Y receptor proteins in striatum and substantia nigra: An immunohistological study. *Purinergic Signal.* 3, 389–398. doi: 10.1007/s11302-007-9069-8

Arbeloa, J., Pérez-Samartín, A., Gottlieb, M., and Matute, C. (2012). $P2X_7$ receptor blockade prevents ATP excitotoxicity in neurons and reduces brain damage after ischemia. *Neurobiol. Dis.* 45, 954–961. doi: 10.1016/j.nbd.2011.12.014

Aristieta, A., Ruiz-Ortega, J. A., Miguelez, C., Morera-Herreras, T., and Ugedo, L. (2016). Chronic L-DOPA administration increases the firing rate but does not reverse enhanced slow frequency oscillatory activity and synchronization in substantia nigra pars reticulata neurons from 6-hydroxydopamine-lesioned rats. *Neurobiol. Dis.* 89, 88–100. doi: 10.1016/j.nbd.2016.02.003

Bartlett, R., Stokes, L., and Sluyter, R. (2014). The $P2X_7$ receptor channel: recent developments and the use of $P2X_7$ antagonists in models of disease. *Pharmacol. Rev.* 66, 638–675. doi: 10.1124/pr.113.008003

Bastide, M. F., Meissner, W. G., Picconi, B., Fasano, S., Fernagut, P. O., Feyder, M., et al. (2015). Pathophysiology of L-dopa-induced motor and non-motor complications in Parkinson's disease. *Prog. Neurobiol.* 132, 96–168. doi: 10.1016/j.pneurobio.2015.07.002

Bernardino, L., Balosso, S., Ravizza, T., Marchi, N., Ku, G., Randle, J. C., et al. (2008). Inflammatory events in hippocampal slice cultures prime neuronal susceptibility to excitotoxic injury: a crucial role of P2X7 receptor-mediated IL-1β release. *J. Neurochem.* 106, 271–280. doi: 10.1111/j.1471-4159.2008.05387.x

Bhattacharya, A., and Biber, K. (2016). The microglial ATP-gated ion channel P2X7 as a CNS drug target. *Glia* 64, 1772–1787. doi: 10.1002/glia.23001

Bortolanza, M., Cavalcanti-Kiwiatkoski, R., Padovan-Neto, F. E., da-Silva, C. A., Mitkovski, M., Raisman-Vozari, R., et al. (2015a). Glial activation is associated with l-DOPA induced dyskinesia and blocked by a nitric oxide synthase inhibitor in a rat model of Parkinson's disease. *Neurobiol. Dis.* 73, 377–387. doi: 10.1016/j.nbd.2014.10.017

Bortolanza, M., Padovan-Neto, F. E., Cavalcanti-Kiwiatkoski, R., Dos Santos-Pereira, M., Mitkovski, M., Raisman-Vozari, R., et al. (2015b). Are cyclooxygenase-2 and nitric oxide involved in the dyskinesia of Parkinson's disease induced by L-DOPA? *Philos. Trans. R. Soc. Lond. B Biol. Sci.* 370:20140190. doi: 10.1098/rstb.2014.0190

Carmo, M. R., Menezes, A. P., Nunes, A. C., Pliássova, A., Rolo, A. P., Palmeira, C. M., et al. (2014). The P2X7 receptor antagonist Brilliant Blue G attenuates contralateral rotations in a rat model of Parkinsonism through a combined control of synaptotoxicity, neurotoxicity and gliosis. *Neuropharmacology* 81, 142–152. doi: 10.1016/j.neuropharm.2014.01.045

Carta, A. R., Mulas, G., Bortolanza, M., Duarte, T., Pillai, E., Fisone, G., et al. (2017). L-DOPA-induced dyskinesia and neuroinflammation: do microglia and astrocytes play a role? *Eur. J. Neurosci.* 45, 73–91. doi: 10.1111/ejn.13482

Crabbé, M., Van der Perren, A., Bollaerts, I., Kounelis, S., Baekelandt, V., Bormans, G., et al. (2019). Increased P2X7 receptor binding is associated with neuroinflammation in acute but not chronic rodent models for Parkinson's disease. *Front. Neurosci.* 13:799. doi: 10.3389/fnins.2019.00799

Cunha, R. A., Vizi, E. S., Ribeiro, J. A., and Sebastião, A. M. (1996). Preferential release of ATP and its extracellular catabolism as a source of adenosine upon high- but not low-frequency stimulation of rat hippocampal slices. *J. Neurochem.* 67, 2180–2187. doi: 10.1046/j.1471-4159.1996.67052180.x

Díaz-Hernández, M., Díez-Zaera, M., Sánchez-Nogueiro, J., Gómez-Villafuertes, R., Canals, J. M., Alberch, J., et al. (2009). Altered P2X7-receptor level and function in mouse models of Huntington's disease and therapeutic efficacy of antagonist administration. *FASEB J.* 23, 1893–1906. doi: 10.1096/fj.08-122275

Díaz-Hernández, J. I., Gomez-Villafuertes, R., León-Otegui, M., Hontecillas-Prieto, L., Del Puerto, A., Trejo, J. L., et al. (2012). *In vivo* P2X7 inhibition reduces amyloid plaques in Alzheimer's disease through GSK3β and secretases. *Neurobiol. Aging* 33, 1816–1828. doi: 10.1016/j.neurobiolaging.2011.09.040

Donnelly-Roberts, D. L., and Jarvis, M. F. (2007). Discovery of P2X7 receptor-selective antagonists offers new insights into P2X7 receptor function and indicates a role in chronic pain states. *Br. J. Pharmacol.* 151, 571–579. doi: 10.1038/sj.bjp.0707265

Donzuso, G., Agosta, F., Canu, E., and Filippi, M. (2020). MRI of motor and nonmotor therapy-induced complications in Parkinson's disease. *Mov. Disord.* 35, 724–740. doi: 10.1002/mds.28025

Ferrazoli, E. G., de Souza, H. D., Nascimento, I. C., Oliveira-Giacomelli, Á., Schwindt, T. T., Britto, L. R., et al. (2017). Brilliant blue G, but not fenofibrate, treatment reverts hemiparkinsonian behavior and restores dopamine levels in an animal model of Parkinson's disease. *Cell Transplant.* 26, 669–677. doi: 10.3727/096368916x695227

Gandelman, M., Levy, M., Cassina, P., Barbeito, L., and Beckman, J. S. (2013). $P2X_7$ receptor-induced death of motor neurons by a peroxynitrite/FAS-dependent pathway. *J. Neurochem.* 126, 382–388. doi: 10.1111/jnc.12286

Gentile, T. A., Simmons, S. J., Tallarida, C. S., Su, S., Rom, S., Watson, M. N., et al. (2019). Synthetic cathinone MDPV enhances reward function through purinergic P2X7 receptor-dependent pathway and increases P2X7 gene expression in nucleus accumbens. *Drug Alcohol Depend.* 197, 22–27. doi: 10.1016/j.drugalcdep.2018.12.022

George, J., Gonçalves, F. Q., Cristóvão, G., Rodrigues, L., Meyer Fernandes, J. R., Gonçalves, T., et al. (2015). Different danger signals differently impact on microglial proliferation through alterations of ATP release and extracellular metabolism. *Glia* 63, 1636–1645. doi: 10.1002/glia.22833

Gonçalves, N., Simões, A. T., Prediger, R. S., Hirai, H., Cunha, R. A., and Pereira de Almeida, L. (2017). Caffeine alleviates progressive motor deficits in a transgenic mouse model of Machado-Joseph disease. *Ann. Neurol.* 81, 407–418. doi: 10.1002/ana.24867

Gourine, A. V., Dale, N., Llaudet, E., Poputnikov, D. M., Spyer, K. M., and Gourine, V. N. (2007). Release of ATP in the central nervous system during systemic inflammation: real-time measurement in the hypothalamus of conscious rabbits. *J. Physiol.* 585, 305–316. doi: 10.1113/jphysiol.2007.143933

Heine, C., Wegner, A., Grosche, J., Allgaier, C., Illes, P., and Franke, H. (2007). P2 receptor expression in the dopaminergic system of the rat brain during development. *Neuroscience* 149, 165–181. doi: 10.1016/j.neuroscience.2007.07.015

Heumann, R., Moratalla, R., Herrero, M. T., Chakrabarty, K., Drucker-Colín, R., Garcia-Montes, J. R., et al. (2014). Dyskinesia in Parkinson's disease: mechanisms and current non-pharmacological interventions. *J. Neurochem.* 130, 472–489. doi: 10.1111/jnc.12751

Hu, S. J., Calippe, B., Lavalette, S., Roubeix, C., Montassar, F., Housset, M., et al. (2015). Upregulation of P2RX7 in Cx3cr1-deficient mononuclear phagocytes leads to increased interleukin-1β secretion and photoreceptor neurodegeneration. *J. Neurosci.* 35, 6987–6996. doi: 10.1523/jneurosci.3955-14.2015

Illes, P., Khan, T. M., and Rubini, P. (2017). Neuronal $P2X_7$ receptors revisited: do they really exist? *J. Neurosci.* 37, 7049–7062. doi: 10.1523/jneurosci.3103-16.2017

Iwata, M., Ota, K. T., Li, X. Y., Sakaue, F., Li, N., Dutheil, S., et al. (2016). Psychological stress activates the inflammasome via release of adenosine triphosphate and stimulation of the purinergic type 2X7 receptor. *Biol. Psychiatry* 80, 12–22. doi: 10.1016/j.biopsych.2015.11.026

Jimenez-Mateos, E. M., Smith, J., Nicke, A., and Engel, T. (2019). Regulation of $P2X_7$ receptor expression and function in the brain. *Brain Res. Bull.* 151, 153–163. doi: 10.1016/j.brainresbull.2018.12.008

Jimenez-Pacheco, A., Díaz-Hernández, M., Arribas-Blázquez, M., Sanz-Rodriguez, A., Olivos-Oré, L. A., Artalejo, A. R., et al. (2016). Transient P2X7 receptor antagonism produces lasting reductions in spontaneous seizures and gliosis in experimental temporal lobe epilepsy. *J. Neurosci.* 36, 5920–5932. doi: 10.1523/jneurosci.4009-15.2016

Jun, D. J., Kim, J., Jung, S. Y., Song, R., Noh, J. H., Park, Y. S., et al. (2007). Extracellular ATP mediates necrotic cell swelling in SN4741 dopaminergic neurons through $P2X_7$ receptors. *J. Biol. Chem.* 282, 37350–37358. doi: 10.1074/jbc.m707915200

Kaczmarek-Hajek, K., Zhang, J., Kopp, R., Grosche, A., Rissiek, B., Saul, A., et al. (2018). Re-evaluation of neuronal P2X7 expression using novel mouse models and a P2X7-specific nanobody. *eLife* 7:e36217. doi: 10.7554/elife.36217

Kimbler, D. E., Shields, J., Yanasak, N., Vender, J. R., and Dhandapani, K. M. (2012). Activation of P2X7 promotes cerebral edema and neurological injury after traumatic brain injury in mice. *PLoS One* 7:e41229. doi: 10.1371/journal.pone.0041229

Kumar, S., Mishra, A., and Krishnamurthy, S. (2017). Purinergic antagonism prevents mitochondrial dysfunction and behavioral deficits associated with dopaminergic toxicity induced by 6-OHDA in rats. *Neurochem. Res.* 42, 3414–3430. doi: 10.1007/s11064-017-2383-9

Lawson, L. J., Perry, V. H., Dri, P., and Gordon, S. (1990). Heterogeneity in the distribution and morphology of microglia in the normal adult mouse brain. *Neuroscience* 39, 151–170. doi: 10.1016/0306-4522(90)90229-w

Lundblad, M., Andersson, M., Winkler, C., Kirik, D., Wierup, N., and Cenci, M. A. (2002). Pharmacological validation of behavioural measures of akinesia and dyskinesia in a rat model of Parkinson's disease. *Eur. J. Neurosci.* 15, 120–132. doi: 10.1046/j.0953-816x.2001.01843.x

Marcellino, D., Suárez-Boomgaard, D., Sánchez-Reina, M. D., Aguirre, J. A., Yoshitake, T., Yoshitake, S., et al. (2010). On the role of $P2X_7$ receptors in dopamine nerve cell degeneration in a rat model of Parkinson's disease: studies with the $P2X_7$ receptor antagonist A-438079. *J. Neural Transm.* 117, 681–687. doi: 10.1007/s00702-010-0400-0

McGrath, J., Drummond, G., McLachlan, E., Kilkenny, C., and Wainwright, C. (2010). Guidelines for reporting experiments involving animals: the ARRIVE guidelines. *Br. J. Pharmacol.* 160, 1573–1576. doi: 10.1111/j.1476-5381.2010.00873.x

Meissner, W., Ravenscroft, P., Reese, R., Harnack, D., Morgenstern, R., Kupsch, A., et al. (2006). Increased slow oscillatory activity in substantia nigra pars reticulata triggers abnormal involuntary movements in the 6-OHDA-lesioned rat in the presence of excessive extracellular striatal dopamine. *Neurobiol. Dis.* 22, 586–598. doi: 10.1016/j.nbd.2006.01.009

Melani, A., Amadio, S., Gianfriddo, M., Vannucchi, M. G., Volontè, C., Bernardi, G., et al. (2006). P2X7 receptor modulation on microglial cells and reduction of brain infarct caused by middle cerebral artery occlusion in rat. *J. Cereb. Blood Flow Metab.* 26, 974–982. doi: 10.1038/sj.jcbfm.9600250

Mulas, G., Espa, E., Fenu, S., Spiga, S., Cossu, G., Pillai, E., et al. (2016). Differential induction of dyskinesia and neuroinflammation by pulsatile versus continuous l-DOPA delivery in the 6-OHDA model of Parkinson's disease. *Exp. Neurol.* 286, 83–92. doi: 10.1016/j.expneurol.2016.09.013

Nishida, K., Nakatani, T., Ohishi, A., Okuda, H., Higashi, Y., Matsuo, T., et al. (2012). Mitochondrial dysfunction is involved in $P2X_7$ receptor-mediated neuronal cell death. *J. Neurochem.* 122, 1118–1128. doi: 10.1111/j.1471-4159.2012.07868.x

Oliveira, J. F., Riedel, T., Leichsenring, A., Heine, C., Franke, H., Krügel, U., et al. (2011). Rodent cortical astroglia express in situ functional $P2X_7$ receptors sensing pathologically high ATP concentrations. *Cereb. Cortex* 21, 806–820. doi: 10.1093/cercor/bhq154

Padovan-Neto, F. E., Echeverry, M. B., Tumas, V., and Del-Bel, E. A. (2009). Nitric oxide synthase inhibition attenuates L-DOPA-induced dyskinesias in a rodent model of Parkinson's disease. *Neuroscience* 159, 927–935. doi: 10.1016/j.neuroscience.2009.01.034

Paxinos, G., and Watson, C. (2005). *The Rat Brain in Stereotaxic Coordinates.* 5th Edn. San Diego, CA: Academic Press.

Rodrigues, R. J., Tomé, A. R., and Cunha, R. A. (2015). ATP as a multi-target danger signal in the brain. *Front. Neurosci.* 9:148. doi: 10.3389/fnins.2015.00148

Ryu, J. K., and McLarnon, J. G. (2008). Block of purinergic $P2X_7$ receptor is neuroprotective in an animal model of Alzheimer's disease. *Neuroreport* 19, 1715–1719. doi: 10.1097/WNR.0b013e3283179333

Sharaf, A., Krieglstein, K., and Spittau, B. (2013). Distribution of microglia in the postnatal murine nigrostriatal system. *Cell Tissue Res.* 351, 373–382. doi: 10.1007/s00441-012-1537-y

Shen, H. Y., Canas, P. M., Garcia-Sanz, P., Lan, J. Q., Boison, D., Moratalla, R., et al. (2013). Adenosine A_{2A} receptors in striatal glutamatergic terminals and GABAergic neurons oppositely modulate psychostimulant action and DARPP-32 phosphorylation. *PLoS One* 8:e80902. doi: 10.1371/journal.pone.0080902

Suarez, L. M., Solis, O., Aguado, C., Lujan, R., and Moratalla, R. (2016). L-DOPA oppositely regulates synaptic strength and spine morphology in D1 and D2 striatal projection neurons in dyskinesia. *Cereb. Cortex.* 26, 4253–4264. doi: 10.1093/cercor/bhw263

Svenningsson, P., Nishi, A., Fisone, G., Girault, J. A., Nairn, A. C., and Greengard, P. (2004). DARPP-32: an integrator of neurotransmission. *Annu. Rev. Pharmacol. Toxicol.* 44, 269–296. doi: 10.1146/annurev.pharmtox.44.101802.121415

Thiele, S. L., Chen, B., Lo, C., Gertler, T. S., Warre, R., Surmeier, J. D., et al. (2014). Selective loss of bi-directional synaptic plasticity in the direct and indirect striatal output pathways accompanies generation of parkinsonism and l-DOPA induced dyskinesia in mouse models. *Neurobiol. Dis.* 71, 334–344. doi: 10.1016/j.nbd.2014.08.006

Volonté, C., Apolloni, S., Skaper, S. D., and Burnstock, G. (2012). $P2X_7$ receptors: channels, pores and more. *CNS Neurol. Disord. Drug Targets* 11, 705–721. doi: 10.2174/187152712803581137

Walker, D. G., Lue, L. F., Serrano, G., Adler, C. H., Caviness, J. N., Sue, L. I., et al. (2016). Altered expression patterns of inflammation-associated and trophic molecules in substantia nigra and striatum brain samples from Parkinson's disease, incidental Lewy body disease and normal control cases. *Front. Neurosci.* 9:507. doi: 10.3389/fnins.2015.00507

Wang, X. H., Xie, X., Luo, X. G., Shang, H., and He, Z. Y. (2017). Inhibiting purinergic $P2X_7$ receptors with the antagonist brilliant blue G is neuroprotective in an intranigral lipopolysaccharide animal model of Parkinson's disease. *Mol. Med. Rep.* 15, 768–776. doi: 10.3892/mmr.2016.6070

Wang, Q., and Zhang, W. (2016). Maladaptive synaptic plasticity in L-DOPA-induced dyskinesia. *Front. Neural Circuits* 10:105. doi: 10.3389/fncir.2016.00105

Wieraszko, A., Goldsmith, G., and Seyfried, T. N. (1989). Stimulation-dependent release of adenosine triphosphate from hippocampal slices. *Brain Res.* 485, 244–250. doi: 10.1016/0006-8993(89)90567-2

Yue, N., Huang, H., Zhu, X., Han, Q., Wang, Y., Li, B., et al. (2017). Activation of $P2X_7$ receptor and NLRP3 inflammasome assembly in hippocampal glial cells mediates chronic stress-induced depressive-like behaviors. *J. Neuroinflammation* 14:102. doi: 10.1186/s12974-017-0865-y

Zhang, X., Zhang, M., Laties, A. M., and Mitchell, C. H. (2005). Stimulation of $P2X_7$ receptors elevates Ca^{2+} and kills retinal ganglion cells. *Invest. Ophthalmol. Vis. Sci.* 46, 2183–2191. doi: 10.1167/iovs.05-0052

Conflict of Interest: RC is a scientific consultant of the Institute for Scientific Information on Coffee (ISIC).

The remaining authors declare that the research was conducted in the absence of any commercial or financial relationships that could be construed as a potential conflict of interest.

frontiers in Molecular Neuroscience

ORIGINAL RESEARCH
published: 02 September 2020
doi: 10.3389/fnmol.2020.00157

Ultra-Endurance Associated With Moderate Exercise in Rats Induces Cerebellar Oxidative Stress and Impairs Reactive GFAP Isoform Profile

Raphael Fabricio de Souza[1,2,3,4], Ricielle Lopes Augusto[1], Silvia Regina Arruda de Moraes[5], Fabio Borges de Souza[1], Lílian Vanessa da Penha Gonçalves[1], Danielle Dutra Pereira[1], Gisele Machado Magalhães Moreno[1], Fernanda Maria Araujo de Souza[6] and Belmira Lara da Silveira Andrade-da-Costa[1,2]*

[1] Laboratory of Neurophysiology, Department of Physiology and Pharmacology, Center of Biosciences, Federal University of Pernambuco, Recife, Brazil, [2] Postgraduate Program in Neuropsychiatry and Behavioral Sciences, Federal University of Pernambuco, Recife, Brazil, [3] Department of Physical Education, Federal University of Sergipe, São Cristovão, Brazil, [4] Group of Studies and Research of Performance, Sport, Health and Paralympic Sports – GEPEPS, Federal University of Sergipe, São Cristovão, Brazil, [5] Laboratory of Neuromuscular Plasticity, Department of Anatomy, Center of Biosciences, Federal University of Pernambuco, Recife, Brazil, [6] Laboratory of Neuropharmacology and Integrative Physiology, Center of Biosciences, Federal University of Alagoas, Maceió, Brazil

OPEN ACCESS

Edited by:
Maria José Diógenes, University of Lisbon, Portugal

Reviewed by:
Tapas C. Nag, All India Institute of Medical Sciences, India
Adelaide Fernandes, University of Lisbon, Portugal

***Correspondence:**
Raphael Fabricio de Souza
desouza@ufs.br; raphaelctba20@hotmail.com

Received: *30 December 2019*
Accepted: *29 July 2020*
Published: *02 September 2020*

Citation:
de Souza RF, Augusto RL, de Moraes SRA, de Souza FB, Gonçalves LVP, Pereira DD, Moreno GMM, de Souza FMA and Andrade-da-Costa BLS (2020) Ultra-Endurance Associated With Moderate Exercise in Rats Induces Cerebellar Oxidative Stress and Impairs Reactive GFAP Isoform Profile. Front. Mol. Neurosci. 13:157. doi: 10.3389/fnmol.2020.00157

Ultra-endurance (UE) race has been associated with brain metabolic changes, but it is still unknown which regions are vulnerable. This study investigated whether high-volume training in rodents, even under moderate intensity, can induce cerebellar oxidative and inflammatory status. Forty-five adult rats were divided into six groups according to a training period, followed or not by an exhaustion test (ET) that simulated UE: control (C), control + ET (C-ET), moderate-volume (MV) training and MV-ET, high-volume training (HV) and HV-ET. The training period was 30 (MV) and 90 (HV) min/day, 5 times/week for 3 months as a continuous running on a treadmill at a maximum velocity of 12 m/min. After 24 h, the ET was performed at 50% maximum velocities up to the animals refused to run, and then serum lactate levels were evaluated. Serum and cerebellar homogenates were obtained 24 h after ET. Serum creatine kinase (CK), lactate dehydrogenase (LDH), and corticosterone levels were assessed. Lipid peroxidation (LP), nitric oxide (NO), Interleukin 1β (IL-1β), and GFAP proteins, reduced and oxidized glutathione (GSH and GSSG) levels, superoxide dismutase (SOD) and catalase (CAT) activities were quantified in the cerebellum. Serum lactate concentrations were lower in MV-ET (∼20%) and HV-ET (∼40%) compared to the C-ET group. CK and corticosterone levels were increased more than ∼ twofold by HV training compared to control. ET increased CK levels in MV-ET vs. MV group ($P = 0.026$). HV induced higher LP levels (∼40%), but an additive effect of ET was only seen in the MV-ET group ($P = 0.02$). SOD activity was higher in all trained groups vs. C and C-ET ($P < 0.05$). CAT activity, however, was intensified only in the MV group ($P < 0.02$). The 50 kDa GFAP levels were enhanced

in C-ET and MV-ET vs. respective controls, while 42 kDa (∼40%) and 39 kDa (∼26%) isoform levels were reduced. In the HV-ET group, the 50 KDa isoform amount was reduced ∼40–60% compared to the other groups and the 39 KDa isoform, increased sevenfold. LDH levels, GSH/GSSG ratio, and NO production were not modified. ET elevated IL-1β levels in the CT and MV groups. Data shows that cerebellar resilience to oxidative damage may be maintained under moderate-volume training, but it is reduced by UE running. High-volume training *per se* provoked systemic metabolic changes, cerebellar lipid peroxidation, and unbalanced enzymatic antioxidant resource. UE after high-volume training modified the GFAP isoform profile suggesting impaired astrocyte reactivity in the cerebellum.

Keywords: oxidative stress, central nervous system, high-volume training, catalase, superoxide dismutase, lipid peroxidation, glial fibrillary acidic protein

INTRODUCTION

In the last decades, a noticeable increase in the number of athletes taking part in long-distance running and ultramarathons has been reported (Agnew et al., 2018). In contrast to regular volume training, some deleterious effects have been described as a result of high volume, repetitive physical effort, and exhaustive and complex competitions (Knechtle and Nikolaidis, 2018). Recent studies have identified physiological impairment resulting from the ultra-endurance race (UE), encompassing cardiac and major artery structural remodeling, indications of pathological condition (O'Keefe et al., 2012; Bonsignore et al., 2017), marked renal and muscle damage (Jastrzębski et al., 2015), hepatic dysfunction (Rama et al., 2015), cartilage wear (Franciozi et al., 2013), and oxidative damage to the peripheral and central nervous systems (CNS) (Chalimoniuk et al., 2015a; Muñoz et al., 2017).

The CNS is especially vulnerable to oxidative damage due to its high O_2-dependent mitochondrial activity, intensified by aerobic exercise, increased oxygen uptake, and cerebral blood flow (40–70%) to meet energy demands (Chalimoniuk et al., 2015a). When subjected to an antioxidant enzymatic imbalance, the CNS is an important target for reactive oxygen species (ROS) and oxidative stress secondary byproducts. Physical exercise can exert neuroprotective or harmful actions in the redox balance, depending on the intensity, volume, duration, and specificity of the brain region, independent of the involvement of this region in the locomotor function (de Souza et al., 2018).

The cerebellum plays a relevant role in motor, cognitive, and limbic activity (Hibi and Shimizu, 2011; Schmahmann, 2019) and promotes movement control, motor learning (Celnik, 2015) balance, muscle coordination, posture (Hibi and Shimizu, 2011; Powell et al., 2015; Jirenhed et al., 2017) and visually guided locomotion (Armstrong, 1996; Rabe et al., 2008; Schmahmann, 2019). Moderate aerobic exercise increased the dendritic density, field area, and total branch length of Purkinje cells (Pysh and Weiss, 1979; Huang et al., 2018) and favors cerebellar angiogenesis (Black et al., 1990; Lee, 2007). Also, cerebellar molecular changes induced by exercise promote plasticity in the motor cortex (Mang et al., 2016), attenuate cerebellar deficiencies (Tercero-Pérez et al., 2019), suppress Purkinje cell loss during Parkinson's disease (Lee et al., 2018), increase mitochondrial biogenesis (Marques-Aleixo et al., 2015), and inhibit oxidative stress, promoting apoptotic signaling (Marques-Aleixo et al., 2016). Purkinje cells have also been shown to have high levels of monocarboxylate transporters (MCTs), which are key proteins in energy metabolism when stimulated, by treadmill running (Hoshino et al., 2016).

Studies that evaluated training over 60 min per day have examined the effects on the entire rodent brain (Radak et al., 2001; Hagen et al., 2018), neglecting metabolic specificities of different brain regions. Notwithstanding the importance of the cerebellum for cognitive planning and execution functions involved in movement control, limited experimental studies have investigated the oxidative impact of high-volume training and UE tests in this brain region. Another aspect that motivated our study was its differential vulnerability and neurochemical profile (Scorziello et al., 2001). To our knowledge, no study has yet investigated whether UE could modify astrocyte function in the cerebellum. Bergman glia is a specialized radial astrocyte of the cerebellum and has a differential genesis, ensheaths, and controls almost all synapses on the Purkinje neurons, conferring to this region distinct plastic responses when compared to the cerebral cortex, for example (Bernardinelli et al., 2014). Moreover, functional modifications in the Bergman glia can affect associative motor learning and/or motor performance (De Zeeuw and Hoogland, 2015). Astrocytes are active players in brain energy delivery, production, utilization, and storage (Sonnay et al., 2017). Brain glycogen is chiefly located in these glial cells and it decreases with extensive and prolonged exercise (Matsui et al., 2012, 2017). However, it is still unknown whether UE running induces altered glial activity as well as modifies antioxidant defense mechanisms when associated with high-volume running training (Jastrzębski et al., 2015; Rama et al., 2015; Knechtle and Nikolaidis, 2018; Millet et al., 2018).

The current discussion on the negative effects of high-volume and UE on runner health (Knechtle and Nikolaidis, 2018; Millet et al., 2018), and the scarcity of knowledge about these effects in locomotion-related brain regions has motivated the present study. We hypothesized that rodent cerebellar resilience to oxidative injuries may be reduced after high-volume training, regardless of the exhaustion test simulating UE running.

MATERIALS AND METHODS

Experimental Animal Groups

Forty-five adult male Wistar rats (60 days; 225.84 ± 24.33 g) were obtained from the animal production unit of the Federal University of Paraíba, João Pessoa, Brazil. The animals were kept on a 12 h light/dark cycle under an inverse photoperiod (lights on 6:00 p.m.), under a controlled environment with temperature (22°C ± 2°C) and had free access to food and water.

After the running training test, the animals were randomized into six groups according to the moderate-intensity training period, followed or not by the exhaustion test (ET): control (C: n = 8, placed on the treadmill off), control + ET (C + ET: n = 7), moderate-volume training (MV: n = 8) moderate-volume training + ET (MV + ET: n = 7), high-volume training (HV: n = 8), and high-volume training + ET (HV + ET: n = 7). All the experimental procedures animals followed the guidelines for the Care and Use of Laboratory Animals previously approved by the Animal Use Ethics Committee of the Federal University of Pernambuco, Brazil (# 0035-2017).

Physical Training Protocol

For running training, a motorized treadmill (AVS products®) with individual tracks and equipped with rear shock (2.0 mA) was used. One week before the beginning of the training, the animals were adapted to a speed of 5 m/min for 10 min, 5 times per week. Subsequently, the animals were submitted to a maximum velocity test (Vmax) to determine the training threshold. Vmax consisted of a graded threshold run and speed increments (5 m/min every 3 min), starting at 5 m/min up to the maximum intensity achieved by each animal (de Senna et al., 2011).

The treadmill trainability test was rated on a scale of 1 to 5 according to the following criteria: (1) refusing to run, (2) below-average runner (sporadically running but stops running constantly), (3) average runner (maintains a steady run but falls or stops running sporadically), (4) above-average runner (consistent runner, occasionally falls backward on the treadmill), and (5) good runner (Dishman et al., 1988). Animals classified as score ≥3 were randomized in the groups for physical training. Only two animals scored <3, and these animals were put in the control groups.

The training protocol was continuous for 12 weeks. Daily exercise sessions 3 to 5 times/week with low to moderate intensity (50–70% of maximum intensity achieved in Vmax tests) were performed by the MV, MV-ET, HV, and HV-ET groups (see **Table 1**). The training times of the MV and MV-ET or HV and HV-ET groups were gradually increased from 10 to 30 min or 10 to 90 min per day, respectively, over 12 weeks (Tarini et al., 2013). Each training session was preceded by 5 min of warm-up at 30% of Vmax and the end of the run 5 min of recovery at 30% of Vmax (de Senna et al., 2011). These times were included in the total protocol period. The rear shock was used only in the early steps of animal adaptation to the treadmill, 1 week before the beginning of the training despite the score obtained in the trainability test. It was not necessary to use rear shock for the 3 months training period.

Twenty-four hours after the training period, the C-ET, MV-ET, and HV-ET groups were submitted to the exhaustion test. This test was performed up to the maximum running distance (low to moderate intensities) when the animals were considered depleted and refused to run (touching the running box 10 times for 1 min) (Tarini et al., 2013), after which tail blood was collected for analysis of serum lactate levels. After 24 h, all animals were weighed, anesthetized with 100% isoflurane, followed by blood collection directly from the heart (left ventricle) before decapitation for immediate removal of the cerebellum tissue (see **Figure 1**).

Running Performance

For analysis of running performance, the running time (min), distance traveled (meters), speed (meters/min), and horizontal workload were evaluated in the groups submitted to the exhaustion test.

Markers of Metabolic Changes in the Serum

Total creatine kinase (CK) and lactate dehydrogenase (LDH) concentrations in the serum were quantified as indicators of potential damage to the tissues. The blood samples (∼4 mL) were collected after euthanasia by cardiac puncture and put in dry tubes for separating serum (InjeXvácuo) with a clot activator. They were subsequently centrifuged for 10 min at 800 g and 4°C, and then the serum was separated for analysis using specific commercial kits (Katal Biotechnology, São Paulo, Brazil for LDH and Labtest Diagnóstica S.A.; Minas Gerais, Brazil for CK) according to the manufacturer's instructions.

For quantification of lactate levels, the tail vein blood sample collection was used; approximately 25 μl of the blood sample was placed directly onto test strips (BM-Lactate) and immediately analyzed with an Accutrend Lactate Accu-Check lactate meter (Roche, Brazil) just after ET.

TABLE 1 | Training protocol.

Week		Training threshold (%–m/min)	Time (Min)		Frequency of weekly sessions	Recovery training (hours)
			MV	HV		
Adaptation	1°	5 m/min	10 min	10 min	3×	24
	2°	50%	10 min	10 min	3×	24
1°Phase	3°	50%	15 min	20 min	3×	24
	4°	50%	20 min	30 min	3×	24
	5°	50%	25 min	40 min	5×	24
	6°	50%	30 min	50 min	5×	24
2°Phase	7°	60%	30 min	60 min	5×	24
	8°	60%	30 min	70 min	5×	24
	9°	60%	30 min	80 min	5×	24
	10°	70%	30 min	90 min	5×	24
3°Phase	11°	70%	30 min	90 min	5×	24
	12°	70%	30 min	90 min	5×	24

MV, moderate-volume training; HV, high-volume training.

For the corticosterone assay, 50 μl of serum was used. Analyses were made in duplicate per sample at a 1:1000 dilution. The entire procedure was performed as recommended by the Corticosterone ELISA kit (Cayman Chemical, No 501320).

Biochemical Analysis of Cerebellum Oxidative Status

Cerebellum Tissue Preparation

The cerebellum dissection was made over a filter paper that was put over an iced buffer, and the wet weight was obtained before the immersion of cerebellum in the saline solution and kept in a deep freezer at –80°C. Then, this tissue was homogenized at 4°C in a lysis buffer containing 10 mM ethylenediaminetetraacetic acid (EDTA), 2 mM phenylmethylsulfonyl fluoride (PMSF), 100 mM sodium fluoride, 10 mM sodium pyrophosphate ($Na_4P_2O_7$), 100 mM Tris (hydroxymethyl) aminomethane, pH 7.4, and a 1% cocktail of protease inhibitors (AEBSF- [4- (2-Aminoethyl) benzenesulfonyl fluoride hydrochloride; Aprotinin, Bestatin hydrochloride, E-64-[N-(*trans*-Epoxysuccinyl)-L-leucine) 4-guanidino butylamine, leupeptin hemisulfate pepstatin A; (Sigma-Aldrich, United States) (1:5 w/v). Thereafter the homogenate was centrifuged for 10 min at 10,000 *g* at 4°C and the supernatants stored at −80°C for further analyses.

Lipid Peroxidation Analysis

Lipoperoxidation (LP) was measured by estimating the malondialdehyde (MDA) levels using the thiobarbituric acid reactive substance (TBARS) assay, which measures the MDA present in the sample, as well as MDA generated from lipid hydroperoxides by the hydrolytic conditions of the reaction (Ohkawa et al., 1979). The reaction was developed by sequential addition of 80 μL 8.1% sodium dodecyl sulfate, 600 μL 20% acetic acid, pH 3.5, and 600 μL 0.8% TBA solutions and 200 μL of cerebellum supernatant, boiled in water for 60 min and then cooled in an ice bath. Afterward, 600 μL of n-butanol was added, the mixture was shaken and centrifuged at 2,500 *g* for 10 min, and the upper phase was collected and analyzed at 532 nm using a plate reader (Thermo Scientific, Varioskan flash spectral scanning multimode reader).

Nitric Oxide Levels

Nitrite levels were estimated using Griess reagent as an indicator of nitric oxide (NO) production (Green et al., 1982). Equal volumes (100 μL) of supernatant and Griess reagent were placed in a 96-well plate and reacted for 10 min at room temperature (∼ 22°C). The absorbance of the diazonium compound was measured at a wavelength of 540 nm. Results were expressed as nmol per mg protein regarding a standard curve constructed with known concentrations of sodium nitrite.

Total Superoxide Dismutase and Catalase Activity

Evaluation of total superoxide dismutase (t-SOD) activity was performed according to Misra and Fridovich (1972) at 25°C. Triplicates of cerebellum supernatants (60 μL) were previously incubated in a water bath at 37°C. Sodium carbonate (920 μL of 0.05% buffer) was added. The reaction was developed by adding 20 μl of 150 mM epinephrine in 0.05% acetic acid. The decay kinetics of absorbance levels at 480 nm was evaluated by measurements every 15 s over a total period of 2 min. One unit of t-SOD was defined as the amount of enzyme that causes 50% inhibition of epinephrine oxidation. The enzymatic activity of t-SOD tissue was expressed in units per milligram of protein (U/mg protein).

Catalase enzymatic activity (CAT) was measured according to Aebi (1984). Triplicates of cerebellum supernatants (60 μL) were added to 905 μL sodium phosphate buffer pH 7.0. The reaction was developed by adding 35 μl of 300 mM hydrogen peroxide in sodium phosphate buffer. The rate constant K decomposition of H_2O_2 under our experimental conditions of temperature (22°C), and pH (7.0) was determined to be 2.3 to measure absorbance changes for 10 s for 1.5 min at 240 nm. Enzyme activity was also expressed as units per milligram of protein (U/mg protein).

Glutathione Levels

Glutathione (GSH) levels were analyzed according to Hissin and Hilf (1976). Thus, 450 μL of 100 mM phosphate buffer with EDTA (5 mM) (pH 8.0) was added to 50 μL of the supernatant; 50 μL of this mixture plus 140 μL of 100 mM phosphate buffer plus 10 μL of o-phthaldialdehyde (OPA; Sigma Aldrich, United States) solutions were placed in plates and incubated for 20 min at room temperature, protected from light. Absorbance was recorded on a spectrofluorometer using a wavelength of 350 nm. Results were expressed in μmol per mg protein regarding a curve pattern constructed with known concentrations of GSH.

Oxidized Glutathione Levels

Oxidized Glutathione (GSSG) levels were analyzed according to Hissin and Hilf (1976). Thus, 50 μL of the supernatant was incubated at room temperature with 20 μL of 0.04M N-ethylmaleimide (NEM) for 30 min to interact with GSH present in the tissue. To this mixture, 430 mL of 0.1 M sodium hydroxide (NaOH) was added; 50 μL of this mixture plus 140 μL of 0.1 M NaOH and 10 mL OPA were placed in the wells of a 96-well plate. This mixture was incubated for 15 min at room temperature and protected from light. The reading was taken on a spectrofluorometer using a wavelength of 350 nm for emission. Results were expressed in μmol per mg protein regarding a standard curve constructed with known concentrations of GSSG.

GFAP and IL-1β Protein Levels in the Cerebellum

Glial fibrillary acidic protein (GFAP) and IL-1 protein levels in the cerebellar tissue were analyzed by Western blotting. Cerebellar homogenate samples were diluted in sample buffer and boiled for 5 min. Forty micrograms of protein per lane were electrophoretically separated in 15% sodium dodecyl sulfate polyacrylamide gel containing 10% sodium dodecyl sulfate, 30% Acrylamide/Bis-Acrylamide Solution, 1.5 M Tris–HCl (pH 8.8), 10% APS, and TEMED at 100V, 0.15A, and 300W. After separation, the proteins were transferred to a nitrocellulose membrane (Maine Manufacturing, United States, 0.22 micron) for 1.5 h at 250V, 0.35A, and 300W. The membranes were blocked for 1 h in a Tris-Tween 20 (TBS-T) solution containing

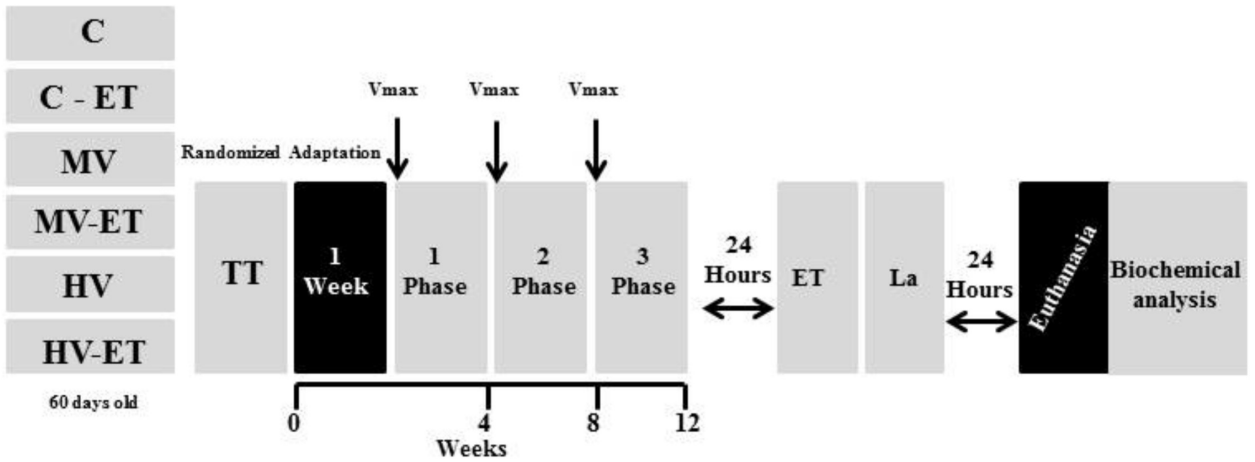

FIGURE 1 | Experimental protocol of aerobic exercise training under different volumes. Vmáx: Max speed test, ET, exhaustion test; TT, trainability test; La, lactate analysis. C, control group; C-ET, control group + exhaustion test; MV, moderate-volume group; MV-ET, moderate-volume + exhaustion test group; HV, high-volume group; HV-ET, high-volume + exhaustion test group.

5% BSA. They were then incubated with rabbit polyclonal anti-GFAP primary antibody (Dako, Agilent Technologies, Germany, 1:1000) or rabbit polyclonal anti-IL-1β (Sino Biological Inc., Beijing, China, 1:2000), both diluted in TBS-T overnight at 4°C. After three washes in TBS-T, the membrane was treated with goat anti-rabbit secondary antibody conjugated to Horseradish peroxidase (Jackson ImmunoResearch, United States; 1:50,000), diluted in TBS-T for 1 h. Subsequently, the membranes were washed in TBS-T and stained with Luminata Western HRP substrate (Millipore, United States) *via* enhanced chemiluminescence using a ChemiDoc imaging system (Bio-Rad, United States). Mouse monoclonal anti-beta-actin antibody (Santa Cruz Biotechnology, CA 1:10,000) was used to normalize the quantitative values. The data were analyzed using the Image Lab 6.0.1 software (Bio-Rad, United States).

Statistical Analysis

The Shapiro-Wilk test was used to verify the normality of the data. Comparisons among groups were made by two-way ANOVA. One-way ANOVA was used for running distance, running time, running velocity, horizontal workload, and lactate variables. *Post hoc* combinations were performed using Bonferroni's or LSD multiple comparison tests. Non-parametric results were compared using the Kruskal Wallis test. To find the effect size, Cohen's *d*-test (Nakagawa and Cuthill, 2007) was applied by adopting the 0.02 to 0.15 points for a small effect, 0.16 to 0.35 medium effect, and greater than 0.35 as a large effect. The software SPSS (version 20.0) was used, considering $P \leq 0.05$ as a significant value.

RESULTS

Body and Cerebellum Weights

Figure 2A illustrates the percentage of body weight gain during the 3 months of training. No intergroup difference in the body weight was detected at the beginning of training [$F(5,44) = 1.99$, $P = 0.101$] and no difference in the percentage of body weight gain was achieved after 3 months of this training (**Figure 2A**), [$F(5,43) = 0.908$, $P = 0.486$]. The area under the curve of the percentage of body weight gain [$F(5,44) = 0.188$, $P = 0.965$] can be seen in **Figure 2B**. There was no difference in the cerebellar weight [**Figure 2C**; $F(5,44) = 1.053$ $P = 0.401$] or in cerebellum/body weight ratio among the groups [**Figure 2D**; ($F(5,44) = 1.791$, $P = 0.137$].

Maximum Velocity Test

Table 2 describes the maximum velocity achieved by the animal groups during the 3 months of training. The training under moderate- or high-volume was able to progressively increase the velocity achieved by the animals when compared to the control condition [$F(17,131) = 2.335$, $P = 0.004$]. A significant increase was found between Vmax 2 vs. Vmax1 in MV; HV and HV-ET ($P < 0.026$). Vmax3 was also higher than Vmax1 in HV-ET and HV ($P < 0.010$). Intergroup differences were detected for Vmax 2 between HV vs. C ($P = 0.021$) and for Vmax3, increase was detected in HV-ET compared to C-ET ($P = 0.016$) and HV vs. C ($P = 0.011$).

Traveled Distance, Duration, Running Speed, and Horizontal Workload During Exhaustion Test

As expected, moderate- and high-volume training promoted a better running performance than the control condition during the exhaustion test (**Figures 2E–H**), evaluated by the running distance [$F(2,20) = 129.019$, $P < 0.001$], running duration [$F(2,20) = 115.743$, $P < 0.001$], running velocity [$F(2,20) = 116.869$, $P < 0.001$], and horizontal workload [$F(2,20) = 15.748$, $P < 0.001$]. The HV-ET group achieved greater running distance at the end of this test when compared to MV-ET (↑ 280.92%; $P < 0.001$; Cohen's $d = 5.13$) and C- ET [↑ 624.75%

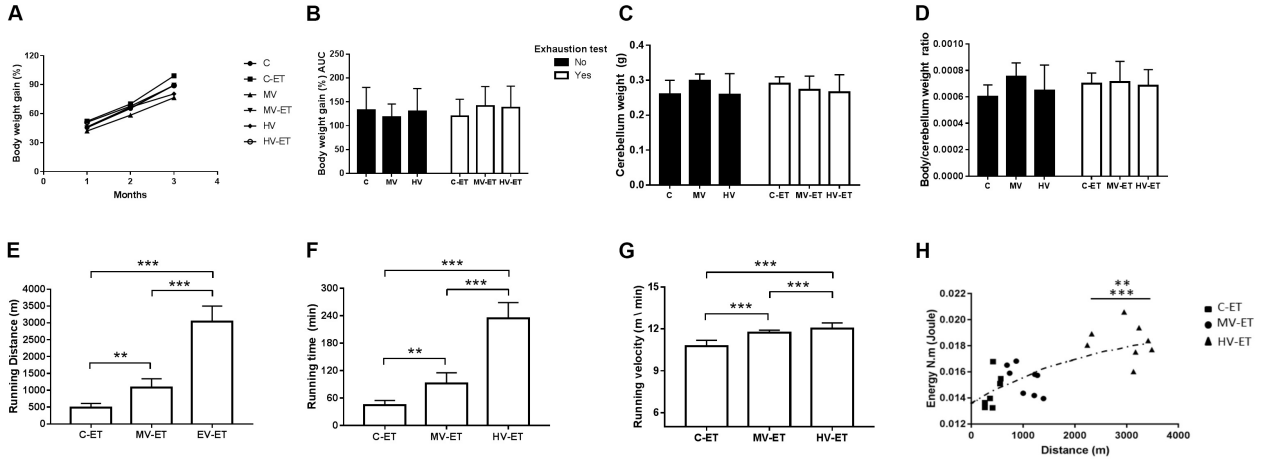

FIGURE 2 | Somatic parameters and Running performance. **(A)** Body weight gain during months of training. **(B)** Area under the curve of body weight gain. **(C)** Cerebellum weight; **(D)** Body weight/cerebellum weight ratio. **(E)** Running distance of exhaustion test: MV-ET vs. C-ET; $P = 0.002$. HV-ET vs. MV-ET; C-ET; $P < 0.001$; **(F)** Running time of exhaustion test: MV-ET vs. C-ET; $P = 0.002$. HV-ET vs. MV-ET; C-ET; $P < 0.001$. **(G)** Velocity of exhaustion test HV-ET vs. MV-ET; C-ET; $P < 0.001$. **(H)** Horizontal Workload vs. running time during exhaustion test HV-ET vs. MV-ET ($P = 0.002$); C-ET; $P < 0.001$. C-ET, control + exhaustion test group; MV, moderate-volume group; MV-ET, moderate-volume + exhaustion test group; HV, high-volume group; HV-ET, high-volume + exhaustion test group. $^{**}P < 0.01$; $^{***}P < 0.001$. Values represent mean ± S.D.

TABLE 2 | Maximum velocity test.

Groups	n	Vmax 1 (m/min)	Vmax 2 (m/min)	Vmax 3 (m/min)
C	8	23.8 ± 2.3	23.1 ± 2.5	21.3 ± 2.3
C-ET	7	20.8 ± 3.8	22.5 ± 5.2	21.4 ± 2.4
MV	8	20.8 ± 3.8	25.0 ± 4.0*	22.9 ± 2.7
MV-ET	7	23.1 ± 3.7	24.3 ± 3.2	24.4 ± 4.2
HV	8	22.9 ± 2.7	27.1 ± 2.6*‡	25.7 ± 1.9‡
HV-ET	7	21.3 ± 3.5	25.6 ± 4.1*	25.6 ± 3.2§#

Vmax, maximum velocity test. C, control group; C-ET, control group + exhaustion test; MV, moderate volume group; MV-ET, moderate volume group + exhaustion test; HV, high group; HV-ET, high group + exhaustion test. $P \leq 0.05$; intragroup (Vmax 2 vs. Vmax1, §Vmax 3 vs. Vmax1); intergroup (‡ HV or MV vs. C, # HV-ET or MV-ET vs. C-ET).*

($P < 0.001$; Cohen's $d = 7.43$]. The running distance traveled by MV-ET was also greater than that achieved by the C-ET group (↑ 222.39%; $P = 0.002$; Cohen's $d = 2.89$) (**Figure 2E**). Similarly, the running duration (**Figure 2F**) in HV-ET animals was higher than in MV-ET (↑ 253.78%; $P < 0.001$ Cohen's $d = 4.79$) and C-ET groups (↑ 522.00%; $P < 0.001$; Cohen's $d = 9.47$. Longer running duration was achieved by MV-ET compared to C-ET (↑ 205.68%; $P = 0.002$; Cohen's $d = 5.62$). The running speed (**Figure 2G**) and the horizontal workload (**Figure 2H**) in the MV-ET and HV-ET groups were also proportionally increased according to the training volume, when compared to the control condition (↑ 6.16 and ↑ 23,96%; $P < 0.001$; Cohen's $d = 0.74$ and 2.60, respectively).

Lactate, CK, Lactate Dehydrogenase, and Corticosterone Levels in the Serum

The ET provoked significant differences in the serum lactate concentration among the groups $F(2,20) = 15.188$, $P < 0.001$). Lower lactate levels were detected in the MV-ET (↓ 30.28%; $P = 0.015$; Cohen's $d = 4.69$) and HV-ET (↓ 53.85%; $P < 0.001$; Cohen's $d = 2.48$) groups when compared to C-TE (**Figure 3A**). Increased serum CK concentration was induced by the training or ET compared to the control condition [$F(5,34) = 4.87$, $P = 0.002$]. The MV-ET group presented higher values when compared to C-ET (↑ 161.68% $P = 0.026$; Cohen's $d = 1.34$) and MV (160.72% $P = 0.033$; Cohen's s $d = 1.24$) groups. In the HV group, CK values were greater than in the C animals (↑ 223.63%; $P = 0.03$; Cohen's $d = 1.31$). No additional increase in the CK values was induced by the exhaustion test in the C-ET or HV-ET groups compared to their respective controls (C and HV) (**Figure 3B**). No statistical difference in serum LDH concentrations was detected among the groups [$F(5,34) = 1.127$, $P = 0.368$] (**Figure 3C**).

Figure 4 shows the results of serum corticosterone levels. A significant difference was found among the groups [$F(5,27) = 4.008$, $P = 0.010$]. The high-volume training *per se* induced higher levels of corticosterone compared to the control condition (↑ 44.44%; $P = 0.038$; Cohen's $d = 0.24$). Values in HV were also greater than in MV-ET group (↑ 90.06%; $P = 0.003$; Cohen's $d = 0.01$) and C-ET (↑ 75.17%; $P = 0.022$; Cohen's $d = 1.33$). No intergroup difference was detected between the HV and HV-ET groups, but corticosterone values in the HV-ET group were elevated compared to MV-ET (↑ 91.74%; $P = 0.002$; Cohen's $d = 0.32$) and C-ET (↑ 79.36%; $P = 0.013$; Cohen's $d = 0.68$).

Lipid Peroxidation in the Cerebellum

Lipid peroxidation levels were differentially affected by the training or exhaustion test [$F(5,27) = 3.396$, $P = 0.020$]. **Figure 5A** illustrates increased levels of lipid peroxidation in the cerebellum of HV versus MV (↑ 26.1%; $P = 0.027$, Cohen's $d = 1.14$) and C (↑ 27.9%; $P = 0.036$, Cohen's $d = 1.26$); MV-ET vs. MV (↑ 25.2%; $P = 0.021$; Cohen's $d = 1.19$).

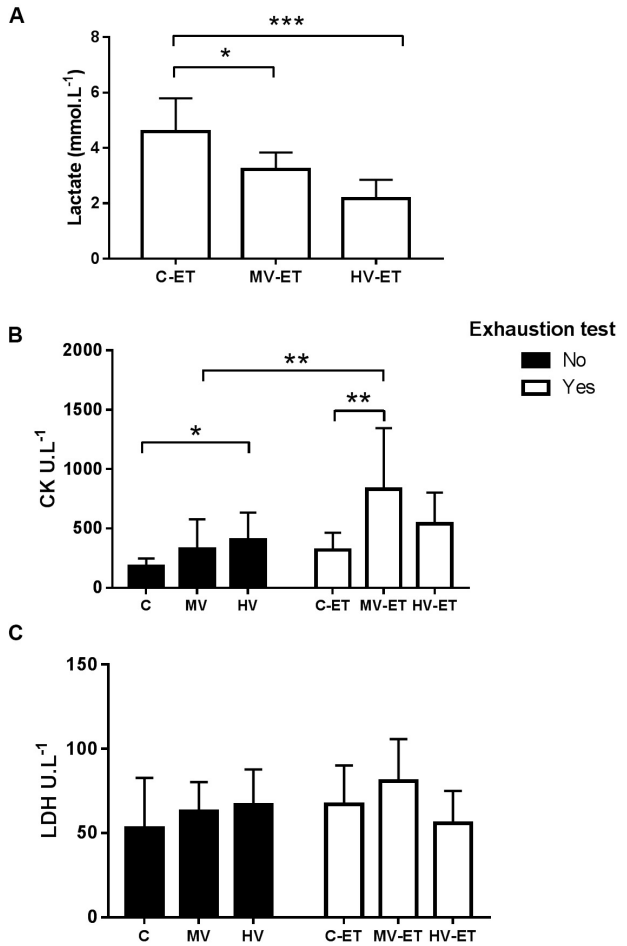

FIGURE 3 | Serum levels of Lactate, Creatine Kinase and Lactate dehydrogenase. **(A)** Lactate: MV-ET vs. C-ET ($P = 0.015$); HV-ET vs. C-ET ($P < 0.001$). **(B)** CK: Creatine Kinase; C-ET ($P = 0.026$) and MV ($P = 0.033$) vs. MV-ET. HV vs. C ($P = 0.015$). **(C)** LDH: Lactate dehydrogenase. C, control group; C-ET, control + exhaustion test group; MV, moderate-volume group; MV-ET, moderate-volume + exhaustion test group; HV, high-volume group; HV-ET, high-volume + exhaustion test group. $^{*}P \leq 0.05$; $^{**}P < 0.01$; $^{***}P < 0.001$. Values represent mean ± S.D. All the experiments were carried out in triplicate.

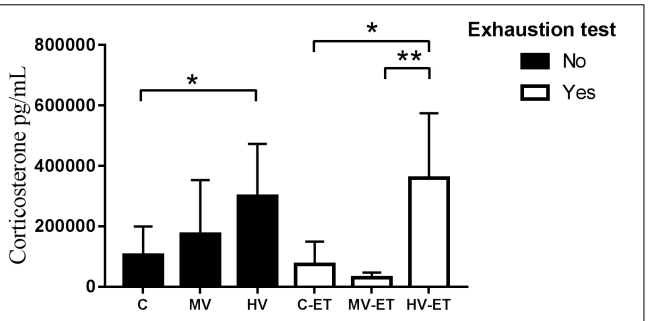

FIGURE 4 | Corticosterone levels in the serum. HV vs. C ($P = 0.038$). HV-ET vs. MV-ET ($P = 0.002$) and C-ET ($P = 0.013$). C, control group; C-ET, control + exhaustion test group; MV, moderate-volume group; MV-ET, moderate-volume + exhaustion test group; HV, high-volume group; HV-ET, high-volume + exhaustion test group. $^{*}P \leq 0.05$; $^{**}P < 0.01$. Values represent mean ± S.D. All the experiments were carried out in triplicate.

No difference was found between C-ET and C or between HV and HV-ET groups. Levels of malondialdehyde were also higher in HV-ET group vs. C-ET (↑ 20.9%; $P = 0.032$; Cohen's $d = 1.12$) but did not differ when compared to values obtained in MV-ET.

Total SOD and CAT Enzymatic Activity

Significant difference among the groups were detected for total SOD activity [$F(5,27) = 5.295$, $P = 0.003$]. High-volume training did not modify SOD activity when compared to moderate-volume training. Nevertheless, both volumes of training, increased SOD activity compared to the control condition: 44.02%; $P = 0.01$; Cohen's $d = 0.16$ for MV vs. C and ↑ 41.81%; $P = 0.02$; Cohen's $d = 0.11$ for HV vs. C groups. Similarly, MV-ET and HV-ET groups do not differ from each other but presented higher SOD activities when compared to C-ET (↑ 31.61%; $P = 0.034$; Cohen's $d = 0.15$) (↑ 63.75%; $P = 0.011$; Cohen's $d = 0.21$), respectively (**Figure 5C**).

Difference for CAT activity was also detected in the comparison among the groups [$F(5,32) = 3.265$, $P = 0.02$]. Higher activity was found in the MV group compared to MV-ET (↑47.82%; $P = 0.001$; Cohen's $d = 0.23$), HV (↑34.78%; $P = 0.043$; Cohen's $d = 0.14$), and C (↑41.44%; $P = 0.006$; Cohen's $d = 0.19$) groups (**Figure 5D**). The exhaustion test did not increase CAT activity in none of the groups.

Nitric Oxide (NO), Glutathione (GSH) and Oxidized Glutathione (GSSG) Levels

No intergroup difference was found for NO [$F(5,35) = 1.123$, $P = 0.370$] (**Figure 5B**), GSH [$F(5,28) = 2.108$, $P = 0.103$] (**Figure 5E**), or GSSG [$F(5,28) = 0.265$, $P = 0.928$] (**Figure 5F**) levels nor for GSH\GSSG ratio [$F(5,28) = 0.775$, $P = 0.577$] (**Figure 5G**) in the cerebellum.

Interleukin-1β Levels

A differential response among the groups was detected in the serum levels of pro-IL-1β (33–34 kDa) [$F(5,35) = 7.396$, $P < 0.0001$] and the active form of IL-1β (17 kDa) in the cerebellum [$F(5,35) = 5.828$, $P = 0.001$]. These levels were not modified by the training volume in both MV and HV groups when compared to the control condition. Nevertheless, 24 h after the ET, an increased concentration of pro-IL-1β was detected in the CT-ET compared to the C (↑53.57%; $P < 0.001$; Cohen's $d = 2.94$). The amount of the active 17 kDa IL-1β was also intensified by the ET in the C-ET (↑22.92%; $P = 0.046$; Cohen's $d = 1.13$) and MV-ET (↑33.15%; $P = 0.006$; Cohen's $d = 1.79$) groups, while no change was detected in the cerebellum of HV-ET animals (**Figure 6**).

GFAP Protein Expression Profile

Four GFAP isoforms were detected in the cerebellum using the Pan-GFAP antibody: the canonical GFAP protein with 50 kDa and the other three proteins with 45, 42, and 39 kDa. **Figure 7**

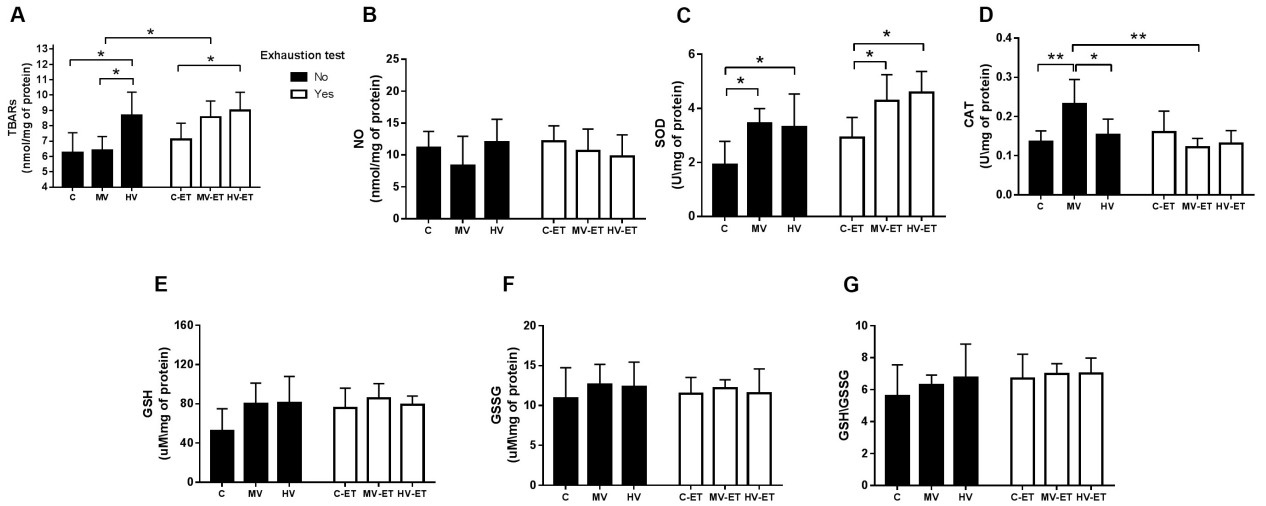

FIGURE 5 | Oxidative Markers in the cerebellum tissue. **(A)** TBARS: MV-ET vs. MV ($P = 0.021$). HV-ET vs. C-ET ($P = 0.032$). HV vs. C ($P = 0.036$) and MV ($P = 0.027$). **(B)** NO: Nitric Oxide; **(C)** SOD: Superoxide dismutase; MV vs. C ($P = 0.020$); MV-ET and C-ET ($P = 0.034$); HV vs. C (0.048); HV-ET vs. C-ET ($P = 0.011$). **(D)** CAT: Catalase; MV vs. MV-ET ($P = 0.001$), HV ($P = 0.043$) and C ($P = 0.006$). **(E)** GSH: Glutathione; **(F)** GSSG: Oxidized Glutathione; **(G)** GSH/GSSG ratio. C, control group; C-ET, control + exhaustion test group; MV, moderate-volume group; MV-ET, moderate-volume + exhaustion test group; HV, high-volume group; HV-ET, high-volume + exhaustion test group. $^{*}P \leq 0.05$; $^{**}P < 0.01$. Values represent mean ± S.D. All the experiments were carried out in triplicate.

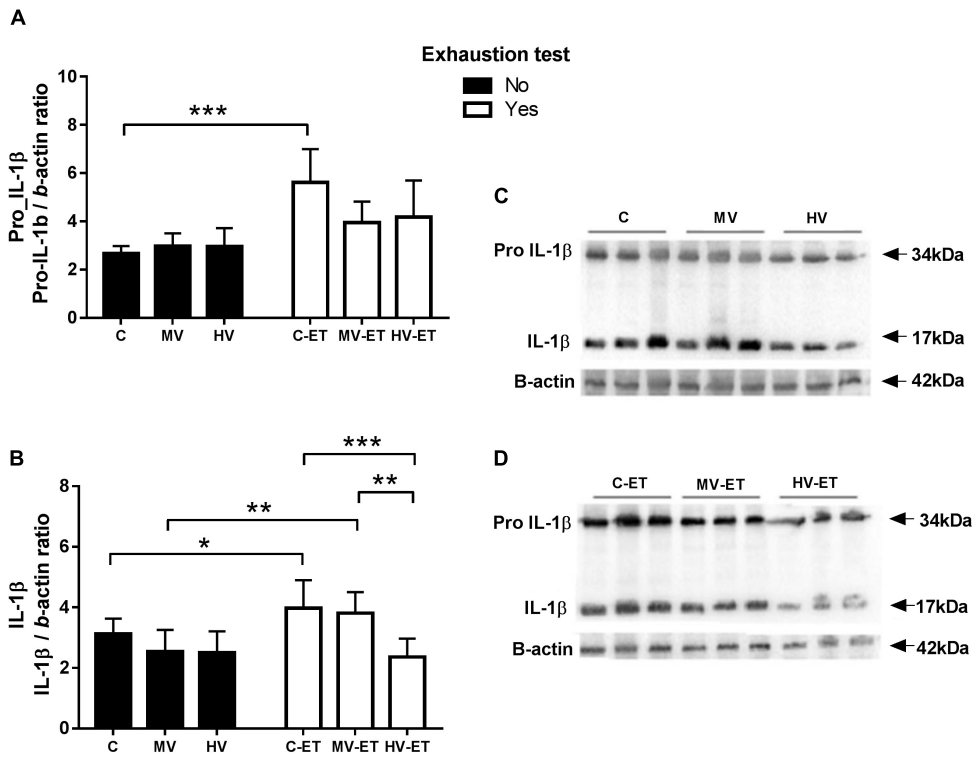

FIGURE 6 | Pro- IL-1B and active IL-1b protein levels assessed by Western blot in the cerebellar tissue. **(A)** Pro IL-1B: C-ET vs. C ($P < 0.001$). **(B)** IL-1B: C-ET vs. C ($P = c0.046$); HV-ET ($P < c0.001$). MV-ET vs. MV ($P = 0.006$); HV-ET ($P = 0.001$). **(C)** Representative Western blotting membrane of groups without exhaustion test. **(D)** Representative Western blotting membrane of groups with exhaustion test. C, control group; C-ET, control + exhaustion test group; MV, moderate-volume group; MV-ET, moderate-volume + exhaustion test group; HV, high-volume group; HV-ET, high-volume + exhaustion test group. $^{*}P \leq 0.05$; $^{**}P < 0.01$; $^{***}P < 0.001$. Values represent mean ± S.D. $N = 3$ independent experiments per group. All the experiments were carried out in triplicate.

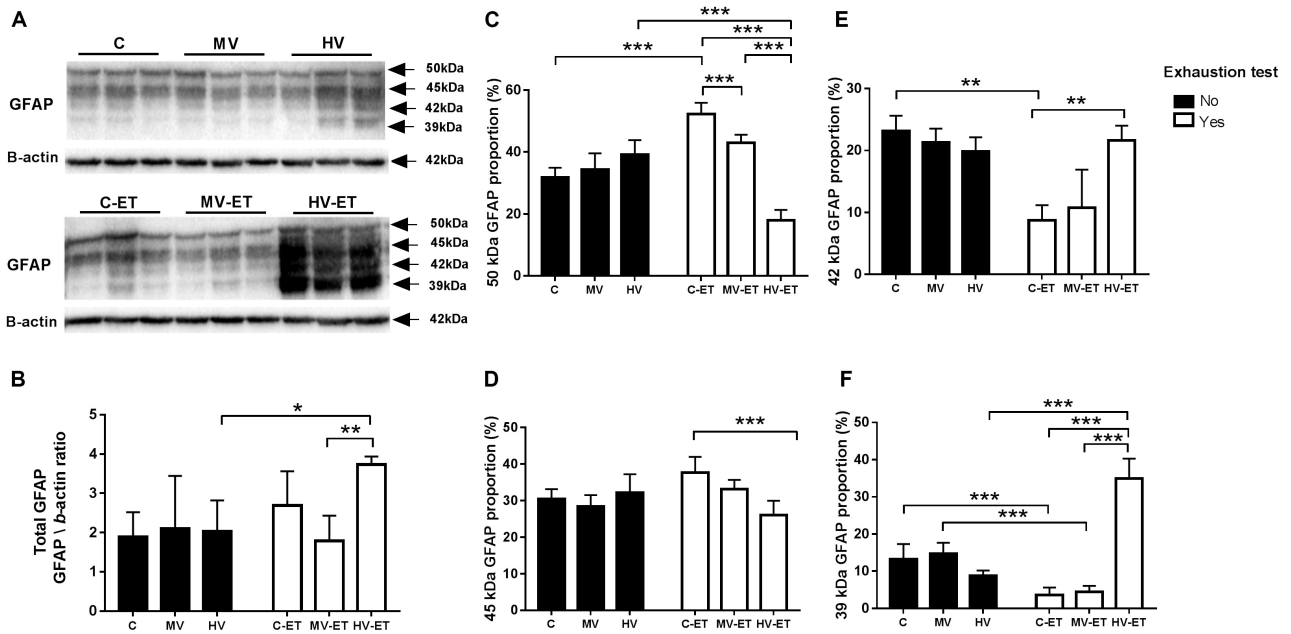

FIGURE 7 | GFAP protein levels assessed by Western blot in the cerebellar tissue. **(A)** Representative Western blotting membrane of groups without and with exhaustion test. **(B)** Quantification of total GFAP (sum of the four isoforms): HV-ET vs. MV-ET ($P = 0.004$); HV ($P = 0.023$). **(C–F)**: The expression profile of each GFAP isoform. **(C)** 50 kDa GFAP: HV-ET vs. C-ET; MV-ET; HV ($P < 0.001$). C-ET vs. C ($P < 0.001$) and MV-ET ($P = 0.013$). **(D)** 45 KDa GFAP: C-ET vs. HV-ET ($P < 0.001$) **(E)** 42 kDa: C-ET vs. C ($P = 0.001$); HV-ET ($P = 0.001$). **(F)** 39 kDa GFAP: HV-ET vs. HV;C-ET;MV-ET ($P < 0.001$); C vs. C-ET ($P < 0.001$). MV vs. MV-ET ($P < 0.001$) C, control; C-ET, control + exhaustion test group; MV, moderate-volume group; MV-ET, moderate-volume + exhaustion test group; HV, high-volume group; HV-ET, high-volume + exhaustion test group. $^{*}P \leq 0.05$; $^{**}P < 0.01$; $^{***}P < 0.001$. Values represent mean ± S.D. N = 3 independent experiments per group. All the experiments were carried out in triplicate.

shows GFAP protein levels illustrated in two different ways. First, we analyzed the total amount of all GFAP isoforms among the groups [$F(5,30) = 3.814$, $P = 0.011$] and observed that the HV-ET group had higher values when compared to MV-ET (↑ 53.80%; $P = 0.002$; Cohen's $d = 4.31$) but not to C-ET. This increase in the total GFAP in the HV-ET was also found when compared to the groups not submitted to exhaustion test: HV (↑ 46 71%; $P = 0.015$; Cohen's $d = 3.12$) and MV (↑ 44.88%; $P = 0.024$; Cohen's $d = 1.79$) groups.

In the separate analysis by isoform, no intergroup difference among C, MV, and HV groups was found for any of the four isoforms. On the other hand, the 50 kDa isoform increased in the C-ET and MV-ET when compared to C (↑ 36.52%; $P < 0.001$; Cohen's $d = 4.23$ and ↑ 20.94%; $P = 0.043$; Cohen's $d = 2.30$, respectively), MV (↑ 34.26%; $P < 0.001$; Cohen's $d = 3.94$), and HV (↑ 36.50%; $P < 0.001$; Cohen's $d = 3.11$). MV-ET and C-ET also differ (19.70%; $P < 0.001$; Cohen's $d = 3.73$). On the other hand, in the HV-ET group, reduced levels of 50 kDa isoform were detected when compared to the other groups submitted to the exhaustion text: C-ET (↓ 65.56%; $P < 0.001$; Cohen's $d = 9.80$), MV-ET (↓ 42.88%; $P < 0.001$; Cohen's $d = 9.44$).

Regarding 45 kDa GFAP isoform [$F(5,35) = 7.018$, $P < 0.0001$] there was an increase in the C-ET when compared to HV-ET (↑ 30.76%; $P = 0.004$; Cohen's $d = 2$) groups. The levels of 42 kDa GFAP did not differ among C, MV, and HV groups. However, in the C-ET, the values were lower (↓ 61.33%; $P = 0.001$; Cohen's $d = 6.07$) than those found in the C ($P = 0.001$; Cohen's $d = 12.48$), MV ($P = 0.001$; Cohen's $d = 5.30$); HV ($P = 0.004$; Cohen's $d = 4.66$) and HV-ET ($P = 0.001$; Cohen's $d = 5.31$) groups.

The exhaustion test had a significant impact on 39 kDa GFAP isoform [$F(5,32) = 51.56$, $P < 0.0001$]. Although these levels did not change in the groups C, MV, and HV, they were reduced in C-ET group compared to C (↓ 27.08%; $P < 0.001$; Cohen's $d = 2.99$) and in the MV-ET vs. MV (↓30.18%; $P < 0.001$; Cohen's $d = 4.35$) groups. On the other hand, 39 kDa GFAP was abundant in the HV-ET group compared to HV (↑74.76%; $P < 0.001$; Cohen's $d = 6.75$); MV-ET (↑87.29%; $P < 0.001$; Cohen's $d = 7{,}80$), and C-ET (↓89.75%; $P < 0.001$; Cohen's $d = 7.82$). These values were also elevated compared to the other group not submitted to the exhaustion test: MV (↓57.87%; $P < 0.001$; Cohen's $d = 0.47$) groups.

DISCUSSION

The findings of the present study indicate that both the moderate- and high-volume training of aerobic exercise on a treadmill were able to reduce the rat body weight similarly and modify the running performance during ET simulating UE. Different responses of serum metabolic markers such as CK and corticosterone levels, as well as in cerebellum oxidative status, were observed in the animals trained under the two distinct conditions of exercise volume. Three months

of high-volume training at moderate intensity impaired the cerebellum antioxidant defense system, resulting in lipid peroxidation. Moreover, when high-volume training was associated with ET, an altered GFAP isoform profile was detected in this brain region.

Running Performance and Serum Lactate Levels

To ascertain whether our exercise training volume did indeed enhance muscular function and provoke adaptive responses, we performed exercise-exhaustion tests on treadmills simulating UE. Although there is no consensus on the definition of UE in rodents, events completed at 4 (Millet et al., 2011) or 6 h of running (Turner et al., 2014) are considered comparable to UE in humans. Our results showed that trained animals submitted to the ET maintained considerable aerobic resistance for up to 4 h. In the animal groups submitted to moderate- or high- training volume, a lower serum lactate concentration was detected 24 h after ET compared to the control. In the control condition, serum lactate concentration exceeded the anaerobic threshold, which typically can be characterized by a lower mitochondrial oxidative capacity, phosphocreatine depletion, increased H^+, and recurrent substrates for adenine nucleotide catabolism (Sahlin et al., 1990; Lewis et al., 2010; Marcinek et al., 2010). The lower lactate concentration observed in the trained groups agreed with previous studies on rodents, that long-term training under aerobic conditions can induce this response, associated to physiological and muscular adaptations such as high mitochondrial sensitivity in oxidizing the pyruvate and muscle angiogenesis and a greater gluconeogenesis capacity (Gaesser and Poole, 1988; Voltarelli et al., 2002; Brito Vieira et al., 2014; Booth et al., 2015; Abreu et al., 2016). Modifications in the liver metabolism accompanied by an increase in the liver monocarboxylate transporter 2 protein levels have also been found in mice submitted to moderate-intensity treadmill exercise for 6 weeks (Lezi et al., 2013).

In long-distance competitions in humans, muscle metabolic changes are accompanied by lactate elevation (Lewis et al., 2010) mostly due to the maximum effort exerted during competition. In our study, different from this, there was no intensity variation during ET. Furthermore, the UE simulation was performed at a lower intensity (50% of maximum speed) than during the preceding protocol of training (70%). Therefore, the findings observed in the MV and HV groups are in agreement with previous evidence that rats submitted to running training under aerobic threshold present lactic stability (Abreu et al., 2016). Moreover, it has been well established that aerobic endurance exercise increases fat consumption as an energy source by decreasing glucose oxidation and pyruvate production (Ferreira et al., 2016).

Creatine Kinase Levels

Ultra-endurance exercises also promote a catabolic state by activating intracellular proteolytic enzyme activity, which can promote muscle protein degradation and augmented cell permeability, allowing the leaking of cell contents into the circulation (Dohm et al., 1987; Baird et al., 2012). For this reason, plasma CK is often used as a biomarker for myocardial and skeletal muscle damage or changes in myocyte membrane permeability after exercise (Yamashita and Yoshioka, 1991). An increase of plasma CK has been also observed in rats after running, even in the absence of histological damage (Kuipers, 1994). In the present study, a significant rise in the serum CK levels was detected in the HV group, and this increase was maintained without modification 24 h after ET. On the other hand, the insult induced by ET was able to elevate CK levels in the MV group. Two peaks in the serum CK levels have been reported after a marathon run and intense exercise, associated with early transient changes in the membrane permeability and a late inflammatory response during 24–48 h of recovery (Clarkson and Ebbeling, 1988). On the other hand, other studies in humans have shown that plasma CK concentration after ultramarathon runs (∼200 Km) declines to basal levels after 24 h of recovery (Son et al., 2015).

The serum CK concentrations here detected in the MV-ET and HV groups were higher than those observed after moderate-intensity protocols in animal models (De Araujo et al., 2012) even when submitted to the eccentric contraction exercise by downhill running (Isanejad et al., 2015) or even when performed at a high intensity (Choi et al., 2013; Rezaei et al., 2017). Wistar rats, when subjected to progressively intense exercise, can reach anaerobic thresholds at velocities exceeding 15 m/min and a maximum CK concentration close to 350 U/L at 17.5 m/min (Rezaei et al., 2017). In the MV-ET and HV groups, higher serum CK concentrations were detected under the aerobic threshold, at a velocity not exceeding 12 m/min and in the absence of increased levels of LDH in the serum. Hepatic and renal function can also become impaired after UE (Lipman et al., 2014; Jastrzębski et al., 2015; Knechtle and Nikolaidis, 2018). Acute kidney injury is relatively common in ultramarathon races (Hoffman et al., 2013; Lipman et al., 2014) and post-race serum CK and creatinine concentrations have been significantly correlated in humans (Hoffman and Weiss, 2016; Hodgson et al., 2017). Exhaustive swimming exercise has been shown to provoke kidney injury in rats (Wu et al., 2012). Although we did not investigate the renal function and histological markers in the muscle of MV-ET and HV animals, we cannot discard the possibility that their increased serum CK levels were related to different types of muscle or renal insults inducing modifications in the clearance of CK (Hodgson et al., 2017). It is possible that that the moderate intensity of the aerobic exercise adopted in the present study could be at least partially responsible for the lack of increased serum LDH levels. Adopting the correlation reported by Rodrigues et al. (2007) between VO2 max and the maximum velocity achieved by the animals in our study, we estimated that the predicted VO2 max was on average 70.5 ± 1.7(mL/Kg/min -1) between 10.78 and 12.9 m/min. Thus, our findings in rodents are in agreement with previous evidence that when aerobic exercise is performed at a value inferior to 80% VO2 max, the release of CK 24 h after the running in the treadmill is not accompanied by increased serum LDH levels, indicating the absence of cardiac stress (Callegari et al., 2017). On the other hand, recent evidence from studies in humans demonstrated that an ultra-endurance mountain

race performed under low intensity and aerobic conditions simultaneously increased CK and LDH levels in the athletes (Ramos-Campo et al., 2016).

Serum Corticosterone Levels

Serum corticosterone levels were also elevated by the training volume in the HV animals when compared to the control or MV groups. However, similarly to what was detected for CK, no additive effect was induced by the ET. Various aspects must be considered in a discussion of these findings. It is well established that exercise induces increased glucocorticoid secretion by stimulation of the hypothalamus-pituitary-adrenal (HPA) axis (Chennaoui et al., 2002). Karkoulias et al. (2008) demonstrated that marathon running in humans causes plasma cortisol elevation just after running and the recovery to basal levels may take a week. According to these authors, the degree of cortisol elevation is dependent on the duration of the run. The importance of glucocorticoids in determining muscle strength and endurance lies in their catabolic effects, especially hyperglycemic effects, and facilitates the conversion of proteins to glycogen, as well as providing amino acids for gluconeogenesis (Chen et al., 2017). These effects are probably involved in the relative resistance of the HV groups. Bernardi et al. (2013) also reported increased corticosterone levels concomitant to reduced serum lactate concentration in rats submitted to treadmill exercise for 4 weeks (20 min/day, 5 days/week during 4 weeks). In addition to acting on the glucose metabolism, increased serum corticosteroid levels may participate in the maintenance of homeostasis and the development of physical fitness as an adaptive mechanism in trained subjects (Mastorakos and Pavlatou, 2005). In the HV group, recovery of the corticosterone to basal values did not occur 24 h after the training period, and the exhaustion test did not modify these levels in the HV-ET animals. It has also been shown that under the long-term exercise of moderate intensity, adaptive mechanisms reducing the sensitivity to glucocorticoids in target tissues including HPA axis can occur both in rats (Chennaoui et al., 2002) and in human marathon runners and triathletes (Duclos et al., 2003, 2007; Duclos and Tabarin, 2016). These mechanisms can prevent deleterious effects of corticosterone (in rodents) or cortisol (in humans) elevation, decreasing additional muscle insult. It remains to be investigated if this type of adaptive mechanism occurred in the HV-ET group.

Effects on the Antioxidant Resource of the Cerebellum

The main hypothesis of the present study was that rodent cerebellar resilience to oxidative injuries could be reduced after high training volumes, regardless of the simulation of UE running. Indeed, we found LP in the HV, MV-ET, and HV-ET groups but not in the MV group. These data indicated that the LP detected was especially due to unbalanced levels of enzymatic antioxidant resources. An intensified CAT activity occurred only in the MV group, concomitant with an increased SOD activity, which was able to efficiently degrade the hydrogen peroxide (H_2O_2) produced by this latter enzyme.

Usually, the exhaustion test on the treadmill can induce systemic oxidative stress depending on the intensity or muscle fatigue (Acikgoz et al., 2006). In the MV-ET group, most of the animals displayed a relative resistance, reaching their point of exhaustion after 2 h of running. The unbalanced levels of the SOD/catalase ratio in the cerebellum associated to the increased levels of systemic CK detected in this group indicated that the previous moderate-volume training for 3 months was not able to confer resistance to a UE simulation, neither by the peripheral organs nor by neural regions involved in locomotion control. Chalimoniuk et al. (2015b) reported increased levels of LP in the cerebellum of rats after 6 weeks of moderate exercise performed during 60 min/day. Nevertheless, no lipid damage was detected in the cerebral cortex of the same animals where balanced levels of SOD and CAT were found (Chalimoniuk et al., 2015b). Falone et al. (2012) also reported increased antioxidant enzyme activity in the cerebral cortex after 16 weeks of training (5 days/week for only 20 min). Despite the differential vulnerability of these brain regions to oxidative insults, the present data reinforce the hypothesis that high-volume training *per se* can be deleterious to the cerebellum even under moderate intensity. However, it is not clear at this moment why the exhaustion test did not provoke an additive effect on the HV group.

Unchanged levels of NO production were here detected in the trained animals either under moderate or high volume when compared to the control condition. Under physiological conditions, NO has been implicated in cerebellar long-term depression and long-term potentiation, which are forms of synaptic plasticity involved in motor learning (Ogasawara et al., 2007). NO also plays an important role in matching blood flow to oxygen demand in the brain during exercise (Toda et al., 2009). A 6-week exercise training protocol on the treadmill (5 days/week), beginning with 40 min at 16 m/min and gradually increased to 60 min/day at 28 m/min was able to enhance nitrergic transmission in the cerebellum, striatum, and midbrain but not in the cortex and hippocampus of adolescent and adult rats (Chalimoniuk et al., 2015a,b). On the other hand, a comparative study analyzing the effect of different modalities of exercise reported different proportions of nitrergic activity in the hippocampus, striatum, and cerebellum (Torres et al., 2006). According to this latter study, only acrobatic exercises increased NADPH-diaphorase activity in the cerebellar granular layer when compared to sedentary and other exercise modalities including the use of a treadmill for 30 min a day, at 12 m/s during 33 days.

The lack of changes in the NO levels inside the cerebellum of MV, MV-ET, HV, and HV-ET groups in the present study was accompanied by an unmodified GSH/GSSG ratio. Crosstalk between NO and GSH has been described as an important mechanism necessary for modulating the cell redox status (Baldelli et al., 2019). Within the cells, besides its antioxidant effect, GSH also has the function of buffering the flux of NO. It has been demonstrated that reduced levels of GSH can trigger a severe NO imbalance, causing neuronal death (Aquilano et al., 2011a). Even a slight and non-toxic decrease of GSH in the brain caused protein nitration which was reversed by inhibiting NO production (Aquilano et al., 2011b). Some studies have analyzed the impact of the exercise of moderate or elevated intensity. These

have reported increased levels of GSH in the brain. Nevertheless, in a systematic review of the effects of aerobic training on redox status, Camiletti-Moirón et al. (2013) did not find a homogeneous response of GSH, GSSG, and GPx, but a slight tendency to a positive effect of aerobic exercise on these parameters. In a recent meta-analysis, we also did not find any tendency for decreased or increased GPx activity after moderate or elevated exercise intensity or volume among several brain regions (de Souza et al., 2018). Therefore, similar values of GSH/GSSG ratio and NO levels between control and trained groups detected in the present study suggest that even after high-volume training and ET a physiological response can still be maintained for keeping the redox balance, favoring modulatory effects of NO in the cerebellum motor function. Future studies are necessary to address this subject.

Inflammatory Markers and Astrocyte Reactivity Profile

Long-term exercise at low-to-moderate intensity has been documented as an important modulator of neuroinflammation and glial activation, inducing adaptive responses (Mee-Inta et al., 2019). The gene expression of IL-1β can be brought about by several transcriptional elements such as cAMP-responsive element, NF-κB, among others (Shirakawa et al., 1993) that can be activated by hypoxia, oxidative stress, hyperosmolarity, thermal injury, gamma radiation, and microbial stimuli (Haddad and Harb, 2005). Translation depends on the activation of MAP kinases producing pro-IL-1β, which must be cleaved by the cysteine protease caspase-1 to adopt biological activity as IL-1β (Hewett et al., 2012). In the healthy brain, the levels of the pro-IL-1β and the active IL-1β are low, and this interleukin can stimulate a variety of signaling pathways, including those involved in synaptic plasticity (Hewett et al., 2012). On the other hand, IL-1β levels in the brain can be increased by local damage and/or peripheral inflammation (Pitossi et al., 1997; Laye et al., 2000; Hewett et al., 2012).

In the present study, moderate and high training volumes did not affect the pro-IL-1β or the active 17-kDa IL-1β levels in the cerebellum. Thus, the lipid peroxidation detected in the group HV was neither correlated with increased levels of IL-1b nor associated with ET. Only in the MV-ET group higher levels of IL-1b occur concomitant to increased lipid peroxidation levels. On the other hand, in the CT-ET group, the amount of Pro-IL-1b and the active IL-1b was elevated by the ET even in the absence of lipid peroxidation. These findings suggest a higher sensitivity of the cerebellum of untrained rats to transcriptional or translational effects on IL-1b levels when submitted to UE simulation. It has been shown that fatigue elicited by the exhaustive test may involve disturbances in the immune system, which can be hampered by long-term training (Chennaoui et al., 2002; Petersen and Pedersen, 2005; Morgado et al., 2012). Our findings indicated that only in the HV-ET animals was the previous training able to prevent the activation of IL-1b induced by the ET, but the mechanism involved in the finding is not clear.

Brain IL-1β is mainly produced by microglia, peri-vascular infiltrating macrophages (Herx et al., 2000), and astrocytes (Rappold and Tieu, 2010) but can be released from some neurons (Silverman et al., 2005) under pathological conditions. In the cerebellum, for example, Purkinje neurons in neonates undergo apoptosis and excitotoxic death when IL-1β and TNF-α levels are released by microglia after acute hypoxia (Kaur et al., 2014). However, current literature also reports that low-intensity exercise is sufficient to reduce the release of IL-1β in part due to modifications in the microglia phenotype (Mee-Inta et al., 2019).

Furthermore, an imbalance in antioxidant and anti-inflammatory neuroprotective mechanisms may also be related to astrocyte reactivity (Liddell, 2017). The relationship between running, pro-inflammatory cytokines, and glial cell activation have been studied in some models of brain injury (Ang et al., 2004). This fact motivated an analysis of the GFAP expression profile in the cerebellum considering the importance of Bergman glia for the homeostasis of this region, locomotor performance, and antioxidant resource (Fernandez-Fernandez et al., 2012). Astrocytes also play trophic, metabolic, and neuronal support functions (Matsui et al., 2017). Besides, they are actively involved in glutamate and GABA metabolism, which contribute to ATP synthesis (Magi et al., 2013). These beneficial actions of astrocytes characterize their neuroprotector phenotype, also called A2 (Cunningham et al., 2019). On the other hand, when overactivated, astrocytes can be neurotoxic acquiring an A1 phenotype and are the main targets of IL-1β released by microglia (Liddell, 2017). Under this condition, astrocytes have a reciprocal interaction with IL-1β, leading to the production of reactive oxygen species (Rappold and Tieu, 2010), and IL-1β can modify the physiological state of Bergman cells.

Exercise can induce astroglial proliferation depending on the brain's demand for energy (Li et al., 2005). The GFAP gene can be alternatively spliced giving rise to at least nine proteins that differ from the first described isoform, called GFAPα with 50 kDa: GFAPβ, GFAPγ, GFAPδ/ϵ, GFAPk, GFAPΔ135, GFAPΔ164, GFAPΔexon6, GFAPΔexon7, and GFAPζ (review in Middeldorp and Hol, 2011). Usually, astrocyte reactivity is accompanied by increased levels of GFAPα protein isoform, which is phosphorylated and mainly expressed in mature and proliferating stages. Augmented levels of this GFAP isoform have also been related to inflammatory status under some pathological conditions (Catts et al., 2014; Sullivan, 2014).

Analyzing the GFAP protein expression, we identified four distinct isoforms in the cerebellum with 50, 45, 42, and 39 kDa, respectively. We have found that neither moderate- nor high-volume training modified the cerebellum GFAP expression profile of these isoforms when compared to the control condition. However, the exhaustion test provoked in the C-ET and MV-ET increased levels of the 50 kDa GFAP isoform, while it concomitantly reduced the 42 and 39 kDa isoforms. Higher levels of the 50 kDa GFAP isoform found in the C-ET were also simultaneous with a higher amount of Pro-IL-1b and the active form of IL-1b. In the HV-ET group, an opposite effect was found in the GFAP isoform profile, where the 50 kDa isoform was about 40% of that found in the control animals and 50–60% of the values in the cerebellum of C-ET, MV-ET, and HV groups. On the other hand, augmented levels of 42 and 39 kDa GFAP were found in HV-ET.

Changes in the expression level of the GFAP isoforms influence the intermediate filament network, which can modify astrocyte mobility and structure (Sullivan, 2014; Sereika et al., 2018). Usually, GFAP phosphorylation contributes to the extensive remodeling of glial networks in mitosis and can also affect its interactions with other intracellular proteins (Moeton et al., 2014). In some neurodegenerative diseases as well as in the astrocytoma of grade IV, GFAP isoforms with lower molecular weight were better expressed when compared to the control condition (Hol et al., 2003; Sereika et al., 2018). Reactive gliosis associated with a drop in GFAP phosphorylation has been reported, for example, in the neurodegenerative condition in Parkinson's disease (Clairembault et al., 2014). It is not clear at this moment which mechanisms are involved in the changed GFAP isoform profile detected here in the cerebellum of the HV-ET group. A recent study using proton magnetic resonance spectroscopy demonstrated that acute exhaustive endurance exercise in rats previously trained on a treadmill increased glutamate signals in the cerebellum. These findings suggested astrocyte dysfunction causing disequilibrium in the glutamate-glutamine cycle and a delay in the return of glutamine from these glial cells to neurons (Swiątkiewicz et al., 2017). Therefore, the modified GFAP profile found in the cerebellum of the HV-ET group suggests impaired astrocyte reactivity. Nevertheless, it remains to be investigated if this molecular change contributes to the lack of response to oxidative and inflammatory insult induced by the UE simulation.

CONCLUSION

In conclusion, the results corroborate the initial hypothesis, indicating that rat cerebellar resilience to oxidative damage is maintained during 3 months of moderate-volume training, but high-volume training at moderate intensity impaired the enzymatic antioxidant defense system of this brain region. Also, we demonstrated for the first time that UE simulation after high-volume training can alter the GFAP isoform profile, suggesting impaired astrocyte reactivity in the cerebellum. The findings also indicate that moderate-volume training, under the aerobic condition for 3 months, does not confer resistance to UE simulation in rats, either for systemic markers or the oxidative and inflammatory status of the cerebellum. Altogether, the data highlights the importance of further studies in other brain regions involved in the movement control given the increase in the number of participants in ultra-marathons nowadays.

DATA AVAILABILITY STATEMENT

The datasets generated for this study are available on request to the corresponding author.

ETHICS STATEMENT

The animal study was reviewed and approved by Animal Use Ethics Committee (CEUA) of the Federal University of Pernambuco, Brazil (# 0035-2017).

AUTHOR CONTRIBUTIONS

RS, BA-C, and SM: designing the experiment. FS, RS, and DP: running training. DP, RA, RS, LG, FS, and GM: biochemical and western blot analysis and data curation. RS and BA-C: writing – original draft. All authors contributed to the final version of the manuscript.

ACKNOWLEDGMENTS

We would like to thank the Coordination for the Improvement of Higher Level or Education Personnel (CAPES, Finance Code 001 and CAPES/PROCAD-2013). Foundation for the Support of Science and Technology of the State of Pernambuco FACEPE (APQ-1037-2.07/15) and National Council for Scientific and Technological Development (CNPq) # 426342/2018-6. The support of the veterinarian Waldo Oliveira Monteiro Filho and the members of Neuromuscular Plasticity Laboratory, where the running training was performed, are greatly appreciated. RA and GM received scholarships from CAPES and LG from CNPq (National Council for Scientific and Technological Development). The English version of this text was revised by Sidney Pratt, Canadian, BA, MAT (The Johns Hopkins University), RSAdip (TEFL—Cambridge University).

REFERENCES

Abreu, P., Mendes, S. V. D., Leal-Cardoso, J. H., and Ceccatto, V. M. (2016). Anaerobic threshold employed on exercise training prescription and performance assessment for laboratory rodents: a short review. *Life Sci.* 151, 1–6. doi: 10.1016/j.lfs.2016.02.016

Acikgoz, O., Aksu, I., Topcu, A., and Kayatekin, B. M. (2006). Acute exhaustive exercise does not alter lipid peroxidation levels and antioxidant enzyme activities in rat hippocampus, prefrontal cortex, and striatum. *Neurosci. Lett.* 406, 148–151. doi: 10.1016/j.neulet.2006.07.034

Aebi, H. (1984). Methods in enzymology. *Acta Chen.* 10, 121–126.

Agnew, J., Hammer, S., Roy, A., and Rahmoune, A. (2018). Central and peripheral pain sensitization during an ultra-marathon competition. *Scand. J. Pain* 18, 703–709. doi: 10.1515/sjpain-2018-0079

Ang, E. T., Wong, P. T., Moochhala, S., and Ng, Y. K. (2004). Cytokine changes in the horizontal diagonal band of Broca in the septum after running and stroke: a correlation to glial activation. *Neuroscience* 129, 337–347. doi: 10.1016/j.neuroscience.2004.06.087

Aquilano, K., Baldelli, S., Cardaci, S., Rotilio, G., and Ciriolo, M. R. (2011a). Nitric oxide is the primary mediator of cytotoxicity induced by GSH depletion in neuronal cells. *J. Cell Sci.* 1, 1043–1054. doi: 10.1242/jcs.077149

Aquilano, K., Baldelli, S., and Ciriolo, M. R. (2011b). Glutathione is a crucial guardian of protein integrity in the brain upon nitric oxide imbalance. *Commun. Integr. Biol.* 4, 477–479. doi: 10.4161/cib.15654

Armstrong, D. M. (1996). Role of the cerebellum and motor cortex in the regulation of visually controlled locomotion. *Can. J. Physiol. Pharmacol.* 74, 443–455. doi: 10.1139/y96-044

Baird, M. F., Graham, S. M., Baker, J. S., and Bickerstaff, G. F. (2012). Creatinekinase- and exercise-related muscle damage implications for muscle

performance and recovery. *J. Nutr. Metab.* 2012:960363. doi: 10.1155/2012/960363

Baldelli, S., Ciccarone, F., Limongi, D., Checconi, P., Palamara, A. T., and Ciriolo, M. R. (2019). Glutathione and nitric oxide: key team players in use and disuse of skeletal muscle. *Nutrients* 11:2318. doi: 10.3390/nu11102318

Bernardi, C., Tramontina, A. C., Nardin, P., Biasibetti, R., Costa, A. P., Vizueti, A. F., et al. (2013). Treadmill exercise induces hippocampal astroglial alterations in rats. *Neural Plast.* 2013, 709–732.

Bernardinelli, Y., Muller, D., and Nikonenko, I. (2014). Astrocyte-synapse structural plasticity. *Neural Plast.* 2014:23210.

Black, J. E., Isaacs, K. R., Anderson, B. J., Alcantara, A. A., and Greenough, W. T. (1990). Learning causes synaptogenesis, whereas motor activity causes angiogenesis, in cerebellar cortex of adult rats. *Proc. Natl. Acad. Sci. U.S.A.* 87, 5568–5572. doi: 10.1073/pnas.87.14.5568

Bonsignore, A., Bredin, S. S. D., Wollmann, H., Morrison, B., Jeklin, A., Buschmann, L., et al. (2017). The influence of race length on arterial compliance following an ultra-endurance marathon. *Eur. J. Sport Sci.* 17, 441–446. doi: 10.1080/17461391.2016.1262453

Booth, F. W., Ruegsegger, G. N., Toedebusch, R. G., and Yan, Z. (2015). Endurance exercise and the regulation of skeletal muscle metabolism. *Prog. Mol. Biol. Transl. Sci.* 135, 129–151.

Brito Vieira, W. H., Halsberghe, M. J. E., Schwantes, M. L. B., Perez, S. E. A., Baldissera, V., Prestes, J., et al. (2014). Increased lactate threshold after five weeks of treadmill aerobic training in rats. *Braz. J. Biol.* 74, 444–449. doi: 10.1590/1519-6984.07912

Callegari, G. A., Novaes, J. S., Neto, G. R., Dias, I., Garrido, N. D., and Dani, C. (2017). Creatine kinase and lactate dehydrogenase responses after different resistance and aerobic exercise protocols. *J. Hum. Kinet.* 58, 65–72. doi: 10.1515/hukin-2017-0071

Camiletti-Moirón, D., Aparicio, V. A., Aranda, P., and Radak, Z. (2013). Does exercise reduce brain oxidative stress? A systematic review. *Scand. J. Med. Sci. Sport.* 23, 202–212.

Catts, V. S., Wong, J., Gregory, S., Fung, S. J., and Shannon, C. (2014). Increased expression of astrocyte markers in schizophrenia: association with neuroinflammation. *Aust. N. Z. J. Psychiatry* 48, 722–723. doi: 10.1177/0004867414531078

Celnik, P. (2015). Understanding, and modulating motor learning with cerebellar stimulation. *Cerebellum* 14, 171–174. doi: 10.1007/s12311-014-0607-y

Chalimoniuk, M., Chrapusta, S. J., Lukaèova, N., and Langfort, J. (2015a). Endurance training upregulates the nitric oxide/soluble guanylyl cyclase/cyclic guanosine 3',5'-monophosphate pathway in the striatum, midbrain and cerebellum of male rats. *Brain Res.* 1618, 29–40. doi: 10.1016/j.brainres.2015.05.020

Chalimoniuk, M., Jagsz, S., Chrapusta, S. J., Klapcinska, B., Langfort, J., Medical, M., et al. (2015b). Diversity of endurance training effects on antioxidant defenses and oxidative damage in different brain regions of adolescent male rats. *J. Physiol. Pharmacol.* 66, 539–547.

Chen, C., Nakagawa, S., An, Y., Ito, K., Kitaichi, Y., and Kusumi, I. (2017). The exercise-glucocorticoid paradox: how exercise is beneficial to cognition, mood, and the brain while increasing glucocorticoid levels. *Front. Neuroendocrinol.* 44:83–102. doi: 10.1016/j.yfrne.2016.12.001

Chennaoui, M., Gomez Merino, D., Lesage, J., Drogou, C., and Guezennec, C. Y. (2002). Effects of moderate and intensive training on the hypothalamo-pituitary-adrenal axis in rats. *Acta Physiol. Scand.* 175, 113–121. doi: 10.1046/j.1365-201x.2002.00971.x

Choi, M., Park, H., Cho, S., and Lee, M. (2013). Vitamin D3 supplementation modulates inflammatory responses from the muscle damage induced by high-intensity exercise in SD rats. *Cytokine* 63, 27–35. doi: 10.1016/j.cyto.2013.03.018

Clairembault, T., Kamphuis, W., Leclair-Visonneau, L., Rolli-Derkinderen, M., Coron, E., and Neunlist, M. (2014). Enteric GFAP expression and phosphorylation in Parkinson's disease. *J. Neurochem.* 130, 805–815. doi: 10.1111/jnc.12742

Clarkson, P. M., and Ebbeling, C. (1988). Investigation of serum creatine kinase variability after muscle-damaging exercise. *Clin. Sci.* 75, 257–261. doi: 10.1042/cs0750257

Cunningham, C., Dunne, A., and Lopez-Rodriguez, A. B. (2019). Astrocytes: heterogeneous and dynamic phenotypes in neurodegeneration and innate immunity. *Neuroscientist* 25, 455–474. doi: 10.1177/1073858418809941

De Araujo, G. G., Papoti, M., Dos Reis, I. G. M., De Mello, M. A. R., Gobatto, C. A., and Kraemer, W. J. (2012). Physiological responses during linear periodized training in rats. *Eur. J. Appl. Physiol.* 112, 839–852. doi: 10.1007/s00421-011-2020-2

de Senna, P. N., Ilha, J., Porto, P., Baptista, A., Gonçalves, C. A., Achaval, M., et al. (2011). Effects of physical exercise on spatial memory and astroglial alterations in the hippocampus of diabetic rats. *Metab. Brain Dis.* 26, 269–279. doi: 10.1007/s11011-011-9262-x

de Souza, R. F., Regina, S., Moraes, A., De Augusto, R. L., Zanona, A. D. F., Matos, D., et al. (2018). Endurance training on rodent brain antioxidant capacity: a meta-analysis. *Neurosci. Res.* 145, 1–9. doi: 10.1016/j.neures.2018.09.002

De Zeeuw, C. I., and Hoogland, T. M. (2015). Reappraisal of Bergmann glial cells as modulators of cerebellar circuit function. *Front. Cell. Neurosci.* 9:246. doi: 10.3389/fncel.2015.00246

Dishman, R., Armstrong, R., Delp, M., Graham, R., and Dunn, A. (1988). Open-field behavior is not related to treadmill performance in exercising rats. *Physiol. Behav.* 43, 541–546. doi: 10.1016/0031-9384(88)90206-5

Dohm, G. L., Tapscott, E. B., and Kasperek, G. J. (1987). Protein degradation during endurance exercise and recovery. *Med. Sci. Sports Exerc.* 19, 166–171.

Duclos, M., Gouarne, C., and Bonnemaison, D. (2003). Acute and chronic effects of exercise on tissue sensitivity to glucocorticoids. *J. Appl. Physiol.* 94, 869–875. doi: 10.1152/japplphysiol.00108.2002

Duclos, M., Guinot, M., and Le Bouc, Y. (2007). Cortisol and GH: odd and controversial ideas. *Appl. Physiol. Nutr. Metab.* 32, 895–903. doi: 10.1139/h07-064

Duclos, M., and Tabarin, A. (2016). Exercise and the hypothalamo-pituitary-adrenal axis. *Front. Horm. Res.* 47:12–26. doi: 10.1159/000445149

Falone, S., D'Alessandro, A., Mirabilio, A., Petruccelli, G., Cacchio, M., Di Ilio, C., et al. (2012). Long-term running biphasically improves methylglyoxal-related metabolism, redox homeostasis and neurotrophic support within adult mouse brain cortex. *PLoS One* 7:e31401. doi: 10.1371/journal.pone.0031401

Fernandez-Fernandez, S., Almeida, A., and Bolaños, J. P. (2012). Antioxidant and bioenergetic coupling between neurons and astrocytes. *Biochem. J.* 443, 3–12. doi: 10.1042/bj20111943

Ferreira, A. R. P., Santos, W. S., Aidar, F. J., Dihogo, G. M., and de Souza, R. F. (2016). Analysis of the response of blood lactate, blood glucose, peripheral oxygen saturation, and heart rate during the trail running competition. *J. Am. Soc. Exerc. Physiol.* 18, 1–9.

Franciozi, C. E. S., Tarini, V. A. F., Reginato, R. D., Gonçalves, P. R. S., Medeiros, V. P., Ferretti, M., et al. (2013). Gradual strenuous running regimen predisposes to osteoarthritis due to cartilage cell death and altered levels of glycosaminoglycans. *Osteoarthr. Cartil.* 21, 965–972. doi: 10.1016/j.joca.2013.04.007

Gaesser, G. A., and Poole, D. C. (1988). Blood lactate during exercise: time course of training adaptation in humans. *Int. J. Sports Med.* 9, 284–288. doi: 10.1055/s-2007-1025023

Green, L. C., Wagner, D. A., Glogowski, J., Skipper, P. L., Wishnok, J. S., and Tannenbaum, S. R. (1982). Analysis of nitrate. nitrite, and [15N] nitrate in biological fluids. *Anal Biochem.* 126, 131–138. doi: 10.1016/0003-2697(82)90118-x

Haddad, J. J., and Harb, H. L. (2005). L-gamma-Glutamyl-L-cysteinyl-glycine (glutathione; GSH) and GSH-related enzymes in the regulation of pro- and anti-inflammatory cytokines: a signaling transcriptional scenario for redox(y) immunologic sensor(s)? *Mol. Immunol.* 42, 987–1014. doi: 10.1016/j.molimm.2004.09.029

Hagen, T., Liu, J., Yeo, H. C., Eva, O., Doniger, S. J., Chu, D. W., et al. (2018). Chronically and acutely exercised rats: biomarkers of oxidative stress and endogenous antioxidants. *J. Appl. Physiol.* 1673, 21–28. doi: 10.1152/jappl.2000.89.1.21

Herx, L. M., Rivest, S., and Yong, V. W. (2000). Central nervous system-initiated inflammation and neurotrophism in trauma: IL-1 beta is required for the production of ciliary neurotrophic factor. *J. Immunol.* 165, 2232–2239. doi: 10.4049/jimmunol.165.4.2232

Hewett, S. J., Jackman, N. A., and Claycomb, R. J. (2012). Interleukin-1β in central nervous system injury and repair. *Eur. J. Neurodegener. Dis.* 1, 195–211. doi: 10.1007/978-4-431-77922-3_47

Hibi, M., and Shimizu, T. (2011). Development of the cerebellum and cerebellar neural circuits. *Dev. Neurobiol.* 72, 282–301. doi: 10.1002/dneu.20875

Hissin, P. J., and Hilf, R. (1976). A fluorometric method for determination of oxidized and reduced glutathione in tissues. *Anal. Biochem.* 74, 214–326. doi: 10.1016/0003-2697(76)90326-2

Hodgson, L. E., Walter, E., Venn, R. M., Galloway, R., Pitsiladis, Y., Sardat, F., et al. (2017). Acute kidney injury associated with endurance events-is it a cause for concern? A systematic review. *BMJ Open Sport Exerc. Med.* 3, 1–14.

Hoffman, M. D., Stuempfle, K. J., Fogard, K., Hew-Butler, T., Winger, J., and Weiss, R. H. (2013). Urine dipstick analysis for identification of runners susceptible to acute kidney injury following an ultramarathon. *J. Sports Sci.* 31, 20–31. doi: 10.1080/02640414.2012.720705

Hoffman, M. D., and Weiss, R. (2016). Does acute kidney injury from an ultramarathon increase the risk for greater subsequent injury? *Clin. J. Sport Med.* 26, 417–422. doi: 10.1097/jsm.0000000000000277

Hol, E. M., Roelofs, R. F., Moraal, E., Sonnemans, M. A., Sluijs, J. A., Proper, E. A., et al. (2003). Neuronal expression of GFAP in patients with Alzheimer pathology and identification of novel GFAP splice forms. *Mol. Psychiatry.* 8, 786–796. doi: 10.1038/sj.mp.4001379

Hoshino, D., Setogawa, S., Kitaoka, Y., Masuda, H., Tamura, Y., Hatta, H., et al. (2016). Exercise-induced expression of monocarboxylate transporter 2 in the cerebellum and its contribution to motor performance. *Neurosci. Lett.* 633, 1–6. doi: 10.1016/j.neulet.2016.09.012

Huang, T., Lin, L., Cho, K., Chen, S., Kuo, Y., Yu, L., et al. (2018). Chronic treadmill exercise in rats delicately alters the Purkinje cell structure to improve motor performance and toxin resistance in the cerebellum. *J. Appl Physiol* 113, 889–895. doi: 10.1152/japplphysiol.01363.2011

Isanejad, A., Saraf, Z. H., Mahdavi, M., Gharakhanlou, R., Shamsi, M. M., and Paulsen, G. (2015). The effect of endurance training and downhill running on the expression of IL-1β, IL-6, and TNF-α and HSP72 in rat skeletal muscle. *Cytokine* 73, 302–308. doi: 10.1016/j.cyto.2015.03.013

Jastrzębski, Z., Zychowska, M., Radzimiński, Ł, Konieczna, A., and Kortas, J. (2015). Damage to liver and skeletal muscles in marathon runners during a 100 km run with regard to age and running speed. *J. Hum. Kinet.* 45, 93–102. doi: 10.1515/hukin-2015-0010

Jirenhed, D.-A., Rasmussen, A., Johansson, F., and Hesslow, G. (2017). Learned response sequences in cerebellar Purkinje cells. *Proc. Natl. Acad. Sci. U.S.A.* 114, 6127–6132. doi: 10.1073/pnas.1621132114

Karkoulias, K., Habeos, I., Charokopos, N., Tsiamita, M., Mazarakis, A., Pouli, A., et al. (2008). Hormonal responses to marathon running in non-elite athletes. *Eur. J. Int. Med.* 19, 598–601. doi: 10.1016/j.ejim.2007.06.032

Kaur, C., Sivakumar, V., Zou, Z., and Ling, E. A. (2014). Microglia-derived proinflammatory cytokines tumor necrosis factor-alpha and interleukin-1beta induce Purkinje neuronal apoptosis via their receptors in hypoxic neonatal rat brain. *Brain Struct. Funct.* 1, 151–170. doi: 10.1007/s00429-012-0491-5

Knechtle, B., and Nikolaidis, P. T. (2018). Physiology and pathophysiology in ultra-marathon running. *Front. Physiol.* 9:634. doi: 10.3389/fphys.2018.00634

Kuipers, H. (1994). Exercise-induced muscle damage. *Int. J. Sports Med.* 15, 132–135.

Laye, S., Gheusi, G., Cremona, S., Combe, C., Kelley, K., Dantzer, R., et al. (2000). Endogenous brain IL-1 mediates LPS-induced anorexia and hypothalamic cytokine expression. *Am. J. Physiol. Regul. Integr. Comp. Physiol.* 279, R93–R98.

Lee, J. M., Kim, T. W., Park, S. S., Han, J. H., Shin, M. S., Lim, B. V., et al. (2018). Treadmill exercise improves motor function by suppressing purkinje cell loss in parkinson disease rats. *Int. Neurourol. J.* 22, S147–S155.

Lee, K. J. (2007). Morphological changes in dendritic spines of Purkinje cells associated with motor learning. *Neurobiol. Learn. Mem.* 88, 445–450. doi: 10.1016/j.nlm.2007.06.001

Lewis, G. D., Farrell, L., Wood, M. J., Martinovic, M., Arany, Z., Rowe, G. C., et al. (2010). Metabolic signatures of exercise in human plasma. *Sci. Transl. Med.* 2, 33–37. doi: 10.1016/j.earlhumdev.2016.01.008

Lezi, E., Lu, J., Burns, J. M., and Swerdlow, R. H. (2013). Effect of exercise on mouse liver and brain bioenergetic infrastructures. *Exp. Physiol.* 98, 207–219. doi: 10.1113/expphysiol.2012.066688

Li, J., Ding, Y. H., Rafols, J. A., Lai, Q., McAllister, J. P., and Ding, Y. (2005). Increased astrocyte proliferation in rats after running exercise. *Neurosci. Lett.* 386, 160–164. doi: 10.1016/j.neulet.2005.06.009

Liddell, J. (2017). Are Astrocytes the predominant cell type for activation of Nrf2 in aging and neurodegeneration? *Antioxidants* 6, 2–35.

Lipman, G. S., Krabak, B. J., Waite, B. L., Logan, S. B., Menon, A., and Chan, G. K. (2014). A prospective cohort study of acute kidney injury in multi-stage ultramarathon runners: the biochemistry in endurance runner study (BIERS). *Res. Sports Med.* 22, 185–192. doi: 10.1080/15438627.2014.881824

Magi, S., Arcangeli, S., Castaldo, P., Nasti, A. A., Berrino, L., Piegari, E., et al. (2013). Glutamate-induced ATP synthesis: relationship between plasma membrane Na+/Ca2+ exchanger and excitatory amino acid transporters in brain and heart cell models. *Mol. Pharmacol.* 84, 603–614. doi: 10.1124/mol.113.087775

Mang, C. S., Brown, K. E., Neva, J. L., Snow, N. J., Campbell, K. L., and Boyd, L. A. (2016). Promoting motor cortical plasticity with acute aerobic exercise: a role for cerebellar circuits. *Neural Plast.* 2016, 1–12. doi: 10.1155/2016/6797928

Marcinek, D. J., Kushmerick, M. J., and Conley, K. E. (2010). Lactic acidosis in vivo: testing the link between lactate generation and H+ accumulation in ischemic mouse muscle. *J. Appl. Physiol.* 108, 1479–1486. doi: 10.1152/japplphysiol.01189.2009

Marques-Aleixo, I., Santos-Alves, E., Balça, M. M., Moreira, P. I., Oliveira, P. J., Magalhães, J., et al. (2016). Physical exercise mitigates doxorubicin-induced brain cortex and cerebellum mitochondrial alterations and cellular quality control signaling. *Mitochondrion* 26, 43–57. doi: 10.1016/j.mito.2015.12.002

Marques-Aleixo, I., Santos-Alves, E., Balça, M. M., Rizo-Roca, D., Moreira, P. I., Oliveira, P. J., et al. (2015). Physical exercise improves brain cortex and cerebellum mitochondrial bioenergetics and alters apoptotic, dynamic and auto(mito)phagy markers. *Neuroscience* 301, 480–495. doi: 10.1016/j.neuroscience.2015.06.027

Mastorakos, G., and Pavlatou, M. (2005). Exercise as a stress model and the interplay between the hypothalamus-pituitary-adrenal and the hypothalamus-pituitary-thyroid axes. *Horm. Metab. Res.* 37, 577–584. doi: 10.1055/s-2005-870426

Matsui, T., Ishikawa, T., Ito, H., Okamoto, M., Inoue, K., Lee, M. C., et al. (2012). Brain glycogen supercompensation following exhaustive exercise. *J. Physiol.* 590, 607–616. doi: 10.1113/jphysiol.2011.217919

Matsui, T., Omuro, H., Liu, Y. F., Soya, M., Shima, T., Mcewen, B. S., et al. (2017). Astrocytic glycogen-derived lactate fuels the brain during exhaustive exercise to maintain endurance capacity. *Proc. Natl. Acad. Sci. U.S.A.* 114, 6358–6363. doi: 10.1073/pnas.1702739114

Mee-Inta, O., Zhao, Z. W., and Kuo, Y. M. (2019). Physical exercise inhibits inflammation and microglial activation. *Cells* 8, 1–17. doi: 10.1155/2015/729509

Middeldorp, J., and Hol, E. M. (2011). GFAP in health and disease. *Prog. Neurobiol.* 93, 421–443. doi: 10.1016/j.pneurobio.2011.01.005

Millet, G., Martin, V., and Temesi, J. (2018). The role of the nervous system in neuromuscular fatigue induced by ultra-endurance exercise. *Appl. Physiol. Nutr. Metab.* 1, 1–34.

Millet, G. Y., Tomazin, K., Verges, S., Vincent, C., Bonnefoy, R., Boisson, R. C., et al. (2011). Neuromuscular consequences of an extreme mountain ultra-marathon. *PLoS One* 22:e17059. doi: 10.1371/journal.pone.0017059

Misra, H., and Fridovich, I. (1972). The role of superoxide anion in the epinephrine and a simple assay for superoxide dismutase. *J. Biol. Chem.* 247, 3170–3175.

Moeton, M., Kanski, R., Stassen, O. M., Sluijs, J. A., Geerts, D., van Tijn, P., et al. (2014). Silencing GFAP isoforms in astrocytoma cells disturbs laminin-dependent motility and cell adhesion. *FASEB J.* 28, 2942–2954. doi: 10.1096/fj.13-245837

Morgado, J. M., Rama, L., Silva, I., de Jesus Inácio, M., Henriques, A., Laranjeira, P., et al. (2012). Cytokine production by monocytes, neutrophils, and dendritic cells is hampered by long-term intensive training in elite swimmers. *Eur. J. Appl. Physiol.* 112, 471–482. doi: 10.1007/s00421-011-1966-4

Muñoz, D., Barrientos, G., Vas, J. A., Pérez, F. J. G., Maria Concepcion, Maynar, M., et al. (2017). Oxidative stress, lipid peroxidation indexes and antioxidant vitamins in long and middle distance athletes during a sport season middle distance athletes during a sport season. *J. Sports Med. Phys. Fitn.* 58, 1713–1719.

Nakagawa, S., and Cuthill, I. C. (2007). Effect size, confidence interval and statistical significance: a practical guide for biologists. *Biol. Rev.* 82, 591–605. doi: 10.1111/j.1469-185x.2007.00027.x

Ogasawara, H., Doi, T., Doya, K., and Kawato, M. (2007). Nitric oxide regulates input specificity of long-term depression and context dependence of cerebellar learning. *PLoS Comput. Biol.* 3:e179. doi: 10.1371/journal.pcbi.0020179

Ohkawa, H., Ohishi, N., and Yagi, K. (1979). Assay for lipid peroxides in animal tissues by thiobarbituric acid reaction. *Anal. Biochem.* 95, 351–358. doi: 10.1016/0003-2697(79)90738-3

O'Keefe, J. H., Patil, H. R., Lavie, C. J., Magalski, A., Vogel, R. A., and McCullough, P. A. (2012). Potential adverse cardiovascular effects from excessive endurance exercise. *Mayo Clin. Proc.* 87, 587–595. doi: 10.1016/j.mayocp.2012.04.005

Petersen, A. M., and Pedersen, B. K. (2005). The anti-inflammatory effect of exercise. *J. Appl. Physiol.* 98, 1154–1162.

Pitossi, F., Del Rey, A., Kabiersch, A., and Besedovsky, H. (1997). Induction of cytokine transcripts in the central nervous system and pituitary following peripheral administration of endotoxin to mice. *J. Neurosci.Res.* 48, 287–298. doi: 10.1002/(sici)1097-4547(19970515)48:4<287::aid-jnr1>3.0.co;2-7

Powell, K., Mathy, A., Duguid, I., and Häusser, M. (2015). Synaptic representation of locomotion in single cerebellar granule cells. *eLife* 4:e07290.

Pysh, J. J., and Weiss, G. M. (1979). Exercise during development induces an increase in purkinje cell dendritic tree size. *Science* 206, 230–232. doi: 10.1126/science.482938

Rabe, K., Livne, O., Gizewski, E. R., Aurich, V., Beck, A., Timmann, D., et al. (2008). Adaptation to visuomotor rotation and force field perturbation is correlated to different brain areas in patients with cerebellar degeneration. *J. Neurophysiol.* 101, 1961–1971. doi: 10.1152/jn.91069.2008

Radak, Z., Kaneko, T., Tahara, S., Nakamoto, H., and Pucsok, J. (2001). Regular exercise improves cognitive function and decreases oxidative damage in rat brain. *Neurochem. Int.* 38, 17–23. doi: 10.1016/s0197-0186(00)00063-2

Rama, L. M., Minuzzi, L. G., Carvalho, H. M., Costa, R. J. S., and Teixeira, A. M. (2015). Changes of hematological markers during a multi-stage ultra-marathon competition in the heat. *Int. J. Sports Med.* 37, 104–111. doi: 10.1055/s-0035-1555929

Ramos-Campo, D. J., Ávila-Gandía, V., Alacid, F., Soto-Méndez, F., Alcaraz, P. E., López-Román, F. J., et al. (2016). Muscle damage, physiological changes, and energy balance in ultra-endurance mountain-event athletes. *Appl. Physiol. Nutr. Metab.* 41, 872–878. doi: 10.1139/apnm-2016-0093

Rappold, P. M., and Tieu, K. (2010). Astrocytesandtherapeutics for Parkinson'sdisease. *Neurotherapeutics* 7, 413–423.

Rezaei, S., Agha-alinejad, H., Molanouri Shamsi, M., Jafari, M., Azevedo Voltarelli, F., Naderi, A., et al. (2017). Evaluation of efforts in untrained Wistar rats following exercise on forced running wheel at maximal lactate steady state. *J. Exerc. Nutr. Biochem.* 21, 26–32. doi: 10.20463/jenb.2017.0040

Rodrigues, B., Figueroa, D. M., Mostarda, C. T., and Angelis, K. (2007). Maximal exercise test is a useful method for physical capacity and oxygen consumption determination in streptozotocin-diabetic rats. *Cardiovasc. Diabetol.* 6, 13–20.

Sahlin, K., Gorski, J., and Edström, L. (1990). Influence of ATP turnover and metabolite changes on IMP formation and glycolysis in rat skeletal muscle. *Am. J. Physiol.* 259, 409–412.

Schmahmann, J. D. (2019). The cerebellum and cognition. *Neurosci. Lett.* 688, 62–75.

Scorziello, A., Pellegrini, C., Forte, L., Tortiglione, A., Gioielli, A., Iossa, S., et al. (2001). Differential vulnerability of cortical and cerebellar neurons in primary culture to oxygen glucose deprivation followed by reoxygenation. *J. Neurosci. Res.* 63, 20–26. doi: 10.1002/1097-4547(20010101)63:1<20::aid-jnr3>3.0.co;2-n

Sereika, M., Urbanaviciute, R., Tamasauskas, A., Skiriute, D., and Vaitkiene, P. (2018). GFAP expression is influenced by astrocytoma grade and rs2070935 polymorphism. *J. Cancer* 9, 4496–4502. doi: 10.7150/jca.26769

Shirakawa, F., Saito, K., Bonagura, C. A., Galson, D. L., Fenton, M. J., Webb, A. C., et al. (1993). The human prointerleukin 1 beta gene requires DNA sequences both proximal and distal to the transcription start site for tissue-specific induction. *Mol. Cell Biol.* 13, 1332–1344. doi: 10.1128/mcb.13.3.1332

Silverman, M. N., Pearce, B. D., Biron, C. A., and Miller, A. H. (2005). Immunemodulation of the hypothalamic–pituitary–adrenal (HPA) axis during viral infection. *ViralImmunol* 18, 41–78. doi: 10.1089/vim.2005.18.41

Son, H. J., Lee, Y. H., Chae, J. H., and Kim, C. K. (2015). Creatine kinase isoenzyme activity during and after an ultra-distance (200 km) run. *Biol. Sport* 32, 357–361.

Sonnay, S., Gruetter, R., and Duarte, J. M. N. (2017). How energy metabolism supports cerebral function: insights from 13C magnetic resonance studies *In vivo*. *Front. Neurosci.* 11:288. doi: 10.3389/fnins.2017.00288

Sullivan, S. M. (2014). GFAP variants in health and disease: stars of the brain.. and gut. *J. Neurochem.* 130, 729–732. doi: 10.1111/jnc.12754

Swiątkiewicz, M., Fiedorowicz, M., Orzeł, J., Wełniak-Kamińska, M., Bogorodzki, P., Langfort, J., et al. (2017). Increases in Brain 1H-MR glutamine and glutamate signals following acute exhaustive endurance exercise in the rat. *Front. Physiol.* 8:19. doi: 10.3389/fphys.2017.00019

Tarini, V. A. F., Carnevali, L. C. Jr., Arida, R. M., Cunha, C. A., Alves, E. S., Seeleander, M. C., et al. (2013). Effect of exhaustive ultra-endurance exercise in muscular glycogen and both Alpha1 and Alpha2 Ampk protein expression in trained rats. *J. Physiol. Biochem.* 69, 429–440. doi: 10.1007/s13105-012-0224-5

Tercero-Pérez, K., Cortés, H., Torres-Ramos, Y., Rodríguez-Labrada, R., Cerecedo-Zapata, C. M., Hernández-Hernández, O., et al. (2019). Effects of physical rehabilitation in patients with spinocerebellar ataxia type 7. *Cerebellum* 18, 397–405.

Toda, N., Ayajiki, K., and Okamura, T. (2009). Cerebral blood flow regulation by nitric oxide: recent advances. *Pharmacol. Rev.* 6, 162–197.

Torres, J. B., Assunção, J., Farias, J. A., Kahwage, R., Lins, N., Passos, A., et al. (2006). NADPH-diaphorase histochemical changes in the hippocampus, cerebellum and striatum are correlated with different modalities of exercise and watermaze performances. *E.xp Brain Res.* 175, 292–304. doi: 10.1007/s00221-006-0549-9

Turner, J. E., Bennett, S. J., Bosch, J. A., Griffiths, H. R., and Aldred, S. (2014). Ultra-endurance exercise: unanswered questions in redox biology and immunology. *Biochem. Soc. Trans.* 42, 989–995. doi: 10.1042/bst20140120

Voltarelli, F. A., Gobatto, C. A., and de Mello, M. A. (2002). Determination of anaerobic threshold in rats using the lactate minimum test. *Braz. J. of Med. Biol. Res.* 35, 1389–1394. doi: 10.1590/s0100-879x2002001100018

Wu, G. L., Chen, Y. S., Huang, X. D., and Zhang, L. X. (2012). Exhaustive swimming exercise-related kidney injury in rats - protective effects of acetylbritannilactone. *Int. J. Sports Med.* 33, 1–7. doi: 10.1055/s-0031-1284397

Yamashita, K., and Yoshioka, T. (1991). Profiles of creatine kinase isoenzyme compositions in single muscle fibres of different types. *J. Muscle Res. Cell Motil.* 12, 37–44. doi: 10.1007/bf01781172

Conflict of Interest: The authors declare that the research was conducted in the absence of any commercial or financial relationships that could be construed as a potential conflict of interest.

Advantages of publishing in Frontiers

OPEN ACCESS
Articles are free to read for greatest visibility and readership

FAST PUBLICATION
Around 90 days from submission to decision

HIGH QUALITY PEER-REVIEW
Rigorous, collaborative, and constructive peer-review

TRANSPARENT PEER-REVIEW
Editors and reviewers acknowledged by name on published articles

Frontiers
Avenue du Tribunal-Fédéral 34
1005 Lausanne | Switzerland

Visit us: www.frontiersin.org
Contact us: frontiersin.org/about/contact

REPRODUCIBILITY OF RESEARCH
Support open data and methods to enhance research reproducibility

DIGITAL PUBLISHING
Articles designed for optimal readership across devices

FOLLOW US
@frontiersin

IMPACT METRICS
Advanced article metrics track visibility across digital media

EXTENSIVE PROMOTION
Marketing and promotion of impactful research

LOOP RESEARCH NETWORK
Our network increases your article's readership